THE EFFECTS OF ALTERED GRAVITY ON PHYSIOLOGY

EDITED BY: Gilles Clement, Richard D. Boyle and Hanns-Christian Gunga
PUBLISHED IN: Frontiers in Physiology

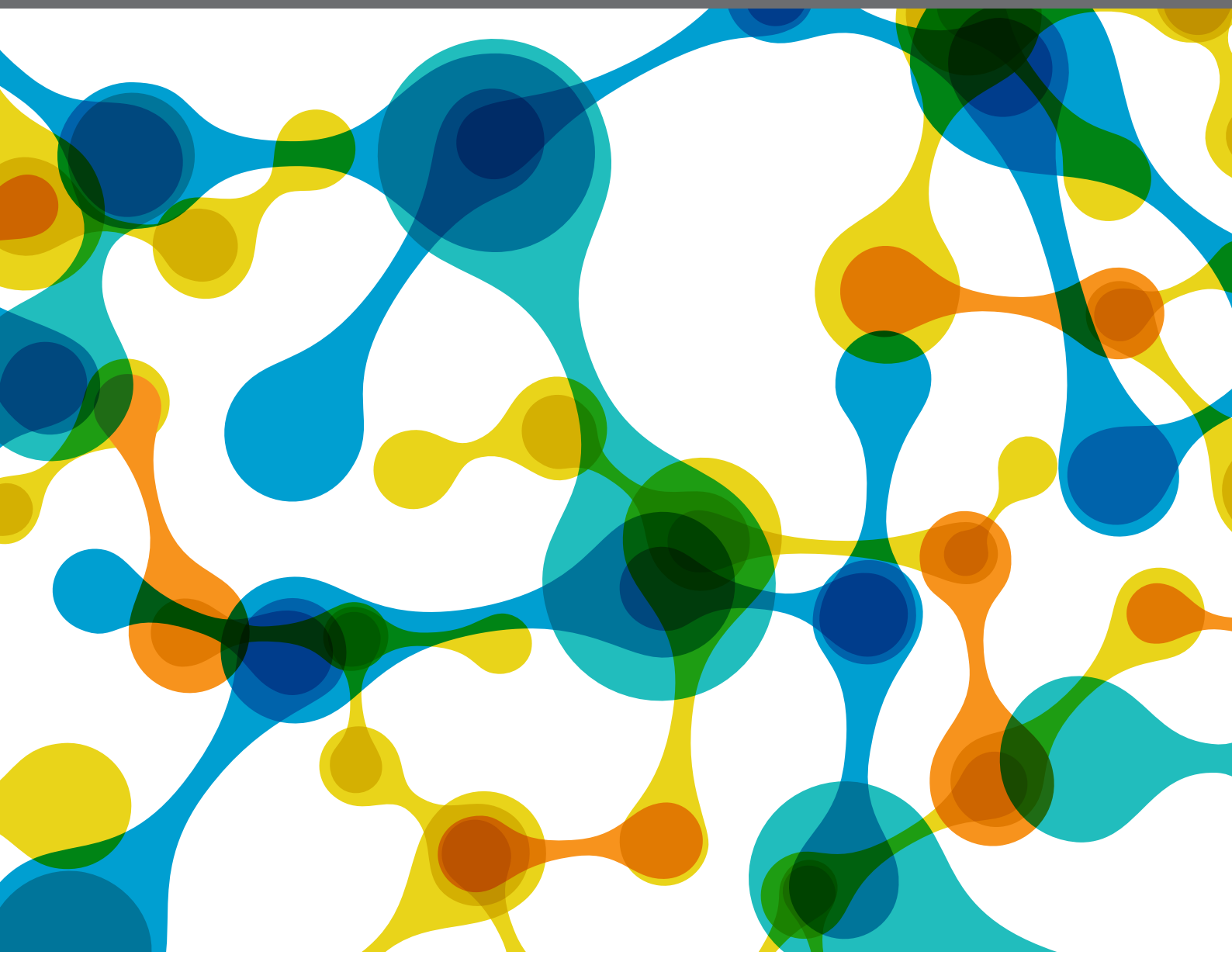

frontiers Research Topics

frontiers

ISSN 1664-8714
ISBN 978-2-88963-350-0
DOI 10.3389/978-2-88963-350-0

About Frontiers

Frontiers is more than just an open-access publisher of scholarly articles: it is a pioneering approach to the world of academia, radically improving the way scholarly research is managed. The grand vision of Frontiers is a world where all people have an equal opportunity to seek, share and generate knowledge. Frontiers provides immediate and permanent online open access to all its publications, but this alone is not enough to realize our grand goals.

Frontiers Journal Series

The Frontiers Journal Series is a multi-tier and interdisciplinary set of open-access, online journals, promising a paradigm shift from the current review, selection and dissemination processes in academic publishing. All Frontiers journals are driven by researchers for researchers; therefore, they constitute a service to the scholarly community. At the same time, the Frontiers Journal Series operates on a revolutionary invention, the tiered publishing system, initially addressing specific communities of scholars, and gradually climbing up to broader public understanding, thus serving the interests of the lay society, too.

Dedication to Quality

Each Frontiers article is a landmark of the highest quality, thanks to genuinely collaborative interactions between authors and review editors, who include some of the world's best academicians. Research must be certified by peers before entering a stream of knowledge that may eventually reach the public - and shape society; therefore, Frontiers only applies the most rigorous and unbiased reviews.
Frontiers revolutionizes research publishing by freely delivering the most outstanding research, evaluated with no bias from both the academic and social point of view. By applying the most advanced information technologies, Frontiers is catapulting scholarly publishing into a new generation.

What are Frontiers Research Topics?

Frontiers Research Topics are very popular trademarks of the Frontiers Journals Series: they are collections of at least ten articles, all centered on a particular subject. With their unique mix of varied contributions from Original Research to Review Articles, Frontiers Research Topics unify the most influential researchers, the latest key findings and historical advances in a hot research area! Find out more on how to host your own Frontiers Research Topic or contribute to one as an author by contacting the Frontiers Editorial Office: researchtopics@frontiersin.org

THE EFFECTS OF ALTERED GRAVITY ON PHYSIOLOGY

Topic Editors:
Gilles Clement, Centre National de la Recherche Scientifique (CNRS), France
Richard D. Boyle, National Aeronautics and Space Administration (NASA), United States
Hanns-Christian Gunga, Charité Medical University of Berlin, Germany

Citation: Clement, G., Boyle, R. D., Gunga, H.-C., eds. (2020). The Effects of Altered Gravity on Physiology. Lausanne: Frontiers Media SA.
doi: 10.3389/978-2-88963-350-0

Table of Contents

frontiers in Physiology

EDITORIAL
published: 27 November 2019
doi: 10.3389/fphys.2019.01447

Editorial: The Effects of Altered Gravity on Physiology

Gilles Clement[1]*, *Richard D. Boyle*[2] *and Hanns-Christian Gunga*[3]

[1] Lyon Neuroscience Research Center, Bron, France, [2] National Aeronautics and Space Administration, Washington, DC, United States, [3] Institute of Physiology, Charité Medical University of Berlin, Berlin, Germany

Keywords: adaptation, microgravity, hypergravity, spaceflight adaptation, extreme environment

Editorial on the Research Topic

The Effects of Altered Gravity on Physiology

In physiology, a graded dose-response curve relates the stimulus input to a specific measured output. Space studies in humans and animals have provided only a snapshot into understanding the role of gravity on physiological responses. Fully understanding this relationship, including adaptive mechanisms, will provide the information required to ensure normal physiological function in crew for long-duration space missions (Clément, 2017).

Various methods can be used for generating altered gravity, including orbital flight, parabolic flight, head down/up tilt, body loading/unloading, and centrifugation (Richter et al.). In this *Frontiers in Physiology* Research Topic, ten papers have used these various methods for studying the effects of altered gravity on sensorimotor, musculoskeletal, cardiopulmonary, and cerebrovascular responses in humans and rodents.

ORBITAL FLIGHT

Long stays in weightlessness take a toll on the human body, as the muscles atrophy, bones lose minerals, and a new set of stimuli imposes novel challenges on the vestibular and cardiovascular systems (Gunga et al., 2016). Stationary bike and treadmill were used on Sklylab and Mir stations; however, they were not completely successful in preventing astronauts' muscle and bone loss. A new exercise device, the Interim Resistive Exercise Device (iRED), was flown on the International Space Station to target weight-bearing structures, such as squats to load the spine, hips and legs (Schneider et al., 2003). McNamara et al. analyzed computed tomography scans of 16 crewmembers before and after long-duration spaceflight and found that crewmembers experienced less decrease in the back, abdominal, and paraspinal muscles after using iRED protocols in orbit.

During spaceflight, the vestibular otolith organs no longer adequately sense gravito-inertial accelerations. Animal studies have shown that otolith afferents are initially hypersensitive to tilt after return to Earth (Boyle et al., 2001). Perhaps as a result of this hypersensitivity, astronauts overestimate pitch and roll tilt for 1–2 days immediately after landing (Clément and Wood, 2013). In addition, their performance during manual motion-based simulation tasks is greatly impaired, which is a navigational concern (Moore et al., 2019). Clément et al. showed that adaptive changes in astronauts' vestibular processing during spaceflight impair their ability to manually control tilt following transitions between gravitational environments; however, simple aids, such as vibrotactile feedback, can be used to improve their performance.

These changes in vestibular processing after spaceflight are confirmed by brain imaging study showing functional connectivity modifications between the vestibular cortex, the vestibular nuclei, and the cerebellum in cosmonauts after long-duration spaceflight (Pechenkova et al.). Interestingly, the severity of space motion sickness symptoms experienced by these subjects was

OPEN ACCESS

Edited and reviewed by:
Rachael D. Seidler,
University of Michigan, United States

***Correspondence:**
Gilles Clement
gilles.r.clement@nasa.gov

Specialty section:
This article was submitted to Environmental, Aviation and Space Physiology, a section of the journal Frontiers in Physiology

Received: *30 September 2019*
Accepted: *08 November 2019*
Published: *27 November 2019*

Citation:
Clement G, Boyle RD and Gunga H-C (2019) Editorial: The Effects of Altered Gravity on Physiology. Front. Physiol. 10:1447. doi: 10.3389/fphys.2019.01447

found to correlate with a post- to pre-flight difference in connectivity between the right and left areas of the vestibular cortex.

PARABOLIC FLIGHT

The parabolic trajectory of an aircraft exposes the passengers to repeated transitions from increased to reduced gravity (Karmali and Shelhamer, 2008). Ritzmann et al. compared postural adjustments in response to perturbations across gravity levels ranging from 0.25 to 1.75 g by varying the aircraft's pitch angle during pull-up. Subjects walked on a split treadmill and changes in their leg muscles activity and ankle and knee joint trajectories were recorded as the speed of the belts suddenly changed. Results showed a linear relationship between gravity level and EMG amplitudes and muscle onset latencies after perturbations.

HEAD DOWN/UP TILT

Body tilt of supine subjects allows for partial mechanical unloading along the subject's longitudinal axis in normal Earth's gravity and simulate cephalad fluid shifts (Pavy-Le Traon et al., 2007). Boschert et al. placed subjects at −12° (head down), corresponding to −0.2 g linear acceleration (Clément et al.), for 3 days and two nights to determine whether changes in cerebral hemodynamics also affected sleep. Results indicated that jugular vein venous congestion occurred faster and that the quality of sleep was poorer at the greater head tilt angle.

Diaz-Artiles et al. compared cardiopulmonary responses of subjects to various gravitational loads along the body longitudinal axis as they exercised on a cycle ergometer while supine with the head-down or head-up. Angles of tilt were −6° (simulating 0 g), 9.5° head up (0.16 g lunar gravity), 22.3° head up (0.38 g Mars gravity), and upright (1 g Earth gravity). Heart rate and respiration tidal volume increased as a function of the gravitational load, whereas respiration rate, and the volume of O_2 and CO_2 uptake decreased as a function of the gravitational loads.

BODY LOADING/UNLOADING

In rodents, a 30° head-down tilt by tail suspension unloads the weight-bearing hindlimbs and creates a cephalad fluid shift and situational stress that are analogs to weightlessness (Morey-Holton and Globus, 2002). Ulanova et al. showed that a 7-days hindlimb suspension resulted in soleus muscle atrophy and a decrease in titin (T1), a protein responsible for the passive elasticity of muscle. Administration of L-Arginine, a semi-essential amino acid, decreased the degree of atrophy and prevented the decrease in T1 levels, thus mitigating the effects of gravitational unloading.

Mortreux et al. used a partial weight suspension system that allowed for reduced loading on all four limbs while still permitting quadrupedal locomotion (Wagner et al., 2010). Here, rats were supported for 14 days under Mars-analog suspension (38% weight bearing) and compared with age-matched (100% weight bearing) controls. Their results demonstrated that resveratrol, a polyphenol that is known to preserve bone and muscle mass, treatment during partial unloading significantly preserves muscle function and mitigates muscle atrophy.

Arntz et al. studied the vestibular drive for standing balance in humans when loading the body downward at 1.5 and 2 times their body weight, and when exposing subjects to hypergravity (1.8 g) during parabolic flights. A stochastic electrical vestibular stimulus (0–25 Hz) delivered during these tasks evoked a vestibular-error signal and corrective muscles responses. With additional load, the magnitude of the vestibular-evoked muscle responses progressively decreased and plateaued at 1.5 times body weight.

CENTRIFUGATION

Diaz-Artiles et al. exposed subjects to 1.4 g at their feet via short-radius centrifugation and measured their cardiovascular responses while exercising on a cycle ergometer. They found that cardiac output, stroke volume, pulse pressure, and heart rate significantly increased with the gravity level. These results confirm that combination of exercise and artificial gravity provide a greater cardiovascular benefit than exercise alone.

AUTHOR CONTRIBUTIONS

All authors listed have made a substantial, direct and intellectual contribution to the work, and approved it for publication.

FUNDING

This work was supported by the NASA/NAG2-945/Neurolab/STS-95 and NIH/NIDCD P01 DC01837 (to RB).

ACKNOWLEDGMENTS

We sincerely thank the authors who have contributed to the success of this Research Topic. Their articles demonstrate the growing popularity of the field of gravitational physiology and point to promising countermeasures for future space exploration.

REFERENCES

Boyle, R. D., Mensinger, A. F., Yoshida, K., Usui, S., Intravaia, A., Tricas, T., et al. (2001). Neural readaptation to 1G following return from space. *J. Neurophysiol.* 86, 2118–2122. doi: 10.1152/jn.2001.86.4.2118

Clément, G. (2017). International roadmap for artificial gravity research. *NPJ Microgravity* 3:29. doi: 10.1038/s41526-017-0034-8

Clément, G., and Wood, S. J. (2013). Motion perception during tilt and translation after spaceflight. *Acta Astronaut.* 92, 48–52. doi: 10.1016/j.actaastro.2012.03.011

Gunga, H. C., von Ahlefeld, V. W., Appell, H. J., Werner, A. U., and Hoffmann, U. (2016). *The Cardiovascular System in Space*. Cham: Springer.

Karmali, F., and Shelhamer, M. (2008). The dynamics of parabolic flight: flight characteristics and passenger percepts. *Acta Astronaut.* 63, 594–602 doi: 10.1016/j.actaastro.2008.04.009

Moore, S. T., Dilda, V., Morris, T. R., Yungher, D. A., MacDougall, H. G., and Wood, S. J. (2019). Long-duration spaceflight adversely affects post-landing operator proficiency. *Sci. Rep.* 9:2677. doi: 10.1038/s41598-019-39058-9

Morey-Holton, E. R., and Globus, R. K. (2002). Hindlimb unloading rodent model: technical aspects. *J. Appl. Physiol. (1985)* 92, 1367–1377. doi: 10.1152/japplphysiol.00969.2001

Pavy-Le Traon, A., Heer, M., Narici, M. V., Rittweger, J., and Vernikos, J. (2007). From space to earth: advances in human physiology from 20 years of bed rest studies (1986–2006). *Eur. J. Appl. Physiol.* 101, 143–194. doi: 10.1007/s00421-007-0474-z

Schneider, S., Amonette, W., Blazine, K., Bentley, J., Lee, S., Loehr, J., et al. (2003). Training with the international space station interim resistive exercise device. *Med. Sci. Sports Exerc.* 35, 1935–1945. doi: 10.1249/01.MSS.0000093611.88198.08

Wagner, E. B., Granzella, N. P., Saito, H., Newman, D. J., Young, L. R., and Bouxsein, M. L. (2010). Partial weight suspension: a novel murine model for investigating adaptation to reduced musculoskeletal loading. *J. Appl. Physiol. (1985)* 109, 350–357. doi: 10.1152/japplphysiol.00014.2009

Conflict of Interest: The authors declare that the research was conducted in the absence of any commercial or financial relationships that could be construed as a potential conflict of interest.

frontiers in Physiology

ORIGINAL RESEARCH
published: 13 November 2018
doi: 10.3389/fphys.2018.01492

Short-Term Cardiovascular Response to Short-Radius Centrifugation With and Without Ergometer Exercise

Ana Diaz-Artiles[1], Thomas Heldt[2†] and Laurence R. Young[3]*

[1] Department of Aerospace Engineering, Texas A&M University, College Station, TX, United States, [2] Institute for Medical Engineering and Science and Department of Electrical Engineering and Computer Science, Massachusetts Institute of Technology, Cambridge, MA, United States, [3] Department of Aeronautics and Astronautics, Massachusetts Institute of Technology, Cambridge, MA, United States

Artificial gravity (AG) has often been proposed as an integrated multi-system countermeasure to physiological deconditioning associated with extended exposure to reduced gravity levels, particularly if combined with exercise. Twelve subjects underwent short-radius centrifugation along with bicycle ergometry to quantify the short-term cardiovascular response to AG and exercise across three AG levels (0 G or no rotation, 1 G, and 1.4 G; referenced to the subject's feet and measured in the centripetal direction) and three exercise intensities (25, 50, and 100 W). Continuous cardiovascular measurements were collected during the centrifugation sessions using a non-invasive monitoring system. The cardiovascular responses were more prominent at higher levels of AG and exercise intensity. In particular, cardiac output, stroke volume, pulse pressure, and heart rate significantly increased with both AG level (in most of exercise group combinations, showing averaged increments across exercise conditions of 1.4 L/min/g, 7.6 mL/g, 5.22 mmHg/g, and 2.0 bpm/g, respectively), and workload intensity (averaged increments across AG conditions of 0.09 L/min/W, 0.17 mL/W, 0.22 mmHg/W, and 0.74 bpm/W respectively). These results suggest that the addition of AG to exercise can provide a greater cardiovascular benefit than exercise alone. Hierarchical regression models were fitted to the experimental data to determine dose-response curves of all cardiovascular variables as a function of AG-level and exercise intensity during short-radius centrifugation. These results can inform future studies, decisions, and trade-offs toward potential implementation of AG as a space countermeasure.

Keywords: artificial gravity, orthostatic intolerance, human experiments, spaceflight deconditioning, spaceflight countermeasure

OPEN ACCESS

Edited by:
Gilles Clement, Centre National de la Recherche Scientifique (CNRS), France

Reviewed by:
Anne Pavy-Le Traon, Centre Hospitalier Universitaire (CHU) de Toulouse, France
Jochen Zange, Helmholtz-Gemeinschaft Deutscher Forschungszentren (HZ), Germany

****Correspondence:***
Ana Diaz-Artiles
adartiles@tamu.edu
orcid.org/0000-0002-0459-9327
†orcid.org/0000-0002-2446-1499

Specialty section:
This article was submitted to Environmental, Aviation and Space Physiology, a section of the journal Frontiers in Physiology

Received: *15 July 2018*
Accepted: *03 October 2018*
Published: *13 November 2018*

Citation:
Diaz-Artiles A, Heldt T and Young LR (2018) Short-Term Cardiovascular Response to Short-Radius Centrifugation With and Without Ergometer Exercise. Front. Physiol. 9:1492. doi: 10.3389/fphys.2018.01492

INTRODUCTION

Astronauts undergo important physiological deconditioning in space due to the weightless environment. Bone loss, muscle atrophy, cardiovascular deconditioning, or neurovestibular alterations are some of the most common issues experienced during space missions (Clément, 2005; Buckey, 2006). The observed changes in cardiovascular performance have been attributed

to the loss of hydrostatic pressure gradients in microgravity (Charles and Lathers, 1991; Williams et al., 2009), causing a series of physiological adaptations, including a fluid shift from the lower extremities to the upper part of the body, a decrease in circulating blood volume, cardiac atrophy, an increase in venous compliance, a reduction of the baroreflex sensitivity (Clément and Bukley, 2007), and other alterations in autonomic function (Mandsager et al., 2015). Oxidative stress (Dhalla et al., 2000), radiation (Baker et al., 2011), and elevated CO_2 levels (Sliwka et al., 1998) may also affect cardiovascular regulation. Previous in-flight investigations have shown significant changes in hemodynamics during both short- (Norsk et al., 2006; Verheyden et al., 2009; Eckberg et al., 2010; Norsk, 2014; Norsk et al., 2015), and long-duration (Baevsky et al., 2007; Verheyden et al., 2009; Hughson et al., 2012; Norsk et al., 2015) spaceflight. This general adaptation of the cardiovascular system to weightlessness, especially if combined with detrimental musculoskeletal changes (LeBlanc et al., 2007; Fitts et al., 2010), may lead to orthostatic intolerance (Buckey, 2006) and a significant reduction in work capacity (Levine et al., 1996) when re-exposure to a significant gravitational environment, like on Earth, occurs.

Currently, there are several countermeasures in place that seek to mitigate the detrimental effects of weightlessness. The introduction of the new Advanced Resistance Exercise Device (ARED) in 2008 has resulted in an attenuation in bone loss when coupled with other countermeasures such as adequate energy intake and vitamin D (Smith et al., 2012), or bisphosphonates (LeBlanc et al., 2013). In general, these countermeasures are specific to individual physiological systems. Cardiovascular countermeasures, for example, have included aerobic and resistive exercise (Buckey, 2006; Trigg, 2013), Lower Body Negative Pressure (LBNP) (Charles and Lathers, 1994; Clément and Bukley, 2007), fluid loading (Clément and Bukley, 2007), intra-vehicular activity suits (Kozlovskaya et al., 1995; Kozlovskaya and Grigoriev, 2004; Waldie and Newman, 2011), landing compression garments (Platts et al., 2009), and nutrition and dietary supplements (Buckey, 2006; Smith et al., 2012). To date, however, countermeasures have failed to consistently preserve pre-flight levels of physiological function, despite the significant crew time that needs to be allocated to them (Clément and Pavy-Le Traon, 2004; Kozlovskaya and Grigoriev, 2004; Buckey, 2006; Clément and Bukley, 2007; Trappe et al., 2009; Lee et al., 2015). Consequently, about two-thirds of returning Shuttle astronauts experienced some degree of orthostatic intolerance (Buckey et al., 1996; Lee et al., 2015), with one out of every four astronauts failing to complete a 10-min stand test on landing day due to light-headedness, palpitations, and syncope (Williams et al., 2009). The incidence of orthostatic intolerance is even greater after longer missions in the ISS, where the proportion of astronauts that could not complete a 10-min orthostatic tilt test is about 33% (Lee et al., 2015). New approaches, possibly combining novel and current countermeasures, are needed for longer missions in the future, such as a trip to the surface of Mars, where astronauts will not have the ground support and resources usually provided on Earth after landing.

Artificial gravity (AG) has been proposed as a promising multisystem countermeasure (Paloski and Charles, 2014; Clément G.R. et al., 2016; Clément, 2017). By intermittently creating a gravitational gradient along the major body axis, AG has the potential to prevent multiple aspects of human deconditioning from occurring during long exposure to weightlessness. Different physiological systems, including the musculoskeletal, cardiovascular, neurovestibular, and immune systems could benefit at the same time from AG exposure while in space (Buckey, 2006; Clément and Bukley, 2007; Paloski and Charles, 2014; Clement et al., 2015; Linnarsson et al., 2015). Furthermore, the benefits of centrifugation could be enhanced if combined with exercise. In addition to its direct contribution to muscle and cardiovascular conditioning, exercise during AG increases tolerance to centrifugation via the muscle pump, protecting astronauts from fainting (Clément and Bukley, 2007; Kaderka et al., 2010). In particular, lower body cycling exercise using an ergometer device mounted on a short-radius centrifuge while rotating has been shown to be effective in preventing cardiovascular deconditioning (Greenleaf et al., 1997; Iwase et al., 2002; Evans et al., 2004; Katayama et al., 2004; Iwase, 2005; Iwasaki et al., 2005; Stenger et al., 2007; Yang et al., 2007, 2010). AG therefore has the potential to provide a greater overall physiological benefit for a given amount of exercise and crew time (Paloski and Charles, 2014; Clement et al., 2015). Similarly, AG could provide similar physiological benefit with less amount of exercise and crew time. Despite the potential benefits and the increasing interest in this area from the scientific community (Paloski and Young, 1999; Young et al., 2009; Paloski and Charles, 2014), many questions still remain concerning its implementation. Aspects such as the appropriate gravity level, centrifuge configuration, radius, angular velocity, exposure time, exercise modality, exercise protocol, or safety concerns are still unanswered, and require further investigation (Clément G. et al., 2016). Of particular interest is to understand the relationship between gravitational dose and physiological response, which is unknown for most human physiological systems (Clément, 2017).

Recent studies have investigated acute cardiovascular responses *while* being exposed to AG using a short-radius centrifuge. A study conducted at the Institute for Space Medicine and Physiology (MEDES), in Toulouse, France, investigated two gravity levels (1 G and 2 G, measured at the feet), and concluded that centrifugation at 2 G provides similar blood pressure regulatory indices (Verma et al., 2018), and similar cardiovascular and cerebral responses (Goswami et al., 2015a) to standing. Another study conducted at the German Aerospace Institute (DLR) also investigated cardiovascular reactions to centrifugation at 1 and 2 G (measured at the feet) showing apparent gender-specific patterns in their cardiovascular responses (Masatli et al., 2018). In both studies, subjects adopted a supine position with the head located near the center of rotation. However, in all cases subjects were laying down passively, without engaging in any exercise or muscle pump-related contraction.

The objective of our research is to characterize the dynamic cardiovascular response during centrifugation, generated by a short-radius centrifuge, combined with lower-body ergometer exercise in healthy human volunteers. An experimental approach

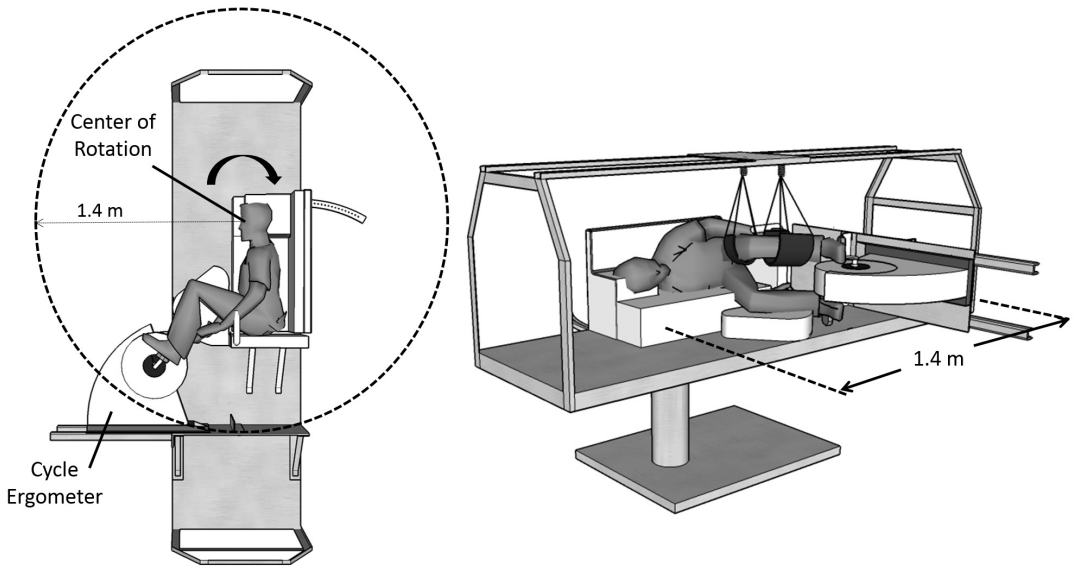

FIGURE 1 | MIT short-radius centrifuge configuration during the experimental sessions. The centrifuge was constrained to a radius of 1.4 m, and a cycle ergometer was used during the centrifugation runs. Subjects were positioned on their right side facing "into the wind."

was implemented to investigate the short-term cardiovascular effects of the gravity level and the exercise intensity, and to generate gravitational dose-response curves in a short-radius centrifuge. It was hypothesized that higher levels of AG would increase the stress upon the cardiovascular system and thereby elicit more pronounced cardiovascular reflex responses in order to maintain blood pressure homeostasis. Additionally, it was further hypothesized that these responses would be more apparent when cardiovascular demand increased further at higher exercise intensities.

EXPERIMENTAL METHODS

Centrifuge Configuration

The experiments were conducted using the Compact-Radius Centrifuge (CRC) at the Massachusetts Institute of Technology (MIT) (Diaz et al., 2015b). Prior to the study, the centrifuge underwent several modifications, primarily driven by the international flight project "Artificial Gravity with Ergometer Exercise" (AGREE) (Diaz et al., 2015b). This project sought to integrate a short-radius centrifuge with an ergometer exercise device for possible deployment in the Permanent Multipurpose Module (PPM) on-board the International Space Station (ISS). Thus, the new configuration of the MIT centrifuge incorporated the majority of requirements from AGREE, particularly the space limitations and subject configuration, resulting in three main modifications. First, the radius of the centrifuge was constrained to 1.4 m (maximum upper radial limit to fit a centrifuge into the PMM). Second, an ergometer device (Lode BV, Groningen, Netherlands) was incorporated into the centrifuge, allowing subjects to engage in lower-body cycling while being rotated. Finally, subjects were positioned in the right-lateral decubitus position with their head located at the center of the rotation and facing "into the wind," and their feet strapped to the ergometer device. This positioning not only minimizes motion sickness, but also minimizes lateral knee deflections caused by Coriolis forces while cycling (Duda et al., 2012). If needed, the ergometer position was slightly adjusted to ensure subjects could properly reach the pedals during cycling. The left leg was suspended using adjustable leg straps to facilitate the exercise in the sidewise position. **Figure 1** shows a schematic of the MIT centrifuge configuration. Subjects were secured using a three-point seat-belt and monitored continuously using a wireless video camera. A detailed description of the CRC MIT centrifuge configuration and subject positioning is available elsewhere (Diaz et al., 2015a,b).

Experimental Design and Instrumentation

We implemented a within-subject, counterbalanced, full factorial experimental design, such that all subjects experienced every combination of AG level and exercise intensity. Each subject participated in three experimental sessions, scheduled on three different days within the same week. The experimental sessions were usually scheduled on consecutive days, although due to subjects' scheduling constraints some sessions occurred every other day. For each subject, the three sessions were scheduled in the morning at approximately the same time to control for possible confounding circadian effects. Additionally, on testing days the subjects were asked to refrain from drinking caffeine and exercising prior to each test session. In each of the three sessions, subjects underwent the same 25-min experimental protocol, under a specific AG level. The AG levels tested were: 0 G (no

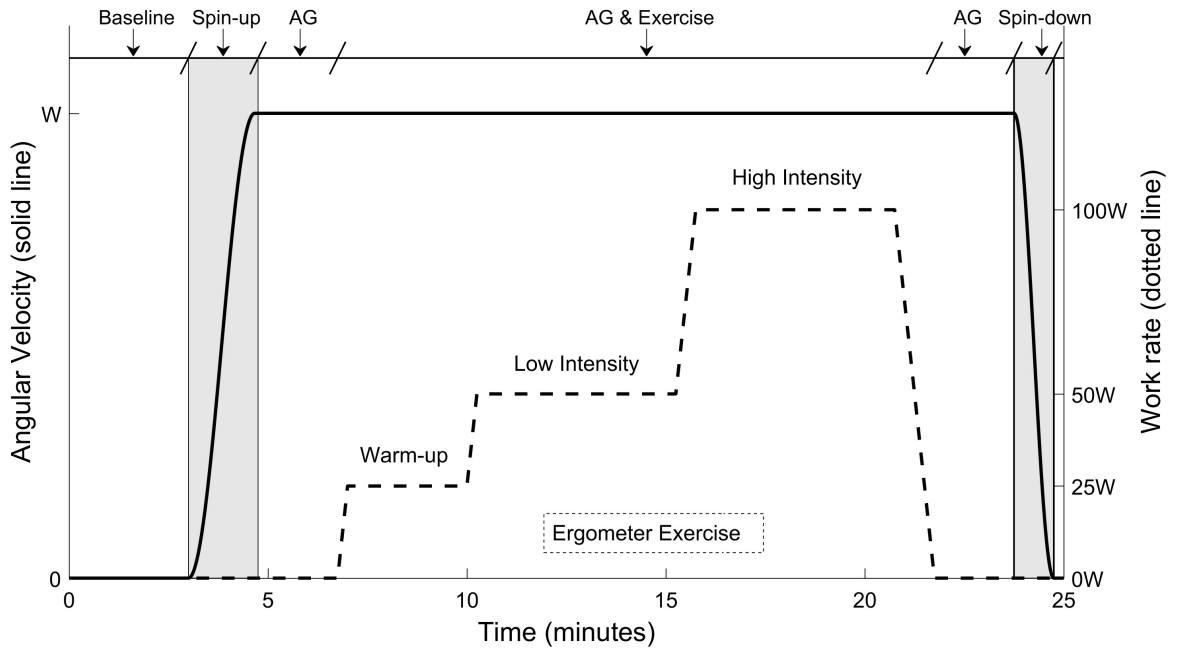

FIGURE 2 | Twenty-five minutes exercise protocol conducted at each experimental session. The protocol included a baseline period (3 min), the spin-up process to the desired G-level (100 s), a first period of AG alone before exercise (125 s), the ergometer exercise period (15-min including work rate transitions), a second period of AG alone after exercise (120 s), and the spin-down process (60 s). The three G-levels tested were 0, 1, and 1.4 G (measured at the feet), corresponding to angular velocities of 0, 28.6, and 33.4 rpm respectively.

rotation), 1 G, and 1.4 G. These levels were chosen based on either their relevance to spaceflight (0 and 1 G), or the maximal rotation capacity of the centrifuge (1.4 G). The order of the three sessions (0 G vs. 1 G vs. 1.4 G) was counterbalanced across subjects, meaning that subjects experienced the three AG conditions in different order to counteract for potential carryover effects. The AG levels were measured at the subject's feet (i.e., the axis of rotation of the ergometer), and they corresponded approximately to rotation rates of 0 rpm (0 G), 28.6 rpm (1 G), and 33.4 rpm (1.4 G). Depending on the ergometer position, these rates were adjusted slightly to ensure that the appropriate gravity level was reached at each subject's feet.

During the experimental sessions, beat-to-beat cardiac output (CO), stroke volume (SV), pulse pressure (PP), heart rate (HR), mean (MBP), systolic (SBP), and diastolic blood pressure (DBP), and total peripheral resistance (TPR) were continuously determined, recorded, and archived using the Nexfin monitor (Edwards Lifesciences Corporation, Irvine, CA, United States). The only interface with the subject was an inflatable finger cuff that includes an infrared photo-plethysmograph sensor to measure the volume of the finger arteries to calculate the real-time finger pressure waveform. The finger pressure waveform is then transformed to brachial pressure waveform to counteract both the pressure drop to resistance, and the pressure wave amplification in peripheral sites like the fingers (Penaz, 1973; Bogert and van Lieshout, 2005; Eeftinck Schattenkerk et al., 2009; Perel et al., 2011). Blood pressure numerics and HR are directly obtained from the branchial pressure waveform while SV, and thus CO = SV*HR and TPR = MAP/CO, are estimated by the Nexfin CO-trek algorithm and depend on subject's age, gender, height, and weight (Truijen et al., 2012). Subjects were instructed to keep their hand with the finger cuff at heart level during the entire protocol to avoid pressure changes due to altered hydrostatic effects caused by the rotating environment and the strong gravity gradient present in a short-radius centrifuge. In addition to the cardiovascular recordings, foot-force data using force plates mounted on the pedals (Vernier Software & Technology), and subjective data related to comfort and motion sickness (using an exit survey) were also collected during the experiments, and these results are available elsewhere (Diaz et al., 2015b).

Artificial Gravity Profile and Exercise Protocol

While the gravity level varied among experimental sessions, the exercise protocol remained the same and it is shown in **Figure 2**. Once subjects were positioned on the centrifuge, their cardiovascular variables were recorded during a baseline period of 3 min. Then, the centrifuge either remained motionless (0 G condition) or was accelerated over approximately 100 s to the desired G-level. The acceleration was sufficiently smooth to ensure subjects were comfortable during this process. Approximately 2 min were provided at the end of the acceleration for the transient effects of the spin-up to subside and for subjects to get used to the new gravitational load. Subjects then executed the exercise portion of the testing protocol. Once completed, an additional 2 min were provided for subjects to partially

recover from the exercise. The centrifuge was then spun-down over the course of 60 s. The shorter duration of the centrifuge deceleration was related to the capabilities of the MIT centrifuge motor. Subjects reported no symptoms of motion sickness during the spin-up or spin-down process, or any other phase of the protocol, with the full motion sickness and comfort data being available elsewhere (Diaz et al., 2015b). Completion of the spin-up, transient wait, exercise period, recovery wait, and spin-down took less than 25 min.

Each exercise period lasted 15 min, and it included three exercise intensities and transitions between them. The work rates tested were: 25 W ("warm-up" intensity during 3 min), 50 W ("low" intensity during 5 min), and 100 W ("high" intensity during 5 min). The exercise work rates were selected to provide a broad range of cardiovascular responses and were based on preliminary data. Changes between workload levels were implemented linearly and smoothly, as indicated in **Figure 2**, to avoid potential injuries. The exercise protocol was created using the Lode Ergometer Manager, Version 9.4.4 (LEM, 2013, Groningen, Netherlands) software package provided with the ergometer. It ran automatically without any intervention from the subject or the operator. In order to avoid confounding factors, subjects were instructed to keep a constant pedal cadence of 60 rpm that was maintained using a metronome. The pedal cadence was also important for the development and validation of a cardiovascular model associated to this investigation and to be reported in separate publications (Diaz Artiles et al., 2016).

Subjects and Study Approval

Twelve healthy subjects (6 males, 6 females) between 23 and 29 years old participated in the study. Given the important changes of the cardiovascular system with age, the age range of selected subjects was limited as much as possible to avoid age-related confounding factors. Average (±standard deviation) age and weight were 25.1 ± 2.1 years, and 69.3 ± 11.6 kg, respectively. Selected subjects exercised regularly and were comfortable engaging in continuous aerobic exercise for at least 1 h. Prior to participating in the study, subjects were asked to complete a questionnaire designed to identify exclusion criteria such as recent musculoskeletal injuries, joint or muscle pain, and cardiovascular defects or conditions. All subjects were able to complete the protocols and experienced no adverse effects. The study protocol was approved by the Committee on the Use of Humans as Experimental Subjects at MIT. Each subject received written and verbal explanations of the study protocols and gave written informed consent to participate in the experiment.

Data Analysis and Statistics

Before analysis, raw cardiovascular signals were filtered using a low-pass Butterworth filter (cut-off frequency between 2 and 8 Hz), both in forward and reverse directions to compensate for phase delays. Additionally, data segments presenting motion artifacts were eliminated from the dataset and not included in the analysis.

Each of the cardiovascular variables was averaged over the last 2 min of each protocol phase. Thus, at each AG level, five values were calculated for each CV variable, per subject, corresponding to the baseline period (BL), and workload intensities of 0 W (centrifugation but no exercise), 25, 50, and 100 W. To study the effects of centrifugation alone (i.e., without exercise), paired, two-sided *t*-tests were used to compare the CV variables at BL with centrifugation (0 W). Since three AG conditions were tested, we implemented a Bonferroni correction for comparisons of multiple groups and used $\alpha = 0.05/3 = 0.017$ to determine statistical significance. To study the effects of centrifugation combined with exercise, a two-way repeated-measures ANOVA was implemented using AG level (0, 1, and 1.4 G) and workload intensity (0, 25, 50, and 100 W) as fixed, within-subjects factors; and gender as a between-subjects factor. All the necessary data assumptions were checked and the Greenhouse–Geisser correction was applied when the data violated the assumption of sphericity (Abdi, 2010). Most of the ANOVAs resulted in significant interaction effects (CO, SV, HR, MBP, and DBP), and therefore the "simple main effects" (difference between groups at each level of each factor; for example the difference between AG levels at 100 W) are also calculated for all variables. The Bonferroni correction for multiple comparisons of the various subgroups was also incorporated in this analysis.

To further quantify and model the effects of AG and exercise work rate (WR) on the cardiovascular variables, we used the following mixed hierarchical regressions to generate dose-response curves between 0 and 1.4 G:

$$(\text{CV Variable})_{ij} = \rho_i + \beta_1(AG^2) + \beta_2(AG) + \beta_3(WR^2) + \beta_4(WR) + \beta_5(AG^*WR) + \varepsilon_{ij} \quad (1)$$

where the measured cardiovascular variable (CV Variable) from the j^{th} measurement combination (3 AG × 4 WR levels: j = 1–12) in the i^{th} subject is a function of the AG term (0, 1, or 1.4 G), the workload intensity (0, 25, 50, or 100 W), and the interaction term (AG * WR). The regression model has subject-dependent intercepts (i.e., biases; ρ_i, where i = 1–12 subjects). In a first step, the subjects' random effects were estimated (ρ_i), accounting for the within-subject experimental design. In the second step, the CV Variable being analyzed was regressed on the rest of the terms. We tested model assumptions, including normality of the error distribution (ε_{ij}) and homogeneity of variances. Statistical tests were performed using SYSTAT 13 Version 13.00.05 (SYSTAT Software Inc. 2009, San Jose, CA, United States).

RESULTS

Continuous recordings from the cardiovascular variables gathered during the centrifuge runs are shown in **Figure 3**. Each graph contains three cardiovascular responses for the 12 subjects (mean ± SE) corresponding to the three AG level experienced (0, 1, and 1.4 G). In addition, the spin-up phase (starting at Time = 3 min) and spin-down phase (starting at Time = 23:45 min), as well as the exercise phase (from Time = 6:45 min to Time = 21:45 min) are also indicated in all figures. Calculated averages (mean ± SE, including all 12 subjects) for the eight cardiovascular variables collected in each AG condition are summarized in **Table 1**.

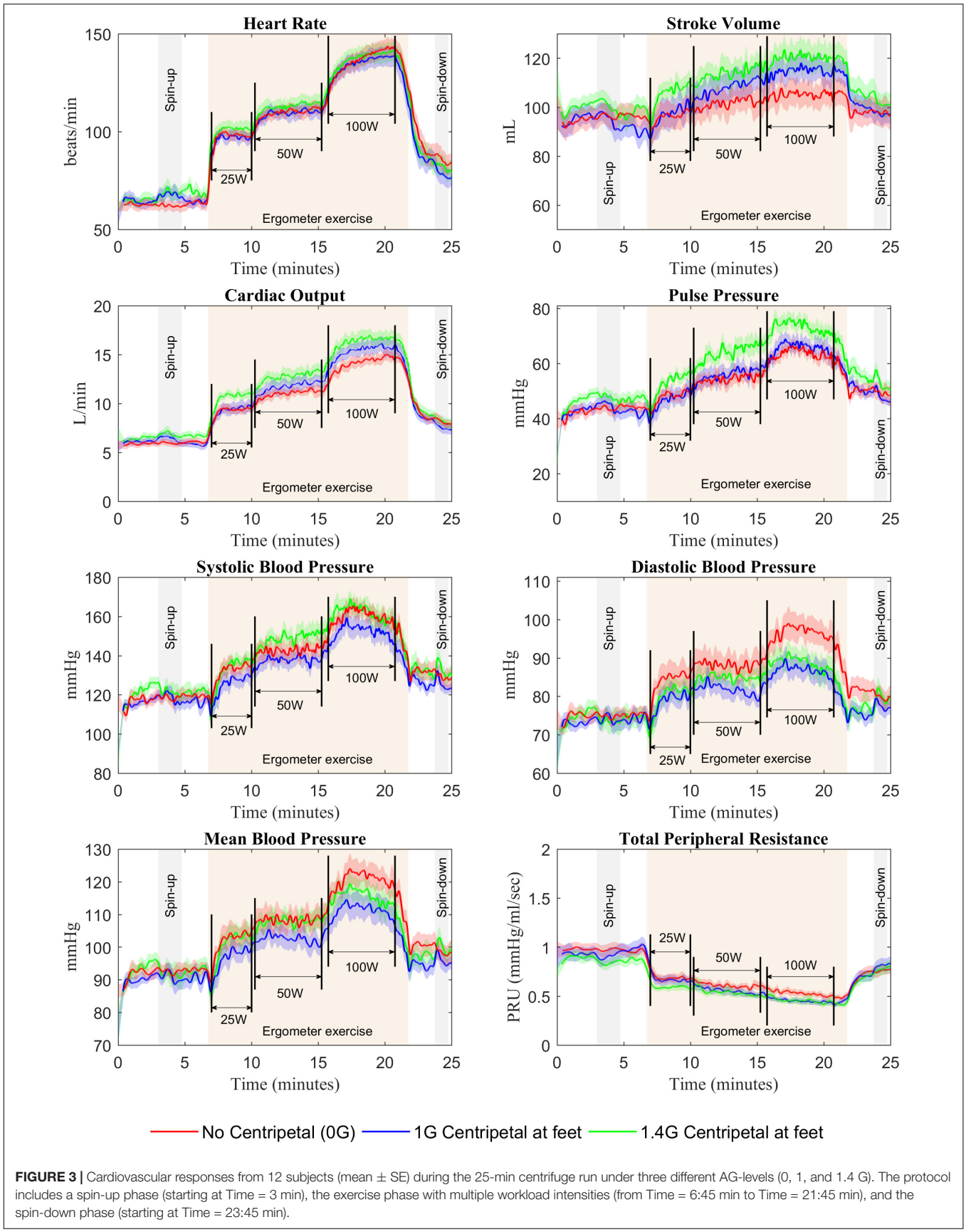

FIGURE 3 | Cardiovascular responses from 12 subjects (mean ± SE) during the 25-min centrifuge run under three different AG-levels (0, 1, and 1.4 G). The protocol includes a spin-up phase (starting at Time = 3 min), the exercise phase with multiple workload intensities (from Time = 6:45 min to Time = 21:45 min), and the spin-down phase (starting at Time = 23:45 min).

TABLE 1 | Calculated averages [mean (SE), including all 12 subjects] during each protocol phase for the 8 CV variables recorded during the centrifuge runs.

AG	Phase	HR (bpm)	SV (mL)	CO (L/min)	PP (mmHg)	SBP (mmHg)	DBP (mmHg)	MAP (mmHg)	TPR (PRU)
0G	BL	62.6 (2.8)	94.8 (4.4)	5.9 (0.3)	42.7 (2.1)	118.0 (3.2)	75.3 (1.8)	92.7 (2.1)	0.98 (0.06)
	0 W	63.5^{b,c,d} (3.0)	96.5 (4.3)	6.1^{b,c,d} (0.3)	44.3^{c,d} (2.1)	119.6^{b,c,d} (3.1)	75.3^{b,c,d} (1.7)	93.1^{b,c,d} (2.2)	0.96^{b,c,d} (0.06)
	25 W	98.1^{a,c,d} (2.7)	97.1^{§,c} (5.3)	9.4^{§,a,c,d} (0.4)	49.0^{c,d} (1.9)	134.3^{a,c,d} (3.8)	85.3^{a,d} (3.4)	103.6^{a,c,d} (3.4)	0.68^{a,c,d} (0.04)
	50 W	111.0^{a,b,d} (3.4)	102.8^{§,b} (5.2)	11.3^{§,a,b,d} (0.5)	55.4^{a,b,d} (2.6)	143.2^{a,b,d} (4.6)	87.9^{a,d} (3.2)	108.3^{a,b,d} (3.4)	0.59^{a,b,d} (0.04)
	100 W	141.6^{‡,a,b,c} (4.8)	102.7§ (5.2)	14.3^{§,a,b,c} (0.5)	62.0^{a,b,c} (1.9)	159.0^{a,b,c} (3.9)	97.0^{‡,§,a,b,c} (3.4)	121.1^{‡,a,b,c} (3.6)	0.52^{a,b,c} (0.03)
1G	BL	64.1 (2.6)	96.2 (4.0)	6.1 (0.3)	43.4 (2.0)	116.6 (1.9)	73.2 (1.2)	90.4 (1.4)	0.93 (0.07)
	0 W	64.5^{§,b,c,d} (2.7)	91.0^{c,d} (4.5)	5.8^{§,b,c,d} (0.4)	42.4^{c,d} (2.6)	116.5^{b,c,d} (3.4)	74.2^{b,c,d} (2.0)	90.5^{b,c,d} (2.4)	0.98^{b,c,d} (0.07)
	25 W	97.0^{§,a,c,d} (3.0)	98.8^{c,d} (6.0)	9.5^{§,a,c,d} (0.6)	48.2^{c,d} (3.1)	128.1^{a,c,d} (3.9)	80.0^{a} (2.5)	98.6^{a,d} (3.0)	0.66^{a,c,d} (0.05)
	50 W	110.3^{§,a,b,d} (3.6)	110.5^{a,b} (5.5)	12.1^{a,b,d} (0.7)	57.4^{a,b,d} (2.8)	138.1^{a,b,d} (4.1)	80.7^{a,d} (2.1)	101.8^{a,d} (3.1)	0.53^{a,b,d} (0.04)
	100 W	138.1^{†,a,b,c} (5.1)	114.8^{a,b} (5.0)	15.8^{a,b,c} (0.8)	65.0^{a,b,c} (2.9)	151.0^{a,b,c} (5.0)	86.0^{†,a,c} (2.8)	110.7^{†,a,b,c} (3.7)	0.44^{a,b,c} (0.03)
1.4G	BL	64.9 (2.9)	101.0 (3.4)	6.5 (0.3)	47.6 (1.7)	123.4 (2.8)	75.8 (1.9)	94.4 (2.1)	0.90 (0.05)
	0 W	69.3^{*,‡,b,c,d} (3.4)	98.2^{b,c,d} (4.1)	6.7^{‡,b,c,d} (0.4)	47.2^{b,c,d} (2.2)	121.7^{b,c,d} (3.4)	74.5^{b,c,d} (2.5)	92.8^{b,c,d} (2.8)	0.86^{b,c,d} (0.05)
	25 W	101.6^{‡,a,c,d} (3.7)	107.9^{†,a,c,d} (4.1)	10.9^{†,‡,a,c,d} (0.4)	54.9^{a,c,d} (1.8)	136.6^{a,c,d} (3.3)	81.7^{a} (2.7)	103.2^{a} (3.2)	0.59^{a,c,d} (0.04)
	50 W	114.4^{‡,a,b,d} (4.1)	115.5^{†,a,b} (5.1)	13.2^{†,a,b,d} (0.6)	66.3^{a,b} (3.2)	151.0^{a,b} (4.8)	84.7^{a} (2.2)	108.1^{a} (3.0)	0.52^{a,b,d} (0.03)
	100 W	140.2^{a,b,c} (5.0)	120.3^{†,a,b} (5.9)	16.7^{†,a,b,c} (0.7)	71.5^{a,b} (3.0)	158.7^{a,b} (5.7)	87.2^{†,a} (3.2)	113.8^{a} (4.2)	0.44^{a,b,c} (0.04)

Cardiovascular variables: HR, heart rate (beats per minute); SV, stroke volume (mL); CO, cardiac output (L/min); PP, pulse pressure (mmHg); SBP, systolic blood pressure (mmHg); DBP, diastolic blood pressure (mmHg); MAP, mean arterial pressure (mmHg); TPR, total peripheral resistance (Peripheral Resistance Units, PRU = mmHg/mL/s). Protocol phases: BL, baseline (no exercise or AG); 0 W, centrifugation alone; 25 W, exercise at 25 W and AG; 50 W, exercise at 50 W and AG; 100 W, exercise at 100 W and AG.

Values are means (SE).

**Different from baseline (paired sample t-test with Bonferroni correction alpha = 0.05/3 = 0.017).*

†Different from 0 G; ‡Different from 1 G, § Different from 1.4 G, all within the same workload levels. (Simple main effects from two-way repeated measures ANOVA with Bonferroni correction).

[a]Different from 0 W; [b]Different from 25 W, [c]Different from 50 W, [d]Different from 100 W, all within the same AG level. (Simple main effects from two-way repeated measures ANOVA with Bonferroni correction).

Centrifugation Alone

A paired, two-sided *t*-test revealed a significant difference in HR between BL and centrifugation alone (0 W) at 1.4 G condition. At this AG level, HR increased by 6.8%, from 64.9 bpm at baseline to 69.3 bpm during centrifugation, and this increase was statistically significant [$t(11) = 2.833$, $P = 0.016$]. Further testing did not reveal significant differences between other averaged values at BL and centrifugation alone (0 W) for any of the AG conditions. Despite the absence of additional statistical significance, transient cardiovascular changes showed the expected tendencies in response to gravitational stress. For example, SV in 1 and 1.4 G conditions (**Figure 3**) decreased when starting the centrifugation phase (from 97.4 to 90.4 mL at 1 G and from 102.6 to 94.9 mL at 1.4 G), and HR increased (from 63.1 to 69.2 bpm at 1 G and from 63.5 to 73.1 bpm at 1.4 G) as well as TPR (from 0.87 PRU to 1.03 PRU at 1 G and from 0.81 PRU to 0.89 PRU at 1.4 G) as compensatory mechanisms to maintain homeostasis. As expected, no changes were observed in the 0 G condition, since subjects were not being centrifuged. We confirmed that, for each CV variable, all three baselines (0, 1, and 1.4 G) were not statistically different from each other using a one-way repeated-measures ANOVA (for all CV variables: $p > 0.05$).

Centrifugation and Exercise

Two-way repeated-measures ANOVAs were conducted to examine the effects of AG level and workload intensity on cardiovascular responses. There were statistically significant effects of AG level on PP [$F(2,22) = 4.147$, $P = 0.03$], and of workload intensity on PP [$F(1.578,17.353) = 53.697$, $P < 0.0005$], SBP [$F(1.402,15.419) = 54.729$, $P < 0.0005$], and TPR [$F(1.465,16.111) = 160.995$, $P < 0.0005$]. In these variables the interaction terms were not statistically significant. However, there was a statistically significant interaction between AG level and workload intensity on the rest of the cardiovascular variables: CO [$F(3.037,33.408) = 4.949$, $P = 0.006$], SV [$F(6,66) = 7.867$, $P < 0.0005$], HR [$F(6,66) = 5.183$, $P < 0.0005$], MBP [$F(6,66) = 2.375$, $P = 0.039$], and DBP [$F(6,66) = 4.561$, $P = 0.001$]. Therefore, for these (and also the rest) CV variables the simple main effects were calculated, and statistical results are summarized in **Table 1** and **Figure 4**. Results from this analysis show that increasing AG level from 0 to 1.4 G significantly increases SV and CO when doing ergometer exercise at 25 W (SV: $P = 0.044$; CO: $P = 0.016$), 50 W (SV: $P = 0.029$; CO: $P = 0.017$) and 100 W (SV: $P = 0.003$; CO: $P = 0.005$). CO also increased from 1 to 1.4 G at 0 W ($P = 0.004$) and at 25 W ($P = 0.015$). Statistical analysis also revealed a significant increase in HR from 1 to 1.4 G at 0 W ($P = 0.007$), 25 W ($P = 0.016$), and 50 W ($P = 0.018$), as well as a decrease from 0 to 1 G when exercising at 100 W ($P = 0.005$). Finally, statistically significant changes in blood pressure also occurred when exercising at 100 W between 0 and 1 G (MAP: $P = 0.029$; DBP: $P = 0.016$), and between 0 and 1.4 G at 100 W (DBP: $P = 0.039$). No statistically significant simple main effects of AG-level were found on SBP, PP, or TPR. Concerning workload intensity, simple main effects were found to be statistically significant in all CV variables in almost all group combinations (see **Table 1**).

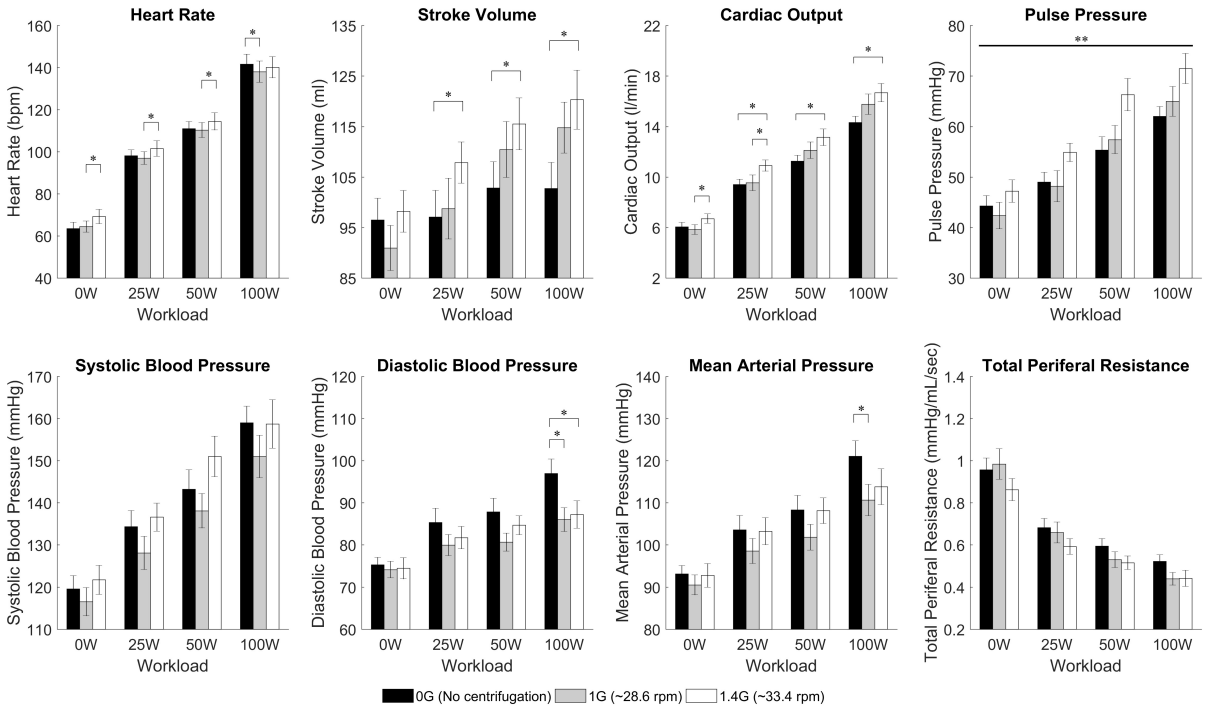

FIGURE 4 | Cardiovascular data from 12 subjects (mean ± SE) by AG-level (0 G, 1 G, and 1.4 G) and workload intensity (0 W, 25 W, 50 W, and 100 W). The figure highlights significant differences between AG-levels within the same workload intensity in HR, SV, CO, DBP, and MAP (simple main effects from 2-factor repeated measures ANOVA with Bonferroni correction, *significantly different at $p < 0.05$). Our analysis also showed a statistically significant overall effect of AG-level on PP (main effects two-way repeated-measures ANOVA, **significantly different at $p < 0.05$) but the simple main effects did not yield a significant result. For clarity, significant differences between work rates have not been included.

Dose-Response Curves

The results of the regression model (Equation 1) applied to the averaged cardiovascular data are given in **Table 2**. Only the significant β coefficients were included in the regression models ($P < 0.05$), and further interaction terms (not shown) were not significant. This specific regression analysis shows that AG level contributes to changes in all CV variables, either directly (β_1 and β_2) and/or through the interaction term (β_5). Specifically, we found statistically significant quadratic relationships between AG level and all CV variables, which could be an indication of the non-linear nature of short-radius centrifugation. Results show that CO, SV, and PP generally increase with AG, especially between 1 and 1.4 G. HR increases with AG level at 0 W but this AG effect seems to disappear at higher work rates. Workload intensity has a significant effect on all variables. The positive β_4 coefficients for PP, SV, CO, MAP, SYS, DIA, and HR indicate that these variables increase with workload intensity, and the negative β_3 coefficient for PP, SV, CO, SYS, DIA, and HR indicates a limitation of this increase at higher work rates. Likewise, the negative β_4 coefficient for TPR indicates that TPR decreases with increasing workload intensity; the positive β_3 coefficient indicates that this reduction is less important at higher work rates. The interaction term was found significant and positive for CO ($\beta_5 > 0$), and significant and negative for HR and DBP ($\beta_5 < 0$). Experimental data and the statistical models fitted to the data are shown in **Figure 5**.

Gender Differences

While the study was not specifically designed to study gender differences, we conducted an exploratory analysis to determine if there was significant differences between genders. We found significant differences during centrifugation between males and females (between-subjects effect of repeated measures ANOVA) in two CV variables: SV ($p < 0.0005$), and PP ($p = 0.006$). We also compared baseline measurements between both genders (two-tailed, two sample *t*-test) and found significant differences in SV ($p < 0.0005$), CO ($p = 0.018$), PP ($p = 0.025$), and SBP ($p = 0.022$). Male and females cardiovascular data at baseline and during centrifugation are shown in **Table 3** and **Figure 6**.

DISCUSSION

Artificial gravity combined with exercise is a promising countermeasure to mitigate human deconditioning in space, particularly during future long duration spaceflight missions beyond Low-Earth Orbit. The use of a compact-radius centrifuge on-board might present an affordable approach to generate gravity in space. However, many questions still remain unanswered regarding the appropriate configuration, parameters, and exercise protocols to keep astronauts in a healthy physiological state. We implemented a comprehensive experimental study on human physiology during ergometer

TABLE 2 | Regression analysis coefficient for all cardiovascular variables based on the following equation:

$$(\text{CV Variable})_{ij} = \rho_i + \beta_1(AG^2) + \beta_2(AG) + \beta_3(WR^2) + \beta_4(WR) + \beta_5(AG^*WR) + \varepsilon_{ij}.$$

	ρ_i	β_1	β_2	β_3	β_4	β_5
HR (bpm)	64.3 (bpm)	3.23 (bpm/g^2)	NS	$-4.76\ 10^{-3}$ (bpm/W^2)	1.24 (bpm/W)	−0.058 (bpm/Wg)
SV (mL)	89.3 (mL)	5.45 (mL/g^2)	NS	$-1.89\ 10^{-3}$ (mL/W^2)	0.37 (mL/W)	NS
CO (L/min)	6.0 (L/min)	1.47 (L/min/g^2)	−1.47 (L/min/g)	$-5.77\ 10^{-3}$ (L/min/W^2)	0.14 (L/min/W)	0.013 (L/min/Wg)
PP (mmHg)	41.4 (mmHg)	11.62 (mmHg/g^2)	−11.05 (mmHg/g)	$-1.35\ 10^{-3}$ (mmHg/W^2)	0.36 (mmHg/W)	NS
SBP (mmHg)	120.1 (mmHg)	19.30 (mmHg/g^2)	−24.91 (mmHg/g)	$-2.51\ 10^{-3}$ (mmHg/W^2)	0.62 (mmHg/W)	NS
DBP (mmHg)	76.3 (mmHg)	7.66 (mmHg/g^2)	−10.91 (mmHg/g)	$-1.15\ 10^{-3}$ (mmHg/W^2)	0.32 (mmHg/W)	−0.067 (L/min/Wg)
MAP (mmHg)	96.9 (mmHg)	11.69 (mmHg/g^2)	−17.83 (mmHg/g)	NS	0.22 (mmHg/W)	NS
TPR (PRU)	0.97 (PRU)	$-43.92\ 10^{-3}$ (PRU/g^2)	NS	$0.07\ 10^{-3}$ (PRU/W^2)	$-11.503\ 10^{-3}$ (PRU/W)	NS

*AG, artificial gravity level; WR, work rate. Only the significant parameters ($p < 0.05$) were included in the regression. A graphical representation of these results is shown in **Figure 5**. NS, non-significant.*

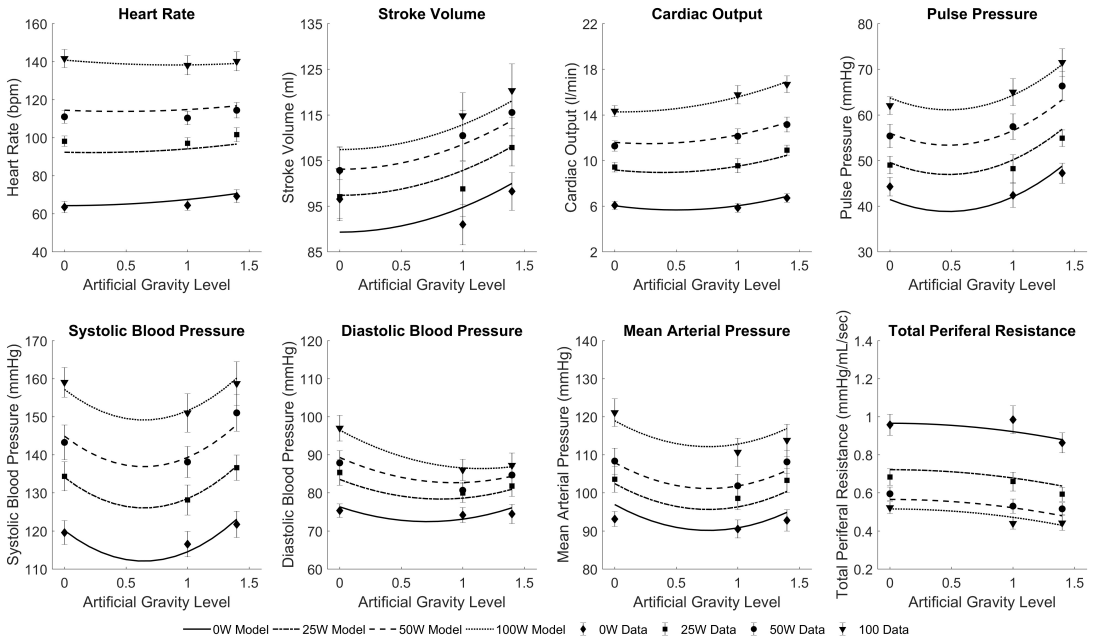

FIGURE 5 | Statistically significant mixed regression models fitted to the cardiovascular experimental data across all conditions: three AG-levels (0 G, 1 G, and 1.4 G) and four workload intensities (0 W, 25 W, 50 W, and 100 W). Symbols and error bars correspond to experimental data from 12 subjects (mean ± SE) in each condition.

exercise using a new configuration of the MIT compact-radius centrifuge, which experienced several modifications in order to be compatible with a future use in the ISS. This experiment contributed to the identification and quantitative characterization of the short-term cardiovascular response to different AG levels and exercise workload intensities. To our knowledge, this is the first experiment that covered multiple exercise and AG levels, including a reference point with no AG.

The amplitude of the cardiovascular responses adapted to the stress level generated, not only by the exercise intensity, but also by the AG level to which the subjects were exposed while exercising. We did find a statistically significant effect of AG-level on PP (main effects two-way ANOVA), which seems to be driven by the reduction in DBP at higher gravitational levels. The average increase across exercise conditions of PP per unit of AG was 5.22 mmHg/g. Additionally, based on the simple main effect and subsequent regression analyses, CO, SV, and HR

TABLE 3 | Cardiovascular variables [mean (SE), 6 females and 6 males] at baseline and during centrifugation separated by gender.

	Gender	Baseline	Gender effect at baseline	0 G	1 G	1.4 G	Gender effect during centrifugation
HR (bpm)	Females	65.6 (2.5)	$p = 0.274$	108.5 (13.6)	107.0 (13.2)	111.0 (13.1)	$p = 0.179$
	Males	62.1 (1.9)		98.6 (11.3)	98.0 (10.7)	101.7 (10.6)	
SV (mL)	Females	88.0 (2.7)	$p < 0.0005$	87.4 (4.2)	90.7 (7.4)	98.6 (6.1)	$p < 0.0005$
	Males	106.6 (1.9)		112.2 (5.3)	116.8 (4.9)	122.3 (5.3)	
CO (L/min)	Females	5.7 (0.3)	$p = 0.018$	9.5 (1.3)	10.0 (1.8)	11.1 (1.6)	$p = 0.067$
	Males	6.6 (0.2)		11.1 (1.4)	11.7 (1.6)	12.7 (1.7)	
PP (mmHg)	Females	42.1 (1.6)	$p = 0.025$	48.4 (4.2)	49.2 (5.9)	58.7 (6.0)	$p = 0.006$
	Males	47.1 (1.4)		56.9 (3.0)	57.3 (4.1)	61.2 (4.5)	
SBP (mmHg)	Females	115.8 (1.9)	$p = 0.022$	132.5 (7.5)	129.4 (7.9)	141.7 (8.7)	$p = 0.078$
	Males	122.9 (2.3)		145.6 (7.6)	137.4 (7.3)	142.3 (8.3)	
DBP (mmHg)	Females	73.7 (0.8)	$p = 0.280$	84.1 (3.9)	80.3 (2.7)	83.0 (3.2)	$p = 0.810$
	Males	75.8 (1.8)		88.7 (6.2)	80.1 (4.5)	81.1 (5.0)	
MAP (mmHg)	Females	91.6 (1.1)	$p = 0.448$	104.0 (5.2)	100.5 (4.7)	106.4 (4.9)	$p = 0.932$
	Males	93.3 (1.9)		109.0 (6.7)	100.3 (5.7)	102.6 (6.2)	
TPR (PRU)	Females	1.0 (0.05)	$p = 0.061$	0.73 (0.09)	0.72 (0.12)	0.66 (0.09)	$p = 0.116$
	Males	0.9 (0.04)		0.65 (0.09)	0.59 (0.09)	0.55 (0.08)	

Female and male data were compared at baseline (two-tailed, two sample t-test) and during centrifugation (between-subjects effects from repeated-measures ANOVA). Results show significant differences in SV, CO, PP, and SBP at baseline and in SV and PP during centrifugation.

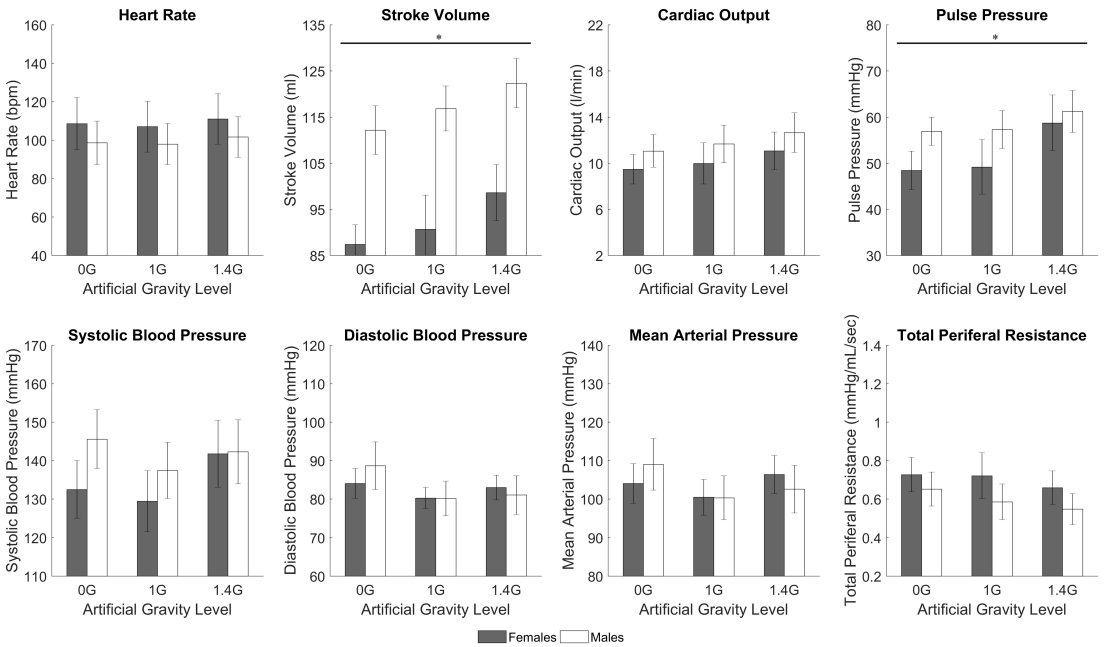

FIGURE 6 | Male and female cardiovascular variables (mean ± SE) during the centrifugation runs, shown at each AG-level across all workload intensity conditions. There was a statistically significant gender effect (between-subjects effect of repeated measures ANOVA, *significantly different at $p < 0.05$) in SV ($p < 0.0005$) and PP ($p = 0.006$). Trends are also present in other variables, namely HR, CO, and TPR.

also increased with AG-level, showing an averaged increment across exercise conditions of 1.4 L/min/g, 7.6 mL/g, 2.0 bpm/g, respectively. Thus, if we consider total blood circulation (in L) an overall index of cardiovascular stress after exercise of a certain duration and intensity, the addition of centrifugation reduces the amount of exercise needed to achieve a similar degree of cardiovascular stress due to exercise alone. For example, a regular 30-min exercise with an average CO of 10 L/min generates a total blood circulation of 300 L. Our results suggest that adding centrifugation at 1 G (which increases CO to ∼11.4 L/min) reduces the exercise length an average of 12.3% to achieve the same amount of total blood circulation. Likewise, the exercise protocol is reduced an average of 16.5% when centrifugation at 1.4 G is superposed to exercise. In a similar manner, the

addition of centrifugation could increase the overall index of cardiovascular stress during a specific exercise protocol of a fixed duration. Thus, superposing 1 and 1.4 G to a 30-min exercise protocol increases the total blood circulation in 14% and 19.6% respectively. While the cardiovascular index used does not capture all the complex physiological mechanisms occurring during exercise, it provides a high-level, quantitative "score" of overall cardiovascular activity, and our results suggest that centrifugation combined with exercise increases this activity with respect to exercise alone. We believe that the addition of AG during exercise protocols could be beneficial during spaceflight, providing additional stress to the cardiovascular system and/or reducing the amount of exercise currently executed during space missions.

The expected cardiovascular dynamics induced by the immediate exposure to AG are well captured during the spin-up phase. Similar to standing up in Earth's gravity, the application of AG introduces a new stress condition that the cardiovascular system needs to overcome in order to assure the appropriate amount of blood flow to all parts of the body. We expect that the orthostatic stress introduced with centrifugation will cause multiple responses in the cardiovascular system. One of the consequences of applying a gravitational stress (applied in the head-to-toe direction) to the human body is blood pooling in the veins of the lower part of the body, which can cause an important, rapid, and transient decrease in blood pressure, particularly if the gravity stress is introduced in a suddenly manner. When there is a significant blood pressure drop, the autonomic nervous system inhibits parasympathetic activity and increases sympathetic stimulation triggered principally by the arterial baroreceptors in the carotid sinus and the aortic arch areas, which are the primary receptors for short-term control of the cardiovascular system. An increase in heart rate and contractility of the heart as well as an increase in TPR (amongst other mechanisms) will act to maintain the appropriate amount of blood flow to all the organs, in particular the brain.

In our experiment, subjects were exposed gently (over 120 s) to two different levels of AG. Our heart rate data showed an increase during the spin-up phase, and this response was more prominent, sustained, and statistically significant in the 1.4 G condition, presumably due to the cardiovascular response to a higher AG environment. Our experimental data also captured the expected dynamics of the vascular resistance: an initial decrease at the beginning of the spin-up process when first exposed to a new gravitational environment, followed by a relatively constant increase due to the sympathetic component of the cardiovascular control system. As a result of these control actions, other cardiovascular variables such as blood pressure, PP, SV, and CO showed only small changes during this phase. This is consistent with previous short-radius centrifugation studies where subjects did not show differences in pressure numerics (MAP, SBP, DBP), between baseline in supine position, 1 G, or 2 G (measured at the feet) (Goswami et al., 2015a; Verma et al., 2018). With the exception of the gravity gradient, which is particularly pronounced during short-radius centrifugation, this follows the same overall cardiovascular mechanisms and responses that someone on Earth experiences when changing from supine to upright position.

Overall, we did not find significant changes in the averaged values in any of the CV variables between BL and centrifugation alone (except HR at 1.4 G), most likely due to a combination of the specific subjects' positioning, the muscle-pump effect, the strong gravity gradient, and the relatively low gravity levels implemented in this experiment. The subjects' head was located at the center of rotation and the gravity level was measured at the feet. Cardiovascular sensors, in particular the baroreceptors, are located in the upper part of the body, and therefore, they were not exposed to gravitational changes as large as the feet or, in general, the lower part of the body. In the 1.4 G condition (i.e., the gravity level at the feet was 1.4 G), the AG level at the baroreceptors was 0.32 G (assuming that these are located at 25 cm from the center of rotation). Similarly, when the feet were exposed to 1 G, the baroreceptors were subjected to just 0.23 G. However, our data did show the expected trend according to the cardiovascular regulation mechanisms and suggest that higher AG-levels (i.e., higher rotation rates AND/OR larger radii) should be investigated in future experiments. Our results are consistent with a previous short-radius centrifugation study where CV responses were not different from baseline (supine) when subjects were subjected to 0.39 G at the heart (equivalent to 1 g at the feet) whereas 0.75 G at the heart (equivalent to 2 g at the feet) provided similar CV reflexes to standing, inducing a significantly higher HR and a significantly lower SV (Goswami et al., 2015a). Limitations in our centrifuge only allowed us to investigate a maximal AG-level of 1.4 G and thus, we did not find the same degree of significance in CV responses than previous studies conducted at 2 G. However, our data show the expected trends and are always consistent with existing results.

Exercise stresses the cardiovascular system and important physiological changes occur. During intense exercise, CO can increase to six or seven times the normal values (Guyton, 1990). Muscle activation increases venous return and therefore mean systemic pressure. Autonomic stimulation increases heart rate and heart contractility. As a consequence, CO also increases to meet the new metabolic demands imposed by the exercise activity. In addition, the higher muscle metabolism causes vasodilatation, and total peripheral resistance decreases to meet the metabolic demand. These cardiovascular changes due to exercise and work rate transitions were observed across all CV variables, and simple main effects analysis showed a statistically significant effect of work rate in all CV variables between most of all group combinations. Averaged changes across AG conditions were: 0.09 L/min/W (CO), 0.17 mL/W (SV), 0.22 mmHg/W (PP), 0.74 bpm/W (HR), 0.34 mmHg/W (MAP), 0.37 mmHg/W (SYS), 0.15 mmHg/W (DIA), and −0.005 PRU/W (TPR).

Exercise increases muscle metabolism and, even though the level of sympathetic stimulation is high, vascular smooth muscle in the exercise muscles dilates to satisfy the increasing local metabolic demands (functional hyperemia). According to this mechanism, in this experiment the vascular resistance decreased during the exercise protocol. In particular, significant reductions can be observed in the 1.4 G condition at the beginning of the 25 and 50 W exercise phases. After these initial reductions, the

resistance seemed to level-off, presumably due to an increase in sympathetic activity, reaching an equilibrium state between two competing mechanisms: dilation due to functional hyperemia, and contraction due to sympathetic activity. Results from the regression fit showed that vascular resistance decreases with AG level, which could be explained by the more important "internal" metabolic demand of exercising muscles at higher AG levels (Bonjour et al., 2010). Bonjour and his colleagues demonstrated that the internal metabolic power during cycling, which includes all sources of metabolic energy other than the external mechanical power, is directly proportional to gravity acceleration (Bonjour et al., 2010). In our experiment, the external mechanical power was fixed (i.e., 25, 50, 100 W), but changes in the total metabolic demand could be possible due to changes in the gravitational environment. The exact nature of those changes in the presence of a gravity gradient requires further investigation, but our results are consistent with the study mentioned above. During the exercise phase at 100 W, the vascular resistances at 1 and 1.4 G seemed to overlap and level off, probably indicating that maximal muscle dilation has been reached.

A number of short-radius centrifugation studies have been reported in which subjects were conducting ergometer exercise while being exposed to AG (Iwase et al., 2002; Evans et al., 2004; Iwasaki et al., 2005; Iwase, 2005; Stenger et al., 2007; Yang et al., 2010; Wang et al., 2011). These studies mainly focused on physiological responses before and after exposure to a specific experimental intervention (typically −6 degrees head-down bed rest, or 1–3 weeks of training) with and/or without exposure to AG + ergometer exercise. Thus, data from subjects *during* centrifugation are scarce and current data do not provide a suitable basis for comparison with our own results.

Although we do not know the exact form of the dose-response relationships between the cardiovascular variables as a function of AG level or exercise intensity, we were able to fit statistically significant linear regressions to our experimental data (**Table 2**). To our knowledge, this is the first time that cardiovascular data have been collected during short-radius centrifugation in such a large number of conditions (3 AG-levels and 4 exercise intensities) in a rigorous and systematic way, with the same set of subjects. Thus, our dataset is unique and constitutes a good starting point to investigate gravitational dose-responses on a centrifuge. When necessary, we used the Bayesian Information Criterion (BIC) to select between multiple model options, which could include more or less parameters from Equation 1. The BIC is a criterion for model selection among a finite set of models and it not only reward a better fitting but also penalizes when adding free parameters, since this could result in overfitting the data (Schwarz, 1978). Thus, each model option has a BIC associated, and the model with a lower BIC is preferred, which implies either fewer explanatory variables, better fit, or both. As an example and based on this criterion, we included a (WR^2) term (i.e., $\beta_3 \neq 0$) in most of the models since this term provided a better explanation of the data even with the penalization related to the addition of an extra parameter (i.e., lower BIC). We decided to use linear models due to the small sample size (3 observations per exercise intensity), and these results should be enriched with additional data to be gathered in future experiments in order to improve the accuracy and goodness of fit of the models, especially if used for prediction purposes at higher G-levels. For example, blood pressure data (particularly SBP, but also MAP and, to a certain extent, DBP) might indicate a more complex curve fitting to capture what appears to be a systematic reduction in pressure at 1 G followed by an increase at 1.4 G (**Figure 5**). This pattern is harder to interpret, but we can mention several factors that could contribute to explain this behavior. First, higher AG levels generate higher sympathetic activity to counteract the gravitational stress and maintain blood pressure at appropriate levels. Additionally, the muscle pump effect during ergometer exercise is theoretically more important at higher AG levels, further facilitating the return of blood to the heart in the 1.4 G condition. This hypothesis is supported by both the larger reduction in vascular resistance (indicating a more important metabolic demand of the exercising muscles) and the higher foot forces exerted on the ergometer in the 1.4 G condition (Diaz et al., 2015b) (presumably indicating a stronger muscle pump effect). Therefore, despite the stronger blood pooling in the lower body at higher AG levels, this exercise effect, combined with the higher sympathetic activity, could contribute to explaining the higher blood pressure values in the 1.4 G condition.

Our sample size is small to conduct a comprehensive study on gender effects. However, we conducted an exploratory analysis and we found gender differences in cardiovascular responses to centrifugation. Specifically, females showed smaller SV and PP than men across all levels of centrifugation and work rates. Although not significant, we also observed trends indicating that females presented larger HR and lower CO, and larger changes in HR with respect to baseline. Females also presented lower SV, CO, PP, and SBP at baseline. This is consistent with previous studies reporting gender specific patterns in cardiovascular responses to AG (Evans et al., 2018; Masatli et al., 2018). Under orthostatic stress, women typically show higher HR and lower SV (Goswami et al., 2015a; Evans et al., 2018), and they present higher incidence of orthostatic intolerance compared to men (Platts et al., 2014). Additional studies on gender effects to AG with larger number of subjects are warranted.

The Nexfin monitor measures the arterial blood pressure waveform from which it derives beat-to-beat cardiovascular parameters, such as SV, CO, and TPR, using a set of assumptions and population-based reference values, including age-related changes in the aortic pressure-area relationship (Wesseling et al., 1993, 1995; Bogert and van Lieshout, 2005; Westerhof et al., 2009; Truijen et al., 2012). A variety of studies has been conducted to evaluate the use of non-invasive devices such as Nexfin to monitor CV responses under different conditions. Cardiovascular measurements derived from the Nexfin algorithm [based on the Modelflow algorithm (Truijen et al., 2012)] showed good correlation with standard methods including traditional blood pressure measurements (e.g., Riva-Rocci/Korotkoff) (Eeftinck Schattenkerk et al., 2009; Martina et al., 2010; Martina et al., 2012; Truijen et al., 2012; Rao et al., 2018), transpulmonary thermodilution, Doppler ultrasound, and rebreathing (Wesseling et al., 1993; Harms et al., 1999; Bogert et al., 2010; Shibata and Levine, 2011; Broch et al., 2012; van der Spoel et al., 2012; Bubenek-Turconi et al., 2013). Additional

studies demonstrated that SV and CO can be estimated by photoplethysmography during open heart cardiac surgery (which involves large hemodynamics changes beyond nominal conditions) (Wesseling et al., 1993), exercise (Bartels et al., 2011), and during conditions where hydrostatic pressures are altered such as fluid challenges (Critchley et al., 2014), moderate orthostatic stress due to LBNP (Harms et al., 1999; Shibata and Levine, 2011; Goswami et al., 2015b), and exposure to hyper-gravity up to +4 Gz (Manen et al., 2015). However, some authors argue that the Nexfin system is not a satisfactory substitute for transpulmonary thermodilution techniques to monitor critical care patients (Fischer et al., 2012). Other studies pointed out potential gravity-dependent limitations of pulse contours methods (PCM) to estimate CO, compared to the rebreathing technique, during microgravity (Limper et al., 2011; Arai et al., 2013) and hyper-gravity (Arai et al., 2013) using parabolic flights. However, these same studies concluded that PCM can be used to track CO dynamics during rapid changes of acceleration profiles (Limper et al., 2011). Another study compared PCM with standard rebreathing techniques in microgravity during long duration spaceflight (>119 days in space), showing limitations presumably due to changes in parameters (i.e., increase in vascular compliance in the splanchnic circulation) affecting the aortic pressure-area relationship assumed in the Modelflow algorithm. While these are important results to consider for future spaceflight applications, our subjects were representative of the normal, healthy population and did not undergo the significant "long-term" physiological changes that astronauts experience during long duration spaceflight. Additionally, it has been shown that in healthy sedentary (i.e., non-masters athletes) young individuals, the assumed "aortic ages" within the PCM were comparable with chronological ages (Shibata and Levine, 2011), supporting the reliability of Modelflow parameters under moderate orthostatic stress conditions. Despite the fact that there are currently no studies that have confirmed the validity of this technique under conditions of altered hydrostatic profiles caused by the rotating environment and presence of a gravity gradient, we took additional measures during our experiment to eliminate this potential source of error. In particular, subjects did not use the Nexfin feature that automatically corrects for hydrostatic differences in pressure when the monitored hand is not at heart level. Instead, subjects kept theirs immobile and aligned with their heart during the entire experiment. This technique has also been used in previous centrifugation studies (Goswami et al., 2015a,b; Verma et al., 2018). While the Nexfin and other similar systems such as Portapres, Finometer, and Finapres certainly have limitations, they currently are the only methods to measure continuous arterial blood pressure and estimate other CV variables continuously and non-invasively. These devices have been used extensively in the human life science space program and ground-based analog studies (Fritsch-Yelle et al., 1994; Di Rienzo et al., 2008; Verheyden et al., 2009; Hughson et al., 2012; Stenger et al., 2013; Goswami et al., 2015a,b; Lee et al., 2015; Linnarsson et al., 2015; Morita et al., 2016; Masatli et al., 2018; Verma et al., 2018), including in conditions where hydrostatic pressures are moderately altered such as Head-Up Tilt and LBNP (Linnarsson et al., 2015; Goswami et al., 2015b). Similarly, our study induced only moderate orthostatic stress, and we are using a device that facilitates comparison with other studies in the field, which is important. Our results are also quantitatively reasonable and in agreement with previous studies (Goswami et al., 2015a; Verma et al., 2018).

Other limitations of the study are related to the facilities and the resources available to conduct the experiment. Subjects' age was not fully representative to the current astronaut population. However, age range was limited to only 6 years to avoid potential alterations in the cardiovascular system related to age differences. Additionally, the duration of the test sessions was limited to 25 min due to structural limitations of the MIT centrifuge and to avoid excessive fatigue of subjects during the exercise protocol. Thus, the relatively short duration of the exercise conditions caused some CV variables to not reach steady state, particularly at higher work rates, and extrapolations of the results outside the timeframes tested should be done with caution. Similarly, other AG levels (both between 0–1 G, and >1.4 G, measured at the subjects' feet) and workload intensities should be tested to expand the results outside the ranges used in this experiment. Additionally, a more exhaustive experiment and analysis should be performed to fully capture proper physiological responses during spin-down. The focus of the experiment presented herein is not the post-exercise and spin-down phase. Here, the effects of both factors (recuperation after intense exercise and centrifuge deceleration) are certainly confounded in the results, since both phases are very close together due to time and protocol constraints on the centrifuge.

CONCLUSION

For the first time, we characterized and quantified continuous cardiovascular response to AG generated by a short-radius centrifuge combined with lower-body ergometer exercise. Different levels of AG and workload intensity were tested and analyzed, informing future decisions and trade-offs regarding the implementation of AG in the future. The orthostatic stress introduced by AG caused the cardiovascular system to increase its overall activity to maintain homeostasis, and these responses were in general more significant at higher AG levels and higher exercise work rates. Our results suggest that AG combined with exercise may be beneficial to cardiovascular conditioning in space, by increasing the overall cardiovascular stress during exercise protocols and/or by reducing the amount of exercise to achieve a similar degree of cardiovascular stress than exercise alone. Based on this analysis, we also recommend to explore both higher AG-levels (to elicit more pronounced CV responses), as well as AG-levels between 0 and 1 G (to fill the gap between this two conditions) in future experiments to get a more comprehensive understanding of short-radius centrifugation during exercise on the CV system.

AUTHOR CONTRIBUTIONS

AD-A designed and conducted the human experiments, developed the statistical model, analyzed the data, and drafted

the manuscript. TH provided expertise concerning the cardiovascular aspects used in this research. Also, he contributed to the modeling and the interpretation of the experimental data, and critically reviewed and approved the final manuscript. LY has contributed through the overall supervision and management of the research project and critically reviewed the experimental results and the manuscript, and approved the final manuscript.

FUNDING

This project was supported by the MIT/Skolkovo development project (Seed Grant 6925991), and the National Space Biomedical Research Institute through NASA Cooperative Agreement NCC 9-58. In addition, the Fulbright Commission has provided additional support.

ACKNOWLEDGMENTS

We appreciate the participation of our anonymous subjects. We thank Chris Trigg, Ankur Kumar, and Aaron Ashley for technical support and assistance in data collection; and Alan Natapoff and Torin Clark for advice in statistics.

REFERENCES

Abdi, H. (2010). "Greenhouse geisser correction," in *Encyclopedia of Research Design*, eds N. J. Salkind, D. M. Dougherty, and B. Frey (Thousand Oaks CA: Sage), 544–548.

Arai, T., Limper, U., Gauger, P., and Beck, L. (2013). Pulse contour methods to estimate cardiovascular indices in micro-and hypergravity. *Aviat. Space Environ. Med.* 84, 1178–1185. doi: 10.3357/ASEM.3683.2013

Baevsky, R. M., Baranov, V. M., Funtova, I. I., Diedrich, A., Pashenko, A. V., Chernikova, A. G., et al. (2007). Autonomic cardiovascular and respiratory control during prolonged spaceflights aboard the International Space Station. *J. Appl. Physiol.* 103, 156–161. doi: 10.1152/japplphysiol.00137.2007

Baker, J. E., Moulder, J. E., and Hopewell, J. W. (2011). Radiation as a risk factor for cardiovascular disease. *Antioxid. Redox Signal.* 15, 1945–1956. doi: 10.1089/ars.2010.3742

Bartels, S. A., Stok, W. J., Bezemer, R., Boksem, R. J., Van Goudoever, J., Cherpanath, T. G. V., et al. (2011). Noninvasive cardiac output monitoring during exercise testing: nexfin pulse contour analysis compared to an inert gas rebreathing method and respired gas analysis. *J. Clin. Monit. Comput.* 25, 315–321. doi: 10.1007/s10877-011-9310-4

Bogert, L. W., and van Lieshout, J. J. (2005). Non-invasive pulsatile arterial pressure and stroke volume changes from the human finger. *Exp. Physiol.* 90, 437–446. doi: 10.1113/expphysiol.2005.030262

Bogert, L. W., Wesseling, K. H., Schraa, O., Van Lieshout, E. J., De Mol, B. A., Van Goudoever, J., et al. (2010). Pulse contour cardiac output derived from non-invasive arterial pressure in cardiovascular disease. *Anaesthesia* 65, 1119–1125. doi: 10.1111/j.1365-2044.2010.06511.x

Bonjour, J., Capelli, C., Antonutto, G., Calza, S., Tam, E., Linnarsson, D., et al. (2010). Determinants of oxygen consumption during exercise on cycle ergometer: the effects of gravity acceleration. *Respir. Physiol. Neurobiol.* 171, 128–134. doi: 10.1016/j.resp.2010.02.013

Broch, O., Renner, J., Gruenewald, M., Meybohm, P., Schöttler, J., Caliebe, A., et al. (2012). A comparison of the nexfin® and transcardiopulmonary thermodilution to estimate cardiac output during coronary artery surgery. *Anaesthesia* 67, 377–383. doi: 10.1111/j.1365-2044.2011.07018.x

Bubenek-Turconi, S. I., Craciun, M., Miclea, I., and Perel, A. (2013). Noninvasive continuous cardiac output by the nexfin before and after preload-modifying maneuvers: a comparison with intermittent thermodilution cardiac output. *Anesth. Analg.* 117, 366–372. doi: 10.1213ANE.0b013e31829562c3

Buckey, J. C. (2006). *Space Physiology*. New York, NY: Oxford University Press.

Buckey, J. C., Lane, L. D., Levine, B. D., Watenpaugh, D. E., Wright, S. J., Moore, W. E., et al. (1996). Orthostatic intolerance after spaceflight. *J. Appl. Physiol.* 81, 7–18. doi: 10.1152/jappl.1996.81.1.7

Charles, B. J., and Lathers, C. M. (1991). Cardiovascular adaption to spaceflight. *J. Clin. Pharmacol.* 31, 1010–1023. doi: 10.1002/j.1552-4604.1991.tb03665.x

Charles, J. B., and Lathers, C. M. (1994). Summary of lower body negative pressure experiments during space flight. *J. Clin. Pharmacol.* 34, 571–583. doi: 10.1002/j.1552-4604.1994.tb02009.x

Clément, G. (2005). *Fundamentals of Space Medicine*. El Segundo, CA: Microcosm Press.

Clément, G. (2017). International roadmap for artificial gravity research. *NPJ Microgravity* 3:29. doi: 10.1038/s41526-017-0034-8

Clément, G., and Bukley, A. P. (2007). *Artificial Gravity*. Hawthorne, CA: Springer. doi: 10.1007/0-387-70714-X

Clément, G., Paloski, W. H., Rittweger, J., Linnarsson, D., Bareille, M. P., Mulder, E., et al. (2016). Centrifugation as a countermeasure during bed rest and dry immersion: what has been learned? *J. Musculoskelet. Neuronal Interact.* 16, 84–91.

Clément, G. R., Charles, J. B., and Paloski, W. H. (2016). Revisiting the needs for artificial gravity during deep space missions. *Reach* 1, 1–10. doi: 10.1016/j.reach.2016.01.001

Clément, G., and Pavy-Le Traon, A. (2004). Centrifugation as a countermeasure during actual and simulated microgravity: a review. *Eur. J. Appl. Physiol.* 92, 235–248. doi: 10.1007/s00421-004-1118-1

Clement, G. R., Bukley, A. P., and Paloski, W. H. (2015). Artificial gravity as a countermeasure for mitigating physiological deconditioning during long-duration space missions. *Front. Syst. Neurosci.* 9:92. doi: 10.3389/fnsys.2015.00092

Critchley, L. A. H., Huang, L., and Zhang, J. (2014). Continuous cardiac output monitoring: what do validation studies tell us? *Curr. Anesthesiol. Rep.* 4, 242–250. doi: 10.1007/s40140-014-0062-9

Dhalla, N. S., Temsah, R. M., and Netticadan, T. (2000). Role of oxidative stress in cardiovascular diseases. *J. Hypertens.* 18, 655–673. doi: 10.1097/00004872-200018060-00002

Di Rienzo, M., Castiglioni, P., Iellamo, F., Volterrani, M., Pagani, M., Mancia, G., et al. (2008). Dynamic adaptation of cardiac baroreflex sensitivity to prolonged exposure to microgravity: data from a 16-day spaceflight. *J. Appl. Physiol.* 105, 1569–1575. doi: 10.1152/japplphysiol.90625.2008

Diaz, A., Heldt, T., and Young, L. R. (2015a). "Cardiovascular responses to artificial gravity combined with exercise," in *Proceedings of the 2015 IEEE Aerospace Conference*, Big Sky, MT. 1–11. doi: 10.1109/AERO.2015.7118969

Diaz, A., Trigg, C., and Young, L. R. (2015b). Combining ergometer exercise and artificial gravity in a compact-radius centrifuge. *Acta Astronaut.* 113, 80–88. doi: 10.1016/j.actaastro.2015.03.034

Diaz Artiles, A., Heldt, T., and Young, L. R. (2016). Effects of artificial gravity on the cardiovascular system: computational approach. *Acta Astronaut.* 126, 395–410. doi: 10.1016/j.actaastro.2016.05.005

Duda, K. R., Jarchow, T., and Young, L. R. (2012). Squat exercise biomechanics during short-radius centrifugation. *Aviat. Space Environ. Med.* 83, 102–110. doi: 10.3357/ASEM.2334.2012

Eckberg, D. L., Halliwill, J. R., Beightol, L. A., Brown, T. E., Taylor, J. A., and Goble, R. (2010). Human vagal baroreflex mechanisms in space. *J. Physiol.* 588, 1129–1138. doi: 10.1113/jphysiol.2009.186650

Eeftinck Schattenkerk, D. W., van Lieshout, J. J., van den Meiracker, A. H., Wesseling, K. R., Blanc, S., Wieling, W., et al. (2009). Nexfin noninvasive continuous blood pressure validated against Riva-Rocci/Korotkoff. *Am. J. Hypertens.* 22, 378–383. doi: 10.1038/ajh.2008.368

Evans, J. M., Knapp, C. F., and Goswami, N. (2018). Artificial gravity as a countermeasure to the cardiovascular deconditioning of spaceflight: gender perspectives. *Front. Physiol.* 9:716. doi: 10.3389/fphys.2018.00716

Evans, J. M., Stenger, M. B., Moore, F. B., Hinghofer-Szalkay, H., Rössler, A., Patwardhan, A. R., et al. (2004). Centrifuge training increases presyncopal orthostatic tolerance in ambulatory men. *Aviat. Space Environ. Med.* 75, 850–858.

Fischer, M. O., Avram, R., Cârjaliu, I., Massetti, M., Gérard, J. L., Hanouz, J. L., et al. (2012). Non-invasive continuous arterial pressure and cardiac index monitoring with nexfin after cardiac surgery. *Br. J. Anaesth.* 109, 514–521. doi: 10.1093/bja/aes215

Fitts, R. H., Trappe, S. W., Costill, D. L., Gallagher, P. M., Creer, A. C., Colloton, P. A., et al. (2010). Prolonged space flight-induced alterations in the structure and function of human skeletal muscle fibres. *J. Physiol.* 588, 3567–3592. doi: 10.1113/jphysiol.2010.188508

Fritsch-Yelle, J. M., Charles, J. B., Jones, M. M., Beightol, L. A., and Eckberg, D. L. (1994). Spaceflight alters autonomic regulation of arterial pressure in humans. *J. Appl. Physiol.* 77, 1776–1783. doi: 10.1152/jappl.1994.77.4.1776

Goswami, N., Bruner, M., Xu, D., Bareille, M. P., Beck, A., Hinghofer-Szalkay, H., et al. (2015a). Short-arm human centrifugation with 0.4g at eye and 0.75g at heart level provides similar cerebrovascular and cardiovascular responses to standing. *Eur. J. Appl. Physiol.* 115, 1569–1575. doi: 10.1007/s00421-015-3142-8

Goswami, N., Evans, J., Schneider, S., Von Der, Wiesche, M., Mulder, E., et al. (2015b). Effects of individualized centrifugation training on orthostatic tolerance in men and women. *PLoS One* 10:e0125780. doi: 10.1371/journal.pone.0125780

Greenleaf, J. E., Gundo, D. P., Watenpaugh, D. E., Mulenburg, G. M., Mckenzie, M. A., Looft-Wilson, R., et al. (1997). "Cycle-powered short radius (1.9 m) centrifuge: effect of exercise versus passive acceleration on heart rate in humans," in *NASA Technical Memorandum 110433*, (Moffett Field, CA: Nasa Ames Research Center), 1–14.

Guyton, A. C. (1990). *Textbook of Medical Physiology*, 8th Edn. St. Louis, MO: Harcourt College Pub.

Harms, M. P., Wesseling, K. H., Pott, F., Jenstrup, M., Van Gj, Secher, N. H., et al. (1999). Continuous stroke volume monitoring by modelling flow from non-invasive measurement of arterial pressure in humans under orthostatic stress. *Clin. Sci.* 97, 291–301. doi: 10.1042/cs0970291

Hughson, R. L., Shoemaker, J. K., Blaber, A. P., Arbeille, P., Greaves, D. K., Pereira-Junior, P. P., et al. (2012). Cardiovascular regulation during long-duration spaceflights to the International Space Station. *J. Appl. Physiol.* 112, 719–727. doi: 10.1152/japplphysiol.01196.2011

Iwasaki, K.-I., Shiozawa, T., Kamiya, A., Michikami, D., Hirayanagi, K., Yajima, K., et al. (2005). Hypergravity exercise against bed rest induced changes in cardiac autonomic control. *Eur. J. Appl. Physiol.* 94, 285–291. doi: 10.1007/s00421-004-1308-x

Iwase, S. (2005). Effectiveness of centrifuge-induced artificial gravity with ergometric exercise as a countermeasure during simulated microgravity exposure in humans. *Acta Astronaut.* 57, 75–80. doi: 10.1016/j.actaastro.2005.03.013

Iwase, S., Fu, Q., Narita, K., Morimoto, E., Takada, H., and Mano, T. (2002). Effects of graded load of artificial gravity on cardiovascular functions in humans. *Environ. Med.* 46, 29–32.

Kaderka, J., Young, L. R., and Paloski, W. H. (2010). A critical benefit analysis of artificial gravity as a microgravity countermeasure. *Acta Astronaut.* 67, 1090–1102. doi: 10.1016/j.actaastro.2010.06.032

Katayama, K., Sato, K., and Akima, H. (2004). Acceleration with exercise during head-down bed rest preserves upright exercise responses. *Aviat. Space Environ. Med.* 75, 1029–1035.

Kozlovskaya, I. B., and Grigoriev, A. I. (2004). Russian system of countermeasures on board of the International Space Station (ISS): the first results. *Acta Astronaut.* 55, 233–237. doi: 10.1016/j.actaastro.2004.05.049

Kozlovskaya, I. B., Grigoriev, A. I., and Stepantzov, V. I. (1995). Countermeasure of the negative effects of weightlessness on physical systems in long-term space flights. *Acta Astronaut.* 36, 661–668. doi: 10.1016/0094-5765(95)00156-5

LeBlanc, A., Matsumoto, T., Jones, J., Shapiro, J., Lang, T., Shackelford, L., et al. (2013). Bisphosphonates as a supplement to exercise to protect bone during long-duration spaceflight. *Osteoporos. Int.* 24, 2105–2114. doi: 10.1007/s00198-012-2243-z

LeBlanc, A. D., Spector, E. R., Evans, H. J., and Sibonga, J. D. (2007). Skeletal responses to space flight & bed rest analogue: a review. *J. Musculoskelet. Neuronal Interact.* 7, 33–47.

Lee, S. M. C., Feiveson, A. H., Stein, S., Stenger, M. B., and Platts, S. H. (2015). Orthostatic intolerance after ISS and space shuttle missions. *Aerosp. Med. Hum. Perform.* 86, 54–67. doi: 10.3357/AMHP.EC08.2015

Levine, B. D., Lane, L. D., Watenpaugh, D. E., Gaffney, F. A., Buckey, J. C., Blomqvist, C. G., et al. (1996). Maximal exercise performance after adaptation to microgravity. *J. Appl. Physiol.* 81, 686–694. doi: 10.1152/jappl.1996.81.2.686

Limper, U., Gauger, P., and Beck, L. E. (2011). Upright cardiac output measurements in the transition to weightlessness during parabolic flights. *Aviat. Space Environ. Med.* 82, 448–454. doi: 10.3357/ASEM.2883.2011

Linnarsson, D., Hughson, R. L., Fraser, K. S., Clément, G., Karlsson, L. L., Mulder, E., et al. (2015). Effects of an artificial gravity countermeasure on orthostatic tolerance, blood volumes and aerobic power after short-term bed rest (BR-AG1). *J. Appl. Physiol.* 118, 29–35. doi: 10.1152/japplphysiol.00061.2014

Mandsager, K. T., Robertson, D., and Diedrich, A. (2015). The function of the autonomic nervous system during spaceflight. *Clin. Auton. Res.* 25, 141–151. doi: 10.1007/s10286-015-0285-y

Manen, O., Dussault, C., Sauvet, F., and Montmerle-Borgdorff, S. (2015). Limitations of stroke volume estimation by non-invasive blood pressure monitoring in hypergravity. *PLoS One* 10:e0121936. doi: 10.1371/journal.pone.0121936

Martina, J. R., Westerhof, B. E., van Goudoever, J., de Beaumont, E. M., Truijen, J., Kim, Y. S., et al. (2012). Noninvasive continuous arterial blood pressure monitoring with nexfin®. *Anesthesiology* 116, 1092–1103. doi: 10.1097/ALN.0b013e31824f94ed

Martina, J. R., Westerhof, B. E., Van Goudoever, J., De Jonge, N., Van Lieshout, J. J., Lahpor, J. R., et al. (2010). Noninvasive blood pressure measurement by the Nexfin monitor during reduced arterial pulsatility: a feasibility study. *ASAIO J.* 56, 221–227. doi: 10.1097/MAT.0b013e3181d70227

Masatli, Z., Nordine, M., Maggioni, M. A., Mendt, S., Hilmer, B., Brauns, K., et al. (2018). Gender-specific cardiovascular reactions to + Gz interval training on a short arm human centrifuge. *Front. Physiol.* 9:1028. doi: 10.3389/fphys.2018.01028

Morita, H., Abe, C., and Tanaka, K. (2016). Long-term exposure to microgravity impairs vestibulo-cardiovascular reflex. *Sci. Rep.* 6:33405. doi: 10.1038/srep33405

Norsk, P. (2014). Blood pressure regulation IV: adaptive responses to weightlessness. *Eur. J. Appl. Physiol.* 114, 481–497. doi: 10.1007/s00421-013-2797-2

Norsk, P., Asmar, A., Damgaard, M., and Christensen, N. J. (2015). Fluid shifts, vasodilatation and ambulatory blood pressure reduction during long duration spaceflight. *J. Physiol.* 593, 573–584. doi: 10.1113/jphysiol.2014.284869

Norsk, P., Damgaard, M., Petersen, L., Gybel, M., Pump, B., Gabrielsen, A., et al. (2006). Vasorelaxation in space. *Hypertension* 47, 69–73. doi: 10.1161/01.HYP.0000194332.98674.57

Paloski, W. H., and Charles, J. B. (2014). *International Workshop on Research and Operational Considerations for Artificial Gravity Countermeasures. (Technical Report)*. Mountain View, CA: Nasa Ames Research Center.

Paloski, W. H., and Young, L. R. (1999). *Artificial Gravity Workshop*. League City, TX: NASA.

Penaz, J. (1973). "Photoelectric measurement of blood pressure, volume and flow in the finger," in *Proceedings of the Digest 10th Int Conf Med Biol Engng*, (Dresden: International Federation for Medical and Biological Engineering), 104.

Perel, A., Wesselink, W., and Settels, J. (2011). "The nexfin monitor – a totally non invasive cardiac output monitor," in *Proceedings of the 23rd Annual Meeting - International Symposium on Critical Care Medicine*, ed. A. Gullo (Italia: Springer-Verlag), 103–108.

Platts, S. H., Merz, N. B., Barr, Y., Fu, Q., Gulati, M., Hughson, R. L., et al. (2014). Effects of sex and gender on adaptation to space: cardiovascular alterations. *J. Womens Heal.* 23, 950–955. doi: 10.1089/jwh.2014.4912

Platts, S. H., Tuxhorn, J. A., Ribeiro, L. C., Stenger, M. B., Lee, S. M. C., and Meck, J. V. (2009). Compression garments as countermeasures to orthostatic intolerance. *Aviat. Space Environ. Med.* 80, 437–442. doi: 10.3357/ASEM.2473.2009

Rao, K. K., Haro, G. J., Ayers, C. R., Patel, P. C., Mishkin, J., Thibodeau, J. T., et al. (2018). 579 blood pressure measurement in patients with continuous flow LVADs: comparing the doppler sphygmomanometer, the nexfin device, and the arterial line. *J. Heart Lung Transplant* 31, S200–S201. doi: 10.1016/j.healun.2012.01.592

Schwarz, G. (1978). Estimating the dimension of a model. *Ann. Stat.* 6, 461–464. doi: 10.1214/aos/1176344136

Shibata, S., and Levine, B. D. (2011). Biological aortic age derived from the arterial pressure waveform. *J. Appl. Physiol.* 110, 981–987. doi: 10.1152/japplphysiol.01261.2010

Sliwka, U., Krasney, J. A., Simon, S. G., Schmidt, P., and Noth, J. (1998). Effects of sustained low-level elevations of carbon dioxide on cerebral blood flow and autoregulation of the intracerebral arteries in humans. *Aviat. Space Environ. Med.* 69, 299–306.

Smith, S. M., Heer, M. A., Shackelford, L. C., Sibonga, J. D., Ploutz-Snyder, L., and Zwart, S. R. (2012). Benefits for bone from resistance exercise and nutrition in long-duration spaceflight: Evidence from biochemistry and densitometry. *J. Bone Miner. Res.* 27, 1896–1906. doi: 10.1002/jbmr.1647

Stenger, M. B., Evans, J. M., Patwardhan, A. R., Moore, F. B., Hinghofer-Szalkay, H., Rössler, A., et al. (2007). Artificial gravity training improves orthostatic tolerance in ambulatory men and women. *Acta Astronaut.* 60, 267–272. doi: 10.3389/fphys.2018.00716

Stenger, M. B., Lee, S. M., Westby, C. M., Ribeiro, L. C., Phillips, T. R., Martin, D. S., et al. (2013). Abdomen-high elastic gradient compression garments during post-spaceflight stand tests. *Aviat. Space Environ. Med.* 84, 459–466. doi: 10.3357/ASEM.3528.2013

Trappe, S., Costill, D., Gallagher, P., Creer, A., Peters, J. R., Evans, H., et al. (2009). Exercise in space: human skeletal muscle after 6 months aboard the International Space Station. *J. Appl. Physiol.* 106, 1159–1168. doi: 10.1152/japplphysiol.91578.2008

Trigg, C. (2013). *Design and Validation of a Compact Radius Centrifuge Artificial Gravity Test Platform*. Ph.D. thesis, Massachusetts Institute of Technology, Cambridge.

Truijen, J., Van Lieshout, J. J., Wesselink, W. A., and Westerhof, B. E. (2012). Noninvasive continuous hemodynamic monitoring. *J. Clin. Monit. Comput.* 26, 267–278. doi: 10.1007/s10877-012-9375-8

van der Spoel, A. G., Voogel, A. J., Folkers, A., Boer, C., and Bouwman, R. A. (2012). Comparison of noninvasive continuous arterial waveform analysis (Nexfin) with transthoracic Doppler echocardiography for monitoring of cardiac output. *J. Clin. Anesth.* 24, 304–309. doi: 10.1016/j.jclinane.2011.09.008

Verheyden, B., Liu, J., Beckers, F., and Aubert, A. E. (2009). Adaptation of heart rate and blood pressure to short and long duration space missions. *Respir. Physiol. Neurobiol.* 169(Suppl.), S13–S16. doi: 10.1016/j.resp.2009.03.008

Verma, A. K., Xu, D., Bruner, M., Garg, A., Goswami, N., Blaber, A. P., et al. (2018). Comparison of autonomic control of blood pressure during standing and artificial gravity induced via short-arm human centrifuge. *Front. Physiol.* 9:712. doi: 10.3389/fphys.2018.00712

Waldie, J. M., and Newman, D. J. (2011). A gravity loading countermeasure skinsuit. *Acta Astronaut.* 68, 722–730. doi: 10.1519/JSC.0000000000001460

Wang, Y. C., Yang, C. B., Wu, Y. H., Gao, Y., Lu, D. Y., Shi, F., et al. (2011). Artificial gravity with ergometric exercise as a countermeasure against cardiovascular deconditioning during 4 days of head-down bed rest in humans. *Eur. J. Appl. Physiol.* 111, 2315–2325. doi: 10.1007/s00421-011-1866-7

Wesseling, K. H., de Wit, B., van der Hoeven, G. M. A., van Goudover, J., and Settels, J. J. (1995). Physiocal, calibrating finger vascular physiology for Finapres. *Homeostasis* 36, 67–82.

Wesseling, K. H., Jansen, J. R., Settels, J. J., and Schreuder, J. J. (1993). Computation of aortic flow from pressure in humans using a nonlinear, three-element model. *J. Appl. Physiol.* 74, 2566–2573. doi: 10.1152/jappl.1993.74.5.2566

Westerhof, N., Lankhaar, J., and Westerhof, B. E. (2009). The arterial Windkessel. *Med. Biol. Eng. Comput.* 47, 131–141. doi: 10.1007/s11517-008-0359-2

Williams, D., Kuipers, A., Mukai, C., and Thirsk, R. (2009). Acclimation during space flight: effects on human physiology. *CMAJ* 180, 1317–1323. doi: 10.1503/cmaj.090628

Yang, C., Bin, Zhang, S., Zhang, Y., Wang, B., Yao, Y.-J., et al. (2010). Combined short-arm centrifuge and aerobic exercise training improves cardiovascular function and physical working capacity in humans. *Med. Sci. Monit.* 16, 575–583.

Yang, Y., Baker, M., Graf, S., Larson, J., and Caiozzo, V. J. (2007). Hypergravity resistance exercise: the use of artificial gravity as potential countermeasure to microgravity. *J. Appl. Physiol.* 103, 1879–1887. doi: 10.1152/japplphysiol.00772.2007

Young, L. R., Yajima, K., and Paloski, W. H. (2009). *Artificial Gravity Research to Enable Human Space Exploration*. Westchester, IL: International Academy of Astronautics (IAA)

Conflict of Interest Statement: The authors declare that the research was conducted in the absence of any commercial or financial relationships that could be construed as a potential conflict of interest.

The handling Editor declared a past co-authorship with one of the authors AD-A.

frontiers in Physiology

ORIGINAL RESEARCH
published: 19 December 2018
doi: 10.3389/fphys.2018.01850

Vibrotactile Feedback Improves Manual Control of Tilt After Spaceflight

Gilles Clément[1,2], Millard F. Reschke[3] and Scott J. Wood[3,4]*

[1] Lyon Neuroscience Research Center, Bron, France, [2] KBRwyle, Houston, TX, United States, [3] Neuroscience Laboratories, National Aeronautics and Space Administration Johnson Space Center, Houston, TX, United States, [4] Azusa Pacific University, Azusa, CA, United States

The objectives of this study were to quantify decrements in controlling tilt on astronauts immediately after short-duration spaceflight, and to evaluate vibrotactile feedback of tilt as a potential countermeasure. Eleven subjects were rotated on a variable radius centrifuge (216°/s <20 cm radius) in a darkened room to elicit tilt disturbance in roll (≤± 15°). Nine of these subjects performed a nulling task in the pitch plane (≤±7.5°). Small tactors placed around the torso vibrated at 250 Hz to provide tactile feedback when the body tilt exceeded predetermined levels. The subjects performed closed-loop nulling tasks during random tilt steps with and without this vibrotactile feedback of tilt. There was a significant effect of spaceflight on the performance of the nulling tasks based on root mean square error. Performance returned to baseline levels 1–2 days after landing. Vibrotactile feedback significantly improved performance of nulling tilt during all test sessions. Nulling performance in roll was significantly correlated with performance in pitch. These results indicate that adaptive changes in astronauts' vestibular processing during spaceflight impair their ability to manually control tilt following transitions between gravitational environments. A simple vibrotactile prosthesis improves their ability to null-out tilt within a limited range of motion disturbances.

Keywords: vestibular system, manual control, vibrotactile feedback, microgravity, subjective vertical

OPEN ACCESS

Edited by:
Jörn Rittweger, Helmholtz-Gemeinschaft Deutscher Forschungszentren (HZ), Germany

Reviewed by:
Ke Lv, China Astronaut Research and Training Center, China
Shu Zhang, Fourth Military Medical University, China

****Correspondence:***
Gilles Clément
gilles.r.clement@nasa.gov

Specialty section:
This article was submitted to Environmental, Aviation and Space Physiology, a section of the journal Frontiers in Physiology

Received: *15 October 2018*
Accepted: *07 December 2018*
Published: *19 December 2018*

Citation:
Clément G, Reschke MF and Wood SJ (2018) Vibrotactile Feedback Improves Manual Control of Tilt After Spaceflight. Front. Physiol. 9:1850. doi: 10.3389/fphys.2018.01850

INTRODUCTION

We previously compared perceptual and ocular changes in astronauts by tilting them in roll and pitch before and immediately after short-duration spaceflight. The astronauts overestimated tilt and translation as a result of their adaptation to weightlessness (Clément and Wood, 2014; Clarke and Schönfeld, 2015). When a spacecraft is accelerating or decelerating, the automated processes for determining the position of the horizon are not very accurate and the pilot must manually correct the tilt of the vehicle. During future exploration mission to Mars where dust clouds are common, it will be critical that the astronaut pilots estimate the amplitude of the vehicle tilt and manually level the vehicle in the absence of any visual cues. Changes in perceived body position caused by adaption to weightlessness could impair an astronaut's ability to manually correct the position of spacecraft and this could have dire consequences (Paloski et al., 2008). To further define this risk of impaired performance, we assessed how spaceflight affects astronauts' abilities to perform a manual-nulling task during passive body tilt in pitch and roll.

Although all the Space Shuttle landings were successful, the pilots' landing performances varied. Landing speeds of the Space Shuttle varied considerably: 20% of the first 100 touchdowns were faster than acceptable, and six were so fast they risked damaging the landing gear tires (Moore et al., 2008). In addition, Clark and Bacal (2008) noted that the two fastest landings were linked to the pilot's momentary spatial disorientation. The degree of neurovestibular dysfunction in the astronauts within several hours of landing (as measured by subjective symptoms, spatial disorientation, impairment in locomotion and coordination of movements, and functional motor performance) was negatively correlated with their performance navigating the spacecraft during the landing procedure.

Previous investigations assessed how nine astronauts manually controlled lateral translations during linear acceleration 2 days after they returned from 10 days Spacelab missions (Arrott and Young, 1986; Arrott et al., 1990). Astronauts were seated in a cabin that was mounted perpendicular to a sled and they were tested while the sled moved in a random appearing velocity profile made of 12 sinusoids added together. Subjects were asked to null out the pseudo-random disturbance of lateral motion using a joystick that controlled the velocity of the sled. On landing day, most astronauts performed this task in the dark better than they did before the mission. No spaceflight-induced change in performance was observed when they completed the same task with visual cues. Unfortunately, the astronauts did not report any sense of roll tilt during lateral translation on the sled. After the mission, the astronauts' performance appeared to improve relative to preflight performance during the higher frequencies of the profile used, which were more likely to generate a sense of translation (Wood, 2002).

Merfeld (1996) measured how two astronauts controlled roll tilt after the 14 days Space Life Science-2 Spacelab mission. Subjects sat on a motion platform that tilted from 0.4 to 2.4° in a pseudo-random sinusoidal profile. On landing day, the two subjects' ability to maintain an upright orientation was greatly impaired compared to their ability before the flight. Clark et al. (2015a) tested a similar manual control task while rotating subjects to 1.5 and 2 Gz in a ground-based centrifuge. Performance of the roll motion-nulling task in darkness degraded during the first trials, but subjects improved their performance over time (Clark et al., 2015b).

Further tests were conducted on the Spacelab astronauts during larger amplitude roll tilts, which correspond to tilts pilots experience when they are flying a spacecraft. Studies using both actual body tilt and centrifugation have shown that immediately after spaceflight the astronauts overestimated the tilt of their body in roll relative to gravity (Reschke and Parker, 1987; Glasauer and Mittelstaedt, 1998; Clément et al., 2001; Clément and Wood, 2013, 2014). We found that subjective estimates of the amplitude of static body tilt in pitch 2 days after landing were unchanged from preflight values (Clément and Wood, 2014). Ocular counter-rolling and counter-pitching, i.e., the compensatory eye movement in response to head roll and pitch tilt, respectively, were not significantly altered (Clément et al., 2007).

The primary goal of the present study was to quantify the decrements in controlling both roll and pitch tilt in a larger group of astronauts immediately after spaceflight. The secondary goal was to test the efficacy of a countermeasure for mitigating these decrements. Vibrotactile feedback (also referred to as haptic feedback) improves balance by using the sense of touch to substitute for, or augment, the sense of sight and balance (Shull and Damian, 2015; Sienko et al., 2017). Vibrotactor arrays placed around the waist of individuals with vestibular deficits can help them reduce tilts of their heads and displacements of their center of pressure while they are standing with their eyes closed (Kentala et al., 2003; Wall and Kentala, 2005; Wall, 2010). The U.S. Navy developed a tactile situation awareness system (TSAS) to cue pilots on the orientation of their aircraft relative to gravity during aerial navigation and combat (Rupert, 2000). The vibration of tactors distributed on the subjects' torso cued them to move in the opposite direction of vibration, and the location of vibrating tactor indicated the degree of desired correction.

More recently, Sienko et al. (2008) found that four tactors spaced evenly around the waist were as effective for correcting posture sway as an array of 48 tactors (3 rows by 16 columns) placed around the waist. In the present study we used a belt with pairs of tactors in each direction of tilt: two tactors were aligned on the front and on the back of the torso during pitch tilt tests, and two were aligned on the right and on the left of the torso during roll tilt tests. We activated the tactors when the chair offset exceeded preset values. We compared tilt nulling performance in pitch and roll before and after spaceflight, and with and without this tactile feedback.

MATERIALS AND METHODS

Subjects

Eleven crewmembers (10 males, 1 female; age 42–55 years, mean 49 years) participated in this experiment. Each crewmember flew on one of eight Space Shuttle missions lasting 11–15 days. All subjects had normal neurological function, as evaluated during the NASA astronaut selection process and subsequent annual medical examination. This study was carried out in accordance with the recommendations of NASA Johnson Space Center Institutional Review Board. The protocol was approved by NASA Johnson Space Center Institutional Review Board. All subjects gave written informed consent in accordance with the Declaration of Helsinki.

All subjects were tested three times before the mission at the Neuroscience Laboratory of the NASA Johnson Space Center (JSC) in Houston at approximately launch minus (L-) 120 days, L-90 days, and L-60 days. The initial post-flight test for the roll tilt stimuli was typically performed between 1 and 4 h after return to Earth (R+0 day) tests at the Space Shuttle landing sites at the Kennedy Space Center or the Dryden (now Armstrong) Space Research Center. Testing was delayed until return to NASA JSC on five subjects due to motion sensitivity or equipment malfunction. Nine subjects participated in the pitch tilt stimuli immediately upon return to NASA JSC during the day following the return to Earth (R+1). Return to baseline performance was

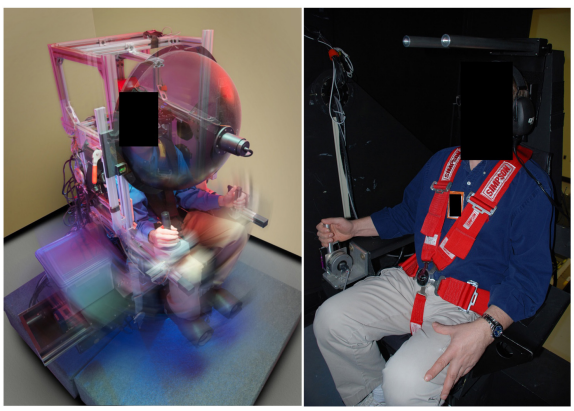

FIGURE 1 | (A) Roll tilt The variable radius centrifuge consisted of a servo-controlled rotator with a small linear track to provide dynamic translation of the chair during constant velocity rotation. Controlling the joystick with their right hand, subjects attempted to keep the chair in the center of the lateral translation stage (maintain a perceived upright orientation). **(B)** Pitch tilt Subjects sat in a chair that tilted in pitch about the interaural axis while they performed a closed-loop nulling task in which they used a joystick to null out perceived tilt motion. Photo credit: NASA.

monitored with continued post-flight testing at NASA JSC on R+2 and R+4 days.

Roll Tilt

A variable radius centrifuge was used to generate a centripetal acceleration along the subjects' interaural axis, which elicited a perception of tilt (somatogravic illusion) in roll without concordant roll cues from the semicircular canals canal or visual cues (Clark and Graybiel, 1966). Subjects were restrained in a chair that was mounted on a small translation stage fixed to rotator that turned about the vertical axis in a light tight enclosure (**Figure 1A**). The restraint system incorporated straps and padding at shoulders, mid-torso, waist, thighs, and feet. Support was provided by moldable Vac-Pacs (Olympic Medical, Seattle, WA, United States) that helped immobilize the body and distribute the pressure uniformly during tilt. A head restraint with adjustable foam pads provided even pressure and head stability relative to the chair. The height and fore-aft position of the head restraint was adjusted to accommodate different subjects while restraining their head in a naturally upright orientation.

The roll stimuli involved an integrated protocol with Clarke and Schönfeld (2015) where the centrifuge was either slowly accelerated ($3°/s^2$) to a constant velocity of 216°/s or decelerated if a unilateral eccentric rotation paradigm was performed first. In either case, subjects rotated for 60 s at constant velocity to allow the post-rotatory response of semicircular canals to decay. After the subjects no longer sensed the rotation, the chair was displaced using the translation stage by ±6.1, ± 12.2, and ±18.5 cm in a random order for 5 s at each position, corresponding to a static roll-tilt of the gravitoinertial acceleration vector at ±5°, ± 10°, and ±15°, respectively. Throughout the random displacements, subjects were instructed to use a chair-mounted joystick to control the chair's translation motion and orient themselves to what they perceived to be an upright orientation.

Pitch Tilt

The subjects were restrained in a tilt chair that was mounted inside a light-tight enclosure. The chair could rotate in pitch about the horizontal axis by means of a direct drive servomotor and a pivoting yoke assembly. The subjects were restrained in the chair with straps and padding around their shoulders, mid-torso, and waist. The chair height was adjusted to align the subject's head inter-aural axis with the tilt axis, and their head was restrained in an upright orientation. The chair was then tilted in pitch at ±2.5°, ± 5°, and ± 7.5° in a random order for 5 s at each angle. As with roll, subjects were instructed to use a chair-mounted joystick to orient the chair to what they perceived as upright (**Figure 1B**), i.e., null out the tilt disturbances. In both the tilt chair and the centrifuge, noise-canceling headphones were used for two-way audio communications and for suppressing any auditory cues of spatial orientation.

Vibrotactile Feedback

Small (0.3 inch in diameter) electromechanical vibrators (C2 model, Engineering Acoustics Inc., Winter Park, FL, United States) provided vibrotactile feedback regarding the direction and amplitude of tilt. The vibration was similar to vibration mode on cell phones (Wood et al., 2009). Before getting into the chair, subjects donned a belt that had four of these tactors. Two tactors were positioned vertically on the front and two on the back of the torso during pitch tilt; two tactors were positioned vertically on the right and two on the left of the torso during roll tilt. Information on body orientation was derived from encoders mounted to the drive axes. Tactors provided a steady pulse rate (250 Hz) that indicated both direction and magnitude of tilt. The lower tactor was activated when body tilt reached 2° relative to gravity; the upper tactor was activated when body tilt reached 4° relative to gravity; both the lower and upper tactors were activated when body tilt reached 6° relative to gravity. Subjects were trained to use the vibrotactile feedback of tilt at the beginning of the first two preflight sessions. To minimize any learning effects, only the last preflight session was compared with the post-flight measures. The order of trials with and without vibrotactile feedback was also counterbalanced across subjects.

Data Analysis

Nulling task performance was derived from the Root Mean Squared (RMS) error in degrees across each entire trial. Thus, lower RMS error represented improved nulling performance relative to higher RMS error. RMS error was obtained from each pitch and roll session for both nulling with and without vibrotactile performance. Based on Shapiro–Wilk tests, the data were not consistently normally distributed. Therefore, only non-parametric statistical tests were utilized.

For both pitch and roll nulling performance, the effect of spaceflight was evaluated with a related samples Friedman's Analysis of Variance by ranks using preflight, R+0/1, R+2, and R+4 measurements. The effect of vibrotactile feedback on nulling performance was based on a related samples Wilcoxon Signed

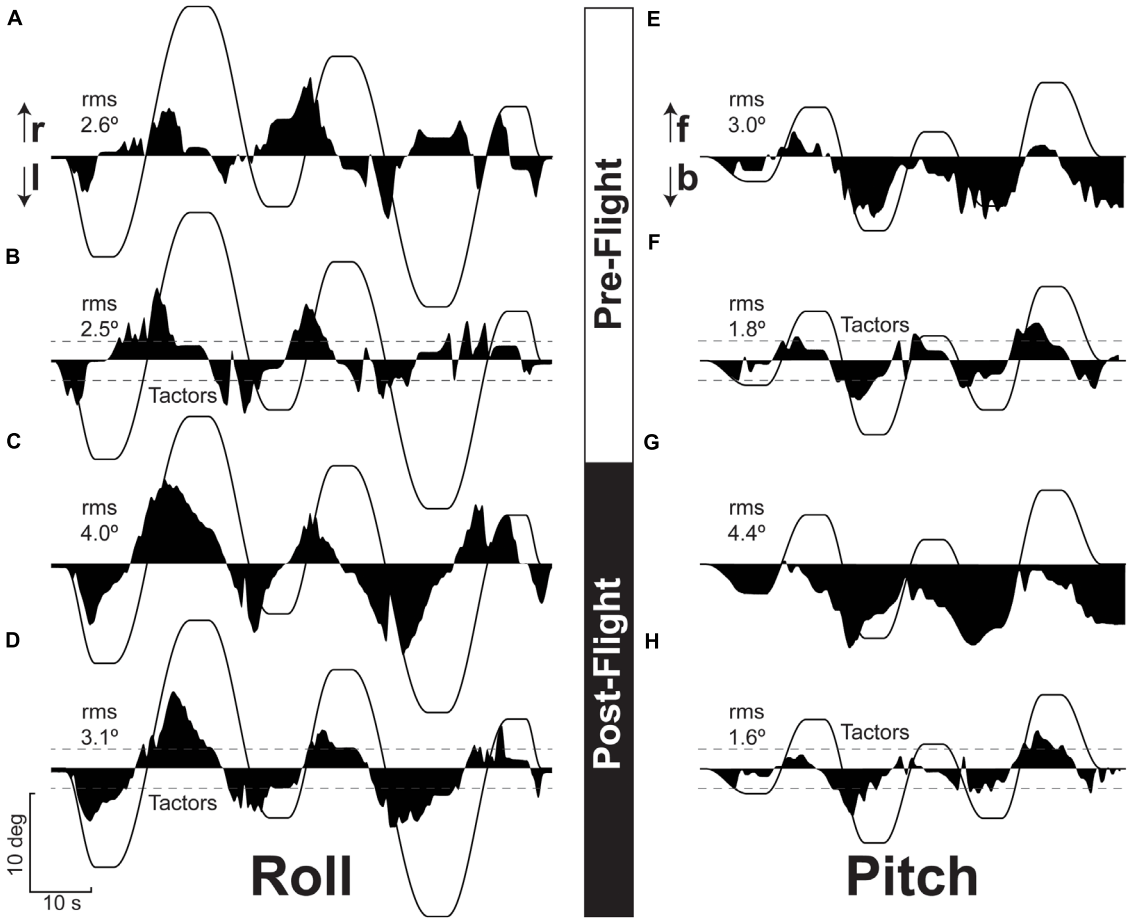

FIGURE 2 | Typical recordings of residual chair tilt after nulling (dark area) in response to imposed chair tilt (thin line) in roll (left side) and pitch (right side) before (top half) and after (bottom half) spaceflight without and with tactile tactile feedback. Performance without vibrotactile feedback is shown in **(A,C,E,G)**. Performance during the same sessions with vibrotactile feedback is shown in **(B,D,F,H)**. The dashed lines on these traces indicate the lowest threshold at which vibrotactile feedback was provided. The RMS error value for each test in also reported. r, right, l, left; f, forward; b, backward.

Rank test. Finally, the relationship between nulling performance in pitch and roll was evaluated with the Spearman's rho. A the critical statistic of $p < 0.05$ was used for all analytical testing.

The first and second preflight sessions were considered familiarization training for the initial exposures to the nulling task. Although there was no significant difference in RMS measures across the three preflight sessions for roll and pitch planes with or without vibrotactile feedback (Friedman's ANOVA), we felt that the latest preflight session was the most appropriate baseline measure since it would minimize any learning or recency effects. There did appear to be a trend of continued improvement during the later post-flight period, presumably due to learning effect with more frequent testing.

RESULTS

Figure 2 illustrates the typical nulling performance during roll and pitch tilt for both preflight and post-flight tests. As seen in this figure, the deviations in roll were typically symmetrical while the deviations in pitch tended to be asymmetrical with deviations more prevalent in the backward direction. The nulling performance was generally better in the roll plane compared to the pitch plane. A comparison of **Figure 2A** with **Figure 2C** and **Figure 2E** with **Figure 2G** exemplifies that larger RMS errors were observed post-flight relative to preflight.

Based on the Friedman's ANOVA, the effect of spaceflight was significant for both roll ($p < 0.001$) and pitch ($p = 0.047$). There was a significant difference in RMS error during roll tilt between preflight and R+0 (Wilcoxon signed rank, $p = 0.017$). RMS error returned to baseline values for both pitch and roll tilt by R+2 days (**Figure 3**).

The effectiveness of vibrotactile feedback to reduce RMS error both preflight and post-flight is illustrated in **Figure 3** by comparing performance without and with vibrotactile feedback. Using Wilcoxon signed rank, the difference in RMS error without and with vibrotactile feedback was significantly reduced during both roll and pitch tilt ($p < 0.001$). The consistency of this improved performance is further illustrated in **Figure 4** by plotting the nulling performance with and without vibrotactile

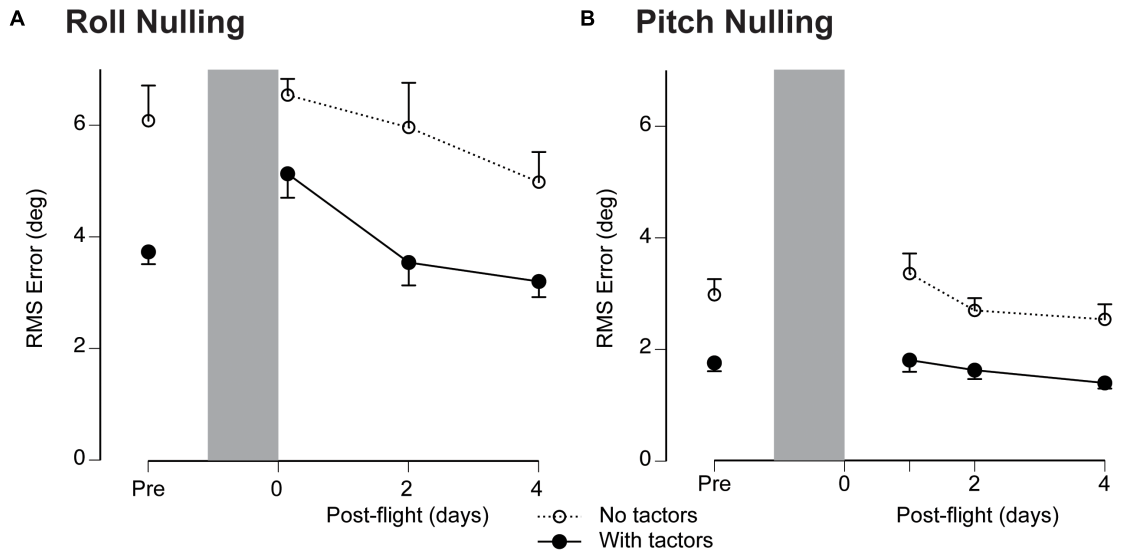

FIGURE 3 | RMS error values averaged for all subjects (±SE) for the nulling tasks during roll tilt **(A)** and pitch tilt **(B)** before (Pre) and after spaceflight without (open symbols) and with (filled symbols) the tactors. Shaded areas represent the flight (not at scale).

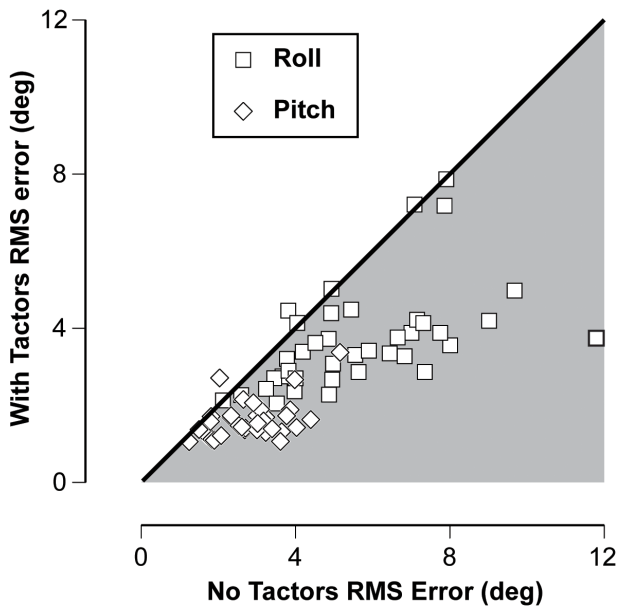

FIGURE 4 | Plot of RMS error values with and without vibrotactile feedback in both the roll and pitch tilt and across all test days for each of the 11 subjects. The unity line illustrates when performance is the same with and without vibrotactile feedback, while the shaded region below this line indicates when performance is improved (RMS error is reduced) with vibrotactile feedback.

performance for each session during roll and pitch tilt. The vast majority of points falls in the shaded region below the unity line, which illustrates that nulling performance was consistently greater with vibrotactile feedback.

The larger RMS errors observed during the roll stimuli (compare **Figure 3A** and **Figure 3B**) are likely attributable to the greater tilt angles in roll. However, differences in vestibular cues between these two stimuli may also explain the larger errors in roll. The roll stimuli elicited tilt disturbances using centripetal accelerations during variable radius centrifugation in contrast to the concordant otolith and canal cues elicited during pitch stimuli. Nevertheless, it is interesting to evaluate the individual performances across both stimuli. **Figure 5** illustrates that there was a significant correlation between an individual's performance in roll and pitch, including trials during which vibrotactile feedback was utilized. The Spearman's rho was 0.496 ($p < 0.001$), suggesting that better performers in roll also tended to be better performers in pitch.

DISCUSSION

The results of the present study agree with those obtained after the Space Life Sciences-2 mission (Merfeld, 1996): astronauts returning from spaceflight missions lasting from 11 to 15 days have difficulties controlling roll tilt in the absence of visual cues. By contrast, their control of pitch tilt is less affected by spaceflight. This difference is in agreement with tilt perception reports that showed astronauts overestimated the amplitude of roll tilt on R+0, but their perception of the amplitude of pitch tilt on R+1 was the same as preflight (Clément and Wood, 2014). Moreover, the improvements in performance using vibrotactile feedback suggests that the astronauts' motor function, i.e., their manipulation of the joystick, was unaffected by exposure to weightlessness.

When trying to null-out an overestimated tilt in roll immediately after landing, the subjects presumably overshoot and this induces a tilt in the opposite direction and therefore generates more instability. These effects, however, are no longer

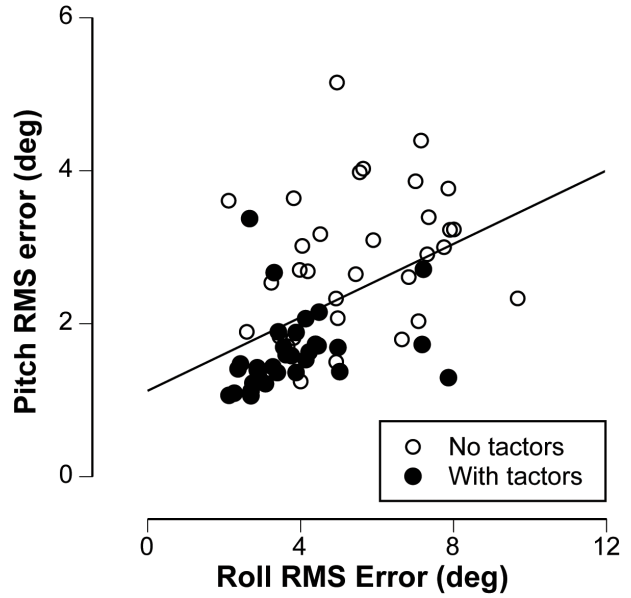

FIGURE 5 | Plot of the relationship between the nulling performance in pitch vs. the nulling performance in roll, including trials without (open symbols) and with (filled symbols) vibrotactile feedback. The line represents best linear fit, characterized by Spearman's correlation (rho = 0.496, $p < 0.001$).

present on R+2, suggesting that the deficits are due to re-adaptation to gravity, which persist throughout the early post-flight period. One limitation in our study was that the first test using the tilt chair took place at R+1, so it is possible that impairment in controlling pitch present at R+0 had recovered in part by R+1. Nevertheless, we demonstrated a significant effect of spaceflight for both pitch and roll tilt.

One possible interpretation for the impaired control of roll tilt after spaceflight is that perception of tilt in darkness becomes useless in weightlessness because body tilt in space will not result in a fall. The otoliths in the inner ear sense both head translation and head tilt relative to gravity. In weightlessness, head tilt no longer stimulates the otoliths, but they are still stimulated by head translation. Researchers have therefore proposed that during adaptation to weightlessness, the brain interprets all otolith output as translation only, and that this interpretation persists during the early post-flight period (Young et al., 1984; Parker et al., 1985). Other authors have suggested that in weightlessness some neural processes that integrate sensory input might use rotational cues for interpreting ambiguous gravitoinertial signals via internal models (Merfeld et al., 1999; Angelaki and Dickman, 2003; Merfeld, 2003; Angelaki et al., 2004; Zupan and Merfeld, 2005; Clark et al., 2015c).

The hypothesis of multi-sensory convergence suggests that in weightlessness, the brain switches from detecting gravity solely based on signals from the otolith organs to including signals from the semicircular canals (Angelaki and Dickman, 2003; Angelaki et al., 2004). In ground-based studies, Angelaki et al. (1999) used monkeys to show the importance of integrating multi-sensory information to discriminate tilt from translation. The monkeys moved their eyes horizontally to compensate for translation at 0.5 Hz, but their eyes moved only slightly during pure roll tilt. However, when their semicircular canals were plugged, the monkeys moved their eyes horizontally during all linear acceleration, regardless of whether the acceleration resulted from translation or tilt. This result is very similar to how the human eye moves in response to constant velocity rotation >0.3 Hz in an off-vertical axis (Wood, 2002). In the present study the semicircular canals were not stimulated during the roll tilt induced by centrifugation, whereas they were stimulated when the chair was tilted in pitch. The origin of the impairment in nulling performance in roll could be intra-vestibular conflict during centrifugation. However, Merfeld (1996) observed impairment in nulling performance when astronauts were tilted in roll relative to the gravity after spaceflight, which stimulated both the semicircular canals and the otoliths.

The other notable finding from the present study is that a simple vibrotactile sensory aid improves control of tilt when attempting to maintain an upright orientation within a limited tilt range. Previous tests have shown that a TSAS is a promising tool for reducing spatial disorientation in unusual acceleration environments (Rupert, 2000) when sensory cues are limited and sensorimotor function is compromised. Similar technology has been used to aid orientation in aeronautic and space environment (Rochlis and Newman, 2000; Van Erp et al., 2002) and to control balance in vestibular-compromised patients.

A study of one astronaut on board the International Space Station showed that localized vibration on the torso to indicate "down" made orienting in weightlessness faster, better, and easier (Van Erp and Van Veen, 2006). The effectiveness of this tactile aid increased over the first 7 days of staying in microgravity while the relative contribution of visual information to spatial orientation decreased over the same period.

In the recent years, vibrotactile feedback has been used successfully in aviation and to improve rehabilitation of individuals with balance disorders (Rupert, 2000; Wall, 2010). Tactile displays can help individuals to learn and change the limits of their stability while they stand or walk and to "tune" the motion inputs from their extra-vestibular system, which helps them improve their postural control. Wall and Kentala (2005) demonstrated that patients with vestibular dysfunction had improvements in postural performance when using tactile displays that record anterior-posterior motion at their waist. Vibrotactile feedback of tilt may also help the elderly or individuals with injuries that cause them to struggle with acute and chronic imbalance. Balance and vestibular rehabilitation therapy could be initiated in a laboratory setting, then the patients could supplement the clinical training at home using another version of the feedback device, and they could continuously wear a portable version to help prevent falls (Wall, 2010).

Since these effects may be attributable to vestibular (primarily otolith) adaptation to spaceflight, one would expect the differences to be larger following long duration spaceflight. Unfortunately, crewmembers now return from the International Space Station on the Soyuz, which lands in the Kazakhstan desert, and the earliest opportunity to perform post-flight measurements in a laboratory is >22 h after landing. Once

the NASA Multipurpose Crew Vehicle or the Space-X Dragon spacecraft are operational, it may be possible to test crewmembers of these vehicles sooner after landing, as it was the case with the Space Shuttle crewmembers.

CONCLUSION

The results of this study demonstrate that a simple belt using two tactors on each side improved the performance of a nulling task during all the sessions. An even simpler system that uses only one tactor on each side, cycling from a slow pulse rate to a steady pulse to indicate both the direction and magnitude of tilt, is currently being tested on astronauts returning from long-duration spaceflight on board the International Space Station. Our current understanding of the risk of impaired control of a spacecraft due to vestibular alterations associated with spaceflight is limited. The pilots' landing performance has been less than desired for both the Space Shuttle and the lunar lander during the Apollo program. Because of the extent physiological adaptation to weightlessness plays in these performance decrements, we can anticipate that the risk of failure will become much greater after a 6 months outbound exploration trip (without artificial gravity) than after a Space Shuttle mission lasting 1–2 weeks. Moreover, the effects of transition from weightlessness to Mars gravity rather than Earth gravity (0.38 g vs. 1 g) is unknown. Tactile feedback, as well as other sensorial countermeasures, including visual, vestibular, auditory, and multisensory displays (Paillard et al., 2014), could potentially mitigate these risks.

AUTHOR CONTRIBUTIONS

GC, MR, and SW contributed to study design, data collection, data analysis, and manuscript. All authors reviewed the manuscript.

FUNDING

This research was funded by the Human Health and Countermeasure Element of NASA's Human Research Program, the European Space Agency, and the Centre National d'Etudes Spatiales.

ACKNOWLEDGMENTS

We would like to thank the participating crewmembers and the personnel of the Neuroscience Laboratory at the NASA Johnson Space Center for their help with data collection and data analysis. We thank Kerry George for editing the manuscript.

REFERENCES

Angelaki, D. E., and Dickman, J. D. (2003). Gravity or translation: central processing of vestibular signals to detect motion or tilt. *J. Vestib. Res.* 13, 245–253.

Angelaki, D. E., McHenry, M. Q., Dickman, J. D., Newlands, S. D., and Hess, B. J. M. (1999). Computation of inertial motion: neural strategies to resolve ambiguous otolith information. *J. Neurosci.* 19, 316–327. doi: 10.1523/JNEUROSCI.19-01-00316.1999

Angelaki, D. E., Shaikh, A. G., Green, A. M., and Dickman, J. D. (2004). Neurons compute internal models of the physical laws of motion. *Nature* 430, 560–564. doi: 10.1038/nature02754

Arrott, A. P., and Young, L. R. (1986). M.I.T./Canadian vestibular experiments on the Spacelab-1 mission: 6. Vestibular reactions to lateral acceleration following ten days of weightlessness. *Exp. Brain Res.* 64, 347–357. doi: 10.1007/BF00237751

Arrott, A. P., Young, L. R., and Merfeld, D. M. (1990). Perception of linear acceleration in weightlessness. *Aviat. Space Environ. Med.* 61, 319–326.

Clark, B., and Graybiel, A. (1966). Factors contributing to the delay in the perception of the oculogravic illusion. *Am. J. Psychol.* 79, 377–388. doi: 10.2307/1420878

Clark, J. B., and Bacal, K. (2008). "Neurologic concerns," in *Principles of Clinical Medicine for Space Flight*, eds M. R. Barratt and S. L. Pool (New York, NY: Springer), 361–380. doi: 10.1007/978-0-387-68164-1_17

Clark, T. K., Newman, M. C., Merfeld, D. M., Oman, C. M., and Young, L. R. (2015a). Human manual control performance in hypergravity. *Exp. Brain Res.* 233, 1409–1420. doi: 10.1007/s00221-015-4215-y

Clark, T. K., Newman, M. C., Oman, C. M., Merfeld, D. M., and Young, L. R. (2015b). Human perceptual overestimation of whole body roll tilt in hypergravity. *J. Neurophysiol.* 113, 2062–2077. doi: 10.1152/jn.00095.2014

Clark, T. K., Newman, M. C., Oman, C. M., Merfeld, D. M., and Young, L. R. (2015c). Modeling human perception of orientation in altered gravity. *Front. Syst. Neurosci.* 9:68. doi: 10.3389/fnsys.2015.00068

Clarke, A. H., and Schönfeld, U. (2015). Modification of unilateral otolith responses following spaceflight. *Exp. Brain Res.* 233, 3613–3624. doi: 10.1007/s00221-015-4428-0

Clément, G., Denise, P., Reschke, M. F., and Wood, S. J. (2007). Human ocular counter-rolling and roll tilt perception during off-vertical axis rotation after spaceflight. *J. Vestib. Res.* 17, 209–215.

Clément, G., Moore, S., Raphan, T., and Cohen, B. (2001). Perception of tilt (somatogravic illusion) in response to sustained linear acceleration during space flight. *Exp. Brain Res.* 138, 410–418. doi: 10.1007/s002210100706

Clément, G., and Wood, S. J. (2013). Eye movements and motion perception during off-vertical axis rotation after spaceflight. *J. Vestib. Res.* 23, 13–22. doi: 10.3233/VES-130471

Clément, G., and Wood, S. J. (2014). Rocking or rolling – Perception of ambiguous motion after returning from space. *PLoS One* 9:e111107. doi: 10.1371/journal.pone.0111107

Glasauer, S., and Mittelstaedt, H. (1998). Perception of spatial orientation in microgravity. *Brain Res. Rev.* 28, 185–193. doi: 10.1016/S0165-0173(98)00038-1

Kentala, E., Vivas, J., and Wall, C. (2003). Reduction of postural sway by use of a vibrotactile balance prosthesis prototype in subjects with vestibular deficits. *Ann. Otol. Rhinol. Laryngol.* 112, 404–409. doi: 10.1177/000348940311200503

Merfeld, D. M. (1996). Effect of spaceflight on ability to sense and control roll tilt: human neurovestibular studies on SLS-2. *J. Appl. Physiol.* 81, 50–57. doi: 10.1152/jappl.1996.81.1.50

Merfeld, D. M. (2003). Rotation otolith tilt-translation reinterpretation (ROTTR) hypothesis: a new hypothesis to explain neurovestibular spaceflight adaptation. *J. Vestib. Res.* 13, 309–320.

Merfeld, D. M., Zupan, L., and Peterka, R. J. (1999). Humans use internal models to estimate gravity and linear acceleration. *Nature* 398, 615–618. doi: 10.1038/19303

Moore, S. T., MacDougall, H. G., Lescue, X., Speyer, J. J., Wuyts, F., and Clark, J. B. (2008). Head-eye coordination during simulated orbiter landings. *Aviat. Space Environ. Med.* 79, 888–898. doi: 10.3357/ASEM.2209.2008

Paillard, A. C., Quarck, G., and Denise, P. (2014). Sensorial countermeasures for vestibular spatial disorientation. *Aviat. Space Environ. Med.* 85, 563–567. doi: 10.3357/ASEM.3735.2014

Paloski, W. H., Oman, C. M., Bloomberg, J. J., Reschke, M. F., Wood, S. J., Harm, D. L., et al. (2008). Risk of sensory-motor performance failures during exploration-class space missions: a review of the evidence and recommendations for future research. *J. Gravit. Physiol.* 15, 1–29.

Parker, D. E., Reschke, M. F., Arrott, A. P., Homick, J. L., and Lichtenberg, B. K. (1985). Otolith tilt translation reinterpretation following prolonged weightlessness: implications for pre-flight training. *Aviat. Environ. Space Med.* 56, 601–609.

Reschke, M. F., and Parker, D. E. (1987). Effects of prolonged weightlessness on self-motion perception and eye movements evoked by roll and pitch. *Aviat. Space Environ. Med.* 58, A153–A158.

Rochlis, J. L., and Newman, D. J. (2000). A tactile display for International Space Station extra-vehicular activity. *Aviat. Space Environ. Med.* 71, 571–578.

Rupert, A. H. (2000). Tactile situation awareness system: proprioceptive prostheses for sensory deficiencies. *Aviat. Space Environ. Med.* 71, A92–A99.

Shull, P. B., and Damian, D. D. (2015). Haptic wearables as sensory replacement, sensory augmentation and trainer – a review. *J. Neuroeng. Rehabil.* 12:59. doi: 10.1186/s12984-015-0055-z

Sienko, K. H., Balkwill, M. D., Oddsson, L. I. E., and Wall, C. (2008). Effects of multi-directional vibrotactile feedback on vestibular-deficient postural performance during continuous multi-directional support surface perturbations. *J. Vestib. Res.* 18, 273–285.

Sienko, K. H., Whitney, S. L., Carender, W. J., and Wall, C. (2017). The role of sensory augmentation for people with vestibular deficits: real-time balance aid and/or rehabilitation device? *J. Vestib. Res.* 27, 63–76. doi: 10.3233/VES-170606

Van Erp, J. B., and Van Veen, H. A. (2006). Touch down: the effect of artificial touch cues on orientation in microgravity. *Neurosci. Lett.* 404, 78–82. doi: 10.1016/j.neulet.2006.05.060

Van Erp, J. B. F., Veltman, J. E., Van Veen, H. A. H. C., and Oving, A. B. (2002). "Tactile torso display as a countermeasure to reduce night vision goggles induced drift," in *Proceedings of the RTA/HFM Symposium on Spatial Disorientation*, La Coruna.

Wall, C. (2010). Application of vibrotactile feedback of body motion to improve rehabilitation in individuals with imbalance. *J. Neurol. Phys. Ther.* 34, 98–104. doi: 10.1097/NPT.0b013e3181dde6f0

Wall, C., and Kentala, E. (2005). Control of sway using vibrotactile feedback of body tilt in patients with moderate and severe postural control deficits. *J. Vestib. Res.* 15, 313–325.

Wood, S. J. (2002). Human otolith-ocular reflexes during off-vertical axis rotation: effect of frequency on tilt-translation ambiguity and motion sickness. *Neurosci. Lett.* 323, 41–44. doi: 10.1016/S0304-3940(02)00118-0

Wood, S. J., Black, F. O., MacDougall, H. G., and Moore, S. T. (2009). Electrotactile feedback of sway position improves postural performance during galvanic vestibular stimulation. *Ann. N. Y. Acad. Sci.* 1164, 492–498. doi: 10.1111/j.1749-6632.2009.03768.x

Young, L. R., Oman, C. M., Watt, D. G. D., Money, K. E., and Lichtenberg, B. K. (1984). Spatial orientation in weightlessness and readaptation to Earth's gravity. *Science* 225, 205–208. doi: 10.1126/science.6610215

Zupan, L. H., and Merfeld, D. M. (2005). Human ocular torsion and perceived roll responses to linear acceleration. *J. Vestib. Res.* 15, 173–183.

Conflict of Interest Statement: The authors declare that the research was conducted in the absence of any commercial or financial relationships that could be construed as a potential conflict of interest.

frontiers in Physiology

ORIGINAL RESEARCH
published: 16 April 2019
doi: 10.3389/fphys.2019.00397

Sleep Is Compromised in −12° Head Down Tilt Position

Alessa L. Boschert[1], David Elmenhorst[2,3], Peter Gauger[1], Zhili Li[4], Maria T. Garcia-Gutierrez[5], Darius Gerlach[1], Bernd Johannes[1], Jochen Zange[1], Andreas Bauer[2,6] and Jörn Rittweger[1,7]*

[1] Department of Muscle and Bone Metabolism, German Aerospace Center (DLR), Institute of Aerospace Medicine, Cologne, Germany, [2] Forschungszentrum Jülich, Institute of Neuroscience and Medicine (INM-2), Jülich, Germany, [3] Division of Medical Psychology, University of Bonn, Bonn, Germany, [4] State Key Laboratory of Space Medicine Fundamentals and Application, China Astronaut Research and Training Center, Beijing, China, [5] High Studies Center Alberta Gimenez (CESAG) University of Comillas, Palma de Mallorca, Spain, [6] Neurological Department, Medical Faculty, Heinrich-Heine-University, Düsseldorf, Germany, [7] Department of Pediatrics and Adolescent Medicine, University of Cologne, Cologne, Germany

Recent studies are elucidating the interrelation between sleep, cranial perfusion, and cerebrospinal fluid (CSF) circulation. Head down tilt (HDT) as a simulation of microgravity reduces cranial perfusion. Therefore, our aim was to assess whether HDT is affecting sleep (clinicaltrials.gov; identifier NCT 02976168). 11 male subjects were recruited for a cross-over designed study. Each subject participated in two campaigns each comprising 3 days and 2 nights. Intervention started on the second campaign day and consisted of maintenance of horizontal position or −12° HDT for 21 h. Ultrasound measurements were performed before, at the beginning and the end of intervention. Polysomnographic measurements were assessed in the second night which was either spent in horizontal posture or at −12° HDT. Endpoints were sleep efficiency, sleep onset latency, number of sleep state changes and arousals, percentages of N3, REM, light sleep stages and subjective sleep parameters. N3 and REM sleep reduced by 25.6 and 19.1 min, respectively (P = 0.002, g = -0.898; P = 0.035, g = -0.634) during −12° HDT. Light sleep (N1/2) increased by 33.0 min at −12° HDT (P = 0.002, g = 1.078). On a scale from 1 to 9 subjective sleep quality deteriorated by 1.3 points during −12° HDT (P = 0.047, g = -0.968). Ultrasonic measurement of the venous system showed a significant increase of the minimum (P = 0.009, $P < 0.001$) and maximum (P = 0.004, P = 0.002) cross-sectional area of the internal jugular vein at −12° HDT. The minimum cross-sectional area of the external jugular vein differed significantly between conditions over time (P = 0.001) whereas frontal skin tissue thickness was not significantly different between conditions (P = 0.077, P = 0.811). Data suggests venous congestion at −12° HDT. Since subjects felt comfortable with lying in −12° HDT under our experimental conditions, this posture only moderately deteriorates sleep. Obviously, the human body can almost compensate the several fold effects of gravity in HDT posture like an affected CSF circulation, airway obstruction, unusual patterns of propioception and effects on the cardiovascular system.

Keywords: head down tilt, simulated microgravity, bed rest, polysomnography, sleep

OPEN ACCESS

Edited by:
Gilles Clement, Centre National de la Recherche Scientifique (CNRS), France

Reviewed by:
Giovanna Zoccoli, University of Bologna, Italy
Nastassia Navasiolava, Centre Hospitalier Universitaire d'Angers, France

****Correspondence:***
Alessa L. Boschert
alessa.boschert@web.de

Specialty section:
This article was submitted to Environmental, Aviation and Space Physiology, a section of the journal Frontiers in Physiology

Received: *29 September 2018*
Accepted: *21 March 2019*
Published: *16 April 2019*

Citation:
Boschert AL, Elmenhorst D, Gauger P, Li Z, Garcia-Gutierrez MT, Gerlach D, Johannes B, Zange J, Bauer A and Rittweger J (2019) Sleep Is Compromised in −12° Head Down Tilt Position. Front. Physiol. 10:397. doi: 10.3389/fphys.2019.00397

Abbreviations: HDT, Head down tilt; NIRS, Near infrared spectroscopy; TCD, Transcranial Doppler ultrasound.

INTRODUCTION

Head down tilt (HDT) reduces intracranial perfusion and leads to jugular vein congestion (Marshall-Goebel et al., 2016; Kramer et al., 2017). Moreover, an increased intracranial pressure is a consequence of HDT (Lawley et al., 2017). Xie et al. (2013) have demonstrated that sleep, among other factors, is vital for cranial fluid exchange and metabolic clearance of by-products via the "glymphatic" system. Transport via the "glymphatic" system is also dependent on body position (Lee et al., 2015). Yet one of the major drivers for intracranial fluid regulation is respiration (Dreha-Kulaczewski et al., 2015; Delaidelli and Moiraghi, 2017). Body position, altered respiration and the accompanying changed intracranial fluid dynamics are likely to affect sleep at HDT.

Of note, HDT is also used as a ground-based model of spaceflight (Kakurin et al., 1976; Pavy-Le Traon et al., 2007). Fluid shifts in the direction of the head and venous congestion in particular are salient effects of both spaceflight and HDT.

Sleep is often disturbed in astronauts. Reduced sleep quality is frequently ascribed to the "multistressor environment" onboard the space station, comprising challenges by noise, workload, lighting, sleep shifting and hypercapnia. All these factors combined eventually result in deteriorated sleep quality and quantity. A daily sleep period of a sufficient time (8.5 h) is set during missions. However, astronauts reported an actual sleep duration of only about three quarters of the available sleeping time (Dinges et al., 2013). Sleep duration is further reduced during periods of circadian misalignment (Flynn-Evans et al., 2016). The shortened and disturbed sleep during shuttle flights and on the International Space Station (Dijk et al., 2001; Whitmire et al., 2009) is changed to an extent that has detrimental effects on cumulative sleep duration and performance in Earth-based studies (Van Dongen et al., 2004). Polysomnographic recordings showed altered sleep architecture with a reduction in deep sleep (Gundel et al., 1997; Dijk et al., 2001). This is in accordance with astronauts specifically complaining about impaired refreshment post-sleep (Dijk et al., 2001) as deep sleep is vital for recovery. The reduction in sleep duration also results in increased susceptibility to stress while physical exhaustion rises due to the impaired sleep quality (Dinges et al., 2013). All these factors combined ultimately result in a higher risk of misconception and errors. Additionally, sleep disturbance is a main reason for medication intake in space (Barger et al., 2014). The effects of these medications – for example sleepiness – can last for several hours. This, again, places the astronauts at higher risk during work periods. The described reasons for inefficient sleep and their possible impact on astronauts' performance necessitate a better understanding of sleep during microgravity as well as during ground-based bed rest studies as a simulation of microgravity.

To the best of our knowledge, it had not been considered that alterations in intracranial fluid regulation, clearance of metabolites and sleep performance can impact each other negatively at −12° HDT. However, based on the alterations above, it seems quite possible. There are two studies reporting a reduction in deep sleep (stage 4 according to Rechtschaffen and Kales) as well as increased arousal frequency during experimental −6° HDT bed rest (Mizuno et al., 2005; Komada et al., 2006) that lasted for 3 days. Both studies used a counterbalanced design with the subjects staying in horizontal position at another session. Gkivogkli et al. (2016) assessed sleep parameters repeatedly during a 50 days −6° bed rest study. Subjects were randomly assigned to two groups. In contrast to the control group, the training group performed reactive sledge jumping three to four times a week. The preliminary results published in the abstract for the SAN2016 Meeting suggest an increase in N1 sleep stage, and a decrease in the total sleep time, N2, N3, and REM sleep stage in the control group between baseline and 21 days of −6° HDT. In the training group N1 and N3 sleep stage seem to increase, N2 sleep stage decreases, while duration REM sleep stage does not change on the 21st day of −6° HDT compared to baseline. Meck et al. (2009) reported that about half of their subjects complained about impaired sleeping, especially in the first week of their 90 day head down bed rest, but also before starting the bed rest. This is in accordance with results from a study conducted by DeRoshia and Greenleaf (1993). Subjects' subjective sleep quality improved after finishing the 30 days −6° bed rest. However, HDT-effects in the last three bed rest studies were assessed longitudinally, and may thus have been confounded with effects of isolation or lack of exercise. Yet, evaluation of objective sleep parameters is not done in most studies.

Therefore, we decided to study the short-term effects of HDT on sleep using the current guidelines of the American Academy of Sleep Medicine (AASM). As our interest was based on postulated effects of intracranial fluid regulation upon metabolic clearance, we decided to limit the exposure to HDT to one night only. We hypothesized that HDT will negatively affect sleep performance. We deliberately used −12° HDT rather than −6° HDT as −12° HDT has shown to be more efficient when measuring possible correlation between intracranial fluid systems (Marshall-Goebel et al., 2016; Kramer et al., 2017).

MATERIALS AND METHODS

Subjects

The study has been registered at clinicaltrials.gov (identifier NCT 02976168). It conformed to the declaration of Helsinki and had been approved by the ethics committee of the regional medical board (Ärztekammer Nordrhein). All subjects gave written informed consent in accordance with the Declaration of Helsinki. The IPCog Study (Intracranial Pressure and brain function: effects of HDT upon brain perfusion and cognitive performance) was conducted at the :envihab, German Aerospace Centre (DLR), Cologne, Germany. Thirteen male subjects were recruited for the study. Volunteers' physical and psychological health was confirmed with questionnaires and medical examination. Exclusion criteria comprised among others a history of sleeping disorders, gastro-esophageal reflux, hiatus hernia, abuse of alcohol, medication or drugs and smoking within a period of 6 months prior to the study (**Table 1**). One week prior to the study onwards, subjects did not consume any caffeine. Two out of the thirteen subjects dropped out after their inclusion. One had to leave during data collection because of family issues, and

TABLE 1 | Exclusion criteria.

Exclusion criteria of the IPCog study	
Medical history	Migraine/chronic headaches Psychological /central nervous disorders Sleeping disorders/inability to sleep on the back Diabetes mellitus Pronounced orthostatic intolerance Kidney disorder Thyroid gland disorder Anemia Lumbar surgery/lumbar spine trauma/ chronic back complaints Elevated risk of thrombosis or coagulopathy Hiatus hernia/gastro-oesophageal reflux Ophthalmological conditions, such as glaucoma etc. weak concentration/previous psychiatric illness
Medication/Substance intake	Drug, medication, alcohol abuse Smoking within 6 months prior to study Medication impairing cognitive function, autonomic function Medication influencing any of the study procedures
Others	Motor/sensory deficits Contraindications against MRI Any medical condition considered a contraindication to study procedures/would make it unsafe/confound measurements

the other reported gastro-esophageal reflux and vomiting during the −12° HDT night. This made it impossible to stay in HDT position. The 11 subjects finishing the study had a age of 30 years ± 10.2 years, a height of 179.82 cm ± 6.6 cm and a weight of 79.82 kg ± 7.3 kg, mean ± SD.

Study Design and Conduction

Polysomnographic recordings were one of the secondary outcome measures of the IPCog study, with the aim to substantiate any detrimental effects of sleeping in −12° HDT position. Primary outcome was the result of the cognitive test battery. The study was carried out in a cross-over design from March 2016 to November 2016, totaling 10 campaigns. Each campaign consisted of 3 days and, therefore, two nights (**Figure 1**). The interventional phase started on the second campaign day, lasting for approximately 21 h. Subjects spent the whole interventional phase either lying in horizontal position or at −12° HDT.

During the first night subjects slept in horizontal posture. The second night belonged to the interventional period. Therefore, subjects slept either at −12° HDT as experimental condition or horizontally as control condition. All subjects participated in both campaigns with approximately a week's time period in between.

Subjects participated in groups of three or two subjects. Each of them slept in their own room which was the same for both campaigns. To maintain −12° HDT and 0°, respectively, subjects did not use pillows.

The polysomnographic device was applied during both nights of each campaign. Lights on and off times were fixed beforehand and arranged stepwise for the subjects participating in the same campaign (21:45–06:00, 22:00–06:30, 22:30–07:15). Stepwise arrangement and the minor difference in lights-off time were due to the arrangement of daytime measurements. Otherwise it would not have been possible to perform two measurement blocks on

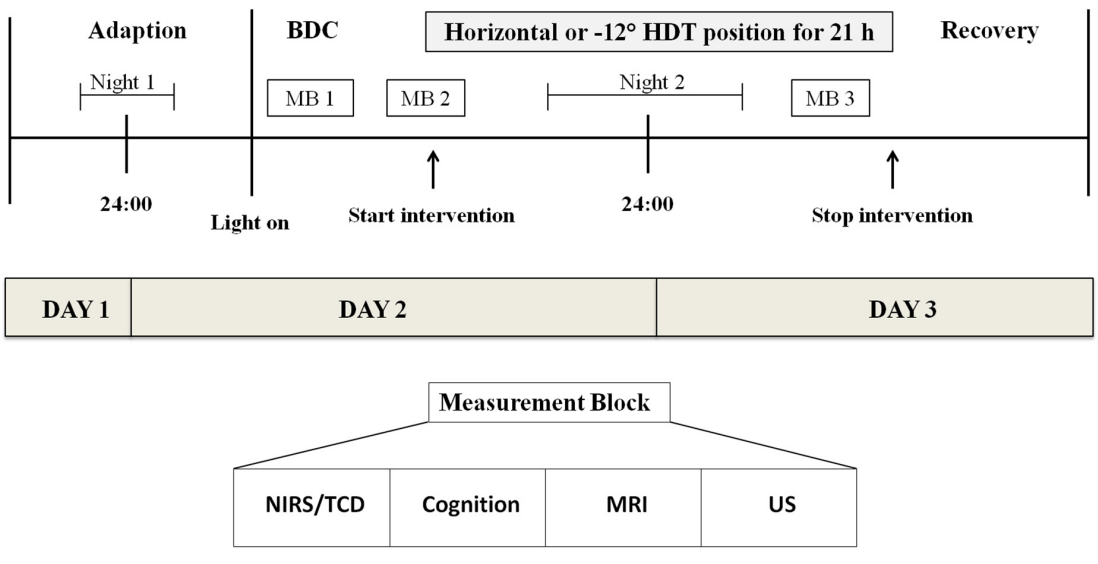

FIGURE 1 | Campaign overview. Each subject participated in two campaigns, once staying in horizontal posture and once being tilted to −12° HDT. Between these two campaigns there was about a week's time. Measurement blocks were carried out on both interventional days comprising five measurements. BDC, Baseline data collection; MB, Measurement block; NIRS, Near-infrared spectroscopy; TCD, Transcranial Doppler ultrasound of the mid-cerebral artery; CTB, cognitive test battery; MRI, (functional) magnetic resonance imaging; US, ultrasound of the jugular vein and facial thickness.

the second campaign day. To record any aberration from the predefined sleeping times, subjects were asked to set a marker when the light was turned off. Subjects were not allowed to sleep outside those predefined sleeping times.

While sleeping at −12° HDT, special mattress pads were used to prevent sliding headwards. Belts were provided to facilitate the subjects pulling themselves up toward feet direction. An additional belt was provided offering the subjects the possibility to fix their feet and, thus, prevent sliding. This was done to minimize any effects on sleeping due to sliding. Additionally, subjects suffering from back pain during −12° HDT were offered a painkiller (Ibuprofen 400 mg) upon request and under medical supervision. Out of all, only subject 0E and 0F were given one tablet each before going to sleep at −12° HDT.

Whether subjects stayed in horizontal or −12° HDT position first was randomized directly before the start of the interventional phase in the afternoon of the campaign's second day. Randomization was done according to even and uneven numbers of a dice throw. To ensure a balanced assignment a maximum two out of three subjects participating in the same campaign could potentially start at −12° HDT. If the group comprised of two subjects, only one of them was tilted to −12° HDT during the first campaign. Randomization was performed by scientific staff members.

Six of the eleven subjects were tilted to −12° HDT during the first campaign and remained in horizontal posture during the second. Five of them started in horizontal position during the first campaign and stayed at −12° HDT during the second campaign.

Data Acquisition

Polysomnographic data were recorded with two portable SOMNOscreen Plus devices (SOMNOmedics, Randersacker, Germany) and with one SOMNOscreen device (SOMNOmedics, Randersacker, Germany). Subjects were tested with the same device type during both interventional phases. Recordings included electroencephalography (EEG), electrooculography (EOG), electrocardiography (ECG), submental electromyography (EMG), peripheral oxygen saturation at finger level, as well as abdominal and thoracic belts to assess breathing movement. With the SOMNOscreen Plus devices, EEG electrodes were placed at positions O1, O2, C3, C4, F3, and F4 according to the international 10–20 System and at O1, C3, C4, and F3 positions with the SOMNOscreen device. Additional electrodes were placed at the mastoids on both sides, ground and reference position in all devices. Cup electrodes by Ambu (Ambu Neuroline Cup, Bad Nauheim, Germany) were used and fixed with EC2 electrode cream by Grass. To further ensure sufficient adhesion of the electrodes small pieces of compresses (Gazin Mullkompressen, Lohmann and Rauscher, Rengsdorf/Neuwied, Germany) were used to fixate the electrodes. For the submental derivations and on other positions where applicable, adhesive electrodes by Ambu (Ambu Neuroline 720, Bad Nauheim, Germany) were used. During the entire study, electrodes were positioned by the same operator. Before attaching the electrodes the skin was prepared with Nuprep skin Prep Gel (Weaver and Company, Aurora, United States) and cleaned with alcoholic disinfectant. This was done to lower skin impedance in order to improve EEG signal strength. An impedance of less than 10 kΩ (calibrated against the mastoid electrodes) was considered to be sufficient.

During the cognitive test battery conducted on the morning of the second and third day subjective sleep quality and subjective refreshment were assessed by using a scale from one to nine. These scales were devised by the scientific team. In both scales, nine represented the best quality of sleeping and resting, respectively. The subjects also indicated their sleep duration by stating their assumed sleeping hours.

Effects of body position on the venous system were assessed during measurement blocks on the second and third campaign day. Frontal tissues thickness was obtained as a surrogate parameter for potential fluid shifts toward the head in general. Measurements were always in the second time slot of each measurement block. Therefore, measurements during the first and third measurement block were performed at the same time of the day. This allowed accounting for potential daytime-dependent effects when comparing measurements of the same campaign.

Data was obtained by B-mode ultrasound using a myLab 25 scanner with a linear 8–10 MHz probe (Esaote, Milan, Italy). The same operator performed the measurement throughout the study. Tissue thickness was assessed on both sides of the front. For each side three measurements during each measurement block were performed. Minimum and maximum cross-sectional areas of the internal and external jugular veins were assessed on both sides. The probe positions were marked on the subject's skin in measurement block 1 for subsequent measurements of the campaign.

Assessment of cranial perfusion included transcranial Doppler ultrasound (TCD), near infrared spectroscopy (NIRS), MRI measurements and a cognitive test battery. TCD and NIRS measurements were assessed simultaneously. Each assessment lasted for at 20 min. Measurements during the first measurement block also included the tilting process: NIRS and TCD assessment was performed for 20 min in horizontal position. The subjects were the tilted during the measurement and data acquisition then continued for further 20 min. MRI measurements were carried out using a special wedge to maintain −12° HDT position. MRI sequences comprised of functional MRI [echo planar imaging – blood oxygenation level dependent (BOLD)], T1 weighed magnetization prepared rapid gradient echo (MPRAGE), pulsed arterial spin level (pASL) with an inversion time (TI) of 1800 ms and phase contrast (PC) imaging. A cognitive test battery was used to assess executive functions, psychomotor vigilance, reaction time, logic, working memory and continuous performance. Analysis is currently ongoing.

Data Processing and Analysis

The manual EEG analysis met the criteria of the AASM. After having applied an ECG filter, each night's sleep was analyzed in intervals of 30 s classifying them as either sleep stages N1–N3 and REM or awake according to the rules of the AASM (Iber et al., 2007). Additionally, we assessed sleep onset latency, changes of sleep states and sleep efficiency (percentage of sleeping time of in bed time). We used the DOMINO Software

(Version 2.7.0, 07.09.2015) by SOMNOmedics (SOMNOmedics, Randersacker, Germany). The channels used were EOG, EEG and submental EMG. Each of the EEG signals was derivated against the signal of the mastoid (M1, M2) electrodes on the opposite side (O1:M2, O2:M1, C3:M2, C4:M1, F3:M2, F4:M1). Where possible, the EEG signals from the left side were used for analysis. Therefore the electrode positions O1, C3, C4, and F3 were used with the SOMNOscreen device. AASM criteria for arousals were applied.

Total sleep time was used, rather than the time in bed, to prevent confounding influences by lights on/off periods. The polysomnographies were all analyzed by the same operator to avoid any interpersonal difference in the analysis. The operator was a scientific staff member of the study and, therefore, not blinded.

Analysis of peripheral tissue oxygenation at the index or middle finger included the mean oxygenation, minimum oxygenation and the time peripheral tissue oxygenation was below 90% as given by the DOMINO Software after the automatic exclusion of artifacts. Abdominal and thoracic belts often shifted out of place due to the subjects' sliding toward head direction. Therefore, an adequate analysis of breathing movement was not possible.

Whilst the polysomnographic devices were applied during the first night for habituation purposes they were not analyzed. This was done to reduce any influences of the first-night effect on the actual experimental night. Therefore, only the second night was statistically analyzed. Likewise, subjective sleep quality was evaluated solely for the experimental night.

The mean of the three measurements performed during one session on one side was used for analysis of frontal tissue thickness. Variation in jugular vein diameter was determined by substracting the minimum diameter of each vein from its maximum diameter.

Due to technical issues, ultrasonic measurements of subject R and S could not be performed. Therefore, they were not included in the statistical analysis.

Data analysis was based on the per protocol approach, therefore excluding the two drop-outs mentioned beforehand. Defining the experimental condition (0° or −12° HDT) as fixed effect and subjects as random effects, linear mixed models were applied. Additionally, the models were checked for non-normal distribution of residuals and heteroscedacity. Box-cox transformations were used when needed. The level of significance was set at $P = 0.05$. R Studio (Version 1.0.136, R Studio) was used to carry out the statistical analysis, hereby using the lme-function to create the linear mixed models. Because of the small sample size Hedge's g was used to calculate the effect size rather than Cohen's d.

RESULTS

A significant increase ($P = 0.002$, $g = 1.078$) of the percentage of light sleep (N1 + N2) of the total sleep time could be detected during −12° HDT (59.9% ± 7.2%) in comparison with 0° (50.9% ± 9.4%). The fraction increased in 10 out of the 11 subjects, the maximum rise being 21.6%. One of the subjects (0J) showed a slight decrease of the light sleep (-3.1%) during the −12° HDT night.

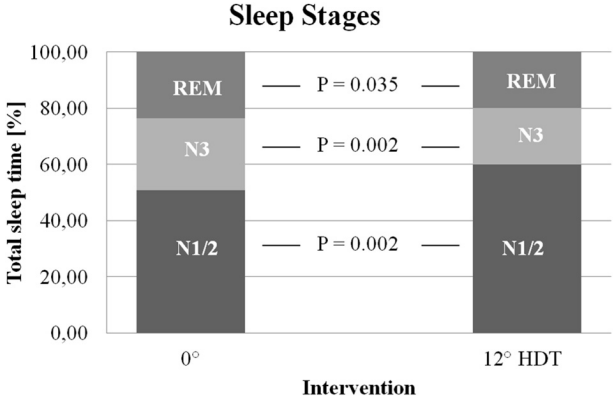

FIGURE 2 | Sleep stages. Percentage of slow wave sleep (20.2% ± 5.2% vs. 25. 4% ± 6.4%) and REM sleep (19.9% ± 5.7% vs. 23.7% ± 6.3%) were reduced during the −12° HDT night. Percentage of light sleep increased (59.9% ± 7.2% vs. 50.9% ± 9.4%) when compared to horizontal position. HDT, Head down tilt.

There was a significant decrease in percentage of slow wave sleep (N3) ($P = 0.002$, $g = -0.898$) from the 0° night (25.4% ± 6.4%) to the −12° HDT night (20.2% ± 5.2%). This decrease ranged between 1.4 and 12.7% in 10 subjects, while the amount of N3 remained the same (17.9%) in the last subject (0E) during both nights.

There was a significant decrease ($P = 0.035$, $g = -0.634$) in the percentage of REM sleep of the total sleep time when comparing the night in horizontal position (23.7% ± 6.3%) to −12° HDT (19.9% ± 5.7%). The extent of the decline varied between 1.5 and 9.7%. 2 Subjects (0J, 0N) showed an increase in the amount of REM sleep during −12° HDT (**Figure 2**).

The mean time period for each of the sleep stages can be seen in **Table 2**. There were no significant differences between 0° position and −12° HDT position.

Sleep efficiency was not significantly different ($P = 0.48$) between the −12° HDT night (80.1% ± 9.6%) compared to that spend in 0° (82.4% ± 14.7%).

Total sleep time was not significantly affected ($P = 0.44$) by −12° HDT (410.4 min ± 55 min vs. 422 min ± 79.1 min at 0°). There was no significant difference in sleep onset latency ($P = 0.30$). Both, maximum (110 min) and minimum (2.0 min) onset latency occurred during the night subjects stayed in horizontal posture. However, when excluding the subject with the maximum sleep onset latency, the latency is significantly prolonged at −12° HDT. We found no significant difference in the number of sleep state changes when comparing the two experimental conditions (−12°: 128.1 ± 37.3; 0°: 119 ± 33.2; $P = 0.19$).

The mean peripheral tissue oxygenation at finger level remained unchanged (94.5%) during both nights with standard variation only differing slightly (2.8% vs. 2.9%). The lowest basal oxygenation of 88% was measured during −12° HDT. There was

TABLE 2 | Objective sleep parameters.

	0° position		−12° HDT position	
TST (min)	422.00 ± 79.10		410.40 ± 55.00	
Sleep onset latency (min)	24.90 ± 29.10		35.00 ± 13.70	
Number of sleep state changes	119.00 ± 33.20		128.10 ± 37.30	
Sleep efficiency (%)	82.40 ± 14.70		80.10 ± 9.60	
Sleep stages	**(min)**	**(% of TST)**	**(min)**	**(% of TST)**
Light sleep (Stage N1/N2)	211.53 ± 45.50	50.9 ± 9.4	244.49 ± 34.10	59.9 ± 7.2*
Slow wave sleep (Stage N3)	107.86 ± 34.77	25.4 ± 6.4	82.23 ± 22.59	20.2 ± 5.2*
REM sleep	102.77 ± 36.37	23.7 ± 6.3	83.64 ± 31.49	19.9 ± 5.7†

*Table giving an overview of the objective sleep parameters at −12° HDT and horizontal position. The values are given in means ± standard deviation. *P = 0.002, †P = 0.035 in comparison to (% of TST) in 0° position. HDT, Head down tilt; TST, Total sleep time.*

no significant change in minimum oxygenation detectable (−12°: 85.9% ± 6.8%; 0°:83.6% ± 11%; $P = 0.41$). The percentage of the mean time with the peripheral tissue oxygenation being lower than 90% showed no significant difference ($P = 0.95$) (**Table 3**).

There was a significant decrease ($P = 0.047$, $g = -0.968$) in subjective sleep quality during the −12° HDT night (4.8 ± 1.5) when compared to the 0° night (6.1 ± 1.1). However, subjective sleep duration did not differ significantly between the experimental conditions (−12°: 5.3 ± 1.8 h; 0°: 6.4 ± 1.4 h; $P = 0.10$). The subjective feeling of refreshment showed no significant difference ($P = 0.09$) between the −12° HDT night (5.6 ± 1.8) and the night spend in horizontal position (6.3 ± 1.3) (**Table 4**).

In comparison to the baseline data collected during measurement block 1 of each campaign frontal tissue thickness did not differ significantly on the first ($P = 0.077$) and the second interventional day ($P = 0.811$) at −12° HDT (**Table 5**). Frontal tissue thickness of the left and right side were differing ($P = 0.009$). There was no difference between conditions over time ($P = 0.116$).

The maximum cross-sectional area of the internal jugular vein increased significantly at −12° HDT on interventional day 1 (1.46 cm^2 ± 0.66 cm^2, $P = 0.004$) and day 2 (−12° HDT: 1.41 cm^2 ± 0.66 cm^2, $P = 0.002$) when compared to the baseline data collection (0.87 cm^2 ± 0.54 cm^2). No difference could be detected when comparing the left and right side ($P = 0.161$). The minimal cross-sectional area of the internal jugular vein was also significantly different between interventional condition (−12° HDT day1: 1.31 cm^2 ± 0.64 cm^2, day 2: 1.18 cm^2 ± 0.62 cm^2) and baseline data (0.65 cm^2 ± 0.52 cm^2) on both interventional days ($P = 0.009$, $P < 0.001$, respectively). It did not differ between both sides over time ($P = 0.369$). The variation of the cross-sectional area of the internal jugular vein was different when comparing both sides ($P = 0.003$). It did not differ significantly between both conditions ($P = 0.686$).

The maximum cross-sectional of the external jugular vein was not significantly different with condition over time ($P = 0.415$), between the HDT- and control group ($P = 0.128$) and between sides ($P = 0.271$). However, the minimal cross-sectional area of the external jugular vein did differ between the conditions over time ($P = 0.001$). There was no significant difference between both sides over time ($P = 0.980$).

TABLE 3 | Measurement of peripheral oxygen saturation at finger level.

	0°	−12° HDT
Mean SpO_2 (%)	94.50 ± 2.90	94.50 ± 2.80
Minimal SpO_2 (%)	85.90 ± 6.80	83.60 ± 11.00
SpO_2 < 90% (%) [(min)]	10.70 ± 22.00 (31.29 ± 83.49)	11.30 ± 21.90 (40.71 ± 89.81)

Mean SpO_2, minimal SpO_2 and the amount of time with an SpO_2 < 90% were assessed. Subject R was excluded during the −12° HDT night because of artifacts. None of those parameters was significantly different between both conditions. The values are given in means ± standard deviation. HDT, head down tilt; SpO_2, Peripheral oxygen saturation at finger level.

TABLE 4 | Subjective sleep parameters.

	0° position	−12° HDT position
Subjective sleep quality (1–9)	6.1 ± 1.1	4.8 ± 1.5*
Subjective refreshment (1–9)	6.3 ± 1.8	5.6 ± 1.8
Subjective sleep duration (h)	6.4 ± 1.4	5.3 ± 1.8

*Subjective sleep parameters were assessed in the morning. Sleep quality and refreshment were assessed by scales from 1 to 9. 9 represented the highest possible sleep quality and refreshment possible. Subjective amount of sleeping hours were given by the subjects. The values are given in means ± standard deviation. *P = 0.047. HDT, head down tilt.*

DISCUSSION

The percentage of slow wave sleep (N3) and REM sleep significantly decreased during −12° HDT, thereby resulting in a compensating significant increase of light sleep (N1/2). The subjective sleep quality was significantly lower when sleeping in HDT. These results are consistent with recent findings (Mizuno et al., 2005; Komada et al., 2006).

Despite these changes in sleep, the respective percentages of the sleep stages still are within the normal range for young adults (Carskadon and Dement, 2005) – although at the ends. This might be due to the subjects' ages ranging between 21 and 55 years. This and the fact that the number of sleep stage changes

TABLE 5 | Jugular vein diameters and frontal tissue thickness.

	Baseline data collection		Measurement block 2		Measurement block 3	
	0° visit	−12° visit	0° visit	−12° visit	0° visit	−12° visit
Internal Jugular Vein						
Minimum cross-sectional area (cm^2)	0.57 ± 0.42	0.65 ± 0.52	0.70 ± 0.49	1.31 ± 0.64††	0.54 ± 0.45	1.18 ± 0.62†††
Maximum cross-sectional area (cm^2)	0.84 ± 0.49	0.87 ± 0.54	0.86 ± 0.60	1.46 ± 0.66††	0.76 ± 0.51	1.41 ± 0.66††
Variation (cm^2)	0.27 ± 0.26	0.21 ± 0.21	0.16 ± 0.17	0.15 ± 0.10	0.22 ± 0.19	0.23 ± 0.19
External Jugular Vein						
Minimum cross-sectional area (cm^2)	0.15 ± 0.07	0.15 ± 0.07	0.15 ± 0.08	0.20 ± 0.15††	0.15 ± 0.09	0.18 ± 0.12††
Maximum cross-sectional area (cm^2)	0.17 ± 0.08	0.17 ± 0.09	0.16 ± 0.09	0.22 ± 0.16	0.16 ± 0.09	0.20 ± 0.13
Variation (cm^2)	0.019 ± 0.027	0.025 ± 0.022	0.012 ± 0.019	0.015 ± 0.022	0.012 ± 0.010	0.018 ± 0.018
Frontal skin thickness (mm)	4.11 ± 0.95	4.04 ± 0.88	4.12 ± 1.01	4.26 ± 1.11	4.03 ± 0.88	4.10 ± 0.94

B-mode ultrasound was used to assess the minimum and maximum diameters of external and internal jugular veins on both sides. Frontal tissue thickness was measured on both sides of the front. Baseline data collection in both groups was performed in horizontal posture. The values are given in means ± standard deviation. ††$P < 0.01$, †††$P < 0.001$ for interaction between measurement block and visit.

remained similar during both positions suggest normal sleep architecture. Mizuno et al. (2005) drew the same conclusion at −6° HDT.

Minimum and maximum cross-sectional area of the internal jugular vein increased significantly at −12° HDT. The minimum cross-sectional area of the external jugular vein was significantly larger at −12° HDT compared to horizontal posture. Both findings indicate venous congestion at −12° HDT.

Frontal skin tissue thickness did not increase significantly during both interventional days at −12° HDT.

We had hypothesized that HDT induced changes on cerebral hemodynamics (Marshall-Goebel et al., 2016) would affect metabolic clearance and sleep. These changes in sleep might influence the transport capability of the "glymphatic" as this transport predominantly takes place during sleep (Xie et al., 2013) resulting in a reciprocal relation.

Dreha-Kulaczewski et al. (2017) showed that venous flow is a major driver for cerebrospinal fluid (CSF) circulation with both systems having opposed flow directions. Therefore, venous congestion as assessed in our study most likely results in a decreased flow of CSF into the cranium. This might directly affect metabolic clearance via CSF circulation.

Although we were not able to analyze the data of the thoracic and abdominal belts, respiration is likely to be affected by HDT: Negative thoracic pressure during inspiration is a main driver for CSF circulation (Dreha-Kulaczewski et al., 2015) as it results in a venous flow out of the cranium. Thereby, CSF flows toward the cranium. Therefore, a potential underlying cause of the increased venous congestion we observed is a change in respiration.

Respiratory obstruction may play a role in sleeping at −12° HDT. Resistance in the upper airway is associated with the lung volume (Begle et al., 1990; Stanchina et al., 2003). During HDT, lung volume decreases due to the shift of abdominal organs toward the head. This possibly results in an increased airflow resistance. The data of the abdominal and thoracic belts could not be evaluated efficiently and no difference was detected for continuous measurements of peripheral oxygen saturation. Therefore, a definite conclusion cannot be drawn.

The resulting effects of the decrease in cranial perfusion (Marshall-Goebel et al., 2016) and increased venous congestion at HDT might be similar albeit not identical to those in chronic heart failure. Chronic heart failure has a strong correlation to the obstructive sleep apnea syndrome. Although the reason for this is multifactorial one cause is possibly the fluid increase in the pharynx (Bradley and Floras, 2003).

This might also be one cause for impaired sleeping at HDT. Due to this shift, fluid also accumulates in the upper airways. The subjects were young, healthy males and the obstruction might not be as severe as in patients suffering from chronic heart failure. Thus, the full disease pattern of obstructive sleep apnea syndrome is not displayed.

In patients suffering from chronic heart failure, the retention of CSF within the cranial cavity might be the cause for cognitive impairment similar to that of idiopathic intracranial hypertension patients (Caplan, 2006). Assumed pathophysiologies for idiopathic intracranial hypertension include an increased outflow resistance of CSF (McGeeney and Friedman, 2014). Additionally, sleep apnea syndrome is related to idiopathic intracranial hypertension (Biousse et al., 2012; McGeeney and Friedman, 2014). Yet, it remains unclear whether it may be one of the causes or the result of the disease. The interactions of arterial, venous and CSF systems described above in addition with respiratory changes might be a possible approach.

With regards to obstruction, the individual build has to be taken into account. Fat distribution is an important risk factor for obstructive sleep apnea syndrome (Horner et al., 1989; Shinohara et al., 1997). Yuan et al. could show a correlation between neck circumference and pharynx collapsibility (Yuan et al., 2013) in adolescents. All our subjects' BMIs were within the normal range but minor influences of individual body fat distribution cannot be completely ruled out.

The change of sleep stages observed in our study could also be explained by a raised level of physiological stress hormones

during HDT as Norepinephrine is one of the transmitters influencing REM sleep stage (McCarley and Hobson, 1975; Winokur et al., 2001). Although, Rai and Kaur (2011). found that said increase in stress hormones took place only after the first week of bed rest, subjects were only positioned at −6° HDT. −12° HDT might lead to a quicker response of the stress system.

Mood, especially an increase in depression, plays a major role during HDT bed rest studies (Styf et al., 2001; Pavy-Le Traon et al., 2007) – even though not always reaching clinically significant level (Liu et al., 2012). As depression and sleep influence each other mutually (Kaneita et al., 2006), this has to be taken into account. However, −12° HDT was applied for less than 24 h and depressive disorders were an exclusion criterion. Liu et al. found no significant changes in anxiety level at −6° HDT (Liu et al., 2012) rendering altered mood an unlikely confounder of sleep (Rosa et al., 1983).

Gundel et al. observed a change in circadian rhythm of astronauts (Gundel et al., 1997) assessed by measuring the body temperature. During bed rest studies these changes generally occur at a later time (Pavy-Le Traon et al., 2007). Therefore, this factor did most likely not affect sleep in our study.

Whereas the subjective feeling of refreshment and estimated sleep duration were not influenced by the body position, subjective sleep quality was significant lower at −12° HDT which might be explained by the significant reduction of slow wave sleep (N3). Both slow wave sleep and sleep efficiency affect subjective sleep quality (Keklund and Akerstedt, 1997). Yet, when comparing subjective with objective sleep quality the results remain inconsistent (Akerstedt et al., 1994).

One limitation of our study regarding sleep was the issue of sliding at −12° HDT. Despite applying several countermeasures, subjects still described wakening because of reaching the head-end of the bed. This impedes the distinction between the effects of HDT itself and those of the sliding on the sleep behavior. The issue of sliding might also have contributed to deterioration in subjective comfort.

The study was designed to diminish any impact of the first night effect. A recent finding indicates REM sleep might even be influenced up to four nights (Le Bon et al., 2001). This might have affected our measurements. However, the counterbalanced design of the study should have reduced the possible impact on sleep.

Before sleeping, two subjects were given painkillers. Although none of the subjects woke up due to pain, the general increase in back pain, stomach pain and headache during bed rest (Styf et al., 2001) might still have influenced their sleeping. Apart from that, several subjects described a feeling of distention in their upper abdomen during −12° HDT contributing to general discomfort. Ibuprofen could affect sleep (Murphy et al., 1994) via inhibition of prostaglandin synthesis and the consequential change in body temperature and melatonin synthesis (Murphy et al., 1996). Yet, these results could not be confirmed (Gengo, 2006).

As with every bed rest study, there remains the question to what extent results are valid for actual space missions. With the observations being generally applicable this comparison might still be impeded due to surrounding circumstances during spaceflight, such as noise and mission parameters (Monk et al., 1998; Mallis and DeRoshia, 2005).

Overall, we could confirm previous findings from bed rest studies regarding sleep stage changes and sleep architecture. We also hypothesized that interrelations between the cranial perfusion systems and metabolic clearance would be a possible explanation for the poorer sleep behavior at −12° HDT. All in all, a better understanding of sleep and its relation to the intracranial fluid system is not only relevant for future space missions but might also have implications for clinical medicine.

ETHICS STATEMENT

This study was carried out in accordance with recommendations of the Declaration of Helsinki in its latest version, Datenschutzgesetz (Data Protective Act), Medizinproduktgesetz (MPG) (Medical Device Law), and Medizinprodukte – Betreiber Verordnung (MPBetrV). The protocol was approved by the ethics committee of the regional medical board (Ärztekammer Nordrhein). All subjects gave written informed consent in accordance with the Declaration of Helsinki.

AUTHOR CONTRIBUTIONS

All authors contributed to the hypothesis development, study design, data acquisition, and manuscript finalization. Analysis of the IPCog study results were carried out by ALB, ZL, DG, BJ, JZ, and JR. PG and JR supervised the study. ALB wrote the first draft of the manuscript and designed the graphs.

FUNDING

This study was funded by the DLR – Institute of Aerospace Medicine Department: Space Physiology.

ACKNOWLEDGMENTS

This study was performed at the German Areospace Centre (DLR) in Cologne. We would like to thank the whole team of the Muscle and Bone Metabolism Department for helping to prepare and conduct the study. Finally, we are indebted to the study participants, as this research would not have been possible without their valuable contribution.

REFERENCES

Akerstedt, T., Hume, K., Minors, D., and Waterhouse, J. (1994). The meaning of good sleep: a longitudinal study of polysomnography and subjective sleep quality. *J. Sleep Res.* 3, 152–158. doi: 10.1111/j.1365-2869.1994.tb00122.x

Barger, L. K., Flynn-Evans, E. E., Kubey, A., Walsh, L., Ronda, J. M., Wang, W., et al. (2014). Prevalence of sleep deficiency and use of hypnotic drugs in astronauts before, during, and after spaceflight: an observational study. *Lancet Neurol.* 13, 904–912. doi: 10.1016/S1474-4422(14)70122-X

Begle, R. L., Badr, S., Skatrud, J. B., and Dempsey, J. A. (1990). Effect of lung inflation on pulmonary resistance during NREM sleep. *Am. Rev. Respir. Dis.* 141, 854–860. doi: 10.1164/ajrccm/141.4_Pt_1.854

Biousse, V., Bruce, B. B., and Newman, N. J. (2012). Update on the pathophysiology and management of idiopathic intracranial hypertension. *J. Neurol. Neurosurg. Psychiatry* 83, 488–494. doi: 10.1136/jnnp-2011-302029

Bradley, T. D., and Floras, J. S. (2003). Sleep apnea and heart failure. part i: obstructive sleep apnea. *Circulation* 107, 1671–1678. doi: 10.1161/01.CIR.0000061757.12581.15

Caplan, L. R. (2006). Cardiac encephalopathy and congestive heart failure: a hypothesis about the relationship. *Neurology* 66, 99–101. doi: 10.1212/01.wnl.0000191327.62136.b1

Carskadon, M. A., and Dement, W. C. (2005). Normal human sleep: an overview. *Princ. Pract. Sleep Med.* 4, 13–23. doi: 10.1016/B0-72-160797-7/50009-4

Delaidelli, A., and Moiraghi, A. (2017). Respiration: a new mechanism for CSF circulation? *J. Neurosci.* 37, 7076–7078. doi: 10.1523/JNEUROSCI.1155-17.2017

DeRoshia, C. W., and Greenleaf, J. E. (1993). Performance and mood-state parameters during 30-day 6 degrees head-down bed rest with exercise training. *Aviat. Space Environ. Med.* 64, 522–527.

Dijk, D.-J., Neri, D. F., Wyatt, J. K., Ronda, J. M., Riel, E., Ritz-De Cecco, A., et al. (2001). Sleep, performance, circadian rhythms, and light-dark cycles during two space shuttle flights. *Am. J. Physiol Regul. Integr. Comp. Physiol.* 281, R1647–R1664. doi: 10.1152/ajpregu.2001.281.5.R1647

Dinges, D. F., Basner, M., Dj, M., Goel, N., and Braun, M. (2013). "ISS missions: elevated workload and reduced sleep duration," in *Proceedings of the NASA Human Research Program Investigators' Workshop*, (Galveston, TX).

Dreha-Kulaczewski, S., Joseph, A. A., Merboldt, K. D., Ludwig, H. C., Gartner, J., and Frahm, J. (2015). Inspiration is the major regulator of human CSF flow. *J. Neurosci.* 35, 2485–2491. doi: 10.1523/JNEUROSCI.3246-14.2015

Dreha-Kulaczewski, S., Joseph, A. A., Merboldt, K. D., Ludwig, H. C., Gartner, J., and Frahm, J. (2017). Identification of the upward movement of human CSF In vivo and its relation to the brain venous system. *J. Neurosci.* 37, 2395–2402. doi: 10.1523/JNEUROSCI.2754-16.2017

Flynn-Evans, E. E., Barger, L. K., Kubey, A. A., Sullivan, J. P., and Czeisler, C. A. (2016). Circadian misalignment affects sleep and medication use before and during spaceflight. *NPJ Microgravity* 2:15019. doi: 10.1038/npjmgrav.2015.19

Gengo, F. (2006). Effects of ibuprofen on sleep quality as measured using polysomnography and subjective measures in healthy adults. *Clin. Ther.* 28, 1820–1826. doi: 10.1016/j.clinthera.2006.11.018

Gkivogkli, P. T., Frantzidis, C., Karagianni, M., Rosenzweig, I., Papadeli, C. K., and Bamidis, P. D. (2016). Sleep macro-architecture disturbances during a 60 days 60 head down tilt bed-rest and the effect of Sledge Jumping System (SJS) as a countermeasure to prevent those changes. *Front. Hum. Neurosci.* 12:106. doi: 10.3389/conf.fnhum.2016.220.00106

Gundel, A., Polyakov, V. V., and Zulley, J. (1997). The alteration of human sleep and circadian rhythms during spaceflight. *J. Sleep Res.* 6, 1–8. doi: 10.1046/j.1365-2869.1997.00028.x

Horner, R. L., Mohiaddin, R. H., Lowell, D. G., Shea, S. A., Burman, E. D., Longmore, D. B., et al. (1989). Sites and sizes of fat deposits around the pharynx in obese patients with obstructive sleep apnoea and weight matched controls. *Eur. Respir. J.* 2, 613–622.

Iber, C., Ancoli-Israel, S., Chesson, A., and Quan, S. (2007). *The AASM manual for the scoring of sleep and associated events : rules, terminology and technical specifications*. Westchester, IL: American Academy of Sleep Medicine.

Kakurin, L. I., Lobachik, V. I., Mikhailov, V. M., and Senkevich, Y. A. (1976). Antiorthostatic hypokinesia as a method of weightlessness simulation. *Aviat Space Environ. Med.* 47, 1083–1086.

Kaneita, Y., Ohida, T., Uchiyama, M., Takemura, S., Kawahara, K., Yokoyama, E., et al. (2006). The relationship between depression and sleep disturbances: a Japanese nationwide general population survey. *J. Clin. Psychiatry* 67, 196–203. doi: 10.4088/JCP.v67n0204

Keklund, G., and Akerstedt, T. (1997). Objective components of individual differences in subjective sleep quality. *J. Sleep Res.* 6, 217–220. doi: 10.1111/j.1365-2869.1997.00217.x

Komada, Y., Inoue, Y., Mizuno, K., Tanaka, H., Mishima, K., Sato, H., et al. (2006). Effects of acute simulated microgravity on nocturnal sleep, daytime vigilance, and psychomotor performance: comparison of horizontal and 6 degrees head-down bed rest. *Percept. Mot. Skills* 103, 307–317. doi: 10.2466/PMS.103.6.307-317

Kramer, L. A., Hasan, K. M., Sargsyan, A. E., Marshall-Goebel, K., Rittweger, J., Donoviel, D., et al. (2017). Quantitative MRI volumetry, diffusivity, cerebrovascular flow, and cranial hydrodynamics during head-down tilt and hypercapnia: the SPACECOT study. *J. Appl. Physiol.* 122, 1155–1166. doi: 10.1152/japplphysiol.00887.2016

Lawley, J. S., Petersen, L. G., Howden, E. J., Sarma, S., Cornwell, W. K., Zhang, R., et al. (2017). Effect of gravity and microgravity on intracranial pressure. *J. Physiol.* 595, 2115–2127. doi: 10.1113/JP273557

Le Bon, O., Staner, L., Hoffmann, G., Dramaix, M., San Sebastian, I., Murphy, J. R., et al. (2001). The first-night effect may last more than one night. *J. Psychiatr. Res.* 35, 165–172. doi: 10.1016/S0022-3956(01)00019-X

Lee, H., Xie, L., Yu, M., Kang, H., Feng, T., Deane, R., et al. (2015). The effect of body posture on brain glymphatic transport. *J. Neurosci.* 35, 11034–11044. doi: 10.1523/JNEUROSCI.1625-15.2015

Liu, Q., Zhou, R., Chen, S., and Tan, C. (2012). Effects of head-down bed rest on the executive functions and emotional response. *PLoS One* 7:e52160. doi: 10.1371/journal.pone.0052160

Mallis, M. M., and DeRoshia, C. W. (2005). Circadian rhythms, sleep, and performance in space. *Aviat Space Environ. Med.* 76, B94–B107.

Marshall-Goebel, K., Ambarki, K., Eklund, A., Malm, J., Mulder, E., Gerlach, D., et al. (2016). Effects of short-term exposure to head-down tilt on cerebral hemodynamics: a prospective evaluation of a spaceflight analog using phase-contrast MRI. *J. Appl. Physiol.* 120, 1466–1473. doi: 10.1152/japplphysiol.00841.2015

McCarley, R. W., and Hobson, J. A. (1975). Neuronal excitability modulation over the sleep cycle: a structural and mathematical model. *Science* 189, 58–60. doi: 10.1126/science.1135627

McGeeney, B. E., and Friedman, D. I. (2014). Pseudotumor cerebri pathophysiology. *Headache* 54, 445–458. doi: 10.1111/head.12291

Meck, J. V., Dreyer, S. A., and Warren, L. E. (2009). Long-duration head-down bed rest: project overview, vital signs, and fluid balance. *Aviat Space Environ. Med.* 80, A1–A8. doi: 10.3357/ASEM.BR01.2009

Mizuno, K., Inoue, Y., Tanaka, H., Komada, Y., Saito, H., Mishima, K., et al. (2005). Heart rate variability under acute simulated microgravity during daytime waking state and nocturnal sleep: comparison of horizontal and 6 degrees head-down bed rest. *Neurosci. Lett.* 383, 115–120. doi: 10.1016/j.neulet.2005.03.058

Monk, T. H., Buysse, D. J., Billy, B. D., Kennedy, K. S., and Willrich, L. M. (1998). Sleep and circadian rhythms in four orbiting astronauts. *J. Biol. Rhythms* 13, 188–201. doi: 10.1177/074873098129000039

Murphy, P. J., Badia, P., Myers, B. L., Boecker, M. R., and Wright, K. P. Jr. (1994). Nonsteroidal anti-inflammatory drugs affect normal sleep patterns in humans. *Physiol. Behav.* 55, 1063–1066. doi: 10.1016/0031-9384(94)90388-3

Murphy, P. J., Myers, B. L., and Badia, P. (1996). Nonsteroidal anti-inflammatory drugs alter body temperature and suppress melatonin in humans. *Physiol. Behav.* 59, 133–139. doi: 10.1016/0031-9384(95)02036-5

Pavy-Le Traon, A., Heer, M., Narici, M. V., Rittweger, J., and Vernikos, J. (2007). From space to Earth: advances in human physiology from 20 years of bed rest studies (1986-2006). *Eur. J. Appl. Physiol.* 101, 143–194. doi: 10.1007/s00421-007-0474-z

Rai, B., and Kaur, J. (2011). Salivary stress markers and psychological stress in simulated microgravity: 21 days in 6 degrees head-down tilt. *J. Oral. Sci.* 53, 103–107. doi: 10.2334/josnusd.53.103

Rosa, R. R., Bonnet, M. H., and Kramer, M. (1983). The relationship of sleep and anxiety in anxious subjects. *Biol. Psychol.* 16, 119–126. doi: 10.1016/0301-0511(83)90058-3

Shinohara, E., Kihara, S., Yamashita, S., Yamane, M., Nishida, M., Arai, T., et al. (1997). Visceral fat accumulation as an important risk factor for obstructive sleep apnoea syndrome in obese subjects. *J. Intern. Med.* 241, 11–18. doi: 10.1046/j.1365-2796.1997.63889000.x

Stanchina, M. L., Malhotra, A., Fogel, R. B., Trinder, J., Edwards, J. K., Schory, K., et al. (2003). The influence of lung volume on pharyngeal mechanics, collapsibility, and genioglossus muscle activation during sleep. *Sleep* 26, 851–856. doi: 10.1093/sleep/26.7.851

Styf, J. R., Hutchinson, K., Carlsson, S. G., and Hargens, A. R. (2001). Depression, mood state, and back pain during microgravity simulated by bed rest. *Psychosom Med.* 63, 862–864. doi: 10.1097/00006842-200111000-00002

Van Dongen, H. P., Baynard, M. D., Maislin, G., and Dinges, D. F. (2004). Systematic interindividual differences in neurobehavioral impairment from sleep loss: evidence of trait-like differential vulnerability. *Sleep* 27, 423–433.

Whitmire, A. M., Leveton, L. B., Barger, L., Brainard, G., Dinges, D. F., Klerman, E., et al. (2009). "Risk of performance errors due to sleep loss, circadian desynchronization, fatigue, and work overload," in *Human Health and Performance Risks of Space Exploration Missions: Evidence Reviewed by the NASA Human Research Program. NASA SP-2009-3405*, (Washington, DC: National Aeronautics and Space Administration).

Winokur, A., Gary, K. A., Rodner, S., Rae-Red, C., Fernando, A. T., and Szuba, M. P. (2001). Depression, sleep physiology, and antidepressant drugs. *Depress Anxiety* 14, 19–28. doi: 10.1002/da.1043

Xie, L., Kang, H., Xu, Q., Chen, M. J., Liao, Y., Thiyagarajan, M., et al. (2013). Sleep drives metabolite clearance from the adult brain. *Science* 342, 373–377. doi: 10.1126/science.1241224

Yuan, H., Schwab, R. J., Kim, C., He, J., Shults, J., Bradford, R., et al. (2013). Relationship between body fat distribution and upper airway dynamic function during sleep in adolescents. *Sleep* 36, 1199–1207. doi: 10.5665/sleep.2886

Conflict of Interest Statement: The authors declare that the research was conducted in the absence of any commercial or financial relationships that could be construed as a potential conflict of interest.

frontiers in Physiology

ORIGINAL RESEARCH
published: 30 April 2019
doi: 10.3389/fphys.2019.00476

The Vestibular Drive for Balance Control Is Dependent on Multiple Sensory Cues of Gravity

*Anne I. Arntz[1,2], Daphne A. M. van der Putte[1], Zeb D. Jonker[1,3,4], Christopher M. Hauwert[1], Maarten A. Frens[1] and Patrick A. Forbes[1,2]**

[1] Department of Neuroscience, Erasmus MC, Erasmus University Medical Center, Rotterdam, Netherlands, [2] Department of Biomechanical Engineering, Faculty of Mechanical, Maritime and Materials Engineering, Delft University of Technology, Delft, Netherlands, [3] Department of Rehabilitation Medicine, Erasmus MC, Erasmus University Medical Center, Rotterdam, Netherlands, [4] Rijndam Rehabilitation Centre, Rotterdam, Netherlands

OPEN ACCESS

Edited by:
Gilles Clement, Centre National de la Recherche Scientifique (CNRS), France

Reviewed by:
Rahul Goel, Baylor College of Medicine, United States
Brian H. Dalton, University of British Columbia Okanagan, Canada
Ajitkumar Mulavara, Universities Space Research Association (USRA), United States

***Correspondence:**
Patrick A. Forbes
p.forbes@erasmusmc.nl

Specialty section:
This article was submitted to Environmental, Aviation and Space Physiology, a section of the journal Frontiers in Physiology

Received: *07 January 2019*
Accepted: *04 April 2019*
Published: *30 April 2019*

Citation:
Arntz AI, van der Putte DAM, Jonker ZD, Hauwert CM, Frens MA and Forbes PA (2019) The Vestibular Drive for Balance Control Is Dependent on Multiple Sensory Cues of Gravity. Front. Physiol. 10:476. doi: 10.3389/fphys.2019.00476

Vestibular signals, which encode head movement in space as well as orientation relative to gravity, contribute to the ongoing muscle activity required to stand. The strength of this vestibular contribution changes with the presence and quality of sensory cues of balance. Here we investigate whether the vestibular drive for standing balance also depends on different sensory cues of gravity by examining vestibular-evoked muscle responses when independently varying load and gravity conditions. Standing subjects were braced by a backboard structure that limited whole-body sway to the sagittal plane while load and vestibular cues of gravity were manipulated by: (a) loading the body downward at 1.5 and 2 times body weight (i.e., load cues), and/or (b) exposing subjects to brief periods (20 s) of micro- (<0.05 g) and hyper-gravity (∼1.8 g) during parabolic flights (i.e., vestibular cues). A stochastic electrical vestibular stimulus (0–25 Hz) delivered during these tasks evoked a vestibular-error signal and corrective muscles responses that were used to assess the vestibular drive to standing balance. With additional load, the magnitude of the vestibular-evoked muscle responses progressively increased, however, when these responses were normalized by the ongoing muscle activity, they decreased and plateaued at 1.5 times body weight. This demonstrates that the increased muscle activity necessary to stand with additional load is accompanied a proportionally smaller increase in vestibular input. This reduction in the relative vestibular contribution to balance was also observed when we varied the vestibular cues of gravity, but only during an absence (<0.05 g) and not an excess (∼1.8 g) of gravity when compared to conditions with normal 1 g gravity signals and equivalent load signals. Despite these changes, vestibular-evoked responses were observed in all conditions, indicating that vestibular cues of balance contribute to upright standing even in the near absence of a vestibular signal of gravity (i.e., micro-gravity). Overall, these experiments provide evidence that both load and vestibular cues of gravity influence the vestibular signal processing for the control of standing balance.

Keywords: gravity, vestibular system, balance control, electrical vestibular stimulation, vestibular-evoked responses

INTRODUCTION

Whenever we stand, the downward pull of gravity requires that we make continuous motor corrections to remain upright. Critical to this process is the ability to accurately estimate our orientation relative to gravity. The sensory cues that inform the brain about gravity, in the absence of vision, are derived primarily from the somatosensory and vestibular systems (see Dakin and Rosenberg, 2018 for a review). The somatosensory system encodes the gravitational load (i.e., forces) throughout the body within the local reference frame of the support surface, whereas the vestibular system's otolith organs, together with the semicircular canal organs, encode head orientation within a fixed gravito-inertial reference frame. These sensory signals shape the corrective motor commands that maintain balance such that any change they undergo has an influence on the postural responses necessary to stand. For example, changes in body load (i.e., added or deducted weight) alters vestibular-evoked postural responses, whereby force rate production increases with loading and decreases with unloading (Marsden et al., 2003). Similar effects can also be observed when subjects take on asymmetric standing postures (Marsden et al., 2002), suggesting that load-related afferent feedback of gravity influences the processing of vestibular signals for the control of balance (Marsden et al., 2003).

Otolith-driven cues of gravity, in contrast to load-cues, appear to influence vestibulospinal reflexes only after prolonged (>24 h) exposures to changes in gravity. For example, in astronauts exposed to vertical drops on the first day of space flight, otolith-modulated motoneuron sensitivities (i.e., H-reflexes evoked during the drop) are analogous to levels tested pre-flight, but are almost absent after 7 days of space flight (Reschke et al., 1984, 1986). This change in otolith-driven motoneuron sensitivity suggests that the adaptation of vestibulospinal reflexes to changes in otolith cues of gravity may occur over longer periods than those observed for load cues of gravity during standing (Marsden et al., 2002, 2003). Vestibulospinal reflexes evoked by the drop conditions, however, arise from the otolith activity produced by the linear acceleration during freefall in absence of any requirement to stand. Therefore, these results may not be generalizable to the compensatory responses arising from the vestibular system during standing balance. Indeed, recent work has proposed that the characteristics of vestibular-evoked muscle corrections when standing reflect highly flexible responses centrally organized to compensate for vestibular disturbances (Britton et al., 1993; Fitzpatrick et al., 1994; Luu et al., 2012; Forbes et al., 2016). For instance, vestibular-induced lower-limb muscle responses during balance occur ∼30 ms later than those evoked by cortex stimulation (Britton et al., 1993; Dakin et al., 2016), even though the pathways conveying each signal have comparable conduction velocities. More notably, when standing subjects are restricted to balance in a single plane, vestibular-evoked muscle responses are greatest when the direction of a vestibular disturbance is aligned with the balance direction, and decrease to zero when the two directions become orthogonal (Forbes et al., 2016). This indicates that muscles compensate only for the component of the vestibular disturbance that is aligned with the balance direction, and not to the net vestibular activity that would be expected for vestibulospinal reflexes such as those produced during freefall. Therefore, we performed experiments to assess whether changes in otolith-driven signals of gravity – analogous to load cues of gravity – also modify the vestibular-evoked muscles responses for standing balance.

We used electrical vestibular stimulation (EVS) to evaluate the effects of varying load and vestibular cues of gravity on the corrective muscle responses required to stand. Electrical current applied to the mastoid processes distorts the firing rate of canal and otolith vestibular afferents (Kim and Curthoys, 2004; Kwan et al., 2019), and in a bilateral-bipolar configuration increases afferent activity on the side of the cathode and decreases afferent activity on the side of the anode (Goldberg et al., 1984; Kim et al., 2011; Kwan et al., 2019). The net sum of the afferent activity induces an isolated virtual signal of head rotation that is fixed in head coordinates (Fitzpatrick and Day, 2004; Day and Fitzpatrick, 2005; Peters et al., 2015) and is interpreted by the CNS as an unexpected vestibular disturbance. When standing, this vestibular disturbance evokes stereotypical muscle and whole-body postural corrections to maintain upright balance (Nashner and Wolfson, 1974; Lund and Broberg, 1983; Fitzpatrick et al., 1994; Dakin et al., 2007; Mian and Day, 2014; Forbes et al., 2016). Using this electrical stimulus, we performed experiments on ground and in parabolic flights to independently modulate load- and vestibular-related cues of gravity for balance. Load-related cues of gravity from the somatosensory system (i.e., cutaneous, proprioception) were modulated by loading subjects with 1.5 and 2 times their body weight using springs attached to the floor while subjects stood in 1 g gravitational conditions. Vestibular-related cues of gravity from the otolith end organs were then modulated by having subjects stand in micro-gravity (<0.05 g) and hyper-gravity (1.8 g) conditions while maintaining equivalent load cues via the springs. We found that the relative contribution of vestibular input to the corrective muscle responses was largest when subjects stood with normal 1 g related load and vestibular cues of gravity, and decreased when these cues were modulated. Specifically, with increased load cues of gravity, the relative vestibular-evoked responses decreased but remained constant when the load exceeded 1.5 times the body weight. Furthermore, responses decreased with modified vestibular cues of gravity, however, this effect was only observed in the absence (i.e., micro-g) and not the excess (i.e., hyper-g) of gravity. Despite these reductions, vestibular-evoked responses were observed in all conditions, indicating that vestibular contributions to balance are maintained even in the near absence of a vestibular signal of gravity (i.e., micro-gravity). Overall, these experiments provide evidence that both load and vestibular cues of gravity influence the vestibular signal processing for the control of standing balance.

MATERIALS AND METHODS

Subjects

Twenty-one healthy subjects (*Experiment 1:* 16 subjects, mean age ± SD = 24 ± 4.2 years, mean height ± SD = 176 ± 7.1 cm,

mean weight ± SD = 68 ± 7.7 kg, 10 men; *Experiment 2:* 6 subjects, mean age ± SD = 38 ± 8.3 years, mean height ± SD = 173 ± 9.4 cm, mean weight ± SD = 76 ± 9.7 kg, 5 men) with no known history of neurological disease or injury participated in this study. Subjects that participated in Experiment 2 completed both a training session under normal gravity conditions (*Experiment 2A*) and a flight session under variable gravity conditions (*Experiment 2B*) in the airplane. One subject participated in both Experiment 1 and Experiment 2. Experiment 1 was approved by the Medical Research Ethics Committee Erasmus MC and Experiment 2 by the University of Caen's Ethics Committee. The experiments were conducted in accordance with the Declaration of Helsinki. All subjects gave their written informed consent prior to participation.

Experimental Set-Up

Two separate experiments were performed to study the effects of load and vestibular cues of gravity on the vestibular-evoked muscle responses. Experiment 1 assessed the influence of load cues of gravity under a constant gravitational level of 1 g. Experiment 2 assessed the influence of vestibular (otolith) cues of gravity under constant load levels of ∼1 and 2 times body weight. For both experiments, subjects maintained upright balance while being exposed to the stochastic EVS signal (see "Vestibular Stimuli"). In both experiments, subjects stood barefoot on a force plate (BP400600HF; AMTI, Watertown, MA, United States) with their feet 5 cm apart and their body secured to a backboard structure positioned immediately behind them (**Figure 1**). The backboard structure was used to eliminate any stabilizing effect of the subject loading system in the mediolateral direction (i.e., the downward pull of the springs, see below). The weight of the backboard structure was 10 kg with the center of mass at a height of ∼0.7 m. The backboard structure was supported by two bearings, such that the mass of the backboard only increased the subjects' inertia by ∼6.5%. The backboard's axis of rotation was fixed at a height of 7.5 cm above the top surface of the force plate and passed through the approximate location of the ankle joints (Huryn et al., 2010). As a result, whole-body sway was limited to the sagittal plane only. This pivoting direction corresponds with the direction of EVS-evoked whole-body sway responses when the head is turned over the shoulder (Lund and Broberg, 1983; Britton et al., 1993; Fitzpatrick et al., 1994). Angular limits of 10° anterior and 6° posterior from vertical prevented the subjects from falling forward or backward, respectively. Seatbelts across the chest and waist secured the subjects to the backboard. A laser distance sensor (optoNCDT-1401; Micro-Epsilon, Orteburg, Germany) attached to the backboard was used to record whole-body sway angle.

To control the vertical loading forces under varying gravitational levels (see section "Experiment 1" and "Experiment 2"), subjects wore a subject loading system to provide additional vertical load. The subject loading system consisted of a body-harness (German Aerospace Center (DLR), Cologne, Germany) and four springs. The body-harness was secured over the subject's shoulders and tightened at the waist. The springs were attached to both sides (two springs on each side) of the body-harness using straps located at the height of the hips (i.e., at the subject's approximate center of mass) and to a low-friction rail-trolley system secured to the floor. This rail-trolley system ensured that ground attachment of the springs moved with the center of mass of the subject such that the springs were always pulling vertically downward. This way, the intrinsic dynamics of the subject (i.e., the load-stiffness relationship) would match conditions appropriate for each load and gravitational level.

Vestibular Stimuli

Stochastic electrical vestibular stimulation was delivered to the subjects in a bilateral bipolar electrode configuration via carbon rubber electrodes (∼15 cm^2). The electrodes were coated with Spectra360 electrode gel (Parker Laboratories, Fairfield, NJ, United States) and secured over the mastoid processes with tape and an elastic headband. The skin over the mastoid processes was anesthetized with Pliaglis cream [lidocaine and tetracaine] (Galderma, Lausanne, Switzerland) to minimize cutaneous sensations under the electrodes. The stimuli were generated on a laptop with custom MATLAB software (MathWorks, Natick, MA, United States) and were sent to an isolated bipolar current stimulator (DS5; Digitimer, Hertfordshire, United Kingdom) via a data acquisition board (USB-6259; National Instruments, Austin, TX, United States). For both experiments, the electrical stimuli were designed as bandwidth limited stochastic signals (0–25 Hz, zero-mean low-pass filtered white noise, 25 Hz cutoff, zero lag, third-order Butterworth) with a peak amplitude of 5 mA [root mean square (RMS) of ∼1.7 mA]. The frequencies (0–25 Hz) contained in our electrical stimuli capture the entire bandwidth of vestibular-evoked muscle activity contributing to postural corrections (Dakin et al., 2007, 2010, 2011). This allowed us to provide a detailed assessment of any changes in vestibular contributions across conditions. In Experiment 1, a stimulus of 40 s was repeated four times in each condition (see section "Experimental protocol"; "Experiment 1"). In Experiment 2, a stimulus of 20 s was used to fit within the different gravitational phases of the parabola (see section "Experimental protocol"; "Experiment 2") and repeated seven or eight times in each condition.

Experimental Protocol

Prior to each experiment, a target whole-body sway angle was defined for each subject. This angle was 3° forward from their subjective zero angle; i.e., the position that subjects perceived as requiring minimal effort to stand upright. For each trial, subjects were instructed to stand upright, lean forward to their target sway angle, cross their arms over their chest, and rotate their head axially to the left (i.e., leftward yaw). The head was also rotated in extension such that the Reid plane was tilted up by 18° horizontally. This head position maximizes the postural responses to binaural bipolar EVS in the anterior-posterior direction along the line of action of the right medial gastrocnemius and soleus muscles due to the well-established orientation of the EVS vector (Lund and Broberg, 1983; Fitzpatrick and Day, 2004; Cathers et al., 2005; Day and Fitzpatrick, 2005) produced by the activation of all vestibular afferents (Kwan et al., 2019). Symmetry of otolith afferents across the striola of the utricle (Tribukait and Rosenhall, 2001) is

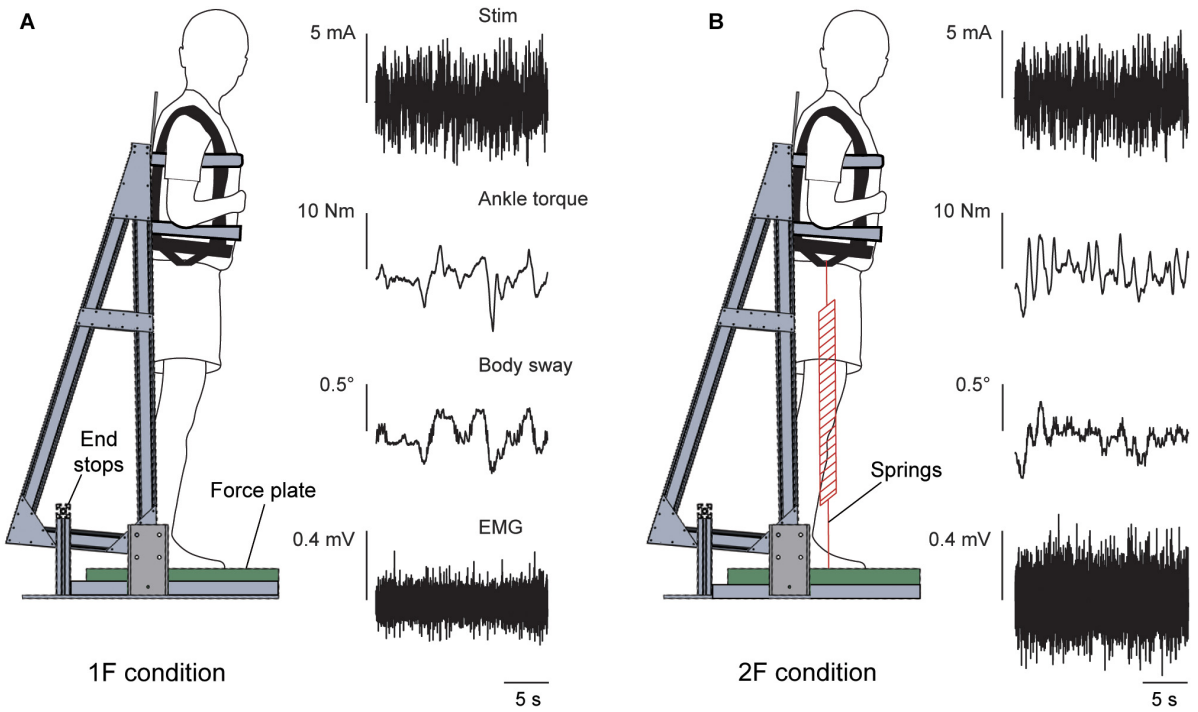

FIGURE 1 | Experimental setup. The subject stood on a force plate and was strapped to a backboard setup that rotated in the sagittal plane about an axis that passed through the subject's ankles. End stops functioned as angular limits to prevent the subject and backboard system from falling forward or backward. The subject remained upright in a slightly forward whole-body sway angle with normal 1 g body load or with added load. Raw data of the vestibular stimulus, ankle torque, whole-body sway angle and EMG activity of the right medial gastrocnemius are shown during a trial of Experiment 1 in the 1F **(A)** and 2F conditions **(B)**.

estimated to result in the cancelation of an otolithic signal during electrical stimulation and a net EVS-vector that predominantly reflects canal activation (i.e., rotation) (Fitzpatrick and Day, 2004). To guide the subjects to their appropriate head and body position before each trial, they were given a subject-specific visual target that was placed on the wall to their left. In Experiment 1, a laser pointer attached to the subject's head was used to orient the head in the desired position. In Experiment 2, the subject was instructed to align their head visually by looking at a target placed ∼1.5 m away on the aircraft wall since for safety reasons a head mounted laser could not be used in the aircraft. Subjects closed their eyes throughout each trial and were given verbal feedback regarding the whole-body sway angle and head position to help maintain a similar position over all trials.

Experiment 1

Experiment 1 assessed three different load conditions to examine the influence of load cues on the vestibular control of balance. Subjects stood with cumulative load forces through the feet equivalent to 1, 1.5 and 2 times their own body weight (conditions 1F, 1.5F and 2F, respectively) by progressively increasing the tension in the springs of the subject loading system. For each condition (1F, 1.5F, and 2F), subjects completed four 40-second trials (12 trials total) providing a total of 160 s of data for analysis under each condition. The order of the trials was randomized for each subject. Prior to delivering the electrical stimulus, subjects were instructed to lean forward to their offset angle, point the head-mounted laser to the mark and close their eyes. Experiment 1 was performed in the Department of Neuroscience at Erasmus Medical Center.

Experiment 2

Experiment 2 was performed with six subjects during the 68th ESA Parabolic Flight Campaign in a modified A310 Zero-G airplane (Novespace, Bordeaux, France) and consisted of a training session (Experiment 2A) and a flight session (Experiment 2B). The training session was completed on-ground in the aircraft 1 day prior to each subject's participation in a parabolic flight (i.e., Experiment 2B). The training session familiarized the subjects with the experimental protocol and provided base-line data for qualitative comparison to Experiment 1 and Experiment 2B. The experiment was performed under two different loading conditions – 1F and 2F – following a similar protocol as described for Experiment 1. A 20-second electrical stimulus was used for Experiment 2A (and Experiment 2B), resulting in eight trials for each loading condition per subject. The order of trial condition (1F and 2F loading) was randomized for each subject.

During the in-flight session, the airplane carried out parabolic flight maneuvers (**Figure 2**) that produced periods of weightlessness (i.e., micro-g or ∼0 g) and increased gravity (i.e., hyper-g or 1.8 g), which modified the vestibular cues of gravity.

Each parabola started and ended with hyper-g periods of ∼20–25 s, separated by a ∼20–25 s micro-g period. Between each parabola the plane was in steady-flight (i.e., normal-g or 1 g) for approximately 100 s. The onset of the electrical stimulus was automatically triggered by acceleration along the *z*-axis of the plane (i.e., the gravitational loading direction). For the micro-gravity (micro-g) phase, the stimulus was triggered 2 s after *z*-acceleration fell below 0.2 g, and for the hyper-gravity (hyper-g) phase, the stimulus was triggered 2 s after z-acceleration exceeded 1.5 g. In the normal-gravity (normal-g) phase, stimulation was started 20 s after the second hyper-g phase of the parabola ended, i.e., when z-acceleration fell below 1.2 g. Offline examination of acceleration data confirmed that the 20 s stimulus occurred within the specific gravity phase for all trials.

Subjects participated in the experiment for 15 parabolic maneuvers (**Figure 2**) under four different conditions with varying levels of gravity (i.e., 0G, 1G or 1.8G) and load via the springs (i.e., 1F or 2F). During seven parabolas, subjects performed normal-gravity/normal-load trials (i.e., 1G-1F) and hyper-gravity/additional-load trials (i.e., 1.8G-1.8F) without spring loading in the normal-g and hyper-g phases, respectively. Hyper-gravity trials (i.e., 1.8G-1.8F) were performed during the first hyper-g phase of the parabola since a more consistent gravity could be achieved during this phase of the parabola. During the other eight parabolas, subjects performed the micro-gravity/normal-load trials (i.e., 0G-1F) and normal-gravity/additional-load trials (i.e., 1G-2F) with spring loading in the micro-g and normal-g phase, respectively (**Figure 2**). The order of the two groups of parabolas (with and without spring loading) was counter balanced across subjects. The subject load system was set per subject to exert a constant force equal to their own weight. Due to the strict timing of consecutive parabolic phases, we were unable to adjust the subject loading system such that the loading level in a steady flight (i.e., 1G-2F) was exactly the same as the load level during the hyper-g phase (i.e., 1.8G-1.8F). Therefore, comparisons of the vestibular-evoked responses were made between 0G-1F and 1G-1F trials, where foot loading forces were matched, and between 1.8G-1.8F and 1G-2F trials, where foot loading forces differed slightly (see **Figure 2**). These comparisons allowed us to evaluate whether changes in gravity-driven otolith signals (i.e., 1 vs. 0 g, and 1 vs. 1.8 g) influence the vestibular control of balance, while maintaining approximately equal load-related afferent cues.

During Experiment 2B, unexpected plane accelerations due to turbulence caused some subjects to fall into the backboard end stops in the middle of a trial. When this occurred, the trial was removed from further analysis. In addition, two subjects experienced motion sickness during the flight and skipped 1–3 parabolas. Nevertheless, all subjects performed a minimum of four trials (i.e., 80 s) per condition without falling into the end stops. For subjects who performed more than four trials without falling into the end stops, the four trials with the lowest mean variability of whole-body sway angle per condition were used for data analysis. This was necessary to maintain equivalent significance thresholds for all subject data (see section "Signal Analysis").

Data Recordings

In all experiments, surface EMG was collected from the medial gastrocnemius (mGAS) and soleus (SOL) muscles in the right leg using self-adhesive Ag-AgCl surface electrodes (BlueSensor M; Ambu, Copenhagen, Denmark). The recordings were made using a bipolar set-up with electrodes placed in-line with the muscle fibers at an inter-electrode (i.e., center-to-center) distance of 18 mm. The skin of the subject's right leg was shaved and cleaned with skin preparation gel (NuPrep; Weaver and Company, Aurora, CO) and alcohol (MediSwab; BSN Medical, Hamburg, Germany) before the electrodes were secured. Acceleration of the plane was measured with a 3-axis accelerometer (3D Accelerometer; TMSi, Oldenzaal, Netherlands) and together with EMG was digitized at 2000 Hz on a data acquisition board (Porti7; TMSi, Oldenzaal, Netherlands). Vestibular stimuli, force plate signals and laser sensor data were digitized at 2000 Hz and recorded via a separate data acquisition board (USB-6259; National Instruments) using a custom MATLAB script (MathWorks, Natick, MA, United States). The two recording systems received a trigger signal at the onset of the vestibular stimulus to synchronize the data.

Signal Analysis

Digitized EMG was high pass filtered offline using a zero-lag sixth order Butterworth filter with a cut-off frequency of 30 Hz and full-wave rectified. EMG signals for each trial were time-locked to EVS onset using the shared trigger signal. Data were concatenated per condition per subject, producing a single 160 (Experiments 1 and 2A) or 80 s (Experiment 2B) data array for a subject's responses for each condition. Data from all subjects were then concatenated to create a single 2560 (Experiments 1 and 2A) and 480 s (Experiment 2B) pooled data set for each condition. Coherence and cumulant density functions were calculated with the individual and pooled data from each condition to evaluate the correlation between the electrical stimulus input and the rectified EMG of the two muscles (Dakin et al., 2007, 2010; Forbes et al., 2014). Data from all experiments were cut into 1 s segments, yielding a frequency resolution of 1 Hz, before computing the auto-spectra and cross-spectrum for the EVS and EMG data.

Coherence provides a measure of the linear relationship between the electrical stimulus (i.e., input) and rectified EMG (i.e., output) across a given range of frequencies. At each frequency point, coherence varies between 0 (no linear relation) and 1 (a linear relation with no noise). Coherence was defined as significant when exceeding the 95% confidence limit, as derived from the number of disjoint segments (Halliday et al., 1995). Coherence was estimated for each condition with concatenated data within each participant as well as concatenated pooled data for each condition across all subjects (see section "Statistics" below). Individual-subject coherence estimates were used to ensure responses were exceeding significance and consistent with the pooled data. The absence of significant coherence at all frequencies between the input stimulus and output muscle activity would indicate the suppression of vestibular contributions to balance.

Cumulant density functions provide a time domain measure of the relationship (i.e., cross-covariance) between the stochastic

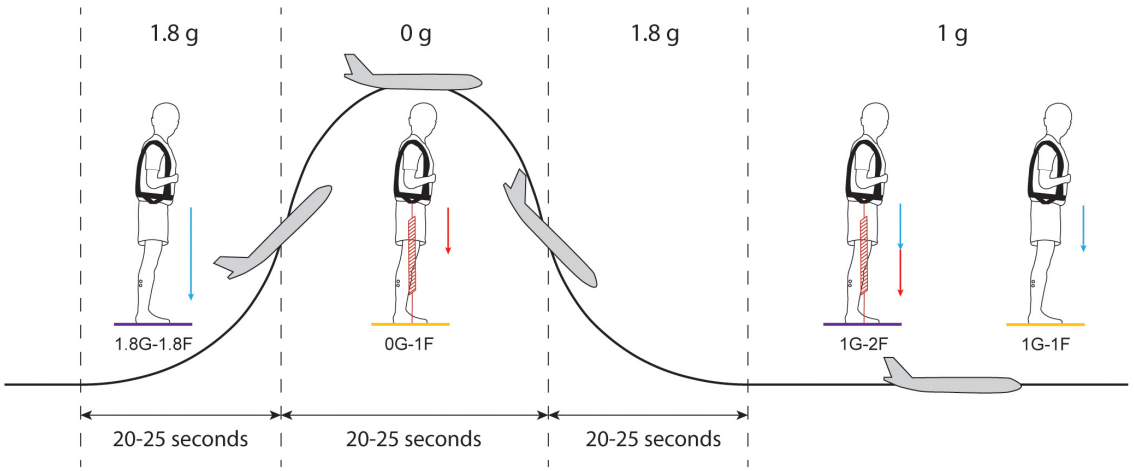

FIGURE 2 | Protocol of Experiment 2B. Each parabolic maneuver starts with a hyper-g phase that is followed by a micro-g phase and ends with a second hyper-g phase. In between each parabola, there is a ∼100 s period of steady flight. For each gravitational phase, subjects performed standing balance tasks under different spring loading conditions while being exposed to the electrical vestibular stimulus. Blue arrows represent the load induced by gravity and red arrows represent the load induced by the subject loading system. Statistical comparisons were made between the results of the 0G-1F and 1G-1F conditions (yellow) and between the results of the 1.8G-1.8F and 1G-2F conditions (purple).

signal and the muscle responses and were calculated by taking the inverse Fourier transform of the cross-spectra (Halliday et al., 1995). Cumulant densities of individual-subject data are used throughout this study to assess the magnitude of the vestibular-evoked muscle response. To account for differences in EMG level between conditions, the cumulant density responses were normalized (between −1 and +1) by the product of the vector norms of the EVS input signal and EMG output signal (Dakin et al., 2010), allowing for inter- and intra-subject comparisons by minimizing potential bias induced by changes in EMG activity. Although this normalized cumulant density is more commonly used to evaluate changes in vestibular-evoked responses (Dakin et al., 2010; Reynolds, 2010; Dalton et al., 2014; Forbes et al., 2014, 2016), we also examined the non-normalized cumulant density responses to assess whether any changes in the normalized responses were modulated simply because of increased non-vestibular input to the motoneuron pool at higher load levels where muscle activity is expected to increase. Because this additional measure is not normalized by ongoing muscle activity, it is not expected to change between conditions if only non-vestibular input (e.g., corticospinal, reticulospinal, spinal reflexes, etc.) leads to increasing EMG magnitude. In contrast, a proportional increase (or decrease) in both vestibular and non-vestibular input is expected to increase (or decrease) only the non-normalized response. Therefore, by comparing the normalized and non-normalized cumulant density responses together with EMG magnitudes, we estimated how the relative vestibular contribution co-varies with the net input to motoneurons. In lower limb muscles, both the normalized and non-normalized cumulant density function exhibit a typical biphasic pattern with peaks defined as short (50–70 ms) and medium (100–120 ms) latency and occurring in opposing directions (Nashner and Wolfson, 1974; Britton et al., 1993; Fitzpatrick et al., 1994; Fitzpatrick and Day, 2004; Dakin et al., 2007, 2011). For comparison across conditions, the peak-to-peak amplitude of the normalized and non-normalized cumulant density was extracted from each subject's response. We also extracted the timing of the peaks for each subject since changes in body load are known to modify the rate of vestibular-evoked postural responses (Marsden et al., 2003). Changes in the timing of the peaks could indicate a slower or more rapid development of a vestibular-evoked postural response. Finally, we estimated the ankle torque generated by subjects using the measured forces and moments, and the anatomical location of the ankle relative to the force-plate surface (Luu et al., 2011).

Statistics

Because most subjects had never balanced under conditions with altered load and vestibular cues of gravity, we first evaluated changes in general balance behavior across conditions, including RMS muscle activity, vertical loading forces, estimated ankle torque, and whole-body sway angle (mean and mean-removed RMS). Analyses of these measures from Experiment 1 showed that the data were normally distributed, therefore the effect of load was identified using a repeated-measures ANOVA (Experiment 1: 1F/1.5F/2F). However, given the low subject numbers in Experiment 2A and 2B, for these data we used a Wilcoxon signed rank test to compare general balance behaviors across conditions (Experiment 2A: 1F vs. 2F; Experiment 2B: 1G-1F vs. 0G-1F and 1G-2F vs. 1.8G-1.8F).

To test the hypothesis that sensory cues of gravity modify the vestibular control of balance, we then examined the pooled coherence, the amplitude of the normalized and non-normalized cumulant density responses and the timing of the normalized cumulant density response across our various experimental conditions. We first evaluated the effect of load cues of gravity in Experiment 1 (i.e., 1F vs. 1.5F vs. 2F) on the pooled coherence using a difference of coherence (DoC) test. The DoC test was

applied on the Fisher transform ($\tanh^{-1}$) of the coherency (square root of the coherence) values and compared to a χ^2-distribution with k - 1 degrees of freedom (k is the number of conditions included in the comparison; k = 2). We then evaluated the effect of load cues of gravity (i.e., 1F vs. 1.5F vs. 2F) on the normalized and non-normalized cumulant density responses using a Friedman test. We used a non-parametric test because the peak-to-peak amplitudes and peak timing of the cumulant density responses were not normally distributed. When significant differences were observed, we performed pairwise comparisons (Wilcoxon signed rank test, Bonferroni corrected) to decompose the main effect of load across our three conditions. We also assessed whether a comparable trend in responses was observed in subjects participating in the parabolic flights by comparing responses across the lowest and highest load conditions in Experiment 2A (i.e., 1F vs. 2F) using a DoC test on the pooled coherence and a Wilcoxon signed-rank test on the cumulant density responses. Finally, we evaluated the effect of vestibular cues of gravity on the vestibular-evoked responses in Experiment 2B – 1g vs. 0g under normal load (i.e., 1G-1F vs. 0G-1F), and 1g vs. 1.8 g under additional load (i.e., 1G-2F vs. 1.8G-1.8F) – using a DoC test on the pooled coherence and Wilcoxon signed-rank tests on the cumulant density responses. All normal data are expressed as means ± standard deviations (SD) and non-normal data are expressed as medians and interquartile ranges (IQR). For all tests, statistical significance was set at 0.05.

RESULTS

Effect of Load Cues of Gravity on Vestibular-Evoked Muscle Responses (Experiments 1 and 2A)

During Experiments 1 and 2A, all subjects were able to balance themselves at the identified target angle (see **Table 1**) in all loading conditions without difficulty. During Experiment 1, mean whole-body sway angle was comparable across the 1F, 1.5F and 2F loading conditions [$F_{(1.37,20.59)} = 0.411$, $p = 0.592$], however, the mean removed RMS sway angle varied depending on the specific load [$F_{(2,30)} = 7.650$, $p = 0.002$] (see **Figure 3**). Pairwise comparisons revealed that the highest load (2F) increased RMS sway compared to 1F and 1.5F conditions ($p = 0.036$ and $p = 0.006$, respectively), whereas there was no difference between the two lower load conditions ($p = 0.659$). As expected, the additional load during 1.5F and 2F conditions required increased medial gastrocnemius [84.4 and 128.6%, respectively, $F_{(2,30)} = 77.3$, $p < 0.001$] and soleus muscle activity [44.6 and 73.6%, respectively, $F_{(2,30)} = 69.083$, $p < 0.001$] relative to the 1F condition (see **Figure 4C**), as well as ankle increased torque [86.9 and 142.0%, respectively, $F_{(1.21,18.08)} = 156.1$, $p < 0.001$] (see **Figure 3**). Mean vertical loading forces in the 1.5F and 2F conditions were slightly below (145.9 and 187.3%, respectively) the intended load levels of 1.5 and 2 times body weight. This was likely due to a downward shift of the subject loading system over the pelvis throughout the trials, which reduced the load applied by the springs.

Lower limb muscle activity showed significant correlation with the electrical stimulus for all subjects and in all conditions. Data from a representative subject show that coherence in both muscles was significant at frequencies up to about 20 Hz (**Figure 4A**). The associated biphasic muscle response (i.e., normalized cumulant density) produced short-latency (∼70 ms) and medium-latency (∼100 ms) peaks exceeding the 95% confidence interval (**Figure 4A**). With increasing load (1.5F and 2F), the coherence and the normalized cumulant density responses decreased by similar amounts across the two conditions, while the non-normalized cumulant density progressively increased with load (see **Figure 4A** insets). A similar trend was observed in the group data (see **Figure 4B**): the DoC test revealed a significant decrease in pooled coherence in both muscles between 0 and ∼10 Hz when the load was elevated (1.5F and 2F), however, between the two load conditions (1.5F vs. 2F) there was no change in coherence. This was associated with a significant effect of load condition on the peak-to-peak amplitude of the normalized cumulant density responses in both muscles (mGAS: $\lambda^2 = 18.375$, $p < 0.001$; SOL: $\lambda^2 = 13.625$, $p = 0.001$). Pairwise analysis revealed that normalized cumulant density responses in both muscles were largest for the 1F condition and decreased by ∼27–33% when load was increased to 1.5F (mGAS: $Z = -3.516$, $p = 0.001$; SOL: $Z = -3.361$, $p = 0.002$) (**Figure 4D**). When the load was increased further to 2F, however, responses were similar to those observed in the 1.5F condition (mGAS: $Z = -0.414$, $p = 0.679$; SOL: $Z = -1.086$, $p = 0.278$), and decreased only relative to the normal load condition (mGAS: $Z = -3.309$, $p = 0.002$; SOL: $Z = -3.154$, $p = 0.005$). Non-normalized cumulant density responses, in contrast, showed a progressive increase with additional load (see **Figure 4B** insets) in both the gastrocnemius (47 and 74%, respectively, $\lambda^2 = 17.375$, $p < 0.001$) and soleus muscles (7 and 50%, respectively, $\lambda^2 = 19.500$, $p < 0.001$). Our results also indicated that the timing of the short and medium latency peaks in both muscles were effected by additional load (short latency: mGAS – $\lambda^2 = 12.132$, $p = 0.002$, SOL – 12.984, $p < 0.002$; medium latency: mGAS – $\lambda^2 = 26.000$, $p < 0.001$, SOL – $\lambda^2 = 17.322$, $p < 0.001$) (see **Table 2**). Pairwise analysis indicated that with elevated load (1.5 and 2F), the short latency peaks occurred ∼1.4–2.4 ms earlier (mGAS: multiple $p < 0.002$; SOL: multiple $p < 0.006$), and the medium latency peaks occurred ∼2.0–4.9 ms earlier (mGAS: multiple $p < 0.002$; SOL: multiple $p < 0.04$) compared to the normal 1F load condition (see **Table 2**). Similar to the normalized peak-to-peak amplitudes, we found no differences between the timing of the short and medium latency peaks across the 1.5F and 2F conditions for both muscles (mGAS: multiple $p = 1.0$; SOL: multiple $p = 1.0$).

The six subjects who participated in the on-ground training (Experiment 2A) showed similar patterns of balancing behavior and vestibular-evoked muscle responses with changing load levels as seen in Experiment 1 (see **Table 1**). Under increased load (2F), muscle activity (mGAS: 89.6%, $Z = -2.201$, $p = 0.028$; SOL: 71.6 %, $Z = -2.201$, $p = 0.028$) and ankle torque (114.6%, $Z = -2.201$, $p = 0.028$) increased substantially relative to 1F loading. Furthermore, vertical load forces in the 2F condition (185.6%) were slightly below the intended

TABLE 1 | Group data for measures of general balance behavior.

		RMS EMG		Foot-loading	Ankle torque	Sway angle	RMS angle
		mGAS [μV]	SOL [μV]	[N]	[Nm]	[°]	[°]
		mean ± SD	*mean ± SD*	*mean ± SD*	*mean ± SD*	*mean ± SD*	*mean ± SD*
Exp 1 (*n* = 16)	*1F*	46.79 ± 24.16	38.54 ± 10.82	714 ± 88	31.44 ± 9.71	2.90 ± 0.26	0.41 ± 0.10
	1.5F	86.28 ± 36.78	55.74 ± 14.31	1042 ± 123	58.77 ± 13.82	2.94 ± 0.20	0.37 ± 0.07
	2F	106.97 ± 45.78	66.90 ± 17.01	1337 ± 176	76.08 ± 21.22	2.96 ± 0.46	0.48 ± 0.12
		median/IQR	*median/IQR*	*median/ IQR*	*median/IQR*	*median/IQR*	*median/ IQR*
Exp 2A (*n* = 6)	*1F*	53.33/23.09	40.27/15.31	817/118	40.06/13.69	2.96/0.09	0.58/0.19
	2F	89.64/31.31	69.11/19.18	1517/243	85.96/24.78	3.05/0.05	0.47/0.14
Exp 2B (*n* = 6)	*0G-1F*	39.79/28.28	43.57/12.56	647/166	36.91/16.51	2.73/0.99	1.28/0.57
	1G-1F	64.85/31.09	50.17/9.86	795/101	51.96/18.07	2.07/0.62	1.18/0.81
	1.8G-1.8F	118.28/34.99	98.87/16.94	1325/179	85.01/17.29	-2.00/0.67	3.08/ 0.92
	1G-2F	92.91/37.28	72.26/12.66	1405/259	85.21/30.15	2.19/0.46	0.70/0.41

For normally distributed data, mean and standard deviation (SD) are given, while for non-normally distributed data, median and interquartile range (IQR) are given. mGAS, medial gastrocnemius muscle; SOL, soleus muscle.

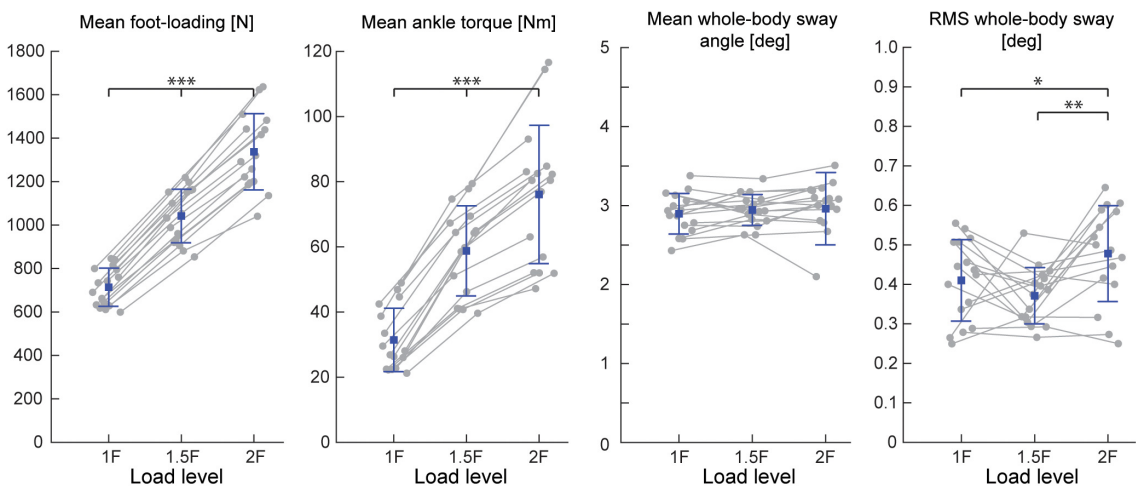

FIGURE 3 | Outcome measures of general balance behavior during Experiment 1 (*n* = 16). Responses include vertical loading forces, ankle torque and whole-body sway angle (mean and mean-removed RMS). Individual subjects are plotted as gray dots. Group responses are plotted with means (blue dots) and standard deviations (whiskers). *$p < 0.05$, **$p < 0.01$, and ***$p < 0.001$ indicates significant differences between conditions. mGAS = medial gastrocnemius muscle, SOL = soleus muscle.

level of 2 times the subjects' body weight (**Table 1**). Minor differences relative to Experiment 1, however, were observed; mean whole-body sway angle increased by 3% ($Z = -1.992$, $p = 0.046$) during 2F loading, while RMS sway was similar across conditions ($Z = -1.153$, $p = 0.249$). Nevertheless, the vestibular-evoked muscle responses in these six subjects also showed similar changes with increasing load when compared to those observed in Experiment 1. During 2F loading, DoC tests revealed that pooled coherence in both muscles decreased between 0 and ∼8 Hz (data not shown). Similarly, in both muscles, the normalized cumulant density responses decreased during 2F loading (mGAS: 42%, $Z = -2.201$, $p = 0.028$; SOL: 19%, $Z = -2.201$, $p = 0.028$), while the non-normalized cumulant density responses increased (mGAS: 62%, $Z = -2.201$, $p = 0.028$; SOL: 27%, $Z = -2.201$, $p = 0.028$) (see **Table 2**). Finally, timing of the short- and medium latency peaks with additional load occurred ∼1.3–2.5 ms (mGAS: $Z = -2.201$, $p = 0.028$) and ∼6.4–7.5 ms earlier (mGAS: $Z = -2.201$, $p = 0.028$; SOL: $Z = -2.207$, $p = 0.027$) relative to normal standing, respectively, with the exception of the soleus short latency peak which did not differ across conditions (SOL: $Z = -0.949$, $p = 0.343$).

Overall, the results of Experiments 1 and 2A indicate that although non-normalized vestibular-evoked muscle responses increase with additional load, the relative vestibular contribution (i.e., normalized cumulant density) is reduced and slightly advanced compared to normal balance conditions. However, no further changes in the amplitude and timing of the relative

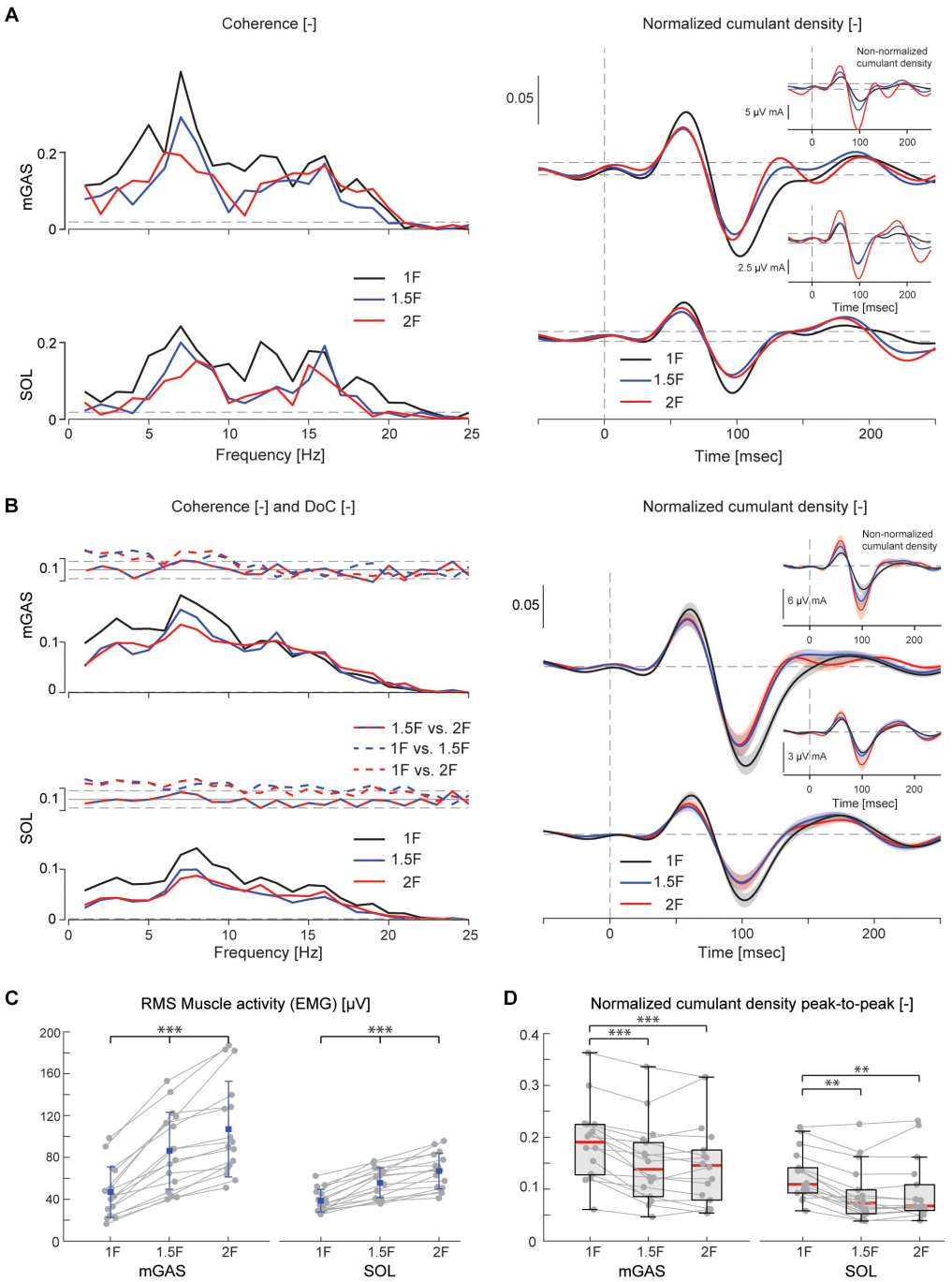

FIGURE 4 | Vestibular-evoked muscle responses with varying load levels from Experiment 1. Data from the medial gastrocnemius and soleus muscles are shown for a single subject **(A)** and group responses (n = 16) **(B)**. Horizontal dotted lines indicate the 95% confidence limits for coherence, difference-of-coherence (DoC) and cumulant density responses. DoC results are plotted above the group pooled coherence results. A positive value for the DoC indicates greater coherence for the first condition listed in each comparison; whereas a negative value represents greater coherence for the second condition in each comparison. Cumulant density plots show the normalized and non-normalized (insets) responses for both individual subject and group data. In the group cumulant density responses, bold lines are group means and for illustrative purposes shaded areas show the standard error. For comparison, data from the group (n = 16) root-mean-square of muscle activity (EMG) **(C)** and peak-to-peak amplitudes of the normalized cumulant density responses **(D)** are shown. Individual subjects are plotted as gray dots. Group responses for normally distributed data are plotted with means (blue dots) and standard deviations (whiskers), while non-normally distributed data are plotted with medians (red line), 25 and 75 percentiles (gray box) and extreme data points (whiskers). $^{**}p < 0.01$ and $^{***}p < 0.001$ indicates significant differences between conditions. mGAS = medial gastrocnemius muscle, SOL = soleus muscle.

TABLE 2 | Group data of peak-to-peak normalized and non-normalized cumulant density responses responses, as well as timing of the short- and medium latency responses.

		Normalized cumlant density peak-to-peak [-]		Non-normalized cumulant density peak-to-peak [uV mA]		Short latency [msec]		Medium latency [msec]	
		Gas	Sol	Gas	Sol	mGAS	SOL	mGAS	SOL
		median / IQR	*median / IQR*	*median / IQR*	*median / IQR*	*median / IQR*	*median / IQR*	*median / IQR*	*median / IQR*
Exp 1	*1F*	0.19/0.10	0.11/0.05	11.41/10.12	6.62/5.92	61.3/2.8	62.3/3.8	103.3/3.8	101.8/5.0
	1.5F	0.14/0.10	0.07/0.05	16.81/21.70	6.97/7.59	59.5/4.5	59.8/4.4	98.5/5.0	99.3/4.9
	2F	0.15/0.10	0.07/0.05	19.87/24.99	9.54/9.48	59.8/3.0	58.8/3.5	97.8/4.5	100.0/3.9
Exp 2A	*1F*	0.16/0.08	0.10/0.09	8.65/18.48	5.64/9.18	61.9/7.9	62.8/6.9	107.3/18.5	114.8/19.5
	2F	0.13/0.09	0.06/0.08	13.98/17.72	7.17/14.43	60.8/8.6	63.0/5.6	98.3/14.8	103.3/15.4
Exp 2B	*0G-1F*	0.12/0.05	0.09/0.06	6.94/5.25	7.85/5.37	62.5/7.8	66.5/5.5	108.5/12.0	113.5/11.5
	1G-1F	0.17/0.12	0.12/0.10	15.68/11.66	10.97/9.22	60.8/2.1	62.5/5.0	107.8/6.4	109.5/7.5
	1.8G-1.8F	0.12/0.07	0.11/0.05	23.21/13.41	15.65/12.09	57.3/5.3	61.0/3.5	99.3/7.5	102.0/9.5
	1G-2F	0.16/0.06	0.09/0.04	21.20/14.29	12.40/6.46	60.3/7.4	61.5/4.0	97.8/13.4	104.5/7.1

mGAS, medial gastrocnemius muscle; SOL, soleus muscle.

vestibular contribution are observed when the load exceeds 1.5 times the body weight.

Effect of Vestibular Cues of Gravity on Vestibular-Evoked Muscle Responses (Experiment 2B)

When subjects balanced during the in-flight experiments (i.e., Experiment 2B), we observed an increased difficulty in maintaining upright stance. Plane turbulence and unexpected loads throughout the parabola caused some subjects to fall into the end stops. As a result, the mean-removed RMS whole-body sway was ∼2–3 times higher during in-flight testing as compared to on-ground training (**Table 1**). Nevertheless, the general balance behavior from Experiment 2B showed similar trends as Experiment 2A when the total load was increased (i.e., 0G-1F/1G-1F vs. 1.8G-1.8F/1G-2F). Specifically, mean foot loading, ankle torque and muscle activity increased under conditions with higher load. Variations in balance behaviors, however, were observed when comparing responses across the different gravity levels as detailed below.

Comparison of 0G-1F and 1G-1F Conditions

During the micro-g phase of the parabola (i.e., 0G-1F condition), all subjects were able to maintain upright balance without difficulty. Load forces during the 0G-1F condition, however, were 18.6% lower than the 1G-1F conditions ($Z = -2.201$, $p = 0.028$) (see **Figure 5**). As a result, ankle torque ($Z = -2.201$, $p = 0.028$) and medial gastrocnemius muscle activity ($Z = -2.201$, $p = 0.028$) were also 31.9 and 38.6% lower during the micro-g condition, respectively. Notably, however, there was no difference in the soleus muscle activity across gravitational conditions ($Z = -0.943$, $p = 0.345$) (see **Figure 6C**). Finally, mean whole-body sway angle during the micro-g condition was larger relative to the normal 1G-1F condition ($Z = -2.201$, $p = 0.028$) – though this was attributed to a single subject who leaned too far forward – while mean-removed RMS sway was not significantly different ($Z = -0.734$, $p = 0.463$) (**Table 1** and **Figure 5**).

The electrical stimulus evoked significant muscle responses in all subjects during trials both with and without gravity. Data from a representative subject show that during the micro-g condition, both coherence and cumulant density responses in the medial gastrocnemius muscle decreased relative to the normal condition (**Figure 6A** black and green traces). Similar responses were observed in the group data (**Figure 6B** black and green traces): the DoC test indicated that pooled coherence decreased when subjects stood without gravity at frequencies between 0 and ∼10 Hz, but only in the medial gastrocnemius muscle (see **Figure 6A** black and green traces; note SOL muscle data not shown). This decrease in medial gastrocnemius coherence was associated with a 30% decrease in the normalized cumulant density ($Z = -1.992$, $p = 0.046$) (**Figure 6D**), and was accompanied by a 29% decrease in the non-normalized cumulant density ($Z = -2.201$, $p = 0.028$) (**Figure 6B** inset, black and green traces). In the soleus muscle, a similar decreasing trend in the responses of both cumulant density measures was observed during micro-g conditions, however, these differences were not significant (normalized: $Z = -1.782$, $p = 0.075$; non-normalized: $Z = -1.363$, $p = 0.173$) (**Figure 6D**). Furthermore, we also found no change in the timing of the short and medium latency peaks across gravity conditions for both the medial gastrocnemius (short: $Z = -0.535$, $p = 0.593$; medium: $Z = -0.135$, $p = 0.892$) and soleus muscle (short: $Z = -0.184$, $p = 0.854$; medium: $Z = -0.674$, $p = 0.500$) (see **Table 2**).

Comparison of 1.8G-1.8F and 1G-2F Conditions

Throughout the hyper-g phase of the parabola (i.e., 1.8G-1.8F condition), plane accelerations in the direction of balance (i.e., longitudinal axis of the plane) progressively increased and tended to push the subjects forward. This additional load made it difficult for subjects to maintain the desired whole-body sway angle without falling into the forward end stop. Consequently, the subjects were instructed to stand leaning forward at an angle that required similar effort as the condition when additional load was provided by the springs with normal 1 g gravity (i.e., 1G-2F).

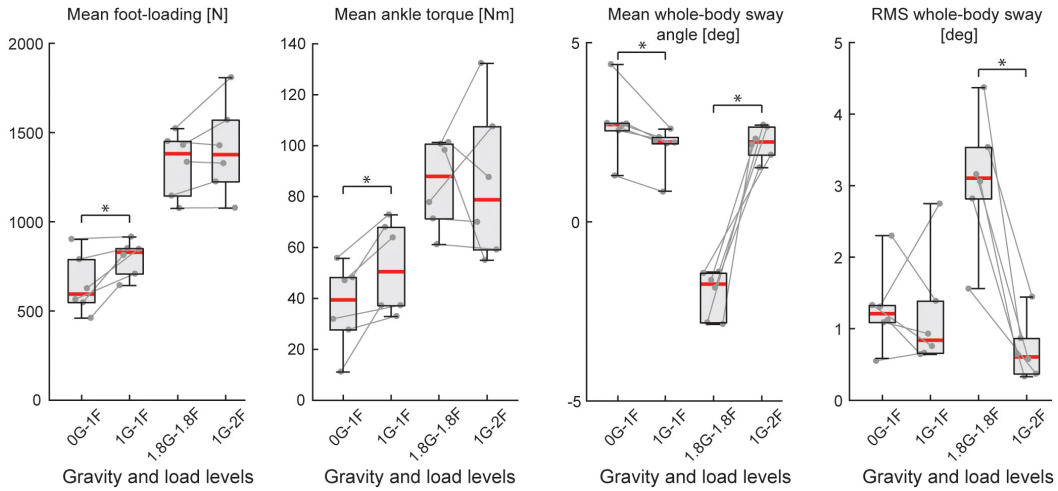

FIGURE 5 | Outcome measures of general balance behavior during Experiment 2B (n = 6). Responses include vertical loading forces, ankle torque and whole-body sway angle (mean and mean-removed RMS). Individual subjects are plotted as gray dots. Data are plotted as median (red line), 25 and 75 percentiles (gray box) and extreme data points (gray whiskers). *$p < 0.05$ indicates significant differences between conditions.

This ensured that the muscles were engaged in a task to remain upright but required that subjects stand at a mean whole-body sway angle that was ∼4° anterior relative to the 1G-2F condition ($Z = -2.201$, $p = 0.028$). Despite this difference in sway angle, load forces and ankle torque were similar across normal and hyper-g conditions (i.e., 1.8G-1.8F vs. 1G-2F, see **Table 1** and **Figure 5**; load forces: $Z = -1.153$, $p = 0.249$; ankle torque: $Z = -0.314$, $p = 0.753$). However, muscle activity was ∼21–27% higher during hyper-g trials (mGAS: $Z = -2.201$, $p = 0.028$; SOL: $Z = -2.201$, $p = 0.028$) and the mean-removed RMS sway was about three times higher ($Z = -2.201$, $p = 0.028$). These differences in muscle activity and sway variability were likely due to the variation in longitudinal acceleration that occurred during the hyper-g phase.

Despite the differences in general balance behavior, the electrical stimuli evoked significant muscle responses in conditions with and without the additional gravity. Data from a representative subject show that during the hyper-g condition, coherence and normalized cumulant density responses in the medial gastrocnemius muscle decreased relative to the normal condition (**Figure 6A** red and blue traces). The non-normalized cumulant density response, however, showed no obvious variation in response magnitude across conditions (**Figure 6A** inset, red and blue traces). A similar effect of the additional gravity was observed in the group data: the DoC test showed coherence decreased during hyper-g trials at most frequencies between 0 and ∼10 Hz, but only in the medial gastrocnemius muscle (**Figure 6B** red and blue traces; note SOL muscle data not shown). Further, this decrease in medial gastrocnemius coherence was associated with a 29% decrease in the normalized cumulant density ($Z = -2.201$, $p = 0.028$), but no significant difference in the non-normalized cumulant density ($Z = -0.105$, $p = 0.917$) (see **Figure 6B** inset, red and blue traces). Soleus muscle responses, in contrast, showed no significant difference with the additional gravity for both the normalized and non-normalized cumulant density responses (both: $Z = -0.105$, $p = 0.917$) (see **Table 2**). Similar to the micro-g conditions, timing of the short and medium latency peaks showed no change between conditions for both the medial gastrocnemius (short: $Z = -1.604$, $p = 0.109$; medium: $Z = -0.943$, $p = 0.345$) and soleus muscle (short: $Z = -1.095$, $p = 0.273$; medium: $Z = -1.625$, $p = 0.104$) (see **Table 2**).

Overall, the results of Experiment 2B indicate that vestibular input to muscle activity persist across varying levels of gravity, but that the relative contribution of vestibular input to ongoing muscle activity decreases when vestibular cues of gravity decrease (but perhaps not increase) relative to normal 1 g gravity.

DISCUSSION

The aim of the present study was to determine whether both somatosensory and vestibular cues of gravity modify the corrective muscle actions to vestibular-evoked postural disturbances. Our results show that when subjects balanced with added load and a constant 1 g vestibular signal, the relative vestibular contribution to the evoked muscle responses (i.e., coherence and normalized cumulant density) decreased and occurred earlier relative to responses during normal standing. In addition, when subjects balanced with varying levels of gravity while the overall load was held relatively constant, the relative vestibular contribution to evoked muscle responses also decreased. This modulation, however, was primarily limited to micro-g conditions when vestibular cues of gravity were absent. Furthermore, these response reductions with changes in gravity occurred in absence of any significant change in their timing. These results demonstrate that load-related cues of gravity from the somatosensory system (i.e., cutaneous and proprioception) and vestibular-related cues of gravity from the otolith end organs influence the vestibular drive for standing balance, such that the relative vestibular contribution to corrective postural

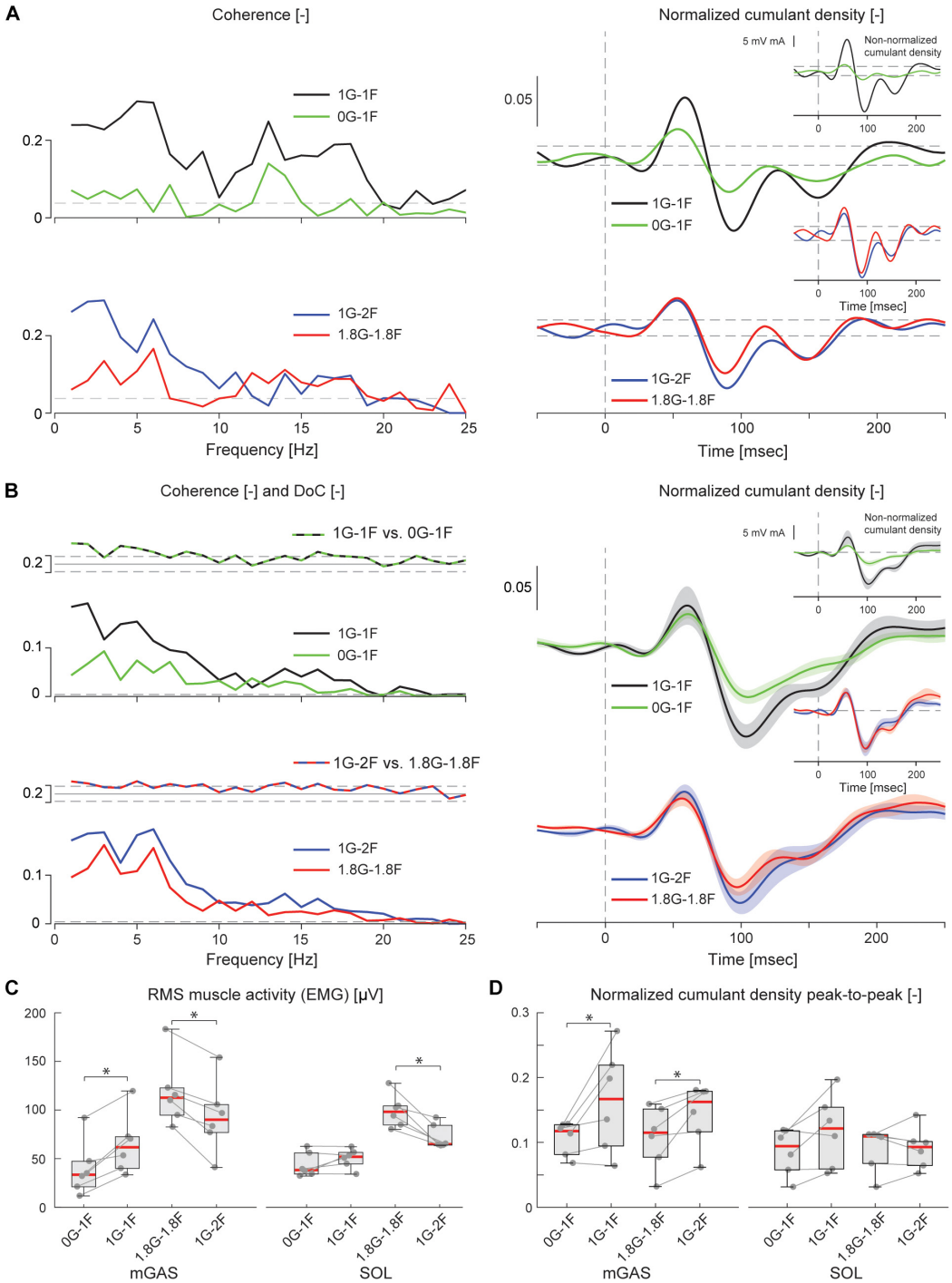

FIGURE 6 | Vestibular-evoked muscle responses with varying load and gravity levels from Experiment 2B. Data from the medial gastrocnemius muscle are shown for a single subject **(A)** and group responses (n = 6) **(B)**. In general, variations in gravity and load level relative to normal standing conditions resulted in lowered coherence and cumulant density responses. Horizontal dotted lines indicate the 95% confidence limits for coherence, difference-of-coherence and cumulant density responses. DoC results are plotted above the group pooled coherence results. A positive value for the DoC indicates greater coherence for the first condition listed in each comparison; whereas a negative value represents greater coherence for the second condition in each comparison. Cumulant density plots show the normalized and non-normalized (insets) responses for both individual subject and group data. In the group cumulant density responses, bold lines are group means and for illustrative purposes shaded areas show the standard error. For comparison, data from the group (n = 6) root-mean-square of muscle activity (EMG) **(C)** and peak-to-peak amplitudes of the normalized cumulant density responses **(D)** are shown. Individual subjects are plotted as gray dots. Group data are plotted as median (red line), 25 and 75 percentiles (gray box) and extreme data points (whiskers). *$p < 0.05$ indicates significant differences between conditions.

responses decreases when sensory cues of gravity differ from normal 1 g conditions.

Despite the reduction in the normalized vestibular-evoked responses across varying load and gravity levels, significant muscle responses to the electrical stimulus were observed for all subjects in all conditions. This aligns with the notion that vestibular-evoked muscle corrections during quiet standing are only evoked when both vestibular information and a muscle's contribution are relevant to the process of balancing the body (Britton et al., 1993; Fitzpatrick et al., 1994; Luu et al., 2012; Forbes et al., 2016). For instance, responses are absent when standing subjects balance a body-equivalent inverted pendulum while being supported by a rigid backboard, a condition where somatosensory signals – but not vestibular signals – are relevant to the balance task (Fitzpatrick et al., 1994). Therefore, it is not entirely surprising that vestibular-evoked muscle responses were observed across our changing load and gravity conditions since both the vestibular feedback and the muscle corrections were always engaged in, and/or relevant to, balancing the body against a downward pulling force. Under micro-gravity conditions, the otolith sensory cues produced by gravity were removed, limiting the available sensory cues of the downward pulling force to somatosensors only. Our results therefore demonstrate that vestibular contributions to standing can be maintained with sensory feedback signals of load and balance that are absent of the otolithic signal of gravity (e.g., somatosensory and/or dynamic vestibular signals). Accordingly, it may be possible that even after prolonged exposure to micro-gravity in space-flight, vestibular-evoked muscle responses continue to compensate for vestibular disturbances while balancing the body against a downward load, in contrast to the reduced otolith-spinal reflexes during the specific freefall drop conditions (Reschke et al., 1984, 1986; Watt et al., 1986). The sustained influence of a vestibular signal for balance in the absence of gravity also parallels the observation that when balancing without proprioceptive signals of ankle angle (i.e., sway referenced balance) (Nashner and Wolfson, 1974; Luu et al., 2012; Forbes et al., 2016) or visual signals of body sway (i.e., in the dark or with eyes closed) (Fitzpatrick et al., 1996; Welgampola and Colebatch, 2001) vestibular-evoked muscle responses are retained.

The changes in vestibular-evoked responses observed here also align with the influence that varying sensory cues of standing can have on the vestibular control of balance (Nashner and Wolfson, 1974; Lund and Broberg, 1983; Britton et al., 1993; Welgampola and Colebatch, 2001; Muise et al., 2012). Cooling of the feet, for example, reduces the sensitivity of cutaneous receptors and increases vestibular-evoked muscle responses (Muise et al., 2012). Similarly, additional load on the body decreases cutaneous receptor sensitivity (Mildren et al., 2016), and progressively increases the associated vestibular-evoked postural responses (Marsden et al., 2003). At first glance, our results when increasing the load (Experiments 1 and 2A) seem to contradict the study of Marsden et al. (2003), since the normalized vestibular-evoked muscle responses reported here (a) decreased with additional load, and (b) ceased to vary (or plateau) when the load was increased from 1.5 to 2 times the body weight. Marsden et al. (2003) however, examined the rate of reaction force development evoked by a transient electrical stimulus, a non-normalized response that reflects the net contribution of vestibular input to postural control. Indeed, similar to Marsden et al. (2003) we found that the non-normalized cumulant density responses also increased with additional load. Our normalized cumulant density results therefore extend the findings of Marsden et al. (2003) showing that although the total vestibular contribution progressively increases with the excitability of the motoneuron pool at higher loads, the relative contribution of vestibular signals decreases. As the load increases beyond 1.5 times body weight, however, the relative vestibular input remains constant.

Our results from Experiment 2B further demonstrate that a decreasing vestibular cue of gravity also influences the processing of vestibular information for balance. Under micro-g conditions, normalized vestibular-evoked muscle responses decreased relative to standing with 1 g vestibular cues and matching load cues (1F). The covariation of both the normalized and non-normalized cumulant density responses together with EMG magnitude (i.e., all measures decreasing) during micro-g trials suggests that the net decrease in the input to the motoneuron was accompanied by a proportionally larger decrease in the vestibular contribution. During hyper-g conditions, in contrast, we saw a reduction only in the normalized cumulant density together with an increase in EMG magnitudes. It appears likely that the decrease in the normalized cumulant density responses during hyper-g was simply due to a net increase in the input to motoneuron arising from non-vestibular sources (Bacsi and Colebatch, 2005; Heroux et al., 2015). A confounding factor in interpreting these hyper-g results, however, is that the loading conditions were substantially different across the two conditions. In particular, the mean sway angle during hyper-g trials was ∼4 degrees posterior and the RMS sway angle was three times higher relative to the 1 g (i.e., 1G-2F) condition. Accordingly, we cannot rule out the possibility that variations in balance state across conditions (i.e., sway angle, sway velocity) (Lee Son et al., 2008; Forbes et al., 2018; Rasman et al., 2018) also contributed to any effect caused by changing gravity. Finally, an additional limitation to these results is that the observed changes in vestibular contributions across gravity conditions in the medial gastrocnemius muscles were not observed in the soleus muscle. However, given the reduced sensitivity of the soleus muscle to vestibular input as compared to the medial gastrocnemius muscle (Dakin et al., 2016), it may be possible that an effect could be seen if the number of subjects was increased.

Overall, the results of both experiments indicate that changes in load and vestibular cues of gravity primarily decrease the relative contribution of vestibular signals to ongoing muscle activity. This reduction in the normalized vestibular-evoked muscle responses with changes in multiple sensory cues of gravity may be compatible with previous observations that the amplitude of vestibular-induced balance responses are dependent upon the congruency between actual and expected sensory consequences of postural motor actions (Luu et al., 2012). The balance system is thought to predict the sensory consequences of postural tasks using an internal model of the standing body's dynamics under normal 1 g loading (van der Kooij et al., 2001; Kuo, 2005;

Heroux et al., 2015; Forbes et al., 2018). When the sensory predictions produced by the internal model do not match actual sensory feedback, vestibular input to standing balance decreases. Therefore, when subjects balance with altered load or vestibular cues of gravity, the change in congruent sensory signals relative to normally expected 1 g standing produces similar changes (i.e., reductions) in the vestibular-evoked motor responses. Importantly, this does not exclude the possibility for adaptation to any of these altered sensory conditions, which over sufficient exposure may allow the vestibular-evoked responses to return to expected levels (Heroux et al., 2015).

CONCLUSION

The present study shows that the vestibular drive for standing balance was always present across variations in load- and vestibular-related cues of gravity, but that the relative vestibular contribution was attenuated when these signals were altered from normal 1 g conditions. This suggests that multiple afferent feedback cues of gravity influence the contribution of vestibular signals for the control of upright stance. Our study provides unique insight into the effect that changing levels of gravity can have on the sensorimotor processing for standing balance and may have important implications for astronauts interacting in different levels of gravity.

ETHICS STATEMENT

The study protocol was approved by the Medical Research Ethics Committee Erasmus MC (Experiment 1) and the University of Caen's Ethics Committee (Experiment 2). The experiments were conducted in accordance with the Declaration of Helsinki and all subjects gave their written informed consent prior to participation.

AUTHOR CONTRIBUTIONS

AA and PF contributed to the conception and design of the study, analyzed the data and wrote the first draft of the manuscript. ZJ created the custom MATLAB software. AA, DvP, CH, and PF collected the data. All authors contributed to manuscript revisions, and read and approved the submitted version.

FUNDING

The research leading to these results was supported by Netherlands Organization for Scientific Research (NWO #016.Veni.188.049, PA Forbes) and the FlyYourThesis! 2017 Campaign of the European Space Agency (ESA).

ACKNOWLEDGMENTS

We thank the staff of Novespace and ESA Education for their assistance in preparing and performing the parabolic flight experiments, the subjects who participated in this research and Jean-Sébastien Blouin for critical discussions of the experimental design and results. We also thank Ramona Ritzmann (University of Freiburg), the German Aerospace Center (DLR) and Digitimer (Hertfordshire, United Kingdom) for loaning experimental equipment used in this research.

REFERENCES

Bacsi, A. M., and Colebatch, J. G. (2005). Evidence for reflex and perceptual vestibular contributions to postural control. *Exp. Brain Res.* 160, 22–28. doi: 10.1007/s00221-004-1982-2

Britton, T. C., Day, B. L., Brown, P., Rothwell, J. C., Thompson, P. D., and Marsden, C. D. (1993). Postural electromyographic responses in the arm and leg following galvanic vestibular stimulation in man. *Exp. Brain Res.* 94, 143–151.

Cathers, I., Day, B. L., and Fitzpatrick, R. C. (2005). Otolith and canal reflexes in human standing. *J. Physiol.* 563, 229–234. doi: 10.1113/jphysiol.2004.079525

Dakin, C. J., Heroux, M. E., Luu, B. L., Inglis, J. T., and Blouin, J. S. (2016). Vestibular contribution to balance control in the medial gastrocnemius and soleus. *J. Neurophysiol.* 115, 1289–1297. doi: 10.1152/jn.00512.2015

Dakin, C. J., Inglis, J. T., and Blouin, J.-S. (2011). Short and medium latency muscle responses evoked by electrical vestibular stimulation are a composite of all stimulus frequencies. *Exp. Brain Res.* 209, 345–354. doi: 10.1007/s00221-011-2549-7

Dakin, C. J., Luu, B. L., van den Doel, K., Inglis, J. T., and Blouin, J. S. (2010). Frequency-specific modulation of vestibular-evoked sway responses in humans. *J. Neurophysiol.* 103, 1048–1056. doi: 10.1152/jn.00881.2009

Dakin, C. J., and Rosenberg, A. (2018). Gravity estimation and verticality perception. *Handb. Clin. Neurol.* 159, 43–59. doi: 10.1016/B978-0-444-63916-5.00003-3

Dakin, C. J., Son, G. M. L., Inglis, J. T., and Blouin, J. S. (2007). Frequency response of human vestibular reflexes characterized by stochastic stimuli. *J. Physiol.* 583, 1117–1127. doi: 10.1113/jphysiol.2007.133264

Dalton, B. H., Blouin, J. S., Allen, M. D., Rice, C. L., and Inglis, J. T. (2014). The altered vestibular-evoked myogenic and whole-body postural responses in old men during standing. *Exp. Gerontol.* 60, 120–128. doi: 10.1016/j.exger.2014.09.020

Day, B. L., and Fitzpatrick, R. C. (2005). Virtual head rotation reveals a process of route reconstruction from human vestibular signals. *J. Physiol.* 567, 591–597. doi: 10.1113/jphysiol.2005.092544

Fitzpatrick, R., Burke, D., and Gandevia, S. C. (1994). Task-dependent reflex responses and movement illusions evoked by galvanic vestibular stimulation in standing humans. *J. Physiol.* 478, 363–372. doi: 10.1113/jphysiol.1994.sp020257

Fitzpatrick, R., Burke, D., and Gandevia, S. C. (1996). Loop gain of reflexes controlling human standing measured with the use of postural and vestibular disturbances. *J. Neurophysiol.* 76, 3994–4008. doi: 10.1152/jn.1996.76.6.3994

Fitzpatrick, R. C., and Day, B. L. (2004). Probing the human vestibular system with galvanic stimulation. *J. Appl. Physiol.* 96, 2301–2316. doi: 10.1152/japplphysiol.00008.2004

Forbes, P. A., Chen, A., and Blouin, J. S. (2018). Sensorimotor control of standing balance. *Handb. Clin. Neurol.* 159, 61–83. doi: 10.1016/B978-0-444-63916-5.00004-5

Forbes, P. A., Luu, B. L., Van der Loos, H. F., Croft, E. A., Inglis, J. T., and Blouin, J. S. (2016). Transformation of vestibular signals for the control of standing in humans. *J. Neurosci.* 36, 11510–11520. doi: 10.1523/jneurosci.1902-16.2016

Forbes, P. A., Siegmund, G. P., Happee, R., Schouten, A. C., and Blouin, J. S. (2014). Vestibulocollic reflexes in the absence of head postural control. *J. Neurophysiol.* 112, 1692–1702. doi: 10.1152/jn.00343.2014

Goldberg, J. M., Smith, C. E., and Fernandez, C. (1984). Relation between discharge regularity and responses to externally applied galvanic currents in vestibular

nerve afferents of the squirrel-monkey. *J. Neurophysiol.* 51, 1236–1256. doi: 10.1152/jn.1984.51.6.1236

Halliday, D. M., Rosenberg, J. R., Amjad, A. M., Breeze, P., Conway, B. A., and Farmer, S. F. (1995). A framework for the analysis of mixed time series/point process data - Theory and application to the study of physiological tremor, single motor unit discharges and electromyograms. *Prog. Biophys. Mol. Biol.* 64, 237–278. doi: 10.1016/s0079-6107(96)00009-0

Heroux, M. E., Law, T. C., Fitzpatrick, R. C., and Blouin, J. S. (2015). Cross-modal calibration of vestibular afference for human balance. *PLoS One* 10:e0124532. doi: 10.1371/journal.pone.0124532

Huryn, T. P., Luu, B. L., Van der Loos, H. F. M., Blouin, J. S., and Croft, E. A. (2010). "Investigating human balance using a robotic motion platform," in *Proceedings of the 2010 IEEE International Conference on Robotics and Automation*, (Piscataway, NJ), 5090–5095.

Kim, J., and Curthoys, I. S. (2004). Responses of primary vestibular neurons to galvanic vestibular stimulation (GVS) in the anaesthetised guinea pig. *Brain Res. Bull.* 64, 265–271. doi: 10.1016/j.brainresbull.2004.07.008

Kim, K.-S., Minor, L. B., Della Santina, C. C., and Lasker, D. M. (2011). Variation in response dynamics of regular and irregular vestibular-nerve afferents during sinusoidal head rotations and currents in the chinchilla. *Exp. Brain Res.* 210, 643–649. doi: 10.1007/s00221-011-2600-8

Kuo, A. D. (2005). An optimal state estimation model of sensory integration in human postural balance. *J. Neural Eng.* 2, S235–S249.

Kwan, A., Forbes, P. A., Mitchell, D. E., Blouin, J. S., and Cullen, K. E. (2019). Neural substrates, dynamics and thresholds of galvanic vestibular stimulation in the behaving primate. *Nat. Commun.* 10:1904. doi: 10.1038/s41467-019-09738-1

Lee Son, G. M., Blouin, J. S., and Inglis, J. T. (2008). Short-duration galvanic vestibular stimulation evokes prolonged balance responses. *J. Appl. Physiol.* 105, 1210–1217. doi: 10.1152/japplphysiol.01398.2006

Lund, S., and Broberg, C. (1983). Effects of different head positions on postural sway in man induced by a reproducible vestibular error signal. *Acta Physiol. Scand.* 117, 307–309. doi: 10.1111/j.1748-1716.1983.tb07212.x

Luu, B. L., Huryn, T. P., Van der Loos, H. F. M., Croft, E. A., and Blouin, J.-S. (2011). Validation of a robotic balance system for investigations in the control of human standing balance. *IEEE Trans. Neural. Syst. Rehabil. Eng.* 19, 382–390. doi: 10.1109/TNSRE.2011.2140332

Luu, B. L., Inglis, J. T., Huryn, T. P., Van der Loos, H. F. M., Croft, E. A., and Blouin, J.-S. (2012). Human standing is modified by an unconscious integration of congruent sensory and motor signals. *J. Physiol.* 590, 5783–5794. doi: 10.1113/jphysiol.2012.230334

Marsden, J. F., Blakey, G., and Day, B. L. (2003). Modulation of human vestibular-evoked postural responses by alterations in load. *J. Physiol.* 548, 949–953. doi: 10.1113/jphysiol.2002.029991

Marsden, J. F., Castellote, J., and Day, B. L. (2002). Bipedal distribution of human vestibular-evoked postural responses during asymmetrical standing. *J. Physiol.* 542, 323–331. doi: 10.1113/jphysiol.2002.019513

Mian, O. S., and Day, B. L. (2014). Violation of the craniocentricity principle for vestibularly evoked balance responses under conditions of anisotropic stability. *J. Neurosci.* 34, 7696–7703. doi: 10.1523/JNEUROSCI.0733-14.2014

Mildren, R. L., Strzalkowski, N. D., and Bent, L. R. (2016). Foot sole skin vibration perceptual thresholds are elevated in a standing posture compared to sitting. *Gait Posture* 43, 87–92. doi: 10.1016/j.gaitpost.2015.10.027

Muise, S. B., Lam, C. K., and Bent, L. R. (2012). Reduced input from foot sole skin through cooling differentially modulates the short latency and medium latency vestibular reflex responses to galvanic vestibular stimulation. *Exp. Brain Res.* 218, 63–71. doi: 10.1007/s00221-012-3002-2

Nashner, L. M., and Wolfson, P. (1974). Influence of head position and proprioceptive cues on short latency postural reflexes evoked by galvanic stimulation of human labyrinth. *Brain Res.* 67, 255–268. doi: 10.1016/0006-8993(74)90276-5

Peters, R. M., Rasman, B. G., Inglis, J. T., and Blouin, J. S. (2015). Gain and phase of perceived virtual rotation evoked by electrical vestibular stimuli. *J. Neurophysiol.* 114, 264–273. doi: 10.1152/jn.00114.2015

Rasman, B. G., Forbes, P. A., Tisserand, R., and Blouin, J.-S. (2018). Sensorimotor manipulations of the balance control loop–beyond imposed external perturbations. *Front Neurol* 9:899. doi: 10.3389/fneur.2018.00899

Reschke, M. F., Anderson, D. J., and Homick, J. L. (1984). Vestibulospinal reflexes as a function of microgravity. *Science* 225, 212–214. doi: 10.1126/science.6729475

Reschke, M. F., Anderson, D. J., and Homick, J. L. (1986). Vestibulo-spinal response modification as determined with the H-reflex during the Spacelab-1 flight. *Exp. Brain Res.* 64, 367–379.

Reynolds, R. F. (2010). The effect of voluntary sway control on the early and late components of the vestibular-evoked postural response. *Exp. Brain Res.* 201, 133–139. doi: 10.1007/s00221-009-2017-9

Tribukait, A., and Rosenhall, U. (2001). Directional sensitivity of the human macula utriculi based on morphological characteristics. *Audiol. Neurootol.* 6, 98–107. doi: 10.1159/000046815

van der Kooij, H., Jacobs, R., Koopman, B., and van der Helm, F. C. T. (2001). An adaptive model of sensory integration in a dynamic environment applied to human stance control. *Biol. Cybern.* 84, 103–115. doi: 10.1007/s004220000196

Watt, D. G., Money, K. E., and Tomi, L. M. (1986). M.I.T./*Canadian vestibular experiments on the Spacelab*-1 mission: 3. Effects of prolonged weightlessness on a human otolith-spinal reflex. *Exp. Brain Res.* 64, 308–315.

Welgampola, M. S., and Colebatch, J. G. (2001). Vestibulospinal reflexes: quantitative effects of sensory feedback and postural task. *Exp. Brain Res.* 139, 345–353. doi: 10.1007/s002210100754

Conflict of Interest Statement: The authors declare that the research was conducted in the absence of any commercial or financial relationships that could be construed as a potential conflict of interest.

frontiers in Physiology

ORIGINAL RESEARCH
published: 21 May 2019
doi: 10.3389/fphys.2019.00627

Lumbopelvic Muscle Changes Following Long-Duration Spaceflight

*Kyle P. McNamara[1], Katelyn A. Greene[1], Austin M. Moore[1], Leon Lenchik[2] and Ashley A. Weaver[1]**

[1]Center of Injury Biomechanics, Virginia Tech - Wake Forest University School of Biomedical Engineering and Sciences, Winston-Salem, NC, United States, [2]Department of Radiology, Wake Forest School of Medicine, Winston-Salem, NC, United States

Long-duration spaceflight has been shown to negatively affect the lumbopelvic muscles of crewmembers. Through analysis of computed tomography scans of crewmembers on 4- to 6-month missions equipped with the interim resistive exercise device, the structural deterioration of the psoas, quadratus lumborum, and paraspinal muscles was assessed. Computed tomography scans of 16 crewmembers were collected before and after long-duration spaceflight. The volume and attenuation of lumbar musculature at the L2 vertebral level were measured. Percent changes in the lumbopelvic muscle volume and attenuation (indicative of myosteatosis, or intermuscular fat infiltration) following spaceflight were calculated. Due to historical studies demonstrating only decreases in the muscles assessed, a one-sample *t* test was performed to determine if these decreases persist in more recent flight conditions. Crewmembers on interim resistive exercise device-equipped missions experienced an average 9.5% (2.0% SE) decrease in volume and 6.0% (1.5% SE) decrease in attenuation in the quadratus lumborum muscles and an average 5.3% (1.0% SE) decrease in volume and 5.3% (1.6% SE) decrease in attenuation in the paraspinal muscles. Crewmembers experienced no significant changes in psoas muscle volume or attenuation. No significant changes in intermuscular adipose tissue volume or attenuation were found in any muscles. Long-duration spaceflight was associated with preservation of psoas muscle volume and attenuation and significant decreases in quadratus lumborum and paraspinal muscle volume and attenuation.

Keywords: astronaut, cosmonaut, microgravity, muscle atrophy, muscle attenuation, computed tomography

OPEN ACCESS

Edited by:
Richard D. Boyle, National Aeronautics and Space Administration (NASA), United States

Reviewed by:
Tobias Weber, European Space Agency (ESA), France
Brandon Richard Macias, KBRwyle, United States

***Correspondence:**
Ashley A. Weaver
asweaver@wakehealth.edu

Specialty section:
This article was submitted to Environmental, Aviation and Space Physiology, a section of the journal Frontiers in Physiology

Received: *13 November 2018*
Accepted: *02 May 2019*
Published: *21 May 2019*

Citation:
McNamara KP, Greene KA, Moore AM, Lenchik L and Weaver AA (2019) Lumbopelvic Muscle Changes Following Long-Duration Spaceflight. Front. Physiol. 10:627. doi: 10.3389/fphys.2019.00627

INTRODUCTION

Significant skeletal muscle atrophy has been observed in crewmembers of long-duration spaceflights and persists for months following spaceflight, particularly in the legs and back (LeBlanc et al., 2000; Ploutz-Snyder et al., 2015; Chang et al., 2016). Muscle volume decreases due to prolonged exposure to microgravity during long-duration spaceflight may increase the risk of astronaut injury while on mission, upon return to earth, or later in life (LeBlanc et al., 1998, 2000; Adams et al., 2003; Lang et al., 2004; Ploutz-Snyder et al., 2015). Studies on muscle atrophy during long-duration spaceflight have primarily focused on the lower extremities, but recent spaceflight and bed rest studies have sought to characterize loss in the supporting spinal musculature (Cao et al., 2005; Ploutz-Snyder et al., 2015; Chang et al., 2016; Macias et al., 2017).

Historical magnetic resonance imaging data from 17-day missions have shown a 10% volumetric loss in the intrinsic back muscles (rotatores, multifidus, semispinalis, spinalis, longissimus, and iliocostalis) and 5% volumetric loss in the psoas muscles, while 16- to 28-week missions resulted in 16% loss in the intrinsic back muscles and 5% loss in the psoas muscles (LeBlanc et al., 2000). Long-duration bed rest studies have been used as corollary for spaceflight studies of muscle degradation as they are both associated with increased muscle soreness, decreased muscle performance, and decreased postural stability (Nicogossian et al., 1994; LeBlanc et al., 2000; Cao et al., 2005; Muir et al., 2011; Macias et al., 2017). Nevertheless, these studies may not adequately capture the full degree of lumbopelvic muscle degradation that occurs with long-duration spaceflight (LeBlanc et al., 1992). Back muscles are likely used in bed rest to adjust position. In the 1-g environment on Earth, lumbopelvic muscles are activated in a tonic fashion that is in anticipation of dynamic loads with various up-right movements, offering segmental control and stability of the spine (Hodges and Richardson, 1997; Moseley et al., 2002). In spaceflight, some spinal loading is achieved through intravehicular activities such as treadmill and resistive exercise as well as any extravehicular activities while on the mission. However, these activities do not produce the same type and magnitude of gravitational loading experienced on Earth. Moreover, during spaceflight, even with the use of advanced exercise equipment, microgravity causes an absence of anticipatory loads, disrupting the feedforward mechanism that normally activates the lumbopelvic muscles (Winnard et al., 2017).

A chief goal of NASA's Human Research Roadmap is to investigate whether atrophied and weakened spinal musculature paired with vertebral bone loss will affect their quality of life upon return to Earth, since lost muscle and bone mass are not immediately restored (LeBlanc et al., 2000; McCarthy et al., 2000; Carpenter et al., 2010; Caldwell et al., 2012). In particular, the combination of spaceflight-induced loss of muscle strength, sensorimotor impairment, reduced postural stability, and bone loss may predispose astronauts to herniated discs (Johnston et al., 2010) and vertebral fracture due to dynamic loading encountered in spacecraft launches and landings and/or due to falls in the years following spaceflight (LeBlanc et al., 2000; Lang et al., 2004; Muir et al., 2011; Wood et al., 2011). In addition to risk of injury, in-flight back pain is a known effect of spaceflight with the majority of crewmembers experiencing some degree of back pain during flight (Sayson and Hargens, 2008; Kerstman et al., 2012; Pool-Goudzwaard et al., 2015). The most common location of spaceflight-induced back pain occurs in the lumbar region. It is postulated that both disc and muscle changes are contributing to this phenomenon (Sayson and Hargens, 2008; Belavý et al., 2011; Hides et al., 2016). Spinal musculature provides support for the vertebral column. Chronic back pain studies in terrestrial populations have linked decreases in the paraspinal muscles and psoas to back pain (Hodges and Richardson, 1996; Hides et al., 2011), though the same correlation is not clear with regard to muscle attenuation, a measure of muscle density in which lower values suggest fat infiltration, and back pain (Danneels et al., 2000; Kamaz et al., 2007).

Early exercise equipment in space consisted of bicycle machines, which provided aerobic training that was ineffective in combating muscle loss, highlighting the need for on-board resistance-based exercise equipment (Thornton and Rummel, 1977). Long-duration International Space Station (ISS) missions have retained the important focus on cardiovascular health with the presence of a cycle ergometer with vibration isolation and stabilization (CEVIS) and a treadmill with vibration isolation and stabilization (TVIS) and its 2009 replacement, the second-generation treadmill (T2; Petersen et al., 2016). Efforts to minimize muscle degradation on ISS missions resulted in the introduction of the interim resistive exercise device (iRED), which used elastomers to mimic weight-bearing exercise as a complimentary in-flight countermeasure (Shiba et al., 2015). This was improved upon in 2010 with the introduction of the advanced resistive exercise device (aRED), which simulated inertial loads experienced at earth-based gravitational pull.

Volumetric changes in spinal musculature occurring as a result of prolonged spaceflight can be measured using computed tomography (CT) scans. Additionally, CT scans can provide an insight into the development of intermuscular adipose tissue deposits as well as intramyocellular lipid deposits in the myocyte cytoplasm through measuring muscle attenuation values (Aubrey et al., 2014; Lee et al., 2017). The combination of these analyses allows for investigation into the influence of long-duration spaceflight on muscle health. The objective of this study was to assess pre- to post-flight changes in the psoas, quadratus lumborum, and paraspinal muscles from lumbar spine CT scans of crewmembers (n = 16) on 4- to 6-month iRED-equipped missions. It was hypothesized that the lumbopelvic muscles would experience post-flight decreases in muscle volume and attenuation in these iRED-era missions.

MATERIALS AND METHODS

Retrospective CT scans were obtained from the Life Sciences Data Archive and Lifetime Surveillance of Astronaut Health project. Written informed consent was obtained from each subject, and the study protocols were approved by the Wake Forest School of Medicine and National Aeronautics and Space Administration Institutional Review Boards. Helical CT images at the level of the L1 and L2 vertebrae were acquired using a GE HiSpeed Advantage at 80 kVp and 140 mA with 3 mm slice thickness and 0.94 mm pixel size (Lang et al., 2004). Scans were obtained for 16 crewmembers made up of astronauts and cosmonauts (average age, 45.9 years; 15 males and 1 female) who flew missions between 4 and 6 months in duration during the period when iRED was available to crewmembers. Pre-flight CT scans were performed 30–60 days before launch, and post-flight CT scans were performed within 7–10 days after landing (Lang et al., 2004).

The psoas, quadratus lumborum, and paraspinal (consisting of the erector spinae and multifidus) muscle groups were segmented and analyzed from the CT images to characterize lumbopelvic muscle volume changes (**Figure 1**). Segmentation was standardized using the morphology of the L2 vertebral body to ensure consistent regional analysis on a per-crewmember level. Segmentation was performed in the axial view starting

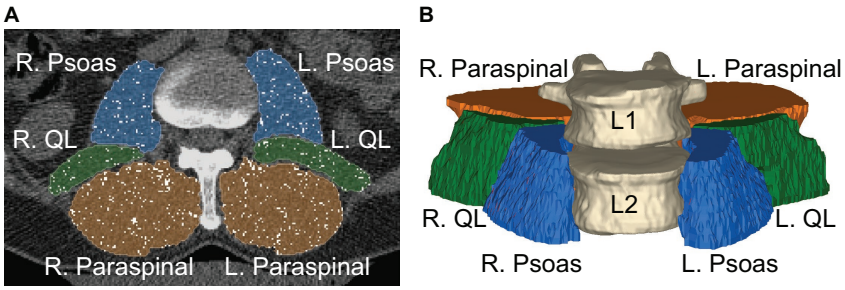

FIGURE 1 | (A) Manual muscle segmentations of the psoas (blue), quadratus lumborum (green), and paraspinal muscles (orange) on a CT scan. Fat voxels (white) have been removed from each of the muscle masks. **(B)** Three-dimensional view of the muscle segmentations represents muscle volumes that span the L2 vertebral body.

with the slice superior to the L2 vertebral body and ending on the slice inferior to the L2 vertebral body. The pre- and post-flight scans per crewmember were quality checked to make sure they encompassed the same regions and had masks of the same height. Semi-automated segmentation was conducted using Mimics software (v20, Materialise, Leuven, Belgium). An initial Hounsfield Unit (HU) threshold for muscle (−29 to 150 HU) was applied and the resulting mask was manually refined to ensure voxels within the external boundary of each lumbopelvic muscle were included in the mask (termed "total muscle mask"). Once all lumbopelvic muscles were segmented, the axial slices were checked for consistent muscle boundary definitions on an intra-subject level. Once lumbopelvic muscle masks were validated, a fat threshold was applied (−190 to −30 HU; Prado et al., 2009) to define voxels representing intermuscular adipose tissue (IMAT; termed "fat mask") within the "total muscle mask." A Boolean operation was then performed to subtract the "fat mask" from the "total muscle mask" to obtain the "true muscle mask." Any fat voxels on the outer layer of the muscle mask were determined to be muscle fascia and were manually removed from the muscle mask to create a "fat infiltration mask" representing IMAT.

From these segmentations, pre- to post-flight changes in muscle volume were quantified. The volume of each true muscle mask was calculated by determining the volume of a 0.94 mm × 0.94 mm × 3.00 mm voxel and multiplying by the number of voxels in the muscle segmentation. Similarly, the volume of IMAT was determined using the same method. The gross fat percentage for each muscle was calculated as the percentage of the combined true muscle and fat infiltration masks occupied by the fat infiltration mask. Muscle and fat attenuation (measure of lipid concentrations in the masks) were calculated as the average HU for each mask. The pre- to post-flight percentage change for the volume and attenuation of each mask was calculated on a per-crewmember level.

Statistical analysis was performed using JMP Pro (JMP®, Version 13. SAS Institute Inc., Cary, NC, USA). Shapiro-Wilk tests were performed on all muscle changes to evaluate for normally distributed results. Paired t tests ($\alpha = 0.05$) were performed to determine the mean change in lumbopelvic muscle and fat volumes on a per-crewmember level. Paired t tests ($\alpha = 0.05$) were also performed to determine the mean change in muscle and fat attenuation on a per-crewmember level. Finally, paired t tests ($\alpha = 0.05$) were performed on the percent change in the volume and attenuation of muscle and fat in the pre- versus post-flight scans. All results are presented as means and standard errors.

A subset consisting of six crewmembers had in-flight workout logs of time spent using CEVIS and TVIS as well as frequency of iRED usage. The crewmembers also had pre- and post-functional fitness assessments consisting of peak torque on 60° knee and trunk flexion and extension. Crewmembers also had pre- and post-fitness assessments for maximum pushups, situps, and pullups performed in 2 min, maximum fingertip distance during a sit and reach exercise, and maximum weight lifted while performing smith bench presses and leg presses. No logs of in-flight nutrition were available in this subset.

Shapiro-Wilk tests were performed on all exercise frequencies and functional fitness assessments to evaluate for normally distributed results. Functional fitness parameters with normal distributions were individually linearly regressed against lumbopelvic muscle changes to assess for any functional changes as a result of radiologically observed findings. Lumbopelvic muscle changes with normal distributions were individually linearly regressed against CEVIS (min/day), TVIS (min/day), and iRED (uses/day) to evaluate for significant changes resulting from crewmembers' choice of in-flight fitness routine. These values were determined by taking the total minutes spent using CEVIS or TVIS and total flight uses of iRED and normalizing by the mission duration in days.

RESULTS

The psoas, quadratus lumborum, and paraspinal muscle volumes were grouped into a single mask to quantify the total change in lumbopelvic muscle volume (**Table 1**). Fourteen of the 16 (88%) crewmembers showed a decrease in total lumbopelvic muscle volume following spaceflight, ranging from 2.4 to 10.5%. One crewmember showed a 4.7% increase in total lumbopelvic muscle volume following spaceflight. One crewmember showed no change in total lumbopelvic muscle volume from baseline. The total lumbopelvic musculature showed an average 5.1% (4.2% SE; $p < 0.001$) decrease following spaceflight (**Figure 2**).

TABLE 1 | Changes in lumbar musculature along the L2 vertebrae for each crewmember.

Subject	Change in muscle volume (cm^3)	Percent change in muscle
1	14.7	4.7
2	–30.4	–9.3
3	–4.5	–2.5
4	–30.2	–10.5
5	–12.1	–3.9
6	–12.8	–5.6
7	–32.9	–11
8	–20.5	–6.2
9	0.5	0.2
10	–22.3	–7.3
11	–12.8	–4.2
12	–23.1	–8.6
13	–28.6	–8.9
14	–2.5	–1.3
15	–16.1	–5.4
16	–6.6	–2.4
Mean (SE)	–15.0 (13.2)	–5.1 (4.2)

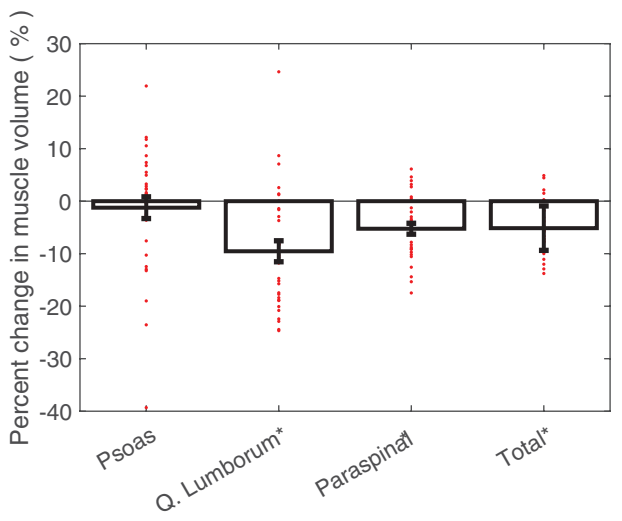

FIGURE 2 | Average percent changes (with standard error bars) in crewmember psoas, quadratus lumborum, paraspinal, and total lumbopelvic muscle volumes, with individual crewmember data points overlaid. Determined from pre- and post-flight manually segmented CT scans of the L2 region. *$p < 0.05$.

Post-flight decreases in individual muscle volumes were observed in the crewmembers (**Figure 2**). Significant decreases in quadratus lumborum muscle volume (mean: 9.5%; 2.0% SE; $p < 0.0001$) and paraspinal muscle volume (mean: 5.3%; 1.0% SE; $p < 0.0001$) were observed. Crewmembers did not experience statistically significant changes in psoas muscle volume.

The individual muscle groups were assessed to determine the overall change in muscle attenuation (measured in HU; **Figure 3**). The quadratus lumborum muscle demonstrated a significant HU decrease in 6.0% (1.5% SE, $p < 0.001$). The paraspinal muscles also demonstrated a significant HU decrease in 5.3% (1.6% SE, $p < 0.01$). The psoas muscles showed no statistically significant changes in HU. The individual muscle groups were assessed to determine the overall change in IMAT among the crewmembers. None of the muscles showed significant changes in fat infiltration volumes and both the psoas and quadratus lumborum fat infiltration volumes were non-normally distributed with outliers experiencing substantial increases in fat infiltration volume (**Figure 4**).

In the subset of individuals with functional fitness assessment test results available, no significant correlations between changes in lumbopelvic muscle volumes or attenuation values were observed with linear regression. However, there were some significant correlations found with lumbopelvic muscle changes when regressed against in-flight iRED and CEVIS use, but not TVIS use.

A significant regression equation to predict total lumbopelvic muscle volume percent change based on the average number of daily iRED workouts while on ISS missions was found ($R^2 = 0.72$, $p < 0.05$). Crewmembers were shown to have a 2.4% improvement in lumbopelvic muscle volume retention for each additional weekly iRED workout performed. Crewmembers who used iRED twice a week were found to have about an 11% decrease in lumbopelvic volume, whereas those who used iRED six times a week were found to have about a 2% decrease in lumbopelvic volume. Similar positive correlations based on iRED exercise frequency were found for paraspinal muscle volume but not for quadratus lumborum or psoas muscle volumes (**Figure 5**). No trends in muscle attenuation were seen with regard to iRED workout frequency.

A significant regression equation to predict paraspinal muscle attenuation percent change based on the average time spent using CEVIS while on ISS missions was found ($R^2 = 0.90$, $p < 0.004$). Crewmembers were shown to have a 1.3% decrease in paraspinal muscle attenuation for each daily minute spent using CEVIS. Crewmembers who used CEVIS for 5 min/day were found to have about a 5% increase in paraspinal muscle attenuation, whereas those who used CEVIS for 20 min/day were found to have about a 14% decrease in paraspinal muscle attenuation. Similar negative correlations based on CEVIS exercise duration were found for percent changes in muscle attenuation of the quadratus lumborum and psoas muscles (**Figure 6**). No trends in muscle volumes were seen with regard to CEVIS workout frequency.

DISCUSSION

The results of this study support the consensus that long-duration spaceflight is detrimental to the overall lumbopelvic muscle volume in astronauts. The study shows the degree to which different lumbopelvic muscles are affected after the implementation of iRED. It is noteworthy that these iRED-era missions had less severe muscle volume degradation than seen in prior studies (LeBlanc et al., 2000), and that the declines in paraspinal musculature and lack of changes to the psoas are in agreement with results from bed-rest studies

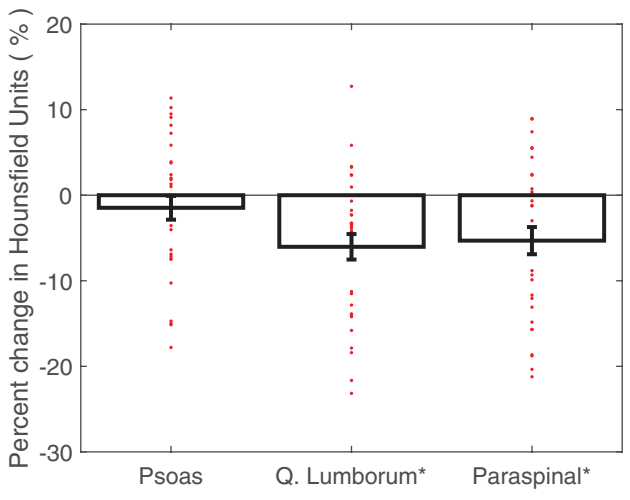

FIGURE 3 | Average percent changes (with standard error bars) in crewmember psoas, quadratus lumborum, and paraspinal muscle attenuation, with individual crewmember data points overlaid. Determined from pre- and post-flight manually segmented CT scans of the L2 region. *$p < 0.05$.

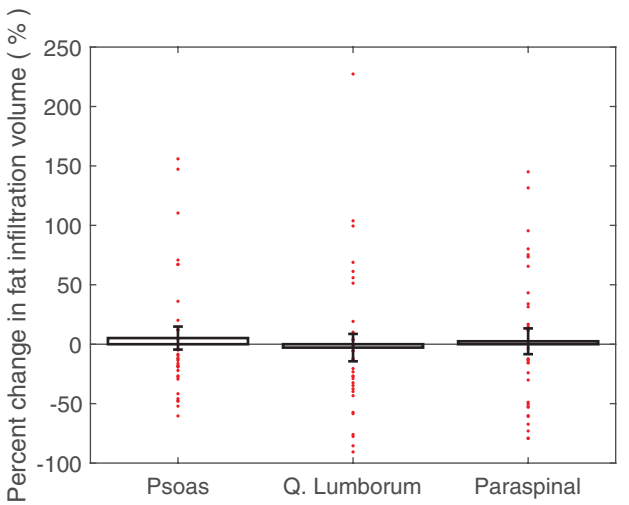

FIGURE 4 | Average percent changes (with standard error bars) in crewmember psoas, quadratus lumborum, and paraspinal muscle fat infiltration mask volume, with individual crewmember data points overlaid. Determined from pre- and post-flight manually segmented CT scans of the L2 region.

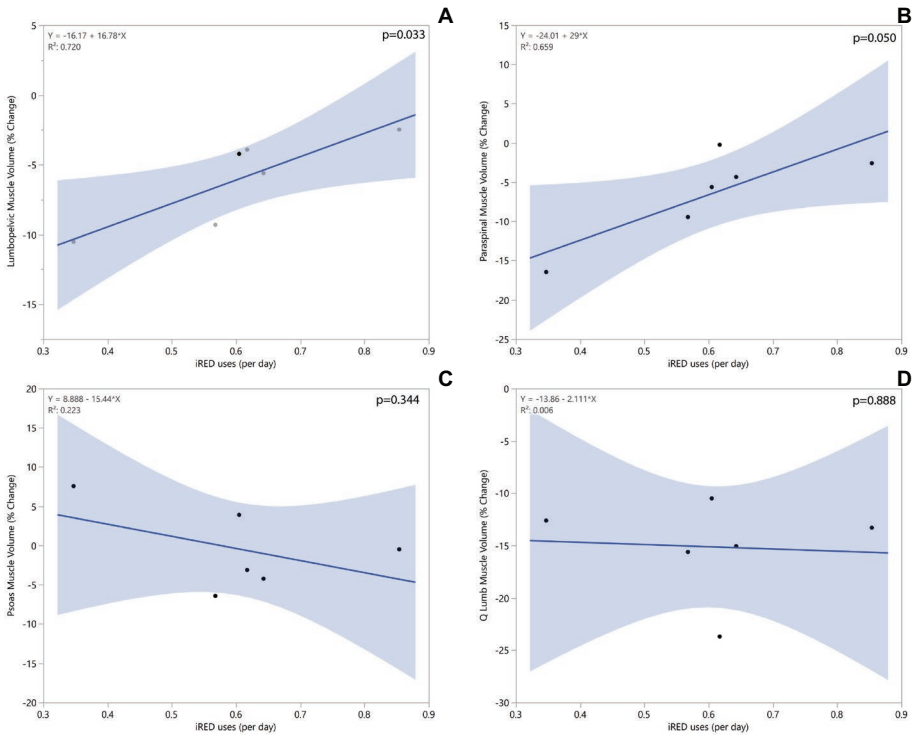

FIGURE 5 | Linear regression models for total lumbopelvic **(A)**, paraspinal **(B)**, psoas **(C)**, and quadratus lumborum **(D)** muscle volume change based on average number of iRED workouts/day while on ISS mission.

(Cao et al., 2005). It is also noteworthy that linear regressions found iRED workouts preserved lumbopelvic muscle volume. Although the paraspinal muscles are still experiencing degradation in space, the volume of muscle degradation has been effectively halved. The psoas muscle is no longer experiencing significant levels of degradation. This may be explained by its function as a hip flexor compared to the paraspinal and quadratus lumborum muscles, which function as posture stabilizers. This discrepancy in degradation of hip flexors and posture stabilizers may indicate that workout

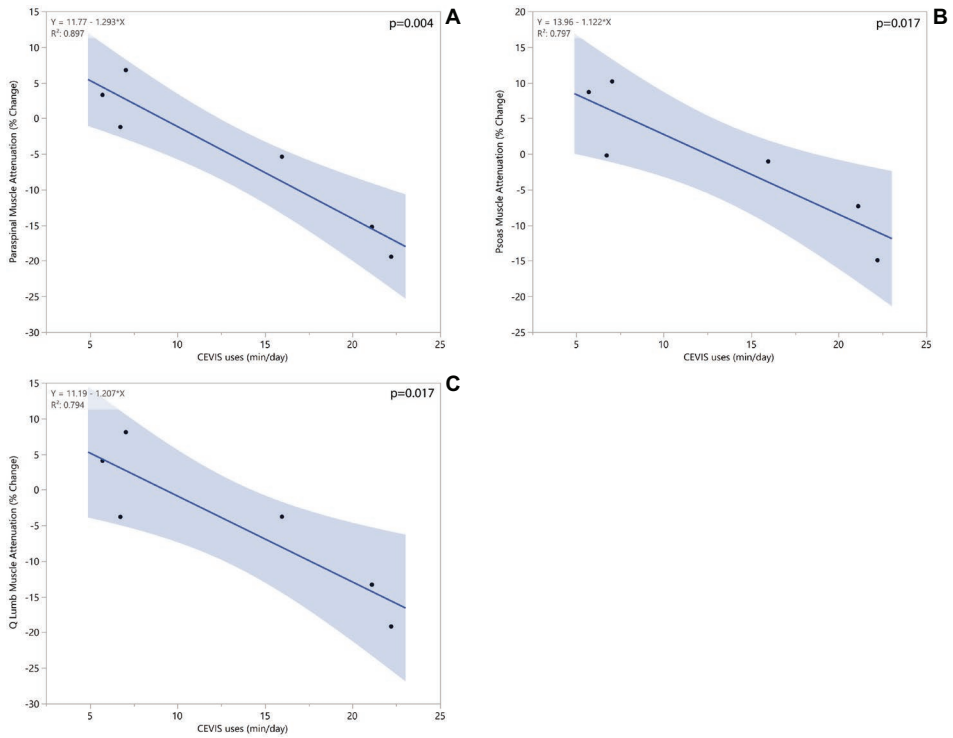

FIGURE 6 | Linear regression models for paraspinal **(A)**, psoas **(B)**, and quadratus lumborum **(C)** muscle attenuation change based on average minutes spent of CEVIS per day while on ISS mission.

equipment is not adequately targeting the muscles responsible for stabilizing the lumbar spine. Loss in these muscles may leave astronauts more susceptible to lumbar injury after spaceflight.

In addition to the volumetric changes exhibited in the muscles responsible for postural stability, the results demonstrate a potential increase in lipid deposition in these muscles. Both the paraspinal and quadratus lumborum muscles exhibited a significant decrease in muscle attenuation. CT muscle attenuation is affected by IMAT. Previous studies have shown that a 1 HU decrease in muscle attenuation corresponds to a 0.01 g ml^{-1} increase in muscle lipid concentration (Goodpaster et al., 2000). This means that approximately 3 HU decrease seen in the quadratus lumborum muscles corresponds to more than 0.03 g ml^{-1} increase in their lipid concentration as a result of prolonged microgravity. A linear regression found that crewmembers spending more time on CEVIS had higher decreases in muscle attenuation. This may indicate that CEVIS is not activating the lumbopelvic musculature in ways to prevent lipid deposition in the muscle fibers. However, it is also possible that this attenuation from CEVIS use is due to a tradeoff in which crewmembers spending more time on CEVIS have less available time to use other in-flight exercise equipment. Studies have found a direct relationship between muscle attenuation and muscle strength even when controlling for cross-sectional area (Goodpaster et al., 2001; Visser et al., 2002). Similarly, many studies have shown an increase in skeletal muscle lipid deposition with age (Ryan and Nicklas, 1999) and with muscle-wasting diseases (Jones et al., 1983; Liu et al., 1993).

The decreases in both muscle volume and quality found in this study may contribute to a decrease strength in lumbopelvic musculature that places crewmembers at risk for injury following spaceflight. Spinal injuries and pain are one of the most common post-flight injuries (Ramachandran et al., 2018). Longitudinal studies of astronauts and matched controls have found a 4.3 times increased incidence of herniated nucleus pulposus in the astronaut population, occurring in 44 of 321 (13.7%) of astronauts (Johnston et al., 2010). In the first-year post-flight, the risk of herniated cervical nucleus pulposus is 35.9 times higher in astronauts than controls (Johnston et al., 2010). Recent studies have found an association between spinal muscle atrophy and decreased lumbar lordosis that can lead to an increased risk of herniated nucleus pulposus (Bailey et al., 2018). These findings further underscore the potential consequences of spinal muscle atrophy quantified in this study, as the decreased strength of lumbar musculature may increase the risk of herniated nucleus pulposus. It is important to highlight the lack of association between the lumbopelvic muscle changes in this study and the crewmembers' trunk extension peak torque values. It is very likely that with a sample size of 6 individuals, associations that may exist between lumbopelvic muscle changes and functional fitness assessments were not adequately powered.

In-flight countermeasures are of great importance in preventing post-flight injuries (Sayson et al., 2013). However, iRED and its replacement (aRED) lack exercise protocols that mimic spine loading on Earth (Sayson et al., 2013), which may explain why

spinal pain has yet to be eliminated with the use of such equipment (Laughlin et al., 2016). NASA's Astronaut Strength, Conditioning, and Rehabilitation (ASCR) team is continually focused on improving both in-flight exercise regimens as well as post-flight rehabilitation to prevent spinal injuries. While the results of this study demonstrate improvement to the lumbar musculature during the iRED-era, the lumbar musculature was still degrading in comparison to pre-flight values. These declines highlight the continued importance of the ASCR team to aid in the maintenance of muscle health in order to offset in-flight deconditioning and promote a shorter re-conditioning period (LeBlanc et al., 2002, 2013; Zhang et al., 2011; Smith et al., 2012; Lloyd et al., 2015; MacNabb et al., 2016; Lang et al., 2017; Ramachandran et al., 2018). Future studies should look at the effects of the newer aRED on lumbopelvic musculature to determine its efficacy over the retired iRED.

Study limitations include a small sample size (n = 16 for muscle changes and n = 6 for fitness data). However, there were only 19 crewmembers on ISS missions during the data collection period. Furthermore, the sample included mostly men, with only one female participant. However, there were only two female ISS crewmembers during the data collection period. Another limitation to the scans was the small region of interest, which only spanned the L1–L2 vertebrae. The physiologic changes to the entire muscle were characterized by the changes experienced at the level of the L2 vertebral body. However, the paraspinal muscles run the entire length of the spine, the psoas runs the entire length of the lumbar spine as well as the entire pelvic region, and the quadratus lumborum runs the entire length of the lumbar spine. Previous literature has shown that measurements taken at the belly (site of maximal cross-sectional area) of a muscle can be used to predict overall muscle volume (Albracht et al., 2008). However, the L1–L2 region is closer to the origin/insertion locations of these muscles and may not entirely capture the significance of changes in these muscles.

CONCLUSIONS

Using pre- and post-flight CT scan analysis, we quantified changes in lumbar musculature in crewmembers of long-duration space missions during the iRED era. Through countermeasures including resistive exercise training (e.g., iRED), crewmembers are effectively combating structural deterioration of the lumbopelvic muscles. While these measures appear to have eliminated degradation in the psoas muscles, there are still deleterious effects in the quadratus lumborum and paraspinal muscles. This may leave crewmembers susceptible to back injuries on re-entry and in the months following spaceflight. Future studies should focus on targeting muscles responsible for postural stability in microgravity to prevent their degradation while on missions.

ETHICS STATEMENT

This study was carried out in accordance with the recommendations of the Institutional Review Boards at the Wake Forest School of Medicine and the National Aeronautics and Space Administration (NASA). All subjects gave written informed consent in accordance with the Declaration of Helsinki. The protocol was approved by the Wake Forest School of Medicine and the NASA Institutional Review Boards.

AUTHOR CONTRIBUTIONS

LL and AW designed the research. KM, KG, and AM performed the data collection, data analysis, and statistical analysis. LL and AW contributed to data interpretation. KM, KG, LL, and AW wrote and revised the manuscript. AW had primary responsibility for final content. All authors listed have made a substantial, direct, and intellectual contribution to the work and approved it for publication.

FUNDING

This study is supported by the NASA Human Research Program (Award No. NNX16AP89G) and the contributions by Nisha Subramanian were made possible by the National Science Foundation [REU Site: Imaging and Mechanics-based Projects on Accidental Cases of Trauma (IMPACT), Award No. 1559700].

ACKNOWLEDGMENTS

The authors would like to acknowledge the contributions of Lisa Maez, Joel Sink, Thomas Noonan, and Nisha Subramanian who assisted with segmentation work.

REFERENCES

Adams, G. R., Caiozzo, V. J., and Baldwin, K. M. (2003). Skeletal muscle unweighting: spaceflight and ground-based models. *J. Appl. Physiol.* 95, 2185–2201. doi: 10.1152/japplphysiol.00346.2003

Albracht, K., Arampatzis, A., and Baltzopoulos, V. (2008). Assessment of muscle volume and physiological cross-sectional area of the human triceps surae muscle in vivo. *J. Biomech.* 41, 2211–2218. doi: 10.1016/j.jbiomech.2008.04.020

Aubrey, J., Esfandiari, N., Baracos, V., Buteau, F., Frenette, J., Putman, C., et al. (2014). Measurement of skeletal muscle radiation attenuation and basis of its biological variation. *Acta Physiol.* 210, 489–497. doi: 10.1111/apha.12224

Bailey, J. F., Miller, S. L., Khieu, K., O'Neill, C. W., Healey, R. M., Coughlin, D. G., et al. (2018). From the international space station to the clinic: how prolonged unloading may disrupt lumbar spine stability. *Spine J.* 18, 7–14. doi: 10.1016/j.spinee.2017.08.261

Belavý, D. L., Armbrecht, G., Richardson, C. A., Felsenberg, D., and Hides, J. A. (2011). Muscle atrophy and changes in spinal morphology: is the lumbar spine vulnerable after prolonged bed-rest? *Spine* 36, 137–145. doi: 10.1097/BRS.0b013e3181cc93e8

Caldwell, E., Gernhardt, M., Somers, J., Younker, D., and Newby, N. (2012). NASA evidence report: Risk of injury due to dynamic loads. Available at: http://humanresearchroadmap.nasa.gov/Evidence/reports/Occupant%20Protection.pdf (Accessed Jan 3, 2019).

Cao, P., Kimura, S., Macias, B. R., Ueno, T., Watenpaugh, D. E., and Hargens, A. R. (2005). Exercise within lower body negative pressure partially counteracts lumbar spine deconditioning associated with 28-day bed rest. *J. Appl. Physiol.* 99, 39–44. doi: 10.1152/japplphysiol.01400.2004

Carpenter, R. D., LeBlanc, A. D., Evans, H., Sibonga, J. D., and Lang, T. F. (2010). Long-term changes in the density and structure of the human hip and spine after long-duration spaceflight. *Acta Astronaut.* 67, 71–81. doi: 10.1016/j.actaastro.2010.01.022

Chang, D. G., Healey, R. M., Snyder, A. J., Sayson, J. V., Macias, B. R., Coughlin, D. G., et al. (2016). Lumbar spine paraspinal muscle and intervertebral disc height changes in astronauts after long-duration spaceflight on the international space station. *Spine* 41, 1917–1924. doi: 10.1097/BRS.0000000000001873

Danneels, L. A., Vanderstraeten, G., Cambier, D. C., Witvrouw, E. E., De Cuyper, H. J., and Danneels, L. (2000). CT imaging of trunk muscles in chronic low back pain patients and healthy control subjects. *Eur. Spine J.* 9, 266–272. doi: 10.1007/s005860000190

Goodpaster, B. H., Carlson, C. L., Visser, M., Kelley, D. E., Scherzinger, A., Harris, T. B., et al. (2001). Attenuation of skeletal muscle and strength in the elderly: the health ABC study. *J. Appl. Physiol.* 90, 2157–2165. doi: 10.1152/jappl.2001.90.6.2157

Goodpaster, B. H., Kelley, D. E., Thaete, F. L., He, J., and Ross, R. (2000). Skeletal muscle attenuation determined by computed tomography is associated with skeletal muscle lipid content. *J. Appl. Physiol.* 89, 104–110. doi: 10.1152/jappl.2000.89.1.104

Hides, J. A., Lambrecht, G., Stanton, W. R., and Damann, V. (2016). Changes in multifidus and abdominal muscle size in response to microgravity: possible implications for low back pain research. *Eur. Spine J.* 25, 175–182. doi: 10.1007/s00586-015-4311-5

Hides, J., Stanton, W., Mendis, M. D., and Sexton, M. (2011). The relationship of transversus abdominis and lumbar multifidus clinical muscle tests in patients with chronic low back pain. *Man. Ther.* 16, 573–577. doi: 10.1016/j.math.2011.05.007

Hodges, P. W., and Richardson, C. A. (1996). Inefficient muscular stabilization of the lumbar spine associated with low back pain: a motor control evaluation of transversus abdominis. *Spine* 21, 2640–2650. doi: 10.1097/00007632-199611150-00014

Hodges, P. W., and Richardson, C. A. (1997). Feedforward contraction of transversus abdominis is not influenced by the direction of arm movement. *Exp. Brain Res.* 114, 362–370. doi: 10.1007/PL00005644

Johnston, S. L., Campbell, M. R., Scheuring, R., and Feiveson, A. H. (2010). Risk of herniated nucleus pulposus among US astronauts. *Aviat. Space Environ. Med.* 81, 566–574. doi: 10.3357/ASEM.2427.2010

Jones, D., Round, J., Edwards, R., Grindwood, S., and Tofts, P. (1983). Size and composition of the calf and quadriceps muscles in Duchenne muscular dystrophy: a tomographic and histochemical study. *J. Neurol. Sci.* 60, 307–322.

Kamaz, M., Kiresi, D., Oguz, H., Emlik, D., and Levendoglu, F. (2007). CT measurement of trunk muscle areas in patients with chronic low back pain. *Diagn. Interv. Radiol.* 13, 144–148.

Kerstman, E. L., Scheuring, R. A., Barnes, M. G., DeKorse, T. B., and Saile, L. G. (2012). Space adaptation back pain: a retrospective study. *Aviat. Space Environ. Med.* 83, 2–7. doi: 10.3357/ASEM.2876.2012

Lang, T., LeBlanc, A., Evans, H., Lu, Y., Genant, H., and Yu, A. (2004). Cortical and trabecular bone mineral loss from the spine and hip in long-duration spaceflight. *J. Bone Miner. Res.* 19, 1006–1012. doi: 10.1359/JBMR.040307

Lang, T., Van Loon, J. J., Bloomfield, S., Vico, L., Chopard, A., Rittweger, J., et al. (2017). Towards human exploration of space: the THESEUS review series on muscle and bone research priorities. *NPJ Microgravity* 3, 1–10. doi: 10.1038/npjmgrav.2016.29

Laughlin, M. S., Murray, J. D., Wear, M. L., and Van Baalen, M. (2016). "Post-flight back pain following international space station missions: evaluation of spaceflight risk factors" in *Human research program Investigators' workshop.* (Galveston, TX). https://ntrs.nasa.gov/archive/nasa/casi.ntrs.nasa.gov/20150020953.pdf

LeBlanc, A., Lin, C., Shackelford, L., Sinitsyn, V., Evans, H., Belichenko, O., et al. (2000). Muscle volume, MRI relaxation times (T2), and body composition after spaceflight. *J. Appl. Physiol.* 89, 2158–2164. doi: 10.1152/jappl.2000.89.6.2158

LeBlanc, A., Matsumoto, T., Jones, J., Shapiro, J., Lang, T., Shackelford, L., et al. (2013). Bisphosphonates as a supplement to exercise to protect bone during long-duration spaceflight. *Osteoporos Int.* 24, 2105–2114.

LeBlanc, A., Shackelford, C., and Schneider, V. (1998). Future human bone research in space. *Bone* 22(5 Suppl.), 113S–116S.

LeBlanc, A. D., Driscol, T. B., Shackelford, L. C., Evans, H. J., Rianon, N. J., Smith, S. M., et al. (2002). Alendronate as an effective countermeasure to disuse induced bone loss. *J. Musculoskelet. Neuronal Interact.* 2, 335–343.

LeBlanc, A. D., Schneider, V. S., Evans, H. J., Pientok, C., Rowe, R., and Spector, E. (1992). Regional changes in muscle mass following 17 weeks of bed rest. *J. Appl. Physiol.* 73, 2172–2178. doi: 10.1152/jappl.1992.73.5.2172

Lee, S. H., Park, S. W., Kim, Y. B., Nam, T. K., and Lee, Y. S. (2017). The fatty degeneration of lumbar paraspinal muscles on computed tomography scan according to age and disc level. *Spine J.* 17, 81–87. doi: 10.1016/j.spinee.2016.08.001

Liu, M., Chino, N., and Ishihara, T. (1993). Muscle damage progression in Duchenne muscular dystrophy evaluated by a new quantitative computed tomography method. *Arch. Phys. Med. Rehabil.* 74, 507–514. doi: 10.1016/0003-9993(93)90115-Q

Lloyd, S. A., Morony, S. E., Ferguson, V. L., Simske, S. J., Stodieck, L. S., Warmington, K. S., et al. (2015). Osteoprotegerin is an effective countermeasure for spaceflight-induced bone loss in mice. *Bone* 81, 562–572.

Macias, B. R., Cao, P., Watenpaugh, D. E., and Hargens, A. R. (2017). LBNP treadmill exercise maintains spine function and muscle strength in identical twins during 28-days simulated microgravity. *J. Appl. Physiol.* 102, 2274–2278. doi: 10.1152/japplphysiol.00541.2006

MacNabb, C., Patton, D., and Hayes, J. (2016). Sclerostin antibody therapy for the treatment of osteoporosis: clinical prospects and challenges. *J. Osteoporos.* 2016, 1–22. doi: 10.1155/2016/6217286

McCarthy, I., Goodship, A., Herzog, R., Oganov, V., Stussi, E., and Vahlensieck, M. (2000). Investigation of bone changes in microgravity during long and short duration space flight: comparison of techniques. *Eur. J. Clin. Investig.* 30, 1044–1054. doi: 10.1046/j.1365-2362.2000.00719.x

Moseley, G. L., Hodges, P. W., and Gandevia, S. C. (2002). Deep and superficial fibers of the lumbar multifidus muscle are differentially active during voluntary arm movements. *Spine* 27, E29–E36. doi: 10.1097/00007632-200201150-00013

Muir, J., Judex, S., Qin, Y. X., and Rubin, C. (2011). Postural instability caused by extended bed rest is alleviated by brief daily exposure to low magnitude mechanical signals. *Gait Posture* 33, 429–435. doi: 10.1016/j.gaitpost.2010.12.019

Nicogossian, A. E., Huntoon, C. L., and Pool, S. L. (1994). "Lean Body Mass and Energy Balance," in *Space Physiology and Medicine*. ed. A. E. Nicogossian (Philadelphia, PA: Lea & Febiger), 189–194.

Petersen, N., Jaekel, P., Rosenberger, A., Weber, T., Scott, J., Castrucci, F., et al. (2016). Exercise in space: the European Space Agency approach to in-flight exercise countermeasures for long-duration missions on ISS. *Extrem. Physiol. Med.* 5:9. doi: 10.1186/s13728-016-0050-4

Ploutz-Snyder, L., Ryder, J., English, K., Haddad, F., and Baldwin, K. (2015). Risk of impaired performance due to reduced muscle mass, strength, and endurance (HRP-47072). Available at: http://humanresearchroadmap.nasa.gov/Evidence/reports/Muscle.pdf (Accessed Jan 3, 2019).

Pool-Goudzwaard, A. L., Belavý, D. L., Hides, J. A., Richardson, C. A., and Snijders, C. J. (2015). Low back pain in microgravity and bed rest studies. *Aerosp. Med. Hum. Perform.* 86, 541–547. doi: 10.3357/AMHP.4169.2015

Prado, C. M., Birdsell, L. A., and Baracos, V. E. (2009). The emerging role of computerized tomography in assessing cancer cachexia. *Curr. Opin. Support. Palliat. Care* 3, 269–275. doi: 10.1097/SPC.0b013e328331124a

Ramachandran, V., Dalal, S., Scheuring, R. A., and Jones, J. A. (2018). Musculoskeletal injuries in astronauts: review of pre-flight, in-flight, post-flight, and extravehicular activity injuries. *Curr. Pathobiol. Rep.* 6, 149–158. doi: 10.1007/s40139-018-0172-z

Ryan, A., and Nicklas, B. (1999). Age-related changes in fat deposition in mid-thigh muscle in women: relationships with metabolic cardiovascular disease risk factors. *Int. J. Obes.* 23, 126–132. doi: 10.1038/sj.ijo.0800777

Sayson, J. V., and Hargens, A. R. (2008). Pathophysiology of low back pain during exposure to microgravity. *Aviat. Space Environ. Med.* 79, 365–373. doi: 10.3357/ASEM.1994.2008

Sayson, J. V., Lotz, J., Parazynski, S., and Hargens, A. R. (2013). Back pain in space and post-flight spine injury: mechanisms and countermeasure development. *Acta Astronaut.* 86, 24–38. doi: 10.1016/j.actaastro.2012.05.016

Shiba, N., Matsuse, H., Takano, Y., Yoshimitsu, K., Omoto, M., Hashida, R., et al. (2015). Electrically stimulated antagonist muscle contraction increased muscle mass and bone mineral density of one astronaut-initial verification on the international space station. *PLoS One* 10:e0134736. doi: 10.1371/journal.pone.0145140

Smith, S. M., McCoy, T., Gazda, D., Morgan, J. L., Heer, M., and Zwart, S. R. (2012). Space flight calcium: implications for astronaut health, spacecraft operations, and Earth. *Nutrients* 4, 2047–2068.

Thornton, W. E., and Rummel, J. (1977). "Muscular deconditioning and its prevention in space flight" in *Biomed. Results from Skylab. NASA SP-377*. eds. R. S. Johnston and L. F. Dietlein (Washington, DC: NASA Johnson Space Center), 191–197.

Visser, M., Kritchevsky, S. B., Goodpaster, B. H., Newman, A. B., Nevitt, M., Stamm, E., et al. (2002). Leg muscle mass and composition in relation to lower extremity performance in men and women aged 70 to 79: the health, aging and body composition study. *J. Am. Geriatr. Soc.* 50, 897–904. doi: 10.1046/j.1532-5415.2002.50217.x

Winnard, A., Nasser, M., Debuse, D., Stokes, M., Evetts, S., Wilkinson, M., et al. (2017). Systematic review of countermeasures to minimise physiological changes and risk of injury to the lumbopelvic area following long-term microgravity. *Musculoskelet. Sci. Pract.* 27(Suppl. 1), S5–S14. doi: 10.1016/j.msksp.2016.12.009

Wood, S. J., Loehr, J. A., and Guilliams, M. E. (2011). Sensorimotor reconditioning during and after spaceflight. *NeuroRehabilitation* 29, 185–195. doi: 10.3233/NRE-2011-0694

Zhang, L., Rajan, V., Lin, E., Hu, Z., Han, H., Zhou, X., et al. (2011). Pharmacological inhibition of myostatin suppresses systemic inflammation and muscle atrophy in mice with chronic kidney disease. *FASEB J.* 25, 1653–1663.

Conflict of Interest Statement: The authors declare that the research was conducted in the absence of any commercial or financial relationships that could be construed as a potential conflict of interest.

frontiers in Physiology

ORIGINAL RESEARCH
published: 21 May 2019
doi: 10.3389/fphys.2019.00576

Stumbling Reactions in Partial Gravity – Neuromechanics of Compensatory Postural Responses and Inter-Limb Coordination During Perturbation of Human Stance

Ramona Ritzmann[1,2], Kathrin Freyler[1], Michael Helm[1], Janek Holubarsch[1] and Albert Gollhofer[1]*

[1] Institute of Sport and Sport Science, University of Freiburg, Freiburg, Germany, [2] Praxisklinik Rennbahn AG, Muttenz, Switzerland

OPEN ACCESS

Edited by:
Gilles Clement, Centre National de la Recherche Scientifique (CNRS), France

Reviewed by:
Jochen Zange, Helmholtz Association of German Research Centers (HZ), Germany
Satoshi Iwase, Aichi Medical University, Japan

****Correspondence:***
Ramona Ritzmann
ramona.ritzmann@sport.uni-freiburg.de

Specialty section:
This article was submitted to Environmental, Aviation and Space Physiology, a section of the journal Frontiers in Physiology

Received: *18 December 2018*
Accepted: *24 April 2019*
Published: *21 May 2019*

Citation:
Ritzmann R, Freyler K, Helm M, Holubarsch J and Gollhofer A (2019) Stumbling Reactions in Partial Gravity – Neuromechanics of Compensatory Postural Responses and Inter-Limb Coordination During Perturbation of Human Stance. Front. Physiol. 10:576. doi: 10.3389/fphys.2019.00576

Spontaneous changes in gravity play a significant role in interplanetary space missions. To preserve the astronauts' capability to execute mission-critical tasks and reduce the risk of injury in transit and on planetary surfaces, a comprehensive understanding of the neuromuscular control of postural responses after balance deterioration in hypo- or hyper-gravity conditions is essential. Therefore, this study aimed to evaluate the effect of acute gravitational variation on postural adjustments in response to perturbations. Gravitational changes were induced using parabolic flight. Postural set was manipulated by randomly providing unilateral left, bilateral or split perturbations which require balance corrections to restore postural stability. In six subjects, postural reactions were recorded after anterior and posterior surface perturbations for progressively increased gravitational conditions spanning from 0.25 to 1.75 g. Ankle and knee joint kinematics and electromyograms (EMG) of eight leg muscles were recorded prior (PRE) and after perturbation onset. Muscle activation onset latencies and amplitudes in the short-, medium-, and long-latency responses (SLR, MLR, LLR) were assessed. Results demonstrate an increased muscle activity ($p < 0.05$) and co-contraction in the lower extremities ($p < 0.05$) prior to perturbation in hypo- and hyper-gravity. After perturbation, reduced muscle onset latencies ($p < 0.05$) and increased muscle activations in the MLR and LLR ($p < 0.05$), concomitant with an increased co-contraction in the SLR, were manifested with a progressive rise in gravity. Ankle and knee joint deflections remained unaffected, whereas angular velocities increased ($p < 0.05$) with increasing gravitation. Effects were more pronounced in bi- compared to unilateral or split perturbations ($p < 0.05$). Neuro-mechanical adaptations to gravity were more distinct and muscle onset latencies were shorter in the displaced compared to the non-displaced leg. In conclusion, the timing and magnitude of postural reflexes involved in stabilization of bipedal stance are gravity-dependent. The approximately linear relationship between gravity and impulse-directed EMG amplitudes or muscle onset latencies after perturbation indicates that the central nervous system correctly predicts the level of gravity. Moreover, it accurately governs contractions in the antigravity

musculature to counterbalance the gravitational pull and to regain upright posture after its disturbance. Importantly, unilateral perturbations evoked fast reflex responses in the synergistic muscles of the non-displaced contralateral leg suggesting a synchronized inter-limb coordination mediated by spinal circuitries.

Keywords: reflex, reduced gravity, balance, electromyography, kinematics, joint, contralateral

INTRODUCTION

The control of bipedal posture and gait and the capacity to regain equilibrium after its deterioration in variable environments is a crucial prerequisite for the success of future manned space discovery (White and Averner, 2001). Surface space walks on the neighboring planets and exploratory activities (Minetti, 2001) require a safe control of the habitual orthograde postural equilibrium with a high demand on the central nervous system (CNS) to immediately adapt muscle forces in accordance with gravity (Mergner and Rosemeier, 1998). With a range from 0 g up to 2 g, scenarios of interplanetary space travel within our solar system will expose humans to habitats where it is imperative to sustain great forces (Ritzmann et al., 2015) or deal with low friction and slippery ground surfaces (Minetti, 2001; Pavei and Minetti, 2016).

In recent debates, scientists have postulated the gravity sensitivity of bipedal stance and gait (Mergner and Rosemeier, 1998; Minetti et al., 2012a). Simulation studies exposing humans to changes in gravity used partial or additional weight-bearing (Hwang et al., 2011; Freyler et al., 2014), water buoyancy (Minetti et al., 2012a) and hypo- or hyper-gravity (Miyoshi et al., 2003). These experiments determined that spontaneous changes in gravity have a significant impact on posture and movement control associated with changes in joint torque (Mergner and Rosemeier, 1998) and neuromuscular activity (Ali and Sabbahi, 2000; Miyoshi et al., 2003). Assuming a constant mass, weight (force) is proportional with gravity (acceleration) based on the equation $F = m^*a$. Thereby, adaptations in somatosensory feedback (Layne et al., 2001) and compensatory reflex activation have been found (Nakazawa et al., 2004; Ritzmann et al., 2015). To date, there is scarce scientific evidence regarding neuromuscular recovery responses to sudden perturbations in such unknown gravity conditions (Ritzmann et al., 2015).

On Earth, gravity provides the reference for spatial orientation that is sensed by the otolith organs and indirectly by the somatosensory system (Nashner and Berthoz, 1978). Studies dealing with compensatory postural responses in fall situations showed that reflexive muscle activations provide appropriate joint torques for an immediate re-stabilization of the center of mass (COM) (Taube et al., 2008). This physiological model is characterized by phase-specific reflex components defined as short- (SLR), medium- (MLR), and long-latency responses (LLR) following the onset of perturbation, indicating different control levels within the CNS that govern the reflectory activation (Horak and Nashner, 1986; Jacobs and Horak, 2007). The temporal distinction of these responses, meaning their onset latency and modulation capacity on specific levels within the CNS, is of functional significance for human stance control (Taube et al., 2006). For instance, slight postural disturbances (i.e., small ankle joint rotations) are compensated by immediate, non-functional monosynaptic stretch reflex responses in the SLR (Gollhofer and Rapp, 1993). Thereby, fast length changes within the muscle elicited by the perturbation of the surface are detected by the muscle spindles and subsequently evoke a muscular response occurring 30–50 ms after perturbation onset (Honeycutt et al., 2012). However, those quick responses are mostly unfunctional, as they are mainly controlled spinally and hence occur too fast to be modulated by supraspinal areas (Dietz, 1992). Studies investigating stance perturbations could further demonstrate that functionally crucial muscle activation (>65 ms after onset, MLR and >85 ms after onset, LLR) occurs when the COM is shifted away from the vertical provoking a quite challenging postural instability (Dietz et al., 1989a, 1991; Gollhofer et al., 1989). Those reflex responses are supposed to be attributed to polysynaptic reflexes via II-afferents, and it is assumed that the CNS intervenes in the spinal pathway by integrating a central control from supraspinal levels to modulate the muscular response appropriately (Jacobs and Horak, 2007; Tokuno et al., 2009).

To control the entire body, neuromuscular activity is synchronized by inter-limb coordination in gait and stance control (Dietz and Berger, 1984; Berger et al., 1987). This is true for bilateral postural disturbances induced by mechanical perturbations, but surprisingly has also manifested for synergistic muscles of both legs when exposed to single mono-lateral perturbations (Dietz et al., 1989a; Habib Perez et al., 2016). This temporal synchronization of electromyograms from each limb in the orthograde stance emphasizes the integrity of the CNS in utilizing contralateral contribution for regulation of the COM within its base of support by producing a symmetric agonistic activation in both limbs (Dietz et al., 1989a). In addition to the ipsi- and contralateral muscle synergies, authors postulate the interplay of antagonistic muscles encompassing the joints of the lower extremity in determination of the quality and safety of postural equilibrium (Rosa, 2015). An increased antagonistic co-activation has been observed to be a major factor in reducing the range of motion (Ritzmann et al., 2015) while mechanically stabilizing joints as a safety and injury prevention mechanism (Tucker et al., 2008; Nagai et al., 2013).

Contradictory results have been observed regarding the timing (Dietz et al., 1989b; Poyhonen and Avela, 2002) and magnitude of reflex responses (Nomura et al., 2001; Nakazawa et al., 2004) Findings in kinematics and intra- and inter-limb coordination are heterogenous as well (Phadke et al., 2006; Hwang et al., 2011). Therefore, despite the substantial number of articles related to this subject, the underlying neuromuscular mechanisms in view of bi-pedal leg coordination and their

functional consequences for the control of posture are poorly understood. It is emphasized that differing methodologies among the gravity-simulating studies may have caused confounding effects such as changes in friction (Dietz et al., 1989b), artificial stabilization (Freyler et al., 2014), hydrostatic pressure (Thornton et al., 1992), and inertia (Mergner and Rosemeier, 1998) leading to a reduced validity or reliability between the measurements (Dietz et al., 1992). To minimize this overlap, auspicious test conditions can be achieved in space-like environments by a gradual change of gravitational force itself in parabolic flights (Mergner and Rosemeier, 1998; Pletser et al., 2012).

The purpose of this study was to elucidate the gravity-dependence of bipedal human stance based on the physiological model of recovery responses to external perturbation. With reference to Dietz et al. (1989a), we set an emphasis on the timing and magnitude of neuromuscular responses coupled with their topographic distinction related to the functional significance of inter-limb coordination (Habib Perez et al., 2016). For that purpose, we recorded electromyograms in the upper and lower limb muscles (Taube et al., 2008), as well as kinematics of both limbs during translational surface perturbations of different modes (physics of bi-, unilateral and split perturbations) during parabolic flight including partial gravity levels. It was hypothesized that acute changes in gravity affect the postural response after perturbation and is required to anticipate neuromuscular control in timing and magnitude. We expected that a gradual increase in gravity from 0.25 to 1.75 g would result in a gradual increase in limb

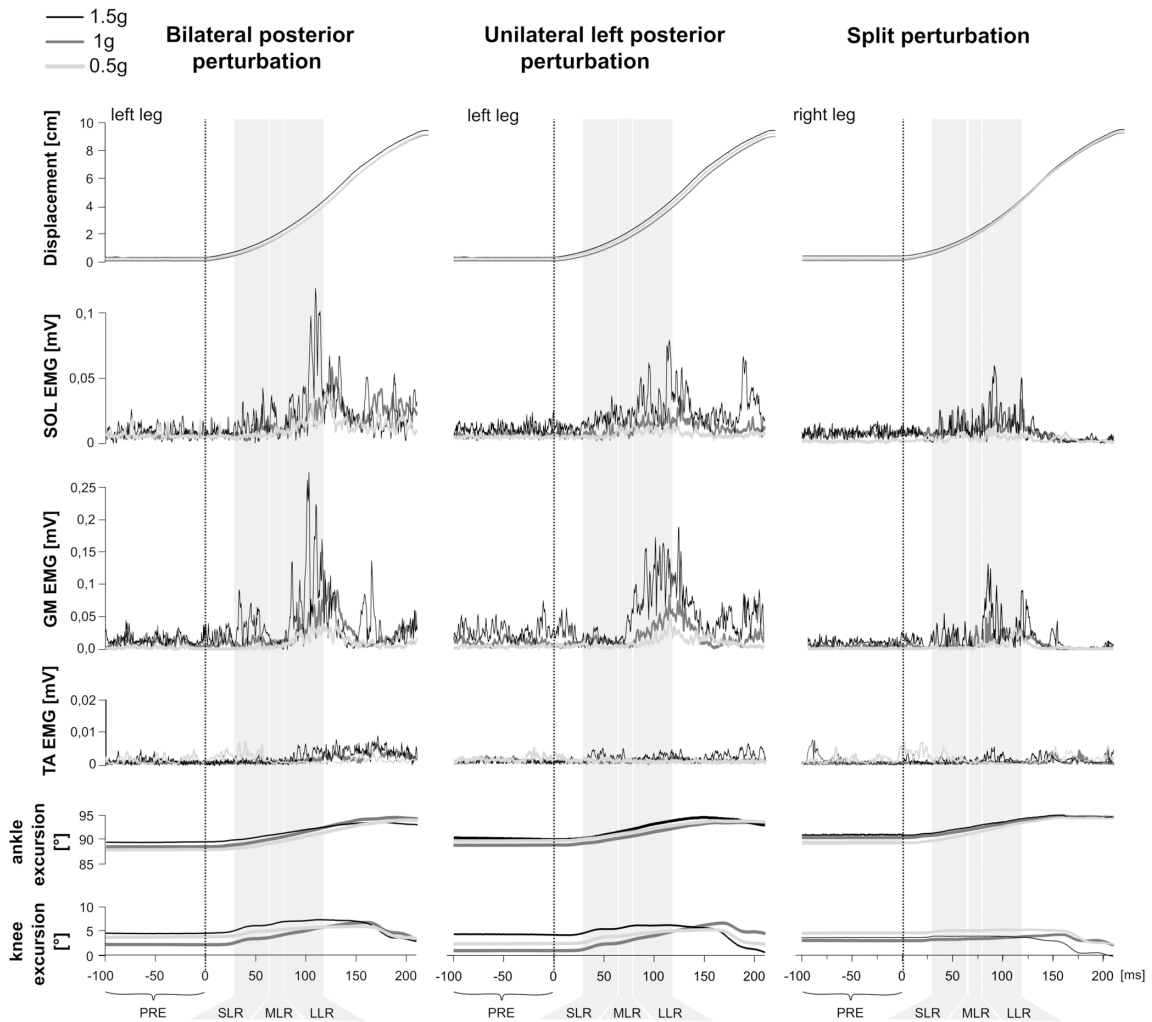

FIGURE 1 | Examples of bilateral **(Left)**, unilateral left **(Middle)**, and split **(Right)** perturbations illustrated by a representative subject. At the top, the trajectory of the platform displacement is illustrated. Below illustrates modulations of the rectified and averaged electromyograms (EMG) of the shank muscles M. soleus (SOL), gastrocnemius medialis (GM) and tibialis anterior (TA) as well as angle and knee joint excursions (bottom) for three gravity conditions that denote hypo-gravity (0.5 g, light gray) Earth gravity (1 g, dark gray) and hyper-gravity (1.5 g, black). Data comprises the means from a minimum of five perturbations for each gravity level. The vertical dashed line indicates the onset of the mechanical displacement. Also marked are the relevant EMG phases: pre-activity (PRE) -100–0 ms before perturbation onset, SLR 30–60 ms, MLR 60–85 ms and LLR 85–120 ms after perturbation onset. Muscular activity progressively increased while muscle activation onset latencies shortened with increasing gravity.

muscle activation intensities and faster muscle onset latencies in response to the perturbation stimulus. We further expected that a phase- and leg-specific reflex adjustment would compensate for the changes in gravitational loading. Three sub-hypotheses have been derived with reference to Dietz et al. (1989a) and Ritzmann et al. (2015): we expect (1) the MLR and LLR to be most affected by changes in gravity, (2) a distinct inter-limb synchronization of neuromuscular activation in response to perturbation and (3) an increase in antagonistic co-activation below and above 1 g.

MATERIALS AND METHODS

Subjects

Six subjects (two females, four males, height 173 ± 6 cm, body mass 66 ± 8 kg, age 33 ± 8 years old) participated in this study. All participants gave written informed consent to the experimental procedure, which was in accordance with the latest revision of the Declaration of Helsinki and approved by the French authorities responsible for the protection of subjects participating in biomedical research (DEMEB of the AFSSAPS) as well as the ethical committee of the University of Freiburg (89/12). The participants underwent two obligatory medical investigations and were healthy with no previous neurological irregularities or injuries of the lower extremities. Exclusion criteria were pregnancy, sickness, injuries, vestibular or proprioceptive dysfunction, fear of flying, previous surgeries on the left or right leg, neurodegenerative diseases or single events associated with neural dysfunctions and an age >41 years.

Study Design

A single-group repeated-measures study design was used to examine differences between postural responses to perturbations in Earth gravity (1 g) with those delivered in hypo- (0.25 g, 0.5 g, and 0.75 g) and hyper-gravity (1.25 g, 1.5 g, and 1.75 g) on the basis of leg joint kinematics and electromyograms (EMG) of lower limb muscles (**Figure 1**). Measurements were performed barefoot on a two-belt treadmill which generated either bi-lateral or unilateral left or split perturbations separated by 3–5 s breaks. Prior to perturbations, subjects stood upright with knee and hip joint extended, arms hanging at the lateral sides and weight equally distributed over both feet.

The order of the recordings in 1 g, hypo- and hyper-gravity was pseudo-randomized between subjects to control for confounding effects such as habituation. Fatigue was avoided by rest pauses (∼2 min) in between the parabolas.

Before the measurements, subjects performed three isometric maximal voluntary contractions (MVCs) for each recorded muscle, according to Wiley and Damiano (1998) and Roelants et al. (2006); the trial with the highest EMG was used for data normalization. The MVCs were executed against resistance for 3 s with recovery pauses of 1 min between trials and repetitions. Body position during MVCs was strictly controlled and supervised through goniometric recordings with standardized knee and hip joint angles by the authors. Antagonistic muscle activation was monitored, and trials were repeated when antagonists were activated.

Parabolic Flights

Gravitational transition was induced using parabolic flight. The experiments were conducted aboard the ZERO-G aircraft (Novespace, Bordeaux, France) during the 1st International Space Life Sciences Working Group Parabolic Flight Campaign (IPFC). This campaign comprised three flight days; each flight lasted 3 h and comprised 31 parabolas for experimentation. Per flight two subjects were measured for 15 parabolas each. The course of one parabola is illustrated in **Figure 2**. The

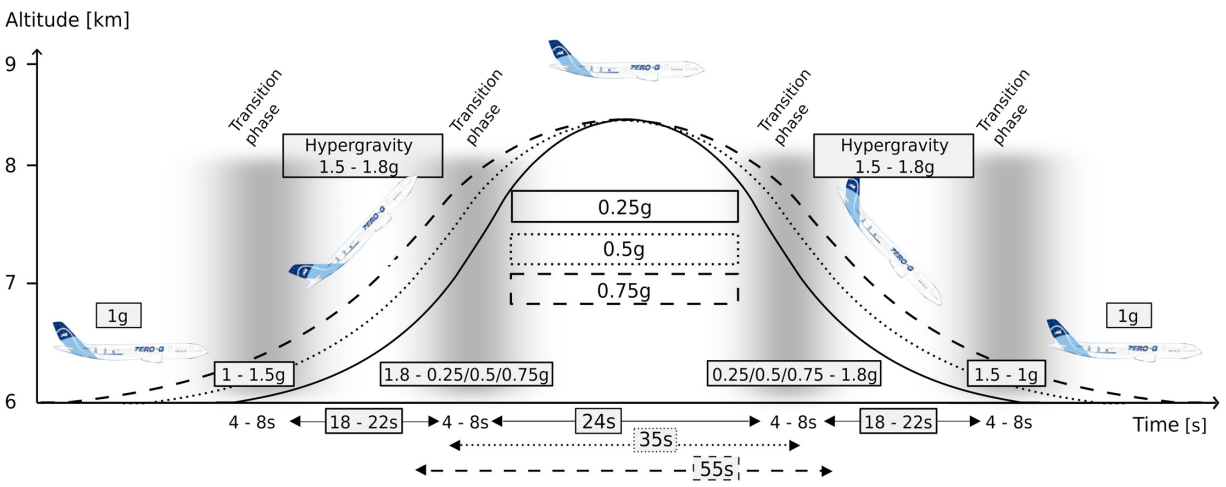

FIGURE 2 | The parabolic flight maneuver and corresponding gravity levels. The level flight (1 g) becomes a steep climb flight inducing hyper-gravity (1.1–1.8 g), followed by hypo-gravity (0.25, 0.5, or 0.75 g) and another hyper-gravity phase before returning to a level flight (1 g), also comprising the respective transition phases between 1 and 1.8 g as well as between the respective hypo-gravity levels and 1.8 g. The maneuver was repeated 31 times in a random order for each of the three flight days. The different gravitational conditions were clustered into equidistant intervals and neuromuscular control and joint kinematics were assessed after surface perturbations.

TABLE 1 | Physical parameters of treadmill perturbations.

	Bilateral anterior		Bilateral posterior		Unilateral left anterior		Unilateral left posterior		Split	
	Left leg	Right leg	Left leg	Right leg	Left leg	Right leg	Left leg	Right leg	Left leg	Right leg
d (cm)	$10.0 \pm 0.0^{\approx}$	$10.0 \pm 0.0^{\approx}$	$-10.0 \pm 0.0^{\approx}$	$-10.0 \pm 0.0^{\approx}$	$10.0 \pm 0.0^{\approx}$	–	$-10.0 \pm 0.0^{\approx}$	–	$-10.0 \pm 0.0^{\approx}$	$10.0 \pm 0.0^{\approx}$
t (ms)	$212 \pm 3^{\approx}$	$211 \pm 4^{\approx}$	$214 \pm 5^{\approx}$	$210 \pm 2^{\approx}$	$209 \pm 5^{\approx}$	–	$214 \pm 4^{\approx}$	–	$211 \pm 2^{\approx}$	$210 \pm 4^{\approx}$
v_{max} (m/s)	$0.8 \pm 0.0^{\approx}$	$0.8 \pm 0.0^{\approx}$	$0.8 \pm 0.0^{\approx}$	$0.8 \pm 0.0^{\approx}$	$0.8 \pm 0.0^{\approx}$	–	$0.8 \pm 0.0^{\approx}$	–	$0.8 \pm 0.0^{\approx}$	$0.8 \pm 0.0^{\approx}$
a_{max} (m/s^2)	$21 \pm 1^{\approx}$	$22 \pm 0^{\approx}$	$22 \pm 3^{\approx}$	$21 \pm 1^{\approx}$	$21 \pm 1^{\approx}$	–	$22 \pm 3^{\approx}$	–	$22 \pm 3^{\approx}$	23 ± 1

Values are absolute values. [v_{max}, maximum speed (m/s); t, impulse duration (ms); a_{max}, maximal acceleration of the treadmill (m/s^2); d, distance (cm)].

partial gravity periods were embedded within two hyper-gravity (1–1.8 g) periods lasting approximately 15–20 s, wherein 10 parabolas included 24-s of 0.25 g, 10 parabolas included 35-s of 0.5 g and 10 parabolas included 55-s of 0.75 g.

Before each flight day, two participants were prepared for the measurements and were given a sex-weight-based injection of 0.2–0.7 ml of Scopolamine 30 min before takeoff to prevent motion sickness (Ritzmann et al., 2016).

Perturbations

Sudden and unexpected acceleration impulses were applied independently to the two belts of the treadmill (physical parameters in **Table 1**). Five different modes of perturbations were elicited in a random order according to Dietz et al. (1989a): (1) simultaneous bilateral anterior perturbation, (2) simultaneous bilateral posterior perturbation, (3) unilateral anterior perturbation on the left leg only, (4) unilateral posterior perturbation on the left leg only, and (5) simultaneous bilateral perturbation in opposing directions. For data analysis, perturbations 2, 4, and 5 were used (**Figure 3A**). The anterior perturbations (1, 3) were applied for the purpose of randomization in order to minimize preparation possibilities for the subjects. As they had to prepare for balance disturbances coming from either anterior or posterior, the initial stance position had to be neutral. The five perturbation modes were applied in random order during seven gravity levels (0.25 g, 0.5 g, 0.75 g, 1 g, 1.25 g, 1.5 g, and 1.75 g). The randomization sequence of the perturbations was performed by software (Labview, Imago, Pfitec, Freiburg). Per g-level, we recorded six to eight perturbations for each of the three analyzed perturbation modes for each subject (**Figure 4**). Hence, we in total recorded approximately 280 perturbations per subject. The mechanical displacement was assessed by a potentiometer (sampling frequency 1 kHz). Subjects wore a safety harness for fall avoidance which was attached to the aircraft ceiling.

Selection of Gravity Levels and Trial Criteria

The g-level was monitored by an accelerometer (sampling frequency 1 kHz). For each subject, we recorded five parabolas per hypo-gravity level (0.25 g, 0.5 g, and 0.75 g). Further, for each of the five parabolas, the two hyper-gravity phases as well as the transition phases (**Figure 2**) were used to record the postural reactions in the hyper-gravity levels (1.25 g, 1.5 g, and 1.75 g). Measurements during steady flight served as a reference in 1 g.

We applied two standardized selection criteria to consider the trial as a valid one without postural interference beyond the mechanical surface translation itself due to pilot, weather or aircraft factors: First, the g-data were extracted for the predefined g-level and needed to lay within boundaries of ± 0.1 g for a time interval of 350 ms (from 100 ms prior to until 250 ms after perturbation onset, Dietz et al., 1989a). If the flight maneuver was instable due to turbulences on the vertical plane or the boundaries of 0.1 g were exceeded, the perturbation trial was excluded. Second, the initial stance position of the subjects prior to each perturbation determined by the COM

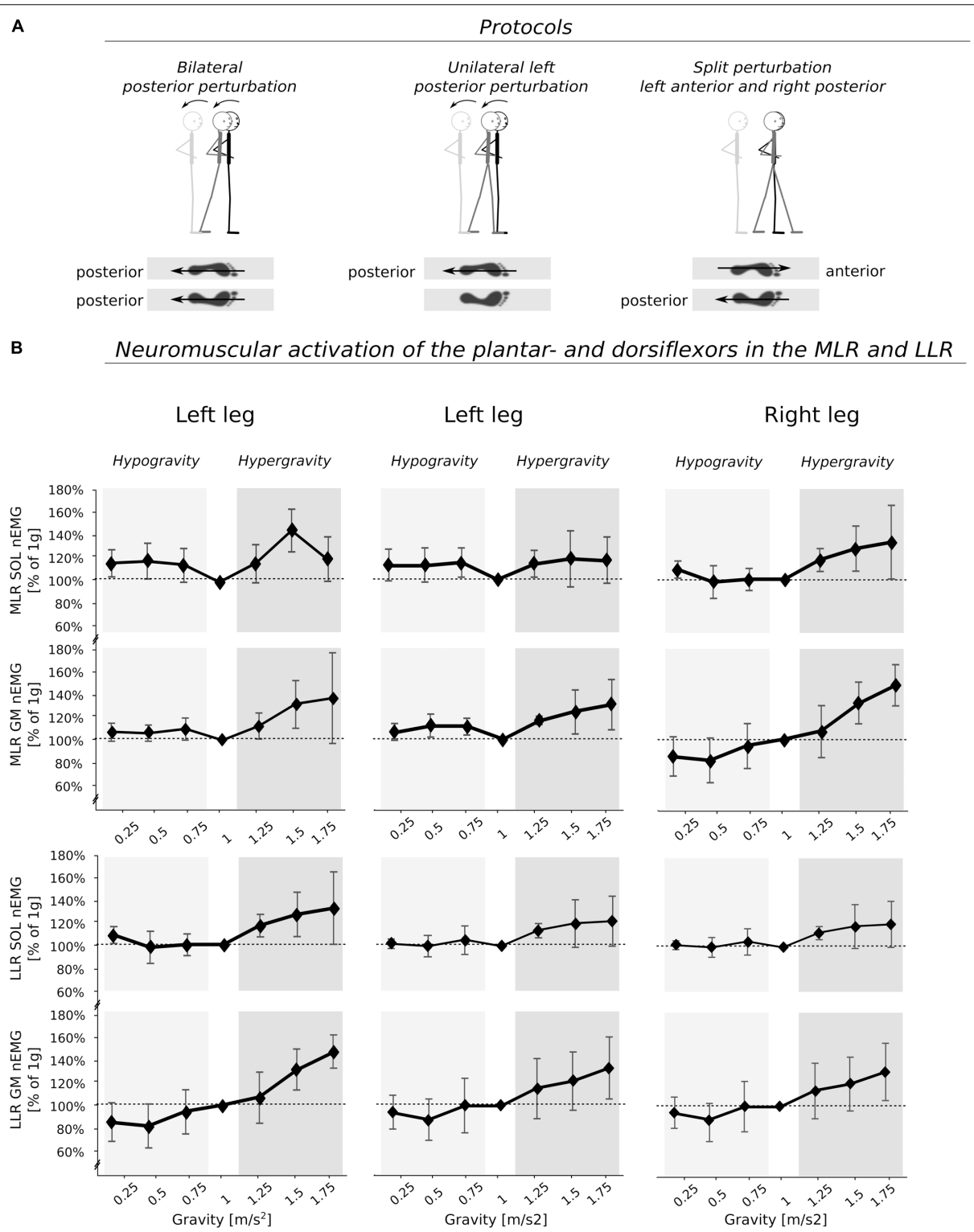

FIGURE 3 | (A) Depiction of the perturbation protocols which were used for analysis as well as **(B)** the means of the electromyograms (EMG) during the medium- and long-latency responses (MLR and LLR) for the plantarflexors [M. soleus (SOL) and M. gastrocnemius medialis (GM)] of the left leg and right leg displayed for the seven gravity levels that span equidistant from hypo- to Earth to hyper-gravity. The MVC normalized iEMG (nEMG) is further normalized to the reference values obtained during the measurements in 1 g. Independent of the postural set (bi-, unilateral left or split perturbation), neuromuscular activity increased progressively with increasing gravity. Note that particularly high gravity levels (>1.5 g) may have led to an inhibition of the neuromuscular activity as shown by the decline in EMG for SOL. The *p*-value refers to the Friedman Test; η_p^2 displays the effect sizes.

position was controlled by a camera [sampling frequency 60 Hz (GoPro, HERO 3, San Mateo, CA, United States)]. If the COM trajectory in the horizontal plane was not within the acceptable bounds of the 90% confidence interval (CI) from trials assessed in 1 g obtained as reference values, the trial was excluded as the initial starting position was considered to be unstable throughout changes in aircraft thrust. In total, we had to exclude nine trials within all six subjects based on one of the aforementioned criteria.

Outcome Measures

Electromyography (EMG)

Bipolar Ag/AgCl surface electrodes (Ambu Blue Sensor P, Ballerup, Denmark, diameter 9 mm, center-to-center distance 34 mm) were placed over the musculus soleus (SOL l), gastrocnemius medialis (GM l), tibialis anterior (TA l), vastus medialis (VM l) and biceps femoris (BF l) of the left leg and over the musculus soleus (SOL r), gastrocnemius medialis (GM r) and tibialis anterior (TA r) of the contralateral right leg. The longitudinal axes of the electrodes were in line with the presumed direction of the underlying muscle fibers. The reference electrode was placed on the patella. Interelectrode resistance was kept below 2 kΩ by means of shaving, light abrasion and degreasing of the skin with a disinfectant. Procedures were executed according to SENIAM (Hermens et al., 2000). The EMG signals were transmitted via shielded cables to the amplifier (band-pass filter 10 Hz to 2 kHz, 200× amplified) and recorded with 1 kHz (A/D-conversion via a National Instruments PCI-6229 DAQ-card, 16 bit resolution).

Kinematics

Ankle (dorsiflexion and plantarflexion) and knee (flexion and extension) joint kinematics of the left as well as the contralateral leg in the sagittal plane were recorded by electro-goniometers

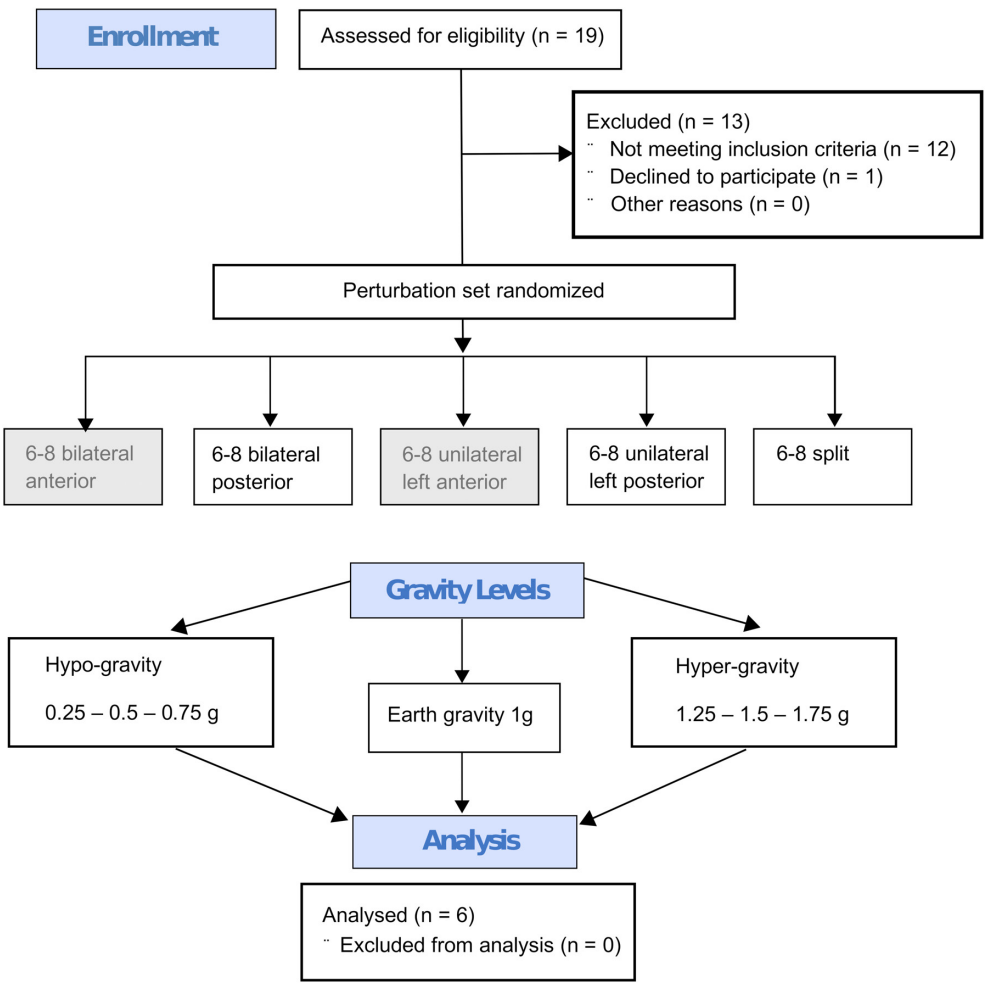

FIGURE 4 | Flow diagram describing the study design with the steps from enrollment to the randomized perturbation modes applied in seven different gravity levels to the analysis. Every subject performed six to eight repetitions under identical conditions (perturbation mode and g-level) and the mean value of these repetitions per subject and g-level were calculated. This mean value was then used for the Friedman test; the statistics for the respective g-levels were calculated separately for all recorded muscles of the left and right leg, phases and perturbation modes with $n = 6$ subjects. The anterior perturbations (gray background) were only applied for randomization purposes and were not included in the analysis.

TABLE 2 | Bilateral posterior perturbation for seven gradually and equidistantly increasing g-levels.

	Hypo gravity			Earth gravity	Hyper gravity			Statistics		
	0.25 g	0.5 g	0.75 g	1 g	1.25 g	1.5 g	1.75 g	*SE*	*P*	η_p^2
PRE SOL l	1.15 ± 0.12	**1.17 ± 0.15**	**1.13 ± 0.14**	**1**	**1.17 ± 0.15**	**1.17 ± 0.11**	**1.16 ± 0.17**	**2%**	**<0.01**	**0.39**
PRE GM l	**1.12 ± 0.10**	**1.10 ± 0.12**	**1.12 ± 0.13**	**1**	**1.13 ± 0.15**	**1.15 ± 0.16**	**1.16 ± 0.14**	**3%**	**0.03**	**0.25**
PRE TA l	1.20 ± 0.18	1.16 ± 0.18	1.16 ± 0.18	1	1.16 ± 0.18	1.17 ± 0.16	1.16 ± 0.18	2%	0.12	0.07
PRE VM l	1.10 ± 0.09	1.08 ± 0.10	1.09 ± 0.10	1	1.09 ± 0.10	1.11 ± 0.09	1.08 ± 0.10	4%	0.35	0.02
PRE BF l	1.14 ± 0.14	1.13 ± 0.16	1.15 ± 0.14	1	1.15 ± 0.17	1.16 ± 0.14	1.11 ± 0.15	3%	0.19	0.05
PRE SOL r	**1.14 ± 0.14**	**1.13 ± 0.14**	**1.13 ± 0.15**	**1**	**1.14 ± 0.16**	**1.16 ± 0.14**	**1.13 ± 0.15**	**5%**	**0.01**	**0.48**
PRE GM r	1.12 ± 011	1.11 ± 0.12	1.12 ± 0.13	1	1.12 ± 0.13	1.14 ± 0.11	1.12 ± 0.12	2%	0.07	0.06
PRE TA r	1.11 ± 0.10	1.10 ± 0.11	1.10 ± 0.11	1	1.10 ± 0.11	1.13 ± 0.11	1.12 ± 0.13	3%	0.19	0.03
SLR SOL l	**1.15 ± 0.11**	**1.17 ± 0.14**	**1.13 ± 0.13**	**1**	**1.15 ± 0.15**	**1.41 ± 0.17**	**1.18 ± 0.18**	**3%**	**<0.01**	**0.56**
SLR GM l	**1.12 ± 0.09**	**1.10 ± 0.11**	**1.11 ± 0.11**	**1**	**1.13 ± 0.11**	**1.40 ± 0.19**	**1.17 ± 0.20**	**2%**	**0.02**	**0.30**
SLR TA l	1.17 ± 0.15	1.17 ± 0.19	1.15 ± 0.18	1	1.15 ± 0.18	1.36 ± 0.22	1.17 ± 0.20	4%	0.18	0.04
SLR VM l	**1.09 ± 0.08**	**1.08 ± 0.10**	**1.10 ± 0.10**	**1**	**1.09 ± 0.09**	**1.17 ± 0.13**	**1.23 ± 0.11**	**5%**	**<0.01**	**0.34**
SLR BF l	1.13 ± 0.14	1.12 ± 0.16	1.15 ± 0.14	1	1.13 ± 014	1.34 ± 0.16	1.12 ± 0.17	5%	0.12	0.09
SLR SOL r	**1.10 ± 0.13**	**1.10 ± 0.12**	**1.13 ± 0.12**	**1**	**1.13 ± 0.15**	**1.42 ± 0.16**	**1.14 ± 0.12**	**7%**	**0.01**	**0.28**
SLR GM r	**1.12 ± 0.11**	**1.11 ± 0.12**	**1.13 ± 0.14**	**1**	**1.13 ± 0.11**	**1.54 ± 0.18**	**1.13 ± 0.17**	**2%**	**0.03**	**0.17**
SLR TA r	1.10 ± 0.09	1.10 ± 0.12	1.10 ± 0.11	1	1.10 ± 0.11	1.31 ± 0.20	1.15 ± 0.16	6%	0.37	0.02
MLR SOL l	**0.99 ± 0.12**	**1.00 ± 0.08**	**1.04 ± 0.08**	**1**	**1.18 ± 0.13**	**1.20 ± 0.10**	**1.19 ± 0.25**	**4%**	**<0.01**	**0.40**
MLR GM l	**1.08 ± 0.09**	**1.07 ± 0.08**	**1.11 ± 0.11**	**1**	**1.14 ± 0.13**	**1.35 ± 0.24**	**1.42 ± 0.45**	**3%**	**<0.01**	**0.71**
MLR TA l	1.19 ± 0.19	1.15 ± 0.17	1.16 ± 0.19	1	1.17 ± 0.20	1.19 ± 0.20	1.19 ± 0.26	5%	0.21	0.03
MLR VM l	1.10 ± 0.10	1.10 ± 0.09	1.09 ± 0.10	1	1.10 ± 0.11	1.12 ± 0.12	1.08 ± 0.09	6%	0.49	0.02
MLR BF l	**1.15 ± 0.15**	**1.14 ± 0.09**	**1.16 ± 0.14**	**1**	**1.18 ± 0.14**	**1.17 ± 0.17**	**1.14 ± 0.14**	**4%**	**0.02**	**0.18**
MLR SOL r	**1.16 ± 0.18**	**1.13 ± 0.16**	**1.12 ± 0.15**	**1**	**1.19 ± 0.29**	**1.28 ± 0.30**	**1.18 ± 0.17**	**3%**	**0.03**	**0.24**
MLR GM r	**1.11 ± 0.15**	**1.09 ± 0.12**	**1.11 ± 0.17**	**1**	**1.23 ± 0.08**	**1.47 ± 0.41**	**1.38 ± 0.27**	**2%**	**<0.01**	**0.52**
MLR TA r	1.13 ± 0.12	1.13 ± 0.07	1.11 ± 0.13	1	1.12 ± 0.13	1.09 ± 0.10	1.05 ± 0.10	6%	0.42	0.02
LLR SOL l	**1.11 ± 0.11**	**1.13 ± 0.14**	**1.11 ± 0.15**	**1**	**1.10 ± 0.16**	**1.17 ± 0.14**	**1.19 ± 0.25**	**6%**	**0.01**	**0.30**
LLR GM l	**1.02 ± 0.08**	**1.01 ± 0.08**	**1.04 ± 0.08**	**1**	**1.13 ± 0.12**	**1.17 ± 0.14**	**1.19 ± 0.16**	**5%**	**0.03**	**0.17**
LLR TA l	**1.18 ± 0.16**	**1.16 ± 0.17**	**1.16 ± 0.20**	**1**	**1.16 ± 0.19**	**1.20 ± 0.18**	**1.22 ± 0.23**	**3%**	**<0.01**	**0.29**
LLR VM l	1.09 ± 0.10	1.09 ± 0.09	1.09 ± 0.10	1	1.08 ± 0.10	1.11 ± 0.10	1.09 ± 0.10	7%	0.35	0.02
LLR BF l	1.07 ± 0.12	1.10 ± 0.16	1.10 ± 0.15	1	1.15 ± 0.19	1.23 ± 0.26	1.19 ± 0.27	4%	0.28	0.04
LLR SOL r	1.06 ± 0.14	1.04 ± 0.08	1.06 ± 0.12	1	1.11 ± 0.15	1.11 ± 0.11	1.15 ± 0.17	8%	0.09	0.13
LLR GM r	**0.97 ± 0.09**	**0.98 ± 0.05**	**0.99 ± 0.07**	**1**	**1.06 ± 0.04**	**1.17 ± 0.15**	**1.16 ± 0.14**	**3%**	**<0.01**	**0.37**
LLR TA r	**1.10 ± 0.10**	**1.09 ± 0.10**	**1.11 ± 0.12**	**1**	**1.09 ± 0.10**	**1.10 ± 0.07**	**1.14 ± 0.16**	**5%**	**0.02**	**0.14**

EMG amplitudes of all subjects (mean ± SD, n = 6 subjects) for the five recorded muscles of the left leg and three recorded muscles of the right leg during four phases (PRE 100 ms before treadmill perturbation until perturbation onset, SLR 30–60 ms, MLR 60–85 ms, LLR 85–120 ms after perturbation). Values are normalized to the iEMG during MVC. The values for hypo- and hyper-gravity are expressed in percent of the 1 g condition. For every leg, muscle and phase the Friedman test was applied to test the effect of the g-level on the EMG amplitude. The p-value refers to the Friedman Test (significant g-effects are labeled with bold letters) and η_p^2 to the effect sizes. Standard errors (SEs) over all seven gravity levels are illustrated.

(Biometrics, Gwent, United Kingdom). The ankle goniometers were fixed at the lateral aspect of the ankle, with its movable endplates attached parallel to the major axis of the foot, in line with the fifth metatarsal, and the major axis of the leg, in line with the fibula. The knee goniometers were placed over the lateral epicondyle of the femur, with one endplate attached to the shank, aligned to the lateral malleolus of the fibula and the other to the thigh, aligned to the greater trochanter. The knee angle was set to zero at 0° during normal upright stance, and joint flexion was reflected by an angle >0°. An angle of 90° between the fifth metatarsal and the fibula corresponded to a 90° ankle angle; an angle >90° reflected plantarflexion. Signals were recorded with a sampling frequency of 2 kHz.

To control the starting position before each perturbation, we monitored the vertical COM projection with 2D video recordings at a distance of 3 m from the treadmill perpendicularly to the sagittal plane (Gambelli et al., 2016). The vertical COM projection was determined using the software SIMI Motion (Unterschleißheim, Germany). Markers were taped on the participants' skin on the anatomical landmark iliac crest representative for the COM.

Data Processing

The joint angles were determined at the onset of perturbation, and the angular joint excursions (°) were calculated from onset of perturbation until 250 ms after the onset. The angular velocity of joint excursions was assessed as follows: $v_{joint} = x^*t$ with

TABLE 3 | Unilateral left posterior perturbation for seven gradually and equidistantly increasing g-levels.

	Hypo gravity			Earth gravity	Hyper gravity			Statistics		
	0.25 g	0.5 g	0.75 g	1 g	1.25 g	1.5 g	1.75 g	*SE*	*P*	η_p^2
PRE SOL l	**1.18 ± 0.16**	1.13 ± 0.13	**1.14 ± 0.14**	**1**	**1.12 ± 0.10**	**1.12 ± 0.11**	**1.15 ± 0.18**	**4%**	**0.04**	**0.14**
PRE GM l	1.11 ± 0.10	1.10 ± 0.13	1.16 ± 0.12	1	1.09 ± 0.12	1.12 ± 0.14	1.14 ± 0.18	4%	0.19	0.08
PRE TA l	1.18 ± 0.17	1.16 ± 0.19	1.09 ± 0.18	1	1.11 ± 0.09	1.14 ± 0.17	1.16 ± 0.21	3%	0.05	0.10
PRE VM l	1.09 ± 0.09	1.08 ± 0.10	1.09 ± 0.10	1	1.07 ± 0.09	1.08 ± 0.10	1.08 ± 0.10	4%	0.27	0.03
PRE BF l	1.13 ± 0.14	1.12 ± 0.16	1.14 ± 0.15	1	1.11 ± 0.16	1.11 ± 0.15	1.11 ± 0.15	6%	0.41	0.02
PRE SOL r	1.14 ± 0.14	1.12 ± 0.15	1.13 ± 0.14	1	1.10 ± 0.14	1.13 ± 0.15	1.12 ± 0.16	2%	0.15	0.05
PRE GM r	1.12 ± 0.11	1.10 ± 0.13	1.12 ± 0.13	1	1.09 ± 0.12	1.12 ± 0.12	1.12 ± 0.14	7%	0.45	0.02
PRE TA r	1.11 ± 0.10	1.09 ± 0.11	1.11 ± 0.11	1	1.09 ± 0.12	1.10 ± 0.11	1.12 ± 0.14	4%	0.35	0.04
SLR SOL l	**1.12 ± 0.14**	**1.12 ± 0.12**	**1.14 ± 0.15**	**1**	**1.13 ± 0.09**	**1.17 ± 0.21**	**1.16 ± 0.16**	**2%**	**0.02**	**0.24**
SLR GM l	**1.12 ± 0.12**	**1.11 ± 0.12**	**1.13 ± 0.13**	**1**	**1.10 ± 0.08**	**1.25 ± 0.28**	**1.25 ± 0.23**	**3%**	**<0.01**	**0.36**
SLR TA l	1.17 ± 0.16	1.14 ± 0.18	1.16 ± 0.18	1	1.12 ± 0.16	1.23 ± 0.21	1.14 ± 0.18	5%	0.05	0.13
SLR VM l	1.10 ± 0.10	1.09 ± 0.10	1.09 ± 0.10	1	1.07 ± 0.09	1.18 ± 0.18	1.09 ± 0.12	4%	0.37	0.05
SLR BF l	1.13 ± 0.14	1.12 ± 0.17	1.15 ± 0.16	1	1.12 ± 0.18	1.20 ± 0.21	1.10 ± 0.14	4%	0.63	0.01
SLR SOL r	1.15 ± 0.14	1.13 ± 0.14	1.14 ± 0.14	1	1.09 ± 0.15	1.24 ± 0.19	1.13 ± 0.15	6%	0.05	0.11
SLR GM r	**1.11 ± 0.11**	**1.09 ± 0.13**	**1.11 ± 0.13**	**1**	**1.07 ± 0.13**	**1.25 ± 0.23**	**1.15 ± 0.16**	**3%**	**0.02**	**0.19**
SLR TA r	1.10 ± 0.11	1.10 ± 0.12	1.11 ± 0.11	1	1.10 ± 0.14	1.17 ± 0.19	1.10 ± 0.12	4%	0.40	0.02
MLR SOL l	**1.14 ± 0.13**	**1.11 ± 0.14**	**1.10 ± 0.12**	**1**	**1.06 ± 0.11**	**1.13 ± 0.23**	**1.12 ± 0.19**	**6%**	**0.03**	**0.21**
MLR GM l	**1.07 ± 0.08**	**1.13 ± 0.11**	**1.12 ± 0.08**	**1**	**1.18 ± 0.04**	**1.26 ± 0.21**	**1.33 ± 0.24**	**6%**	**<0.01**	**0.52**
MLR TA l	1.16 ± 0.17	1.18 ± 0.20	1.16 ± 0.17	1	1.13 ± 0.18	1.20 ± 0.20	1.16 ± 0.21	4%	0.36	0.04
MLR VM l	1.09 ± 0.08	1.10 ± 0.14	1.09 ± 0.10	1	1.08 ± 0.10	1.12 ± 0.12	1.08 ± 0.09	7%	0.61	0.01
MLR BF l	1.13 ± 0.14	1.11 ± 0.17	1.14 ± 0.14	1	1.12 ± 0.15	1.17 ± 0.16	1.10 ± 0.14	3%	0.10	0.07
MLR SOL r	**1.14 ± 0.14**	**1.13 ± 0.16**	**1.14 ± 0.15**	**1**	**1.11 ± 0.17**	**1.16 ± 0.19**	**1.13 ± 0.13**	**4%**	**0.04**	**0.09**
MLR GM r	**1.12 ± 0.11**	**1.12 ± 0.14**	**1.12 ± 0.11**	**1**	**1.08 ± 0.20**	**1.21 ± 0.21**	**1.20 ± 0.17**	**3%**	**0.03**	**0.09**
MLR TA r	1.14 ± 0.13	1.16 ± 0.12	1.11 ± 0.11	1	1.14 ± 0.21	1.15 ± 0.24	1.15 ± 0.21	3%	0.08	0.05
LLR SOL l	**1.02 ± 0.04**	**1.00 ± 0.09**	**1.05 ± 0.12**	**1**	**1.13 ± 0.06**	**1.19 ± 0.20**	**1.21 ± 0.21**	**8%**	**<0.05**	**0.63**
LLR GM l	**0.93 ± 0.18**	**0.85 ± 0.22**	**1.00 ± 0.29**	**1**	**1.18 ± 0.32**	**1.26 ± 0.31**	**1.40 ± 0.33**	**4%**	**<0.01**	**0.42**
LLR TA l	1.18 ± 0.16	1.04 ± 0.14	1.16 ± 0.18	1	1.11 ± 0.15	1.10 ± 0.21	1.16 ± 0.17	3%	0.28	0.03
LLR VM l	1.10 ± 0.10	1.00 ± 0.10	1.05 ± 0.08	1	1.06 ± 0.09	1.05 ± 0.16	1.08 ± 0.10	5%	0.47	0.01
LLR BF l	1.13 ± 0.14	1.11 ± 0.13	1.15 ± 0.16	1	1.08 ± 0.17	1.09 ± 0.16	1.10 ± 0.15	2%	0.31	0.02
LLR SOL r	1.07 ± 0.13	1.03 ± 0.13	0.98 ± 0.12	1	1.12 ± 0.14	1.11 ± 0.17	1.16 ± 0.15	7%	0.05	0.06
LLR GM r	**1.04 ± 0.12**	**1.00 ± 0.14**	**0.98 ± 0.14**	**1**	**1.15 ± 0.09**	**1.19 ± 0.25**	**1.28 ± 0.14**	**6%**	**<0.01**	**0.42**
LLR TA r	1.10 ± 0.10	1.00 ± 0.13	1.11 ± 0.12	1	1.06 ± 0.08	1.07 ± 0.14	1.10 ± 0.11	4%	0.49	0.02

EMG amplitudes of all subjects (mean ± SD, n = 6 subjects) for the five recorded muscles of the left leg and three recorded muscles of the right leg during four phases (PRE 100 ms before treadmill perturbation until perturbation onset, SLR 30–60 ms, MLR 60–85 ms, LLR 85–120 ms after perturbation). Values are normalized to the iEMG during MVC. The values for hypo- and hyper-gravity are expressed in percent of the 1 g condition. For every leg, muscle and phase the Friedman test was applied to test the effect of the g-level on the EMG amplitude. The p-value refers to the Friedman Test (significant g-effects were labeled with bold letters) and η_p^2 to the effect sizes. Standard errors (SEs) over all seven gravity levels are illustrated.

x describing the displacement [°] and t the time to maximal excursion [s] in a timeframe of 0–210 ms.

EMG signals were rectified, averaged, integrated (iEMG) and time-normalized for four time intervals, based on previously reported onset latencies and durations of the reflex components (Lee and Tatton, 1975; Marsden et al., 1978; Sinkjaer et al., 1999): the pre-activation phase (PRE, -100–0 ms before perturbation), the SLR (30–60 ms after perturbation), MLR (60–85 ms after perturbation) and LLR (85–120 ms after perturbation) (Hobara et al., 2008; Taube et al., 2008; Zuur et al., 2010). These integrals were normalized to the MVC of the corresponding muscle. Furthermore, antagonistic co-activation of TA and SOL (TA_SOL), TA and GM (TA_GM) and VM and BF (VM_BF) were calculated for the pre-activation phase for both legs (Hoffrén et al., 2011). Furthermore, muscle activation onset latencies of each muscle after the perturbation were identified as the first burst >2 standard deviations above the baseline EMG and displayed in ms (Henry et al., 1998).

All data were averaged for identical perturbation modes.

Statistics

Data are presented as means ± standard deviations (SD) for each g-level. We used a two-step procedure (**Figure 4**): first, as every subject performed six to eight repetitions under identical conditions (perturbation mode and g-level), we calculated the mean value of these repetitions per subject and g-level for data reduction. Second, this synthesized mean value per subject and g-level was used for the Friedman test. The statistics for the

TABLE 4 | Split perturbation (left leg anterior and right leg posterior) for 7 gradually and equidistantly increasing g-levels.

	Hypo gravity			Earth gravity	Hyper gravity			Statistics		
	0.25 g	0.5 g	0.75 g	1 g	1.25 g	1.5 g	1.75 g	*SE*	*P*	η_p^2
PRE SOL l	1.16 ± 0.13	**1.17 ± 0.17**	**1.14 ± 0.16**	**1**	**1.14 ± 0.15**	**1.09 ± 0.10**	**1.18 ± 0.25**	**2%**	**0.02**	**0.28**
PRE GM l	1.12 ± 0.11	1.09 ± 0.11	1.12 ± 0.13	1	1.15 ± 0.23	1.13 ± 0.15	1.15 ± 0.21	1%	0.07	0.12
PRE TA l	**1.20 ± 0.18**	**1.14 ± 0.17**	**1.17 ± 0.19**	**1**	**1.13 ± 0.17**	**1.15 ± 0.20**	**1.16 ± 0.18**	**3%**	**0.01**	**0.24**
PRE VM l	1.09 ± 0.09	1.07 ± 0.09	1.09 ± 0.10	1	1.07 ± 0.09	1.08 ± 1.10	1.08 ± 0.10	2%	0.38	0.04
PRE BF l	**1.14 ± 0.14**	**1.11 ± 0.14**	**1.15 ± 0.15**	**1**	**1.10 ± 0.15**	**1.11 ± 0.14**	**1.11 ± 0.15**	**4%**	**0.02**	**0.19**
PRE SOL r	1.14 ± 0.14	1.11 ± 0.13	1.14 ± 0.15	1	1.12 ± 0.16	1.13 ± 0.16	1.13 ± 0.15	3%	0.28	0.04
PRE GM r	1.12 ± 0.11	1.10 ± 0.11	1.12 ± 0.13	1	1.10 ± 0.12	1.13 ± 0.17	1.11 ± 0.14	6%	0.17	0.02
PRE TA r	1.12 ± 0.10	1.09 ± 0.10	1.11 ± 0.12	1	1.09 ± 0.12	1.10 ± 0.12	1.11 ± 0.12	2%	0.46	0.02
SLR SOL l	**1.03 ± 0.15**	**1.07 ± 0.18**	**1.00 ± 0.16**	**1**	**0.95 ± 0.15**	**0.97 ± 0.08**	**0.92 ± 0.28**	**5%**	**0.04**	**0.09**
SLR GM l	1.04 ± 0.11	1.02 ± 0.10	1.02 ± 0.12	1	1.00 ± 0.14	0.96 ± 0.13	0.93 ± 0.18	3%	0.06	0.05
SLR TA l	**1.01 ± 0.20**	**0.97 ± 0.16**	**0.95 ± 0.19**	**1**	**1.13 ± 0.16**	**1.25 ± 0.19**	**1.34 ± 0.23**	**3%**	**<0.01**	**0.56**
SLR VM l	1.09 ± 0.08	1.07 ± 0.08	1.10 ± 0.10	1	1.10 ± 0.14	1.07 ± 0.10	1.08 ± 0.10	4%	0.35	0.03
SLR BF l	1.09 ± 0.14	1.05 ± 0.15	1.06 ± 0.15	1	1.09 ± 0.14	1.10 ± 0.15	1.10 ± 0.13	3%	0.47	0.02
SLR SOL r	**1.11 ± 0.12**	**1.08 ± 0.13**	**1.10 ± 0.15**	**1**	**1.18 ± 0.09**	**1.20 ± 0.14**	**1.30 ± 0.13**	**8%**	**0.02**	**0.19**
SLR GM r	**1.12 ± 0.11**	**1.10 ± 0.11**	**1.13 ± 0.12**	**1**	**1.09 ± 0.10**	**1.26 ± 0.14**	**1.33 ± 0.13**	**4%**	**0.04**	**0.14**
SLR TA r	0.99 ± 0.09	1.02 ± 0.09	0.97 ± 0.12	1	0.95 ± 0.17	0.99 ± 0.09	0.97 ± 0.10	2%	0.74	0.02
MLR SOL l	1.02 ± 0.15	1.05 ± 0.18	1.00 ± 0.17	1	0.93 ± 0.17	0.96 ± 0.26	0.99 ± 0.27	4%	0.88	0.01
MLR GM l	0.95 ± 0.13	0.97 ± 0.11	1.02 ± 0.14	1	0.96 ± 0.17	1.04 ± 0.30	1.02 ± 0.15	4%	0.91	0.01
MLR TA l	**0.84 ± 0.18**	**0.90 ± 0.13**	**0.94 ± 0.20**	**1**	**1.14 ± 0.18**	**1.21 ± 0.38**	**1.33 ± 0.18**	**5%**	**<0.01**	**0.42**
MLR VM l	1.10 ± 0.10	1.19 ± 0.18	1.09 ± 0.10	1	1.05 ± 0.09	1.13 ± 0.28	1.07 ± 0.09	4%	0.16	0.03
MLR BF l	1.11 ± 0.15	1.24 ± 0.11	1.15 ± 0.13	1	1.12 ± 0.13	1.15 ± 0.32	1.10 ± 0.12	3%	0.27	0.04
MLR SOL r	**0.91 ± 0.15**	**0.90 ± 0.17**	**0.95 ± 0.17**	**1**	**1.23 ± 0.20**	**1.20 ± 0.30**	**1.27 ± 0.14**	**5%**	**<0.01**	**0.44**
MLR GM r	**0.94 ± 0.14**	**0.99 ± 0.12**	**1.02 ± 0.15**	**1**	**1.13 ± 0.11**	**1.21 ± 0.27**	**1.23 ± 0.14**	**3%**	**0.01**	**0.32**
MLR TA r	0.93 ± 0.14	1.01 ± 0.12	0.97 ± 0.14	1	0.94 ± 0.12	0.90 ± 0.31	0.82 ± 0.14	6%	0.08	0.18
LLR SOL l	**1.03 ± 0.16**	**1.09 ± 0.16**	**1.02 ± 0.18**	**1**	**0.90 ± 0.18**	**0.84 ± 0.10**	**0.81 ± 0.26**	**4%**	**0.02**	**0.24**
LLR GM l	**1.12 ± 0.11**	**1.10 ± 0.08**	**1.13 ± 0.14**	**1**	**0.97 ± 0.12**	**0.96 ± 0.17**	**0.90 ± 0.14**	**3%**	**0.04**	**0.16**
LLR TA l	**1.18 ± 0.17**	**1.07 ± 0.08**	**1.05 ± 0.09**	**1**	**1.15 ± 0.20**	**1.25 ± 0.20**	**1.35 ± 0.22**	**5%**	**<0.01**	**0.47**
LLR VM l	1.09 ± 0.08	1.00 ± 0.09	1.10 ± 0.10	1	1.08 ± 0.12	1.07 ± 0.10	1.08 ± 0.09	5%	0.53	0.02
LLR BF l	**1.12 ± 0.13**	**1.03 ± 0.08**	**1.14 ± 0.15**	**1**	**1.04 ± 0.15**	**1.08 ± 0.10**	**1.21 ± 0.17**	**3%**	**0.04**	**0.13**
LLR SOL r	**1.10 ± 0.10**	**1.00 ± 0.10**	**1.13 ± 0.14**	**1**	**1.21 ± 0.14**	**1.44 ± 0.19**	**1.52 ± 0.22**	**6%**	**<0.01**	**0.48**
LLR GM r	**0.98 ± 0.13**	**1.00 ± 0.16**	**1.03 ± 0.09**	**1**	**1.17 ± 0.10**	**1.20 ± 0.15**	**1.37 ± 0.23**	**2%**	**<0.01**	**0.32**
LLR TA r	0.96 ± 0.14	1.00 ± 0.08	1.02 ± 0.08	1	1.03 ± 0.11	0.98 ± 0.11	0.94 ± 0.13	4%	0.30	0.03

EMG amplitudes of all subjects (mean ± SD, n = 6 subjects) for the five recorded muscles of the left leg and three recorded muscles of the right leg during four phases (PRE 100 ms before treadmill perturbation until perturbation onset, SLR 30–60 ms, MLR 60–85 ms, LLR 85–120 ms after perturbation). Values are normalized to the iEMG during MVC. The values for hypo- and hyper-gravity are expressed in percent of the 1 g condition. For every leg, muscle and phase the Friedman test was applied to test the effect of the g-level on the EMG amplitude. The p-value refers to the Friedman Test (significant g-effects were labeled with bold letters) and η_p^2 to the effect sizes. Standard errors (SEs) over all seven gravity levels are illustrated.

respective g-levels were calculated separately for all recorded muscles of the left and right leg, phases and perturbation modes with $n = 6$ subjects. Standard errors (SEs) were calculated across gravity levels.

To evaluate kinematic and neuromuscular modulations in response to changes in gravitational loading [gravity (7)], the Friedman Test was used for $n = 6$ subjects. The dependent variables were the onset latencies and EMGs normalized to MVC for PRE, SLR, MLR, and LLR for the eight recorded muscles of the lateral and contralateral leg as well as ankle and knee joint excursions and velocities. The level of significance was set to $P = 0.05$. The false discovery rate was controlled according to the Benjamini-Hochberg-Yekutieli method, a less conservative but still stringent statistical approach conceptualizing the rate of type I errors (Benjamini and Hochberg, 1995; Benjamini and Yekutieli, 2005). Partial eta squared (η_p^2) was also used as an estimate of the effect size [$\eta_p^2 < 0.01$ small, $0.01 \leq \eta_p^2 \leq 0.06$ medium, $0.24 < \eta_p^2$ large effect size (Cohen, 1973)].

Bivariate, two-tailed Pearson correlation analyses were conducted to determine the strength of linear relations between the two variables joint velocities and the neuromuscular activity in the reflex phases MLR and LLR, for the muscles SOL and GM, respectively. Furthermore, to compare correlations from dependent samples obtained in the seven progressively increasing gravity levels, correlation coefficients (r0.25, r0.5, r0.75, r1, r1.25, r1.5, and r1.75) were converted into a *z*-score using Fisher's r-to-z transformation (Steiger, 1980). Subsequently,

TABLE 5 | Kinematics for seven gradually and equidistantly increasing g-levels.

	Hypo gravity			Earth gravity	Hyper gravity			Statistics		
Bilateral posterior perturbation	**0.25 g**	**0.5 g**	**0.75 g**	**1 g**	**1.25 g**	**1.5 g**	**1.75 g**	***SE***	***P***	η_p^2
L ankle angle at perturbation onset (°)	94 ± 2	93 ± 2	93 ± 2	94 ± 2	94 ± 3	93 ± 3	95 ± 3	2%	0.91	0.01
R ankle angle at perturbation onset (°)	90 ± 4	91 ± 4	90 ± 3	92 ± 3	89 ± 4	92 ± 4	93 ± 5	1%	0.29	0.04
L max. ankle angular excursion (°)	−4 ± 1	−5 ± 1	−5 ± 1	−6 ± 2	−4 ± 2	−4 ± 1	−4 ± 2	2%	0.15	0.08
R max. ankle angular excursion (°)	−5 ± 1	−5 ± 1	−6 ± 1	−6 ± 2	−5 ± 1	−5 ± 1	−5 ± 1	1%	0.29	0.03
L knee angle at perturbation onset (°)	0 ± 5	0 ± 4	−1 ± 3	−2 ± 2	−1 ± 4	−1 ± 4	−1 ± 4	2%	0.80	0.01
R knee angle at perturbation onset (°)	2 ± 1	3 ± 2	1 ± 3	1 ± 3	1 ± 2	1 ± 1	1 ± 1	1%	0.76	0.02
L max. knee angular excursion (°)	2 ± 1	2 ± 1	2 ± 1	3 ± 2	2 ± 2	2 ± 1	2 ± 2	2%	0.15	0.07
R max. knee angular excursion (°)	2 ± 1	2 ± 1	2 ± 1	2 ± 2	2 ± 1	2 ± 1	2 ± 2	1%	0.29	0.03
Unilateral left posterior perturbation	**0.25 g**	**0.5 g**	**0.75 g**	**1 g**	**1.25 g**	**1.5 g**	**1.75 g**	***SE***	***P***	η_p^2
L ankle angle at perturbation onset (°)	94 ± 2	94 ± 2	93 ± 1	94 ± 2	93 ± 2	95 ± 3	94 ± 6	3%	0.65	0.03
R ankle angle at perturbation onset (°)	92 ± 5	91 ± 4	90 ± 3	92 ± 3	91 ± 2	91 ± 3	93 ± 4	2%	0.40	0.07
L max. ankle angular excursion (°)	−3 ± 1	−4 ± 1	−4 ± 1	−4 ± 1	−4 ± 1	−3 ± 1	−3 ± 1	3%	0.79	0.02
R max. ankle angular excursion (°)	−0 ± 0	−1 ± 1	−0 ± 0	−1 ± 1	−1 ± 1	−1 ± 1	−1 ± 1	1%	0.44	0.02
L knee angle at perturbation onset (°)	2 ± 4	0 ± 4	1 ± 3	1 ± 2	1 ± 2	1 ± 3	1 ± 2	2%	0.52	0.03
R knee angle at perturbation onset (°)	2 ± 1	2 ± 2	1 ± 3	1 ± 2	2 ± 3	1 ± 2	1 ± 2	2%	0.19	0.04
L max. knee angular excursion (°)	2 ± 1	3 ± 1	3 ± 1	3 ± 2	3 ± 2	2 ± 1	2 ± 1	3%	0.73	0.03
R max. knee angular excursion (°)	0 ± 1	1 ± 1	1 ± 1	1 ± 1	1 ± 1	0 ± 0	1 ± 1	1%	0.48	0.05
Split perturbation (left anterior right posterior)	**0.25 g**	**0.5 g**	**0.75 g**	**1 g**	**1.25 g**	**1.5 g**	**1.75 g**	***SE***	***P***	η_p^2
L ankle angle at perturbation onset (°)	92 ± 6	90 ± 2	90 ± 2	90 ± 1	90 ± 2	91 ± 3	93 ± 2	4%	0.16	0.07
R ankle angle at perturbation onset (°)	91 ± 4	91 ± 4	90 ± 3	92 ± 3	89 ± 4	93 ± 4	93 ± 4	1%	0.59	0.02
L max. ankle angular excursion (°)	6 ± 1	6 ± 1	7 ± 1	7 ± 1	5 ± 1	5 ± 1	6 ± 2	2%	0.49	0.02
R max. ankle angular excursion (°)	−3 ± 1	−4 ± 1	−5 ± 2	−5 ± 2	−4 ± 1	−4 ± 1	−4 ± 2	3%	0.19	0.04
L knee angle at perturbation onset (°)	2 ± 3	0 ± 4	−1 ± 3	0 ± 4	1 ± 5	1 ± 4	0 ± 6	4%	0.47	0.02
R knee angle at perturbation onset (°)	2 ± 1	3 ± 3	1 ± 4	0 ± 3	0 ± 3	1 ± 2	1 ± 2	4%	0.15	0.04
L max. knee angular excursion (°)	2 ± 1	3 ± 1	3 ± 1	2 ± 1	2 ± 1	2 ± 0	3 ± 2	4%	0.82	0.01
R max. knee angular excursion (°)	1 ± 1	2 ± 1	2 ± 2	2 ± 3	1 ± 1	1 ± 1	2 ± 1	2%	0.47	0.02

Mean ankle and knee joint angles at perturbation onset and maximal ankle and knee angular excursions of the left (l) and right (r) leg after perturbation. Postural set was manipulated by either bilateral posterior (top), unilateral left posterior (middle) and split perturbation (bottom), each mean value comprises n = 6 participants. For every joint angle of each leg the Friedman test was applied to test the effect of the g-level on the kinematic parameters. The p-value refers to the Friedman Test and η_p^2 to the effect sizes. Standard errors (SEs) over all seven gravity levels are illustrated.

the asymptotic covariance of the estimates was computed according to Steiger (1980).

Equivalence statistics were used to determine if the physics of the treadmill perturbations were statistically equal between the gravity levels below and above 1 g compared to 1 g. For this purpose, the 95% CI was calculated for the differences between 1 g and respective gravity level. If the CI lay within the acceptable boundaries (which were determined based on the variance within the 1 g data set (Borman et al., 2009) the differences were statistically equal and the respective parameter was marked with a $\approx$ symbol.

All statistical analyses were conducted using SPSS 24.0 software (SPSS, Chicago, IL, United States) and calculators from Lee and Preacher (2013).

RESULTS

In all gravity levels and for all perturbation modes, subjects succeeded to regain their postural equilibrium after the mechanical perturbation. There was no trial, in which subjects needed to be secured or were falling.

Physics of Treadmill Perturbation

The treadmill displacement, its maximum speed, the acceleration of the treadmill and the impulse duration for the bilateral, unilateral, and split perturbations are displayed in **Table 1**. The physics were statistically equal between the three perturbation conditions over the seven progressively increased gravity levels.

Neuromuscular Activity

Means of the EMG amplitudes in the recorded shank and thigh muscles are displayed in **Tables 2–4**. Mean rectified EMG signal traces of a representative subject are given in **Figure 1**. Results demonstrate an increased muscle activity in the lower extremities ($p < 0.05$) prior to perturbation in hypo- and hyper-gravity.

After perturbation, compensatory neuromuscular responses in the leg musculature to external stimuli were gravity-sensitive. With progressively increased gravitation the neuromuscular

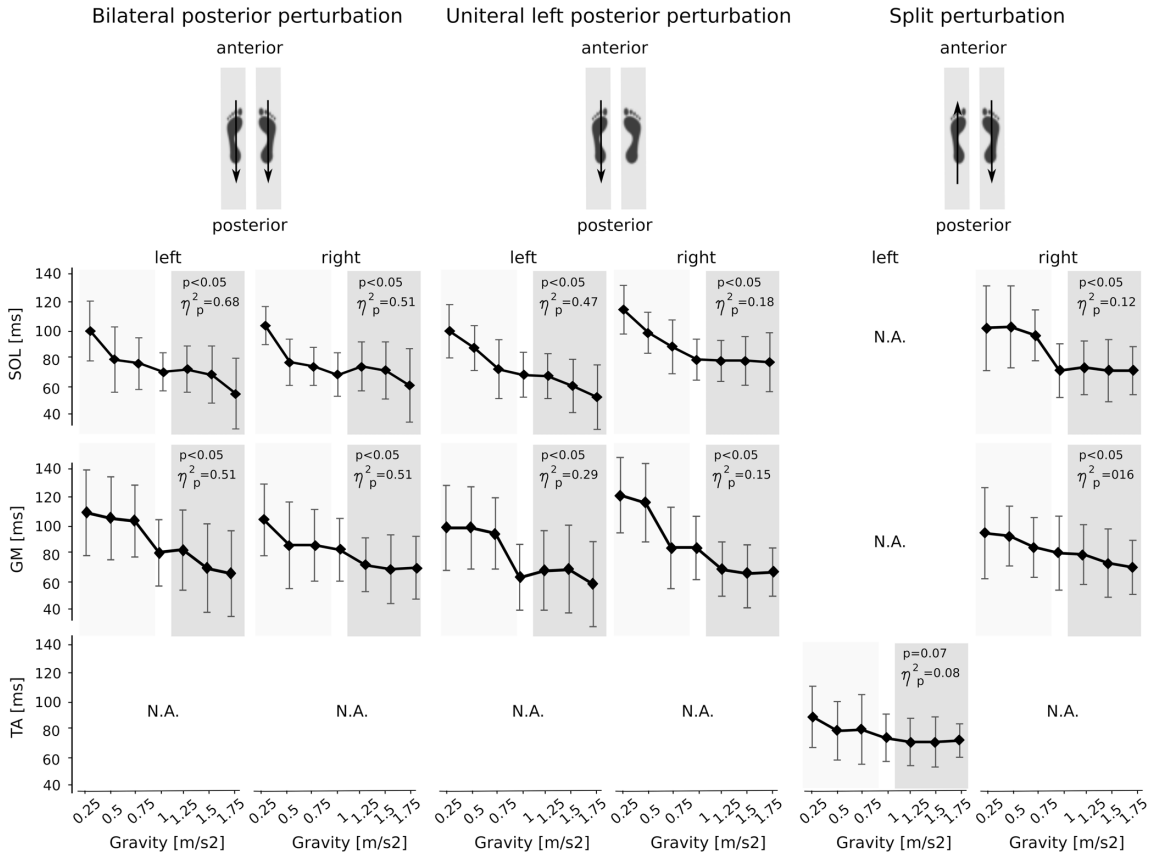

FIGURE 5 | Muscle activation onset latencies for the plantarflexors [M. soleus (SOL) and M. gastrocnemius medialis (GM)] and the dorsiflexor [M. tibialis anterior (TA)] displayed for the seven gravity levels that span from hypo- to Earth to hyper-gravity. Values are displayed in ms. Independent of the postural set (bi- unilateral left or split perturbation), onset latencies shortened progressively with increasing gravity. Note that even the contralateral non-displaced leg (right leg during unilateral left perturbations) showed EMG bursts in response to the left leg's perturbation, however, with longer onset latencies compared to the displaced leg. N.A. denotes the muscles that were not affected by the perturbation and thus did not show onset latencies. The *p*-value refers to the Friedman Test; η^2_p displays the effect sizes.

activity increased. This was true for all three modes of perturbation (**Table 1**) and leg segments, and independent of the muscle's function distinguished by flexors or extensors (**Tables 2**–**4**). As such, the neuromuscular activation intensity increased significantly and gradually as a function of gravity (**Figures 1**, **5**). This increase was phase-specific, more pronounced for MLR and LLR (**Figure 3**) and less visible in the SLR. The M. soleus and M. gastrocnemius medialis were most affected by changes in gravity. In a few muscles, the rise in EMG amplitudes reached saturation and showed an asymptotic behavior or even a minor decline in the highest gravity level (>1.5 g). During unilateral left surface perturbations, the contralateral musculature of the non-displaced leg demonstrated a significant increase in neuromuscular activity with increasing gravity indicating an interlimb-synchronization for the MLR and LLR.

Muscle Onset Latencies

Gravity-induced changes in the muscle onset latencies are illustrated in **Figure 5**. Activation onsets occurred only in the muscles that counteracted the perturbation stimulus. With increasing gravity, onset latencies were significantly reduced in the affected muscles involving the SOL, GM, and TA for the perturbed and not perturbed leg. The gravity-associated reduction in onset latency was also visible in the contralateral non-displaced leg, however, the neuromuscular activation in the contralateral leg was delayed as compared to the perturbed leg ($p < 0.05$).

Antagonistic Co-activation Prior to Perturbation Onset

Means of the co-activation in PRE of antagonistic muscles encompassing the ankle and knee joint are illustrated in **Figure 6**. With both increasing and decreasing gravity above and below 1 g, the antagonistic co-activation increased significantly in the shank and thighs and equally for leg extensors and flexors prior to perturbation compared to the reference values of 1 g indicating a joint stiffening.

Kinematics

Means of the ankle and knee joint kinematics are displayed in **Table 5**. Mean signal traces of the ankle and knee joint excursions

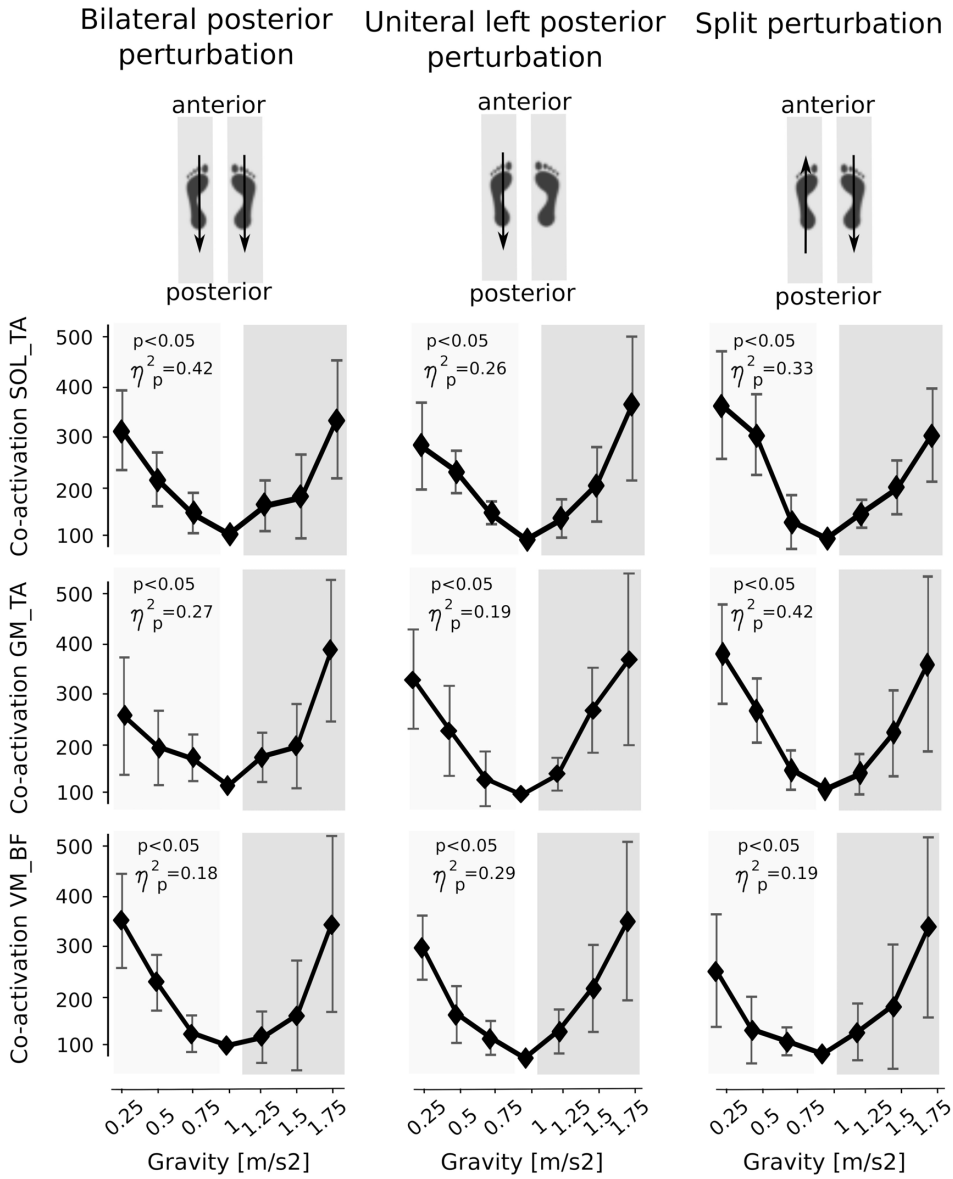

FIGURE 6 | Muscle co-activation of antagonists encompassing the ankle (top and middle) and knee joint (bottom). Graphs illustrate the increase in co-activation above and below Earth gravity. Data are presented illustrate the co-activation of the M. soleus and M. tibialis anterior (SOL_TA), the M. gastrocnemius medialis and M. tibialis anterior (GM_TA) and the M. vastus medialis and M. biceps femoris muscles (VM_BF) for the left leg during the pre-activation phase prior to perturbation. The *p*-value refers to the Friedman Test; η^2_p displays the effect sizes.

of a representative subject collected from a minimum of five perturbations for each gravity level are provided in **Figure 1**. Ankle and knee joint position at perturbation onset and maximal joint defections revealed no statistical differences between the gravity levels. The v_{joint} of ankle joint deflection increased progressively with increasing gravity (**Figure 7**).

Correlations Between Joint Velocities and Neuromuscular Activity

A significant positive correlation was detected for the variable v_{joint} of the ankle with muscle activity in the SOL and GM in the reflex phases MLR and LLR for bi-lateral posterior perturbations. Corresponding graphs to illustrate bivariate correlations and correlation coefficients for bilateral perturbations are displayed in **Figure 8**.

DISCUSSION

With the success of re-gaining postural equilibrium after its perturbation, this study provides a major insight into the gravity-dependency of postural recovery responses after translational surface perturbations. Findings reveal increased muscle activity

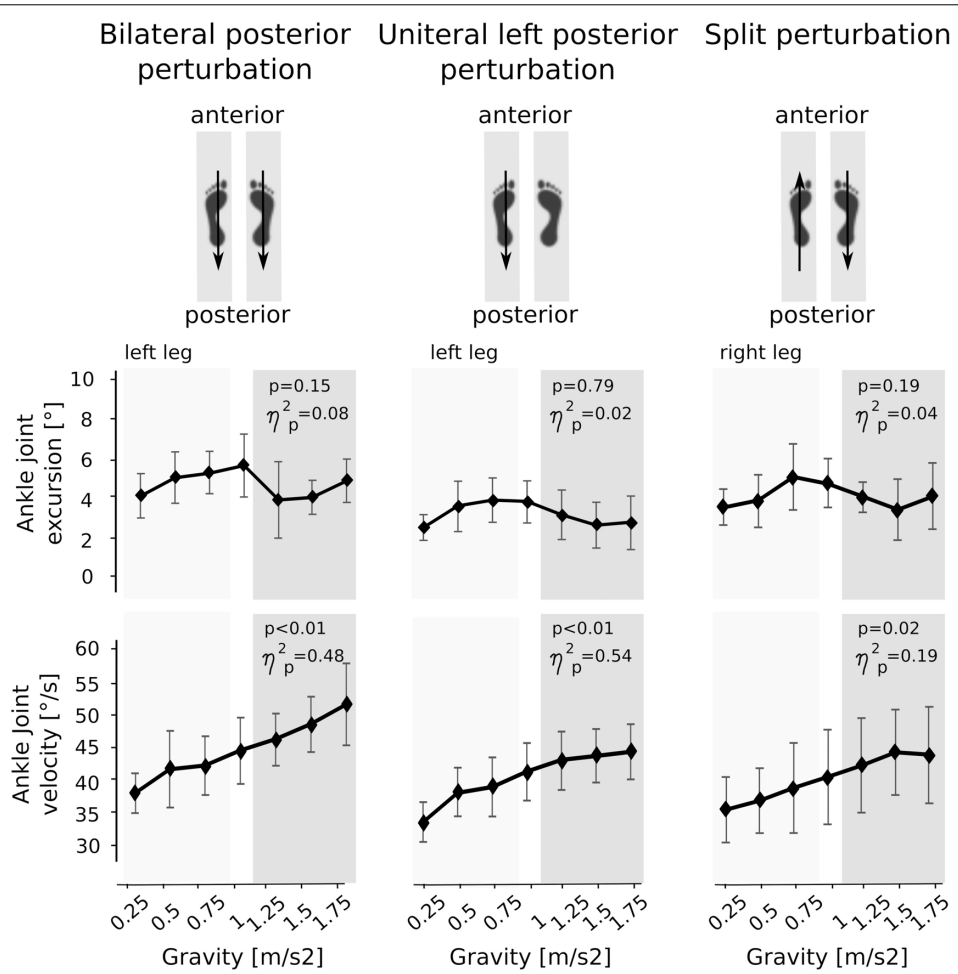

FIGURE 7 | Means of the kinematic parameters for the seven gravity levels that span from hypo- to Earth to hyper-gravity. Adaptation in peak angular excursion of the ankle joint are displayed on the top, while changes in mean angular velocities of the ankle joint are illustrated on the bottom. Whereas angular excursions showed no significant changes over time, the angular velocities progressively increased with increasing gravity. The *p*-value refers to the Friedman Test; η_p^2 displays the effect sizes.

and co-contraction in the lower extremities prior to perturbation in hypo- and hyper-gravity. After perturbation, gradually reduced muscle activation onset latencies and increased neuromuscular activation in the MLR and LLR were manifested with a progressive rise in gravity. Neuro-mechanical adaptations to gravity were more distinct and muscle onset latencies were shorter in the displaced compared to the non-displaced leg. Ankle and knee joint deflections remained unaffected, whereas angular velocities increased with increasing gravitation. Positive correlations were manifested for angular velocities and EMG amplitudes of SOL and GM for the MLR and LLR. Effects were more pronounced in bi- compared to unilateral or split perturbations.

The regulation of human posture in our terrestrial habitat is based on a physiological model (Taube et al., 2008) that involves an accurate coordination of muscle onset and activation patterns between the two legs and their segments (Clement et al., 1984; Dietz et al., 1989a; Rosa, 2015). Slips or stumbles in particular require precise neuronal control of skeletal muscles transmitting the force to the skeleton in order to regain postural equilibrium after its deterioration. At this point, it is important to consider the role of gravity: Counteracting the gravitational force in the vertical plane and compensating for an immediate deterioration of posture control caused by COM shifts in the horizontal plane presupposes an adequate level of activation of the muscle, which may depend on the loading force (**Figure 9**) (Nakazawa et al., 2004; Ritzmann et al., 2015). With reference to gravitational variation, the underlying neuromechanical coupling (Mergner and Rosemeier, 1998) and its proportionality to the ankle joint torque, (Gollhofer et al., 1989) we wish to highlight three major aspects of these concepts:

Timing and Magnitude of Neuromuscular Responses as an Adaptation to Gravity

Our findings indicate that postural perturbations can be counteracted intuitively, appropriate muscle activity can be anticipated, and segmental and COM positioning can

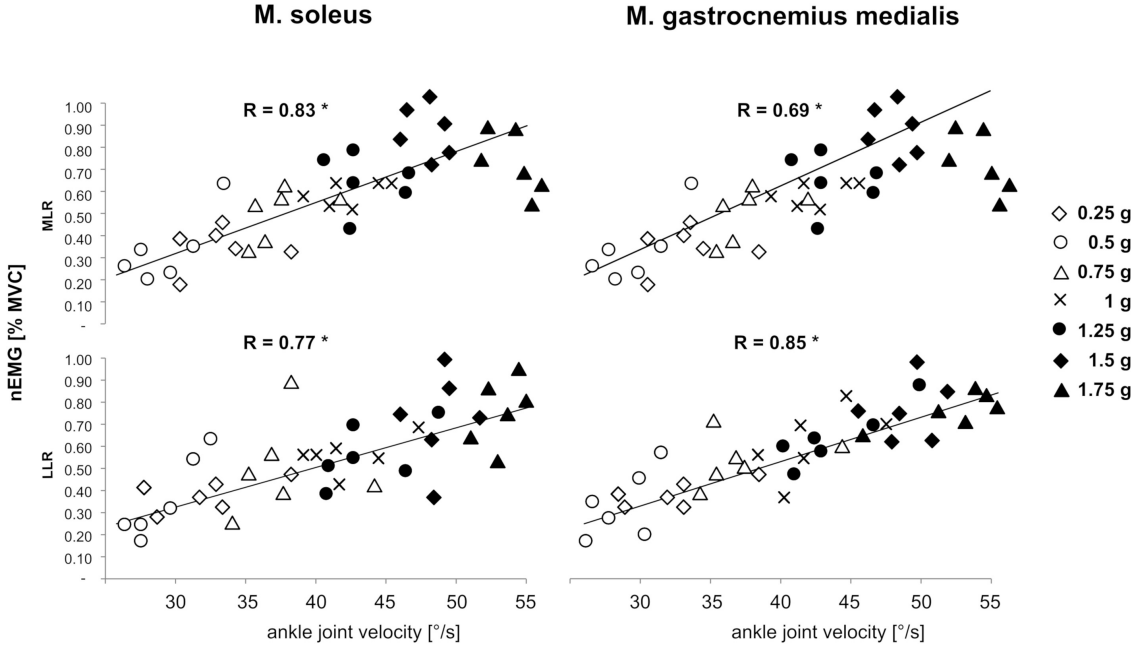

FIGURE 8 | Gravity-dependent bivariate correlations and correlation coefficients among the variable angular velocity of the ankle joint (abscissa) with the normalized EMGs of M. soleus (left leg) and M. gastrocnemius medialis (right leg) in the relevant EMG phases Medium-latency response (MLR, 60–85 ms after perturbation onset) and long-latency response (LLR, 85–120 ms after perturbation onset, ordinate) during left posterior perturbation. Findings revealed that the EMG was positively correlated to ankle joint velocity (* indicate significant findings $p < 0.05$).

be properly adjusted. Subjects adapted their motor control pattern progressively, even though planetary acceleration profiles differ largely between Earth, hyper- and hypo-gravity. With increasing gravity, the EMG amplitudes increased and muscle activation onset latencies diminished. This was true for all muscles counteracting the perturbation, and valid for all types of perturbation modes (**Table 2**) and leg segments, and were independent of muscle function distinguished by flexors or extensors (**Tables 2–4**). The most prominent gravity-induced adaptations were observed in the MLR, which is considered to be governed by supraspinal structures via the brain (Taube et al., 2006) (**Figure 3**). It is assumed that, beyond the massive increase in load, which in turn immediately increases the torques affecting the body, the altered vestibular input results in an excitatory influence exerted by the vestibular organ on muscle and tendon receptors (Lackner and DiZio, 2000). In this context, an increased vestibulo-spinal influence on the excitation of alpha and gamma motoneurons has been shown to be related with the function of the antigravity musculature (Lackner and DiZio, 1993; Kalb and Solomon, 2007). Thus, our physiological model moves functional reflexes into the focus and underlines that the gravity-adjustment under supraspinal control serves as a successful management of posture control preventing falling.

In a few distal muscles, the rise of the neuromuscular activity for MLR and LLR reached saturation and showed an asymptotic behavior or even a minor decline in the highest gravity level (>1.5 g) (**Figure 3**). We expect that this phenomenon could be attributed to neuronal inhibition initiated by supraspinal centers of the CNS (Dietz, 1999; Winters and Crago, 2012; Aagaard, 2018). Extreme gravity levels exceeding 2 g are difficult to tolerate and compensatory motor control in fall-simulations is even more critical in these conditions (**Figure 9**). We can only speculate in terms of the underlying mechanisms that may be found in a segmental shift from distal to proximal body segments, as has been previously reported (Ritzmann et al., 2015).

Neuro-Mechanical Considerations

The positive correlations between muscle activation intensities and the v_{joint} in the ankle emphasizes the neuromechanical coupling which may be determined by gravity (Dietz et al., 1989b; Duysens et al., 2000). As indicated by simulations that utilize the inverted pendulum model to describe the habitual orthograde human posture, ankle joint torque caused by perturbations increased proportional to the gravitational loading (**Figure 9**) (van der Kooij et al., 2005; Bottaro et al., 2008). With reference to the study of Dietz et al. (1989a), it is expected that the neuromuscular responses must increase proportionally to efficiently counteract the perturbation with adequate muscle force. These considerations underline the findings of the current study that highlight an interrelationship between joint mechanics and neuromuscular attributes, and could also be confirmed in experiments using water buoyancy (Dietz et al., 1989b; Minetti et al., 2012b). Within this physiological model, authors postulated the existence of a load receptor system detecting changes in gravity, allowing the integration of this sensory information within the CNS leading to an adequate adjustment of muscle responses and associated joint torques to re-gain a stable posture

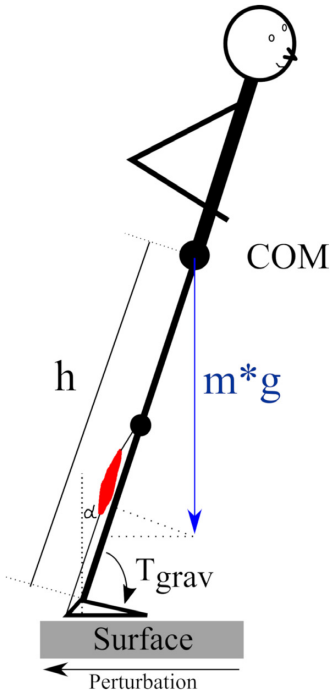

FIGURE 9 | Schematic of the gravity-dependency of the human body in the sagittal plane according to the inverted pendulum model published by van der Kooij et al. (2005) and Bottaro et al. (2008). The pendulum is inclined in the anterior direction due to a translational posterior surface perturbation. The required muscle force of the plantarflexors (red) for a repositioning of the center of mass (COM) above the base of support depends on the body mass (*m*), the COM height (*h*) above the ankle joint and the inclination angle alpha (α) with reference to the vertical. The gravity-dependent ankle joint torque $T_{grav} = m^*g^*h^*\sin(\alpha)$.

after deterioration (Dietz, 1998; Dietz and Duysens, 2000; Bachmann et al., 2008).

Inter-Limb Coordination

Biomechanical models highlight the importance of harmonized inter-limb coordination during perturbed or unperturbed stance (Dietz et al., 1989a) and gait in healthy populations (Russell et al., 2010; Fujiki et al., 2015). It is well in line with previous publications (Dietz et al., 1989a) that leg symmetries were not perfectly synchronous, but showed a small delay in onset latency of approximately 15 ms and slightly diminished amplitudes in the shank musculature (**Figure 5**). The temporal and directional synchronization of activation intensities in both limbs was shown to be paramount in the regulation of the COM within its base of support to safely maintain upright posture in bipedal stance or locomotion (Dietz et al., 1989a; Dietz, 1996; Habib Perez et al., 2016). Changes in gravity may have made the matching of contralateral movement even more important, particularly in conditions in which the subjects were exposed to high gravitation loads (>1 g). For example, unilateral left perturbations directed backward were followed by a bilateral gastrocnemius-EMG response in the left and right leg, and a forward-directed perturbation by a bilateral tibialis anterior-EMG response. However, the first EMG rise in the contralateral non-displaced leg occurred later and was smaller, thus, it may have contributed less to regain a stable posture after deterioration (Dietz et al., 1989a).

Limitation

For a conclusive statement, it is crucial to consider the limitations of the study. Three aspects are of substantial importance; the first one deals with stimulus prediction, the second one with the experimental setting in the parabolic flight and the third one with the generalization of our findings. First, although the perturbation direction, bilateralism and the duration of the pauses have been randomized among the trials (Dietz et al., 1989a), the subjects were aware that a perturbation would come. Despite the unknowledge about the perturbation characteristics, we cannot fully exclude that the subjects pre-activated or co-contracted the muscles in an effort to be prepared for any disturbance of posture control. Second, data collection has been executed during parabolic flight maneuvers. Although the order of the gravity levels has been randomized and the selection criteria for valid attempts and the gravity span have been rigorously pre-defined; parabolic flights are test flights and the time intervals for the data collection are short. They could also include small changes in gravity, which are not existent on the International Space Station. In addition, only a limited number of trials could be collected due to the restricted number of parabolas (Pletser et al., 2012). Third, although our findings highlight adaptability to various gravitation conditions, they cannot be generalized to all types of imposed motion. Besides the wearing of space suits limiting angular excursion in the limb joints (Schmidt, 2001; Gernhardt et al., 2008) and of vision-restricting helmets (Schmidt, 2001), lunar or Martian dust (Gaier, 2018), low friction coefficients (Sperling, 1970; Minetti et al., 2012b) or other surface particularities (Pavei and Minetti, 2016) are likely to impede habitual orthograde stance control on other planets as well.

CONCLUSION

In view of upcoming space missions to the Moon and Mars (Minetti, 2001), the control of posture and locomotion under variable gravitation is paramount. The findings of the current study give a unique insight into neuromuscular regulation of human orthograde stance as a function of gravity. The CNS demonstrated remarkable adaptability to compensate for the sudden deterioration of postural balance among gravity levels spontaneously switching between 0 g and 2 g. This includes the systematic up- and down-regulation of muscle activity and muscle activation onset latencies accompanied by synchronized inter-limb coordination with the success of regaining postural equilibrium in each of the recorded gravity levels.

These results are of functional relevance in view of foreseen interplanetary manned space explorations: first, by integrating habituation sessions in the Astronauts 5-years preparation process and second, by establishing new therapy and space-relevant training modalities addressing particular strategies and adaptations by means of over- or under-loading conditions (Freyler et al., 2014).

ETHICS STATEMENT

All participants gave written informed consent to the experimental procedure, which was in accordance with the latest revision of the Declaration of Helsinki and approved by the French authorities responsible for the protection of subjects participating in biomedical research (DEMEB of the AFSSAPS) as well as the ethics committee of the University of Freiburg (89/12). The participants underwent two obligatory medical investigations and were healthy with no previous neurological irregularities or injuries of the lower extremities. The experiments comply with current German laws and were approved by the local ethics committee.

AUTHOR CONTRIBUTIONS

RR, KF, and AG: conceptualization and funding acquisition. RR, KF, MH, JH, and JK: investigation, methodology, resources, software, and review and editing. RR and KF: project administration. RR and AG: supervision. RR: writing of the original draft and contributed to figures and tables.

FUNDING

This study was funded by the European Space Agency (ESA) and German Aerospace Center (DLR, FKZ 50WB1715). The article processing charge was funded by the German Research Foundation (DFG) and the University of Freiburg in the funding program.

ACKNOWLEDGMENTS

The authors want to thank the ESA and DLR Spaceflight Department, in particular Dr. Katrin Stang, Dr. Jennifer Ngo, Neil Melville-Kenney, and Dr. Hans-Ulrich Hoffmann for the support in parabolic flight experiment preparation.

REFERENCES

Aagaard, P. (2018). Spinal and supraspinal control of motor function during maximal eccentric muscle contraction: effects of resistance training. *J. Sport Health Sci.* 7, 282–293. doi: 10.1016/j.jshs.2018.06.003

Ali, A. A., and Sabbahi, M. A. (2000). H-reflex changes under spinal loading and unloading conditions in normal subjects. *Clin. Neurophysiol.* 111, 664–670. doi: 10.1016/s1388-2457(99)00304-1

Bachmann, V., Müller, R., van Hedel, H. J. A., and Dietz, V. (2008). Vertical perturbations of human gait: organisation and adaptation of leg muscle responses. *Exp. Brain Res.* 186, 123–130. doi: 10.1007/s00221-007-1215-6

Benjamini, Y., and Hochberg, Y. (1995). Controlling the false discovery rate: a practical and powerful approach to multiple testing. *J. R. Stat. Soc. B* 57, 289–300. doi: 10.1111/j.2517-6161.1995.tb02031.x

Benjamini, Y., and Yekutieli, D. (2005). False discovery rate–adjusted multiple confidence intervals for selected parameters. *J. Am. Stat. Assoc.* 100, 71–81. doi: 10.1198/016214504000001907

Berger, W., Quintern, J., and Dietz, V. (1987). Afferent and efferent control of stance and gait: developmental changes in children. *Electroencephalogr. Clin. Neurophysiol.* 66, 244–252. doi: 10.1016/0013-4694(87)90073-3

Borman, P. J., Chatfield, M. J., Damjanov, I., and Jackson, P. (2009). Design and analysis of method equivalence studies. *Ana. Chem.* 81, 9849–9857. doi: 10.1021/ac901945f

Bottaro, A., Yasutake, Y., Nomura, T., Casadio, M., and Morasso, P. (2008). Bounded stability of the quiet standing posture: an intermittent control model. *Hum. Mov. Sci.* 27, 473–495. doi: 10.1016/j.humov.2007.11.005

Clement, G., Gurfinkel, V. S., Lestienne, F., Lipshits, M. I., and Popov, K. E. (1984). Adaptation of postural control to weightlessness. *Exp. Brain. Res.* 57, 61–72.

Cohen, J. (1973). Eta-squared and partial eta-squared in fixed factor anova designs. *Educ. Psychol. Meas.* 33, 107–112. doi: 10.1177/001316447303300111

Dietz, V. (1992). Human neuronal control of automatic functional movements: interaction between central programs and afferent input. *Physiol. Rev.* 72, 33–69. doi: 10.1152/physrev.1992.72.1.33

Dietz, V. (1996). Interaction between central programs and afferent input in the control of posture and locomotion. *J. Biomech.* 29, 841–844. doi: 10.1016/0021-9290(95)00175-1

Dietz, V. (1998). Evidence for a load receptor contribution to the control of posture and locomotion. *Neurosci. Biobehav. Rev.* 22, 495–499. doi: 10.1016/s0149-7634(97)00035-3

Dietz, V. (1999). Supraspinal pathways and the development of muscle-tone dysregulation. *Dev. Med. Child Neurol.* 41, 708–715. doi: 10.1111/j.1469-8749.1999.tb00527.x

Dietz, V., and Berger, W. (1984). Interlimb coordination of posture in patients with spastic paresis. Impaired function of spinal reflexes. *Brain* 107(Pt 3), 965–978. doi: 10.1093/brain/107.3.965

Dietz, V., and Duysens, J. (2000). Significance of load receptor input during locomotion: a review. *Gait Posture* 11, 102–110. doi: 10.1016/s0966-6362(99)00052-1

Dietz, V., Gollhofer, A., Kleiber, M., and Trippel, M. (1992). Regulation of bipedal stance: dependency on "load" receptors. *Exp. Brain Res.* 89, 229–231.

Dietz, V., Horstmann, G. A., and Berger, W. (1989a). Interlimb coordination of leg-muscle activation during perturbation of stance in humans. *J. Neurophysiol.* 62, 680–693. doi: 10.1152/jn.1989.62.3.680

Dietz, V., Horstmann, G. A., Trippel, M., and Gollhofer, A. (1989b). Human postural reflexes and gravity — An under water simulation. *Neurosci. Lett.* 106, 350–355. doi: 10.1016/0304-3940(89)90189-4

Dietz, V., Trippel, M., Discher, M., and Horstmann, G. A. (1991). Compensation of human stance perturbations: selection of the appropriate electromyographic pattern. *Neurosci. Lett.* 126, 71–74. doi: 10.1016/0304-3940(91)90374-3

Duysens, J., Clarac, F., and Cruse, H. (2000). Load-regulating mechanisms in gait and posture: comparative aspects. *Physiol. Rev.* 80, 83–133. doi: 10.1152/physrev.2000.80.1.83

Freyler, K., Weltin, E., Gollhofer, A., and Ritzmann, R. (2014). Improved postural control in response to a 4-week balance training with partially unloaded bodyweight. *Gait Posture* 40, 291–296. doi: 10.1016/j.gaitpost.2014.04.186

Fujiki, S., Aoi, S., Funato, T., Tomita, N., Senda, K., and Tsuchiya, K. (2015). Adaptation mechanism of interlimb coordination in human split-belt treadmill walking through learning of foot contact timing: a robotics study. *J. R. Soc. Interface* 12:0542. doi: 10.1098/rsif.2015.0542

Gaier, J. (2018). *The Effects of Lunar Dust on Advanced EVA Systems: Lessons from Apollo*. Washington, DC: NASA.

Gambelli, C. N., Theisen, D., Willems, P. A., and Schepens, B. (2016). Human motor control of landing from a drop in simulated microgravity. *J. Appl. Physiol.* 121, 760–770. doi: 10.1152/japplphysiol.00305.2016

Gernhardt, M., Jones, J., Scheuring, R., Abercromby, A., Tuxhorn, J., and Norcross, J. (2008). *Risk of Compromised EVA Performance and Crew Health Due to Inadequate EVA Suit Systems*. Houston, TX: NASA's Human Research Program.

Gollhofer, A., Horstmann, G. A., Berger, W., and Dietz, V. (1989). Compensation of translational and rotational perturbations in human posture: stabilization of the centre of gravity. *Neurosci. Lett.* 105, 73–78. doi: 10.1016/0304-3940(89)90014-1

Gollhofer, A., and Rapp, W. (1993). Recovery of stretch reflex responses following mechanical stimulation. *Eur. J. Appl. Physiol. Occup. Physiol.* 66, 415–420. doi: 10.1007/bf00599614

Habib Perez, O., Singer, J. C., and Mochizuki, G. (2016). The effects of predictability on inter-limb postural synchronization prior to bouts of postural instability. *Gait Posture* 46, 167–172. doi: 10.1016/j.gaitpost.2016.03.005

Henry, S. M., Fung, J., and Horak, F. B. (1998). EMG responses to maintain stance during multidirectional surface translations. *J. Neurophysiol.* 80, 1939–1950. doi: 10.1152/jn.1998.80.4.1939

Hermens, H. J., Freriks, B., Disselhorst-Klug, C., and Rau, G. (2000). Development of recommendations for SEMG sensors and sensor placement procedures. *J. Electromyogr. Kinesiol.* 10, 361–374. doi: 10.1016/s1050-6411(00)00027-4

Hobara, H., Kimura, K., Omuro, K., Gomi, K., Muraoka, T., Iso, S., et al. (2008). Determinants of difference in leg stiffness between endurance- and power-trained athletes. *J. Biomech.* 41, 506–514. doi: 10.1016/j.jbiomech.2007.10.014

Hoffrén, M., Ishikawa, M., Rantalainen, T., Avela, J., and Komi, P. V. (2011). Age-related muscle activation profiles and joint stiffness regulation in repetitive hopping. *J. Electromyogr. Kinesiol.* 21, 483–491. doi: 10.1016/j.jelekin.2011.01.009

Honeycutt, C. F., Nardelli, P., Cope, T. C., and Nichols, T. R. (2012). Muscle spindle responses to horizontal support surface perturbation in the anesthetized cat: insights into the role of autogenic feedback in whole body postural control. *J. Neurophysiol.* 108, 1253–1261. doi: 10.1152/jn.00929.2011

Horak, F. B., and Nashner, L. M. (1986). Central programming of postural movements: adaptation to altered support-surface configurations. *J. Neurophysiol.* 55, 1369–1381. doi: 10.1152/jn.1986.55.6.1369

Hwang, S., Jeon, H.-S., Kwon, O.-Y., and Yi, C.-H. (2011). The effects of body weight on the soleus H-reflex modulation during standing. *J. Electromyogr. Kinesiol.* 21, 445–449. doi: 10.1016/j.jelekin.2010.11.002

Jacobs, J. V., and Horak, F. B. (2007). Cortical control of postural responses. *J. Neural. Transm.* 114, 1339–1348. doi: 10.1007/s00702-007-0657-0

Kalb, R., and Solomon, D. (2007). Space exploration, Mars, and the nervous system. *Arch. Neurol.* 64, 485–490. doi: 10.1001/archneur.64.4.485

Lackner, J. R., and DiZio, P. (1993). Multisensory, cognitive, and motor influences on human spatial orientation in weightlessness. *J. Vestib. Res.* 3, 361–372.

Lackner, J. R., and DiZio, P. (2000). Human orientation and movement control in weightless and artificial gravity environments. *Exp. Brain Res.* 130, 2–26. doi: 10.1007/s002210050002

Layne, C. S., Mulavara, A. P., McDonald, P. V., Pruett, C. J., Kozlovskaya, I. B., and Bloomberg, J. J. (2001). Effect of long-duration spaceflight on postural control during self-generated perturbations. *J. Appl. Physiol.* 90, 997–1006. doi: 10.1152/jappl.2001.90.3.997

Lee, I. A., and Preacher, K. J. (2013). *Calculation for the Test of the Difference Between Two Dependent Correlations with One Variable in Common [Computer software]*. Available at: http://quantpsy.org. (accessed November 17, 2018)

Lee, R. G., and Tatton, W. G. (1975). Motor responses to sudden limb displacements in primates with specific CNS lesions and in human patients with motor system disorders. *Can. J. Neurol. Sci.* 2, 285–293. doi: 10.1017/s0317167100020382

Marsden, M., Merton, P., Morton, H., Adam, J., Hallett, M., et al. (1978). "Automatic and voluntary responses to muscle stretch in man," in *Cerebral Motor control in Man: Long Loop Mechanisms*, ed. J. E. Desmedt (Basel: Karger).

Mergner, T., and Rosemeier, T. (1998). Interaction of vestibular, somatosensory and visual signals for postural control and motion perception under terrestrial and microgravity conditions–a conceptual model. *Brain Res. Brain Res. Rev.* 28, 118–135. doi: 10.1016/s0165-0173(98)00032-0

Minetti, A. E. (2001). Walking on other planets. *Nature* 409, 467–469. doi: 10.1038/35054166

Minetti, A. E., Ivanenko, Y. P., Cappellini, G., Dominici, N., and Lacquaniti, F. (2012a). Humans running in place on water at simulated reduced gravity. *PLoS One* 7:e37300. doi: 10.1371/journal.pone.0037300

Minetti, A. E., Pavei, G., and Biancardi, C. M. (2012b). The energetics and mechanics of level and gradient skipping: preliminary results for a potential gait of choice in low gravity environments. *Planet. Space Sci.* 74, 142–145. doi: 10.1016/j.pss.2012.06.004

Miyoshi, T., Nozaki, D., Sekiguchi, H., Kimura, T., Sato, T., Komeda, T., et al. (2003). Somatosensory graviception inhibits soleus H-reflex during erect posture in humans as revealed by parabolic flight experiment. *Exp. Brain Res.* 150, 109–113. doi: 10.1007/s00221-003-1414-8

Nagai, K., Yamada, M., Mori, S., Tanaka, B., Uemura, K., Aoyama, T., et al. (2013). Effect of the muscle coactivation during quiet standing on dynamic postural control in older adults. *Arch. Gerontol. Geriatr.* 56, 129–133. doi: 10.1016/j.archger.2012.08.009

Nakazawa, K., Miyoshi, T., Sekiguchi, H., Nozaki, D., Akai, M., and Yano, H. (2004). Effects of loading and unloading of lower limb joints on the soleus H-reflex in standing humans. *Clin. Neurophysiol.* 115, 1296–1304. doi: 10.1016/j.clinph.2004.01.016

Nashner, L., and Berthoz, A. (1978). Visual contribution to rapid motor responses during postural control. *Brain Res.* 150, 403–407. doi: 10.1016/0006-8993(78)90291-3

Nomura, T., Kawano, F., Ishihara, A., Sato, Y., Mitarai, G., Iwase, S., et al. (2001). Enhanced Hoffman-reflex in human soleus muscle during exposure to microgravity environment. *Neurosci. Lett.* 316, 55–57. doi: 10.1016/s0304-3940(01)02367-9

Pavei, G., and Minetti, A. E. (2016). Hopping locomotion at different gravity: metabolism and mechanics in humans. *J. Appl. Physiol.* 120, 1223–1229. doi: 10.1152/japplphysiol.00839.2015

Phadke, C. P., Wu, S. S., Thompson, F. J., and Behrman, A. L. (2006). Soleus H-reflex modulation in response to change in percentage of leg loading in standing after incomplete spinal cord injury. *Neurosci. Lett.* 403, 6–10. doi: 10.1016/j.neulet.2006.04.058

Pletser, V., Winter, J., Duclos, F., Bret-Dibat, T., Friedrich, U., Francois Clervoy, J., et al. (2012). The first joint european partial-g parabolic flight campaign at moon and mars gravity levels for science and exploration. *Microgravity Sci. Technol.* 24, 383–395. doi: 10.1007/s12217-012-9304-y

Poyhonen, T., and Avela, J. (2002). Effect of head-out water immersion on neuromuscular function of the plantarflexor muscles. *Aviat. Space Environ. Med.* 73, 1215–1218.

Ritzmann, R., Freyler, K., Krause, A., and Gollhofer, A. (2016). No neuromuscular side-effects of scopolamine in sensorimotor control and force-generating capacity among parabolic fliers. *Microgravity Sci. Technol.* 28, 477–490. doi: 10.1007/s12217-016-9504-y

Ritzmann, R., Freyler, K., Weltin, E., Krause, A., and Gollhofer, A. (2015). Load dependency of postural control - kinematic and neuromuscular changes in response to over and under load conditions. *PLoS One* 10:e0128400. doi: 10.1371/journal.pone.0128400

Roelants, M., Verschueren, S. M. P., Delecluse, C., Levin, O., and Stijnen, V. (2006). Whole-body-vibration-induced increase in leg muscle activity during different squat exercises. *J. Strength Cond. Res.* 20, 124–129. doi: 10.1519/R-16674.1

Rosa, M. (2015). Co-contraction role on human control. A neural basis. *J. Nov. Physiother.* 5:248.

Russell, D. M., Kalbach, C. R., Massimini, C. M., and Martinez-Garza, C. (2010). Leg asymmetries and coordination dynamics in walking. *J. Mot. Behav.* 42, 157–168. doi: 10.1080/00222891003697962

Schmidt, P. B. (2001). *An Investigation of Space Suit Mobility with Applications to EVA Operations*. Doctorial Dissertation. Cambridge, MA: Massachusetts Institute of Technology.

Sinkjaer, T., Andersen, J. B., Nielsen, J. F., and Hansen, H. J. (1999). Soleus long-latency stretch reflexes during walking in healthy and spastic humans. *Clin. Neurophysiol.* 110, 951–959. doi: 10.1016/s1388-2457(99)00034-6

Sperling, F. B. (1970). *Technical Memorandum 33-443: Basic and Mechanical Properties of the Lunar Soil Estimated from Surveyor Touchdown Data, no. 19700014154*. Pasadena, CA: California Institute of Technology.

Steiger, J. H. (1980). Tests for comparing elements of a correlation matrix. *Psychol. Bull.* 87, 245–251. doi: 10.1037/0033-2909.87.2.245

Taube, W., Gruber, M., and Gollhofer, A. (2008). Spinal and supraspinal adaptations associated with balance training and their functional relevance. *Acta Physiol.* 193, 101–116. doi: 10.1111/j.1748-1716.2008.01850.x

Taube, W., Schubert, M., Gruber, M., Beck, S., Faist, M., and Gollhofer, A. (2006). Direct corticospinal pathways contribute to neuromuscular control of perturbed stance. *J. Appl. Physiol.* 101, 420–429. doi: 10.1152/japplphysiol.01447.2005

Thornton, W. E., Hedge, V., Coleman, E., Uri, J. J., and Moore, T. P. (1992). Changes in leg volume during microgravity simulation. *Aviat. Space Environ. Med.* 63, 789–794.

Tokuno, C. D., Taube, W., and Cresswell, A. G. (2009). An enhanced level of motor cortical excitability during the control of human standing. *Acta Physiol.* 195, 385–395. doi: 10.1111/j.1748-1716.2008.01898.x

Tucker, M. G., Kavanagh, J. J., Barrett, R. S., and Morrison, S. (2008). Age-related differences in postural reaction time and coordination during voluntary sway movements. *Hum. Mov. Sci.* 27, 728–737. doi: 10.1016/j.humov.2008.03.002

van der Kooij, H., van Asseldonk, E., and van der Helm, F. C. (2005). Comparison of different methods to identify and quantify balance control. *J. Neurosci. Methods* 145, 175–203. doi: 10.1016/j.jneumeth.2005.01.003

White, R. J., and Averner, M. (2001). Humans in space. *Nature* 409, 1115–1118. doi: 10.1038/35059243

Wiley, M. E., and Damiano, D. L. (1998). Lower-extremity strength profiles in spastic cerebral palsy. *Dev. Med. Child Neurol.* 40, 100–107. doi: 10.1111/j.1469-8749.1998.tb15369.x

Winters, J. M., and Crago, P. E. (2012). *Biomechanics and Neural Control of Posture and Movement*. New York, NY: Springer.

Zuur, A. T., Lundbye-Jensen, J., Leukel, C., Taube, W., Grey, M. J., Gollhofer, A., et al. (2010). Contribution of afferent feedback and descending drive to human hopping. *J. Physiol.* 588, 799–807. doi: 10.1113/jphysiol.2009.182709

Conflict of Interest Statement: The authors declare that the research was conducted in the absence of any commercial or financial relationships that could be construed as a potential conflict of interest.

frontiers in Physiology

ORIGINAL RESEARCH
published: 17 June 2019
doi: 10.3389/fphys.2019.00720

Cardiopulmonary Responses to Sub-Maximal Ergometer Exercise in a Hypo-Gravity Analog Using Head-Down Tilt and Head-Up Tilt

Ana Diaz-Artiles[1], Patricia Navarro Tichell[2] and Francisca Perez[2]*

[1] Department of Aerospace Engineering, Texas A&M University, College Station, TX, United States, [2] Sibley School of Mechanical and Aerospace Engineering, Cornell University, Ithaca, NY, United States

After more than 50 years of spaceflight, we still do not know what is the appropriate range of gravity levels that are required to maintain normal physiological function in humans. This research effort aimed to investigate musculoskeletal, cardiovascular, and pulmonary responses between 0 and 1 g. A human experiment was conducted to investigate acute physiological outcomes to simulated altered-gravity with and without ergometer exercise using a head-down tilt (HDT)/head-up tilt (HUT) paradigm. A custom tilting platform was built to simulate multiple gravitational loads in the head-to-toe direction (Gz) by tilting the bed to the appropriate angle. Gravity levels included: Microgravity (−6°HDT), Moon (0.17g-Gz at +9.5°HUT), Mars (0.38g-Gz at +22.3°HUT), and Earth (1g-Gz at +90° upright). Fourteen healthy subjects performed an exercise protocol at each simulated gravity level that consisted of three work rates (50W, 75W, 100W) while maintaining a constant cycling rate of 90 rpm. Multiple cardiopulmonary variables were gathered, including volume of oxygen uptake (VO_2), volume of carbon dioxide output (VCO_2), pulmonary ventilation (V_E), tidal volume (V_T), respiratory rate (R_f), blood pressure, and heart rate (HR) using a portable metabolic system and a brachial blood pressure cuff. Foot forces were also measured continuously during the protocol. Exercise data were analyzed with repeated-measures ANOVA with Bonferroni correction for multiple comparisons, and regression models were fitted to the experimental data to generate dose-response curves as a function of simulated AG-levels and exercise intensity. Posture showed a main effect in all variables except for systolic blood pressure. In particular, VO_2, VCO_2, V_E, V_T, R_f, and HR showed average changes across exercise conditions between Microgravity and 1 g (i.e., per unit of simulated AG) of −97.88 mL/min/g, −95.10 mL/min/g, −3.95 L/min/g, 0.165 L/g, −5.33 breaths/min/g, and 5.05 bpm/g, respectively. In the case of VO_2, further pairwise comparisons did not show significant differences between conditions, which was consistent with previous studies using supine and HDT postures. For all variables (except HR), comparisons between Mars and Earth conditions were not statistically different, suggesting that ergometer exercise at a gravitational stress comparable to Mars gravity (∼3/8 g) could provide similar physiological stimuli as cycling under 1 g on Earth.

Keywords: physiological dose response, artificial gravity, altered gravity, spaceflight countermeasure, head down tilt posture, upright posture

OPEN ACCESS

Edited by:
Hanns-Christian Gunga, Charité – Berlin University of Medicine, Germany

Reviewed by:
Ulrich Limper, Klinikum der Universität Witten/Herdecke, Germany
Tiago Peçanha, University of São Paulo, Brazil

****Correspondence:***
Ana Diaz-Artiles
adartiles@tamu.edu
orcid.org/0000-0002-0459-9327

Specialty section:
This article was submitted to Environmental, Aviation and Space Physiology, a section of the journal Frontiers in Physiology

Received: *08 February 2019*
Accepted: *23 May 2019*
Published: *17 June 2019*

Citation:
Diaz-Artiles A, Navarro Tichell P and Perez F (2019) Cardiopulmonary Responses to Sub-Maximal Ergometer Exercise in a Hypo-Gravity Analog Using Head-Down Tilt and Head-Up Tilt. Front. Physiol. 10:720. doi: 10.3389/fphys.2019.00720

INTRODUCTION

Astronauts on space missions experience various detrimental physiological effects including (but not limited to) muscular atrophy, diminished cardiopulmonary function, and redistribution of internal fluids (Clément, 2005; Buckey, 2006). These changes can lead to orthostatic intolerance (Buckey et al., 1996b; Lee et al., 2015) and diminished exercise capacity (Levine et al., 1996) upon return to a gravitational environment. Currently, crewmembers in the International Space Station (ISS) use a series of countermeasures to attenuate these detrimental effects. For example, astronauts exercise 2.5 h a day (including set-up and cleaning time), 6 days a week, on three different exercise devices: a cycle ergometer, a treadmill, and the advance resistive exercise device (ARED) (Diaz et al., 2015a). Other countermeasures include fluid loading (Clément and Bukley, 2007), and the use of Lower Body Negative Pressure (LBNP) (Charles and Lathers, 1994). Although these countermeasures have greatly diminished the degree of deconditioning experienced during ISS missions (Smith et al., 2012; Moore et al., 2015), especially since the introduction of the ARED, (Smith et al., 2012; Petersen et al., 2016), they still require a significant amount of time and resources. Additionally, the current ISS exercise hardware suite is bulky and most likely, it will not be available in future long duration exploration missions to the Moon, Mars, and beyond due to volume, mass, and power constraints in future exploration vehicles (Ploutz-Snyder et al., 2018). Instead, smaller exercise devices that combine aerobic and resistance exercise capabilities are currently being investigated (Ploutz-Snyder et al., 2018). Thus, new approaches, potentially combining current and novel countermeasures, are likely to be needed for longer space missions in the future, especially on a trip to another planetary surface where there will not be any ground support for astronauts after landing.

Artificial gravity (AG) combined with exercise has been proposed as a multi-system countermeasure that can provide benefits to multiple physiological systems at once (Hargens et al., 2013; Paloski and Charles, 2014; Clément et al., 2016; Clément, 2017). However, the specific parameters and conditions (i.e., gravitational level, intensity, duration) under which this exercise should be ideally performed to be most effective are still unknown. More broadly, there is a lack of fundamental understanding of the relationship between gravity level (i.e., gravitational dose) and physiological response. This relationship, also known as gravitational dose-response curve, will not only contribute to determining physiological responses at Moon and Martian gravity levels, but also the gravity range in which a particular physiological response is closest to "Earth response," and therefore the range of AG that would most likely be effective as a countermeasure (Clément, 2017).

Previous ground-based investigations on cardiopulmonary responses to ergometer exercise in altered-gravity have focused primarily on studying hypergravity conditions (>1 g), especially through the use of small radius centrifuges equipped with cycle ergometers (Bonjour et al., 2010, 2011; Diaz Artiles, 2015; Diaz et al., 2015b; Diaz Artiles et al., 2016; Diaz-Artiles et al., 2018). When hypogravity conditions (<1 g) have been investigated, most studies have been limited to small experiments in actual microgravity conditions during spaceflight that resulted in very few data points, typically less than four subjects, and they only compared 0 to 1 g conditions (Girardis et al., 1999; Trappe et al., 2006; Bonjour et al., 2011). Other studies conducted simulations on Earth that included the use of Lower Body Positive Pressure (LBPP) (Cutuk, 2006; Evans et al., 2013; Schlabs et al., 2013), parabolic flights (Pletser, 2004; Pletser et al., 2012; Widjaja et al., 2015), and head-down tilt (HDT) and head-up-tilt (HUT) paradigms (Lathers et al., 1990, 1993; Louisy et al., 1994; Pavy-Le Traon et al., 1997; Kostas et al., 2014; Baranov et al., 2016). However, few of these hypogravity simulation experiments have studied the effects of exercise (Richter et al., 2017), and those that did focused on walking and running tasks (Cutuk, 2006; Schlabs et al., 2013; Pavei et al., 2015; Pavei and Minetti, 2016), or anaerobic training (Alessandro et al., 2016).

The objective of our research is to investigate and characterize cardiovascular, pulmonary, and musculoskeletal responses (i.e., foot forces) to ergometer exercise in hypogravity conditions (between 0 and 1 g) to fill the gap between those gravitational levels. We conducted a ground-based study on healthy human subjects using a HDT/HUT paradigm to simulate hypogravity conditions on Earth (Clement et al., 2015). Specifically, we investigated the effects of multiple gravity levels (including Microgravity, Moon, Mars, and Earth) by varying posture and exercise intensities to generate gravitational dose-response curves between simulated 0 and 1 g.

EXPERIMENTAL METHODS

Subjects and Study Approval

Fourteen healthy subjects (12 males, 2 females) capable of performing 1 h of cardiovascular exercise were selected to participate in the experiment (mean ± SD, age: 23.5 ± 3.5 years; height: 177.6 ± 8.0 cm; weight: 71.9 ± 7.8 kg). Prior to the experiment, subjects were asked to complete a questionnaire designed to identify exclusion criteria such as cardiopulmonary medical conditions, recent musculoskeletal injuries, or medications that could put subjects at risk or bias the results. Subjects were also instructed to avoid exercising and to abstain from drinking caffeine the morning prior to testing. All subjects were informed about their right to withdraw from the experiment at any point and provided written informed consent to participate. The study was approved by Cornell University's Institutional Review Board for Human Participants (protocol ID #: 1706007254).

Altered-Gravity Exercise Platform Simulator

The Altered-gravity Exercise Platform Simulator (AEPS) is a custom-built platform designed to perform cycling ergometer exercise in multiple, simulated gravitational environments. Using HDT and HUT positions, the AEPS can replicate known gravity-induced fluid shifts based on appropriate tilt angles. Thus, the platform is capable of providing a −6° HDT, a +9.5° HUT, a +22.3° HUT, and a +90° upright orientation, corresponding

to Microgravity, Moon, Mars, and Earth gravitational conditions, respectively (Clement et al., 2015). In the reclined positions (i.e., Microgravity, Moon, and Mars), subjects laid on the platform and handlebars were positioned laterally on either side, to help them avoid sliding down. The handlebars had five different configurations in order to be adjustable for the subjects' anthropometric needs. In the upright position, subjects sat on a bike seat with handlebars positioned in front of them as on a standard bike. The platform also incorporated an ergometer device (Lode BV, Groningen, Netherlands) for subjects to perform cycling exercise while exposed to the different postures (see **Figure 1**). If needed, the cycle ergometer was slightly adjusted to accommodate anthropometric differences between subjects.

Experimental Design

A within-subject experimental design was implemented to determine the effects of artificial gravity (AG) level and exercise work rates (WR) on cardiopulmonary and musculoskeletal responses. The AG levels tested were: Microgravity (−6° HDT), Moon (+9.5° HUT), Mars (+22.3° HUT), and Earth (+90° upright). The exercise intensities tested were: 50, 75, and 100W. Every subject experienced every combination of WR and AG level (i.e., within-subject design). Each subject participated in four sessions scheduled on different days within the same week. The experimental sessions were always performed in the morning approximately at the same time to avoid possible confounding circadian effects that could influence the results. In each of the four sessions, subjects performed the same exercise protocol in a different posture. Earth configuration (i.e., upright) was always tested first in order to allow subjects to get familiar with the exercise protocol and testing equipment. Then, a counterbalanced design was used for the following three test sessions (i.e., Microgravity, Moon, Mars), meaning that subjects experienced these three AG levels in a different order to counteract potential carryover effects.

Instrumentation and Data Collection

Volume of oxygen uptake (VO_2, mL/min), volume of carbon dioxide output (VCO_2, mL/min), pulmonary ventilation (V_E, L/min), tidal volume (V_T, ml), and respiratory rate (R_f, breaths/min) were recorded continuously throughout the experiment sessions using the K4b2 portable gas analyzer (Cosmed, Srl – Italy). Prior to testing, the K4b2 main unit was

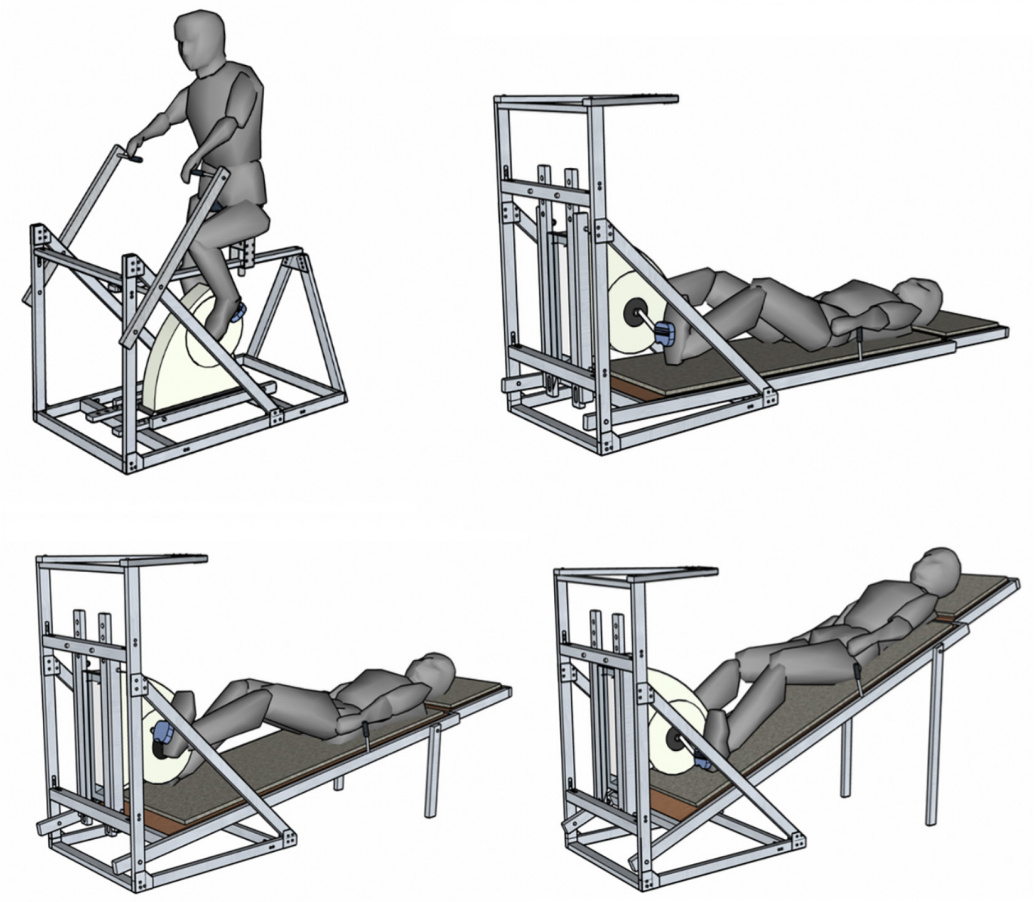

FIGURE 1 | The Altered-gravity Exercise Platform Simulator in upright-Earth configuration (upper left), −6° HDT-Microgravity configuration (upper right), +9.5° HUT-Moon configuration (bottom left), and +22.3° HUT-Mars configuration (bottom right).

warmed-up for a minimum of 45 min as instructed in the system manual. The gas analyzer was calibrated before each test using a reference gas mixture (CO_2: 5%, O_2: 16%; Cosmed, Srl-Italy) and the turbine was calibrated once a week with a 3000-ml syringe. The Cosmed K4b2 equipment also measured continuous heart rate data (HR) using a Polar Heart Rate monitor. Blood pressure measurements were taken every 2 min during the entire protocol using an automated brachial blood pressure (BP) monitor connected to the cycle ergometer and controlled by the Lode Ergometer Manager, Version 9.4.4 (LEM, 2013, Groningen, Netherlands) software package. Although subjects were supporting themselves via the handlebars, we asked them to relax their arm while blood pressure measurements were being taken. In addition to BP, other exercise parameters such as pedaling cadence and workload intensity were continuously measured and recorded. Additionally, foot-force data were also collected using force-plates (Vernier Software & Technology) mounted on the ergometer pedals. These sensors measured forces between −850 and +3500 N with a resolution of 1.2 N, where positive force values correspond to compression forces and negative force values correspond to traction forces. The force plates were calibrated before each experimental session. Finally, an exit survey was conducted to collect subjective data about the subjects' experience during the exercise protocol. Questions included comfort and difficulty of exercise using a 10-point Likert scale (Comfort: 1 = very uncomfortable/ unnatural, 10 = very comfortable/ natural; Strenuousness: 1 = easy, 10 = very strenuous), as well as potential causes contributing to them. Subjects were also asked to report any muscle soreness or discomfort resulting from the platform orientation.

Exercise Protocol

The exercise protocol implemented in all experimental sessions is shown in **Figure 2**. Each exercise session began with a 5-min resting period in the seated position in order to obtain a physiological baseline at rest. After this first period, subjects were positioned on the platform (or sat on the bike upright for Earth configuration) and were required to rest for seven additional minutes to capture their physiological baseline in the new experimental condition. Subjects then executed the exercise portion of the testing protocol, which consisted of three different workload stages of 50W ("warm-up"), 75W ("low" intensity), and 100W ("high" intensity). All exercise stages were 7-min long. To facilitate transition between work rates and to avoid potential injuries, 30-s transition periods between stages were also included. After the exercise period, an additional 7-min resting period was included to allow subjects to partially recover from the exercise. The exercise protocol was created using the Lode Ergometer Manager, Version 9.4.4 (LEM, 2013, Groningen, Netherlands) software package provided with the ergometer, and it ran automatically without intervention from the operator. Subjects were instructed to pedal at 1.5 Hz (i.e., 90 rpm) using a metronome to avoid additional confounding factors. During the entire protocol subjects were instructed to avoid talking and making unnecessary movements that could affect data collection. Additionally, an early termination protocol was in place to ensure the safety of the subjects throughout the experiment. Termination criteria included an increase in heart rate $>0.8^*$(220- Subject Age), an increase in diastolic blood pressure >20 mmHg with respect to seated baseline measurements, and systolic blood pressure >230 mmHg.

Data and Statistical Analysis

Breath-by-breath pulmonary variables (VO_2, VCO_2, V_E, V_T, R_f) were averaged over 5-s intervals, and outliers were removed using a Hampel filter (Pearson et al., 2016). In addition, a 5th order median filter was also applied to reduce noise of the signals. Each of these variables and the heart rate data

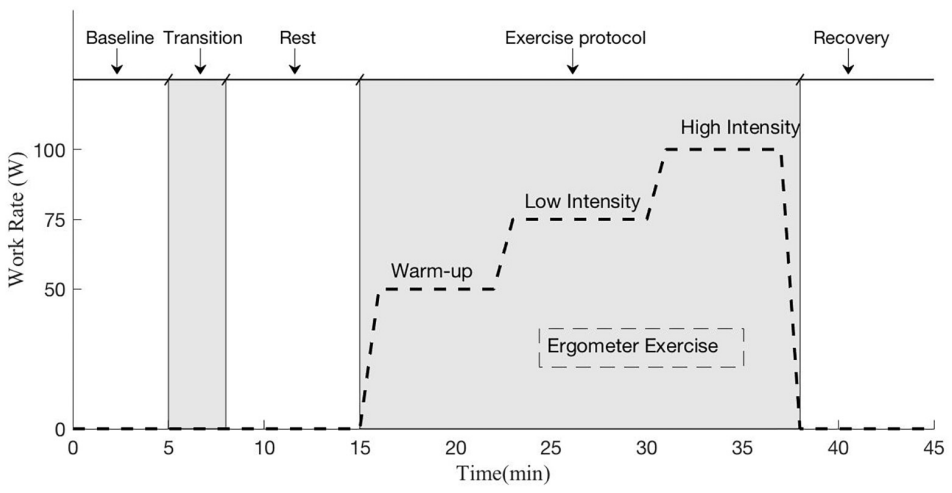

FIGURE 2 | Exercise protocol implemented during each experimental session. The protocol included a baseline session in seated position (5 min), a transition period to position the subject in the desired testing configuration (Microgravity −6° HDT, Moon +9.5° HUT, Mars +22.3° HUT, Earth +90° upright), another period at rest to capture the new baseline in the new gravitational configuration (7 min), the ergometer exercise period (23 min including work rate transitions), and a final recovery period (7 min).

(VO_2, VCO_2, V_E, V_T, R_f, HR), which were collected continuously, were averaged over the last 2 min of each protocol phase, yielding five values per variable, per subject, at each AG configuration. Blood pressure data, which were collected every 2 min, were averaged using the last two values obtained in each protocol phase. Thus, for each posture, we generated averages corresponding to the seated baseline period (BL), at rest (Rest, no exercise in the AG environment of interest), 50, 75, and 100W. To study the effect of postural changes, paired, two-sided *t*-tests were used to compare all cardiopulmonary (CP) variables at BL with Rest at the AG condition being studied. To study the effects of exercise at different postures, a two-way repeated measures ANOVA was implemented using AG-level (Microgravity, Moon, Mars, Earth), and workload intensity (50W, 75W, 100W) as fixed factors. The necessary assumptions including normality, homoscedasticity, and absence of outliers were checked prior to any testing, and the Greenhouse-Geisser correction was applied when the data violated the sphericity assumption (Salkind et al., 2010). Pairwise comparisons were also calculated using the Bonferroni *post hoc* correction.

A quadratic mixed regression model was used to generate dose-response curves between 0 and 1 g for the pulmonary variables measured:

$$y_{ij} = \beta_0 + \beta_1^* AG^2 + \beta_2^* AG + \beta_3^* WR^2 + \beta_4^* WR + \beta_5^* AG^* WR + u_i + \varepsilon_{ij}$$

where y_{ij} represents the response of the variable measured for the subject i (i = 1:14) in the condition j (j = 1:16, combinations of the 4 AG levels and the 4 WR exercise intensities: 0, 50, 75, and 100W). The terms β represent the fixed effects coefficients, with β_0 being the intercept. The term u_i represents the random effects associated with each subject and the within-subject design. When necessary, we used the Akaike Information Criteria (AIC) to select between different regression models (Akaike, 1974). The AIC is a technique for model selection based on information theory that provides a quantitative way to estimate the quality of a model fit. The preferred model is the one that has minimum AIC among all the other models.

Maximum and minimum peak force values for the right and left foot were calculated as the average of the individual maximum and minimum peak forces for each exercise work rate at each of the simulated altered-gravity configuration, following the same methodology reported in a previous publication (Diaz et al., 2015b). Transitions between stages were not included. Data from two subjects were discarded due to problems with the foot sensors and thus, only twelve subjects were considered. A two-way repeated-measures ANOVA and *post hoc* pairwise comparison with Bonferroni correction were conducted to investigate the influence of altered-gravity and workload intensity. AG-levels considered in this study were Microgravity, Moon, and Mars. Earth configuration was not included due to the differences in body position and pedaling strategy between the reclined positions on the platform (i.e., Microgravity, Moon, Mars) and the Earth position, where subjects were seated on a bike saddle. These differences could lead to changes in inertial forces or pedaling effectiveness not caused by changes in the gravitational environment but changes in pedaling configuration, therefore confounding final results. Paired two-sided *t*-tests were used instead to compare Earth results with reclined positions (i.e., Microgravity, Moon, and Mars). Finally, a non-parametric Friedman's test was implemented to compare the results of comfort and strenuousness in the different postures. All statistical tests were performed with IBM SPSS Statistics 25 software (IBM Corporation) and the significance level was set at $\alpha = 0.05$.

RESULTS

All subjects tested were able to successfully complete the exercise protocol except for one subject, who exceeded the maximum blood pressure criteria and thus, the testing session was terminated immediately. The subject was completely excluded from the study (i.e., subject not included in the cohort of 14 subjects analyzed), and therefore any related data have not been included in the results reported in this manuscript.

Continuous responses from the cardiopulmonary variables during the different testing configurations are shown in **Figure 3**. Each graph contains the average cardiopulmonary responses of all 14 subjects (SE not shown for clarity) at each one of the four altered-gravity scenarios investigated (Microgravity −6° HDT, Moon +9.5° HUT, Mars +22.3° HUT, Earth +90° upright). **Figure 3** also shows the average systolic and diastolic blood pressure (measurements taken every 2 min) of all 14 subjects during the exercise protocol for all four conditions.

After the 5-min baseline period, a rise in HR can be observed corresponding to the transition between the seated position and the required position according to the altered-gravity level being studied. During the exercise period, HR increased proportionally with the workload intensity as expected. VO2, VCO2 and VE responses showed a similar pattern along the exercise protocol. Abrupt increases can be observed in each transition between different workload levels followed by the establishment of a new relatively steady state in order to meet the new oxygen demand of the body. In contrast, V_T and R_f showed much more noisy behavior. V_T increased after every change in work rate but instead of staying constant, it showed a tendency to decrease. This phenomenon was compensated by the R_f, which increased during the entire duration of every work rate period. Despite the higher variability, both V_T and R_f seemed to work closely together to maintain V_E at the adequate levels.

Changes in Posture

Calculated averages for the six cardiopulmonary variables (VO_2, VCO_2, V_E, V_T, R_f, HR) and blood pressure measurements (SBP, DBP) for the seated baseline (BL) condition, and at rest (Rest) on the platform at the different simulated altered-gravity environments are summarized in **Figure 4**. Paired, two-sided *t*-tests revealed the expected significant differences in HR between seated position (BL) and all four postural conditions investigated. Thus, with respect to BL, HR decreased in all hypogravity conditions (Microgravity, Moon, Mars) where the Gz hydrostatic column is reduced, increasing central ventricular filling pressure and ventricular end-diastolic volumes

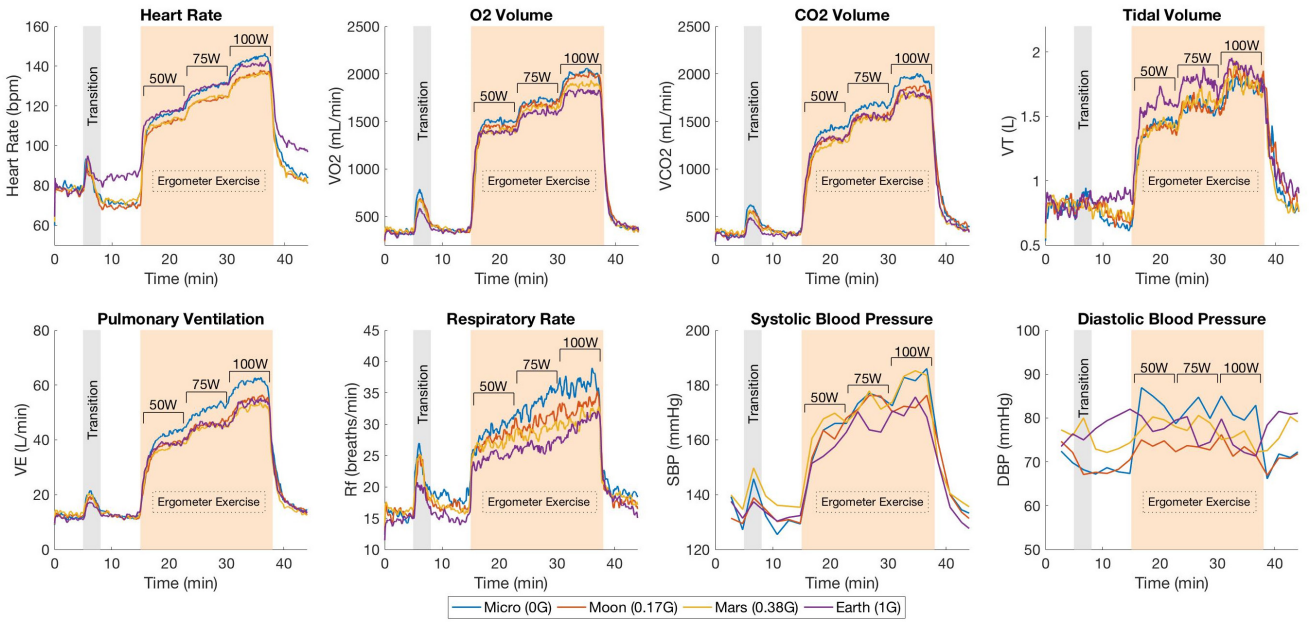

FIGURE 3 | Mean cardiopulmonary responses from 14 subjects during the exercise protocol under the different altered-gravity environments (Microgravity −6° HDT, Moon +9.5° HUT, Mars +22.3° HUT, Earth +90° upright). The protocol includes a baseline period in the upright seated position (5 min), a transition period for the subject to get positioned in the desired testing configuration (Microgravity, Moon, Mars, or Earth), another period at rest to capture the new baseline in the new gravitational configuration (7 min), the exercise phase with three workload intensities (23 min including work rate transitions), and a final recovery period (7 min). Systolic and diastolic blood pressure measurements were collected every 2 min and not continuously as the rest of the variables.

(Nixon et al., 1979; Gaffney et al., 1985). However, it increased in the Earth condition due to the higher gravitational and muscular stresses that result from subjects' exposure to 1 g while positioned on the exercise platform. VO_2, VCO_2, V_T, V_E, and DBP also significantly increased with respect to BL in the Earth configuration. Additionally, we observed significant changes in VCO_2, V_T, and R_f in the Microgravity condition with respect to the seated baseline. With regards to blood pressure, SBP remained fairly constant (i.e., no significant differences were observed) but DBP decreased significantly in Moon and Mars conditions due to vasodilatation, whereas it increased in Earth configuration due to vasoconstriction. DBP also decreased in Microgravity conditions but differences were not statistically significant. For completeness, we also calculated the respiratory exchange ratio ($RER = VCO_2/VO_2$), reported in **Table 1**, and paired two-sided *t*-tests results showed no significant differences between BL and Rest in any of the AG conditions.

Altered-Gravity and Exercise

Calculated averages for all variables measured during the different workload intensities of the exercise period are shown in **Figure 5**. Two-way repeated-measures ANOVAs revealed no significant interaction between AG and WR for all variables studied. Further analysis yielded significant main effects of AG-level on all variables except SBP {HR [$F(1.641,21.337) = 6.148$, $p = 0.011$], VO_2 [$F(3,39) = 5.838$, $p = 0.002$], VCO_2 [$F(3,39) = 6.108$, $p = 0.002$], V_T [$F(3,39) = 5.546$, $p = 0.003$], V_E [$F(3,39) = 10.514$, $p < 0.0005$], R_f [$F(3,39) = 15.088$, $p < 0.0005$], SBP [$F(3,27) = 2.315$, $p = 0.098$], and DBP [$F(3,27) = 5.333$, $p = 0.005$]}. Thus, our results showed that, when exercising, VO_2, VCO_2, V_E, and R_f significantly decreased with higher levels of simulated gravity while V_T and HR (except in the Microgravity condition) increased with higher gravitational stress in the Gz direction. **Figure 5** also indicates *post hoc* pairwise comparisons, yielding significant differences between Microgravity and Moon on HR, VCO_2, V_E, R_f, and DBP; between Microgravity and Mars on VCO_2, V_E, and R_f; between Moon and Earth on V_T and R_f, and between Microgravity and Earth on V_E, and R_f. A similar analysis on RER, shown in **Table 1**, revealed significant main effects of AG-level {RER [$F(3,39) = 8.396$, $p < 0.0005$]}, followed by significant *post hoc* pairwise comparisons between Microgravity and Moon, and between Microgravity and Mars. No significant differences were found between Mars and Earth conditions except for HR.

Workload intensity was found to be a significant factor in all variables except for DBP {HR [$F(1.228,15.96) = 281.1$, $p < 0.0005$], VO_2 [$F(1.169,15.195) = 509.6$, $p < 0.0005$], VCO_2 [$F(1.402,18.221) = 364.2$, $p < 0.0005$], V_T [$F(2,26) = 31.5$, $p < 0.0005$], V_E [$F(2,26) = 220.4$, $p < 0.0005$], R_f [$F(1.313,17.063) = 24.778$, $p < 0.0005$], SBP [$F(2,18) = 35.495$, $p < 0.0005$], and DBP [$F(2,18) = 0.919$, $p = 0.417$]}. For all variables where WR was a significant factor (i.e., all except DBP), WR pairwise comparisons were also found to be statistically significant in all group combinations with no exception. Finally,

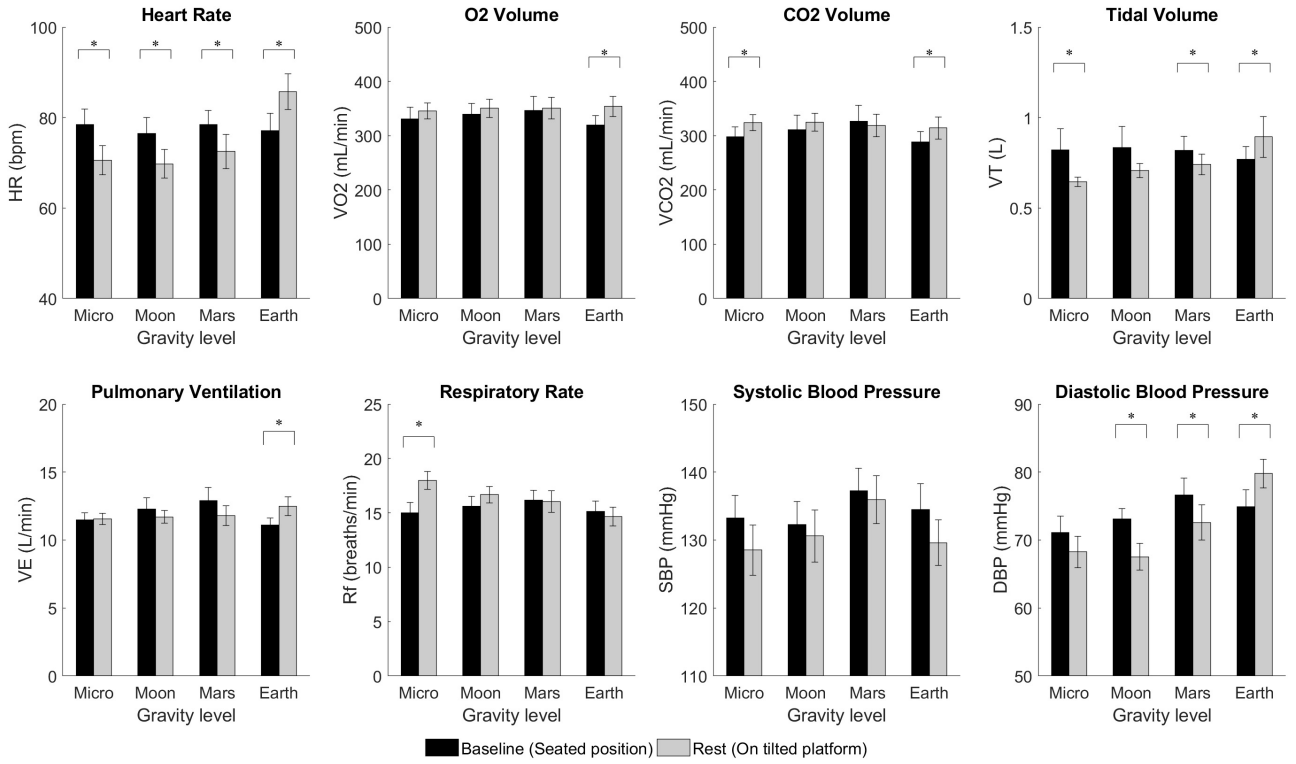

FIGURE 4 | Cardiopulmonary variables from 14 subjects (mean ± SE) at baseline (BL, seated) and at rest (on the platform) for the different altered-gravity environments (Microgravity −6° HDT, Moon +9.5° HUT, Mars +22.3° HUT, Earth +90° upright). The figure highlights significant differences between BL and Rest due to changes in posture (paired *t*-test *significantly different at $p < 0.05$).

TABLE 1 | Respiratory exchange ratio (**RER=VCO_2 /VO_2**) averages [mean (SE), including all 14 subjects] during baseline (BL, seated position), at Rest on the platform, and at each work rate of the exercise protocol (50W, 75W, 100W) at the different simulated altered-gravity positions (Microgravity −6° HDT, Moon +9.5° HUT, Mars +22.3° HUT, Earth +90° upright).

RER	Microgravity −6° HDT	Moon +9.5° HUT	Mars +22.3° HUT	Earth +90° upright
BL	0.91 (0.03)	0.91 (0.03)	0.93 (0.02)	0.90 (0.02)
Rest	0.94 (0.02)	0.93 (0.02)	0.91 (0.02)	0.88 (0.02)
50W	0.96 (0.01)	0.91 (0.01)	0.92 (0.01)	0.95 (0.01)
75W	0.97 (0.01)	0.92 (0.01)	0.93 (0.01)	0.97 (0.01)
100W	0.97 (0.01)	0.93 (0.01)	0.93 (0.01)	0.98 (0.01)

concerning RER, work rate was found to be a significant factor {RER [$F(2,26) = 4.936$, $p = 0.015$}. However, when tested for pairwise comparisons we did not find significant differences between conditions.

Dose-Response Curves

The regression model coefficients applied to the cardiopulmonary data are provided in **Table 2**, and the statistical models fitted to the experimental data are shown in **Figure 6**. Only statistically significant coefficients were included in the regressions, and further interaction terms (not shown) were not significant. Similar to previous gravitational dose-response curves under orthostatic stress generated by short-radius centrifugation (Diaz-Artiles et al., 2018), results show that AG level contributes to changes in all variables, either directly (β_1 and β_2) or through the interaction term (β_5). **Figure 6** shows that generally HR and V_T increase with AG, especially between Moon and Earth condition, while VO_2, VCO_2, V_E, and R_f decrease with gravity level. As expected, workload intensity also has a prominent role in the regressions, as shown by the significant terms β_3 and β_4 in all variables. The positive nature of coefficient β_4 indicates that all variables increase with workload intensity, and the negative coefficient β_3 indicates that this increase becomes less important at higher work rates. Systolic and diastolic blood pressure dose-response curves were not included in this analysis due to poor fitting when generating the models. Blood pressure is the "regulated variable" and experimental data did not show a consistent behavior when changing postures as the other variables did. Thus, within the limits of our testing conditions, we were unable to generate appropriate dose-response curves for neither systolic nor diastolic blood pressure.

Foot Forces

Calculated averages for minimum and maximum right and left foot forces during the different workload intensities of the exercise period at the different simulated altered-gravity environments are shown in **Table 3**. No significant differences were found between right and left foot forces (between subjects'

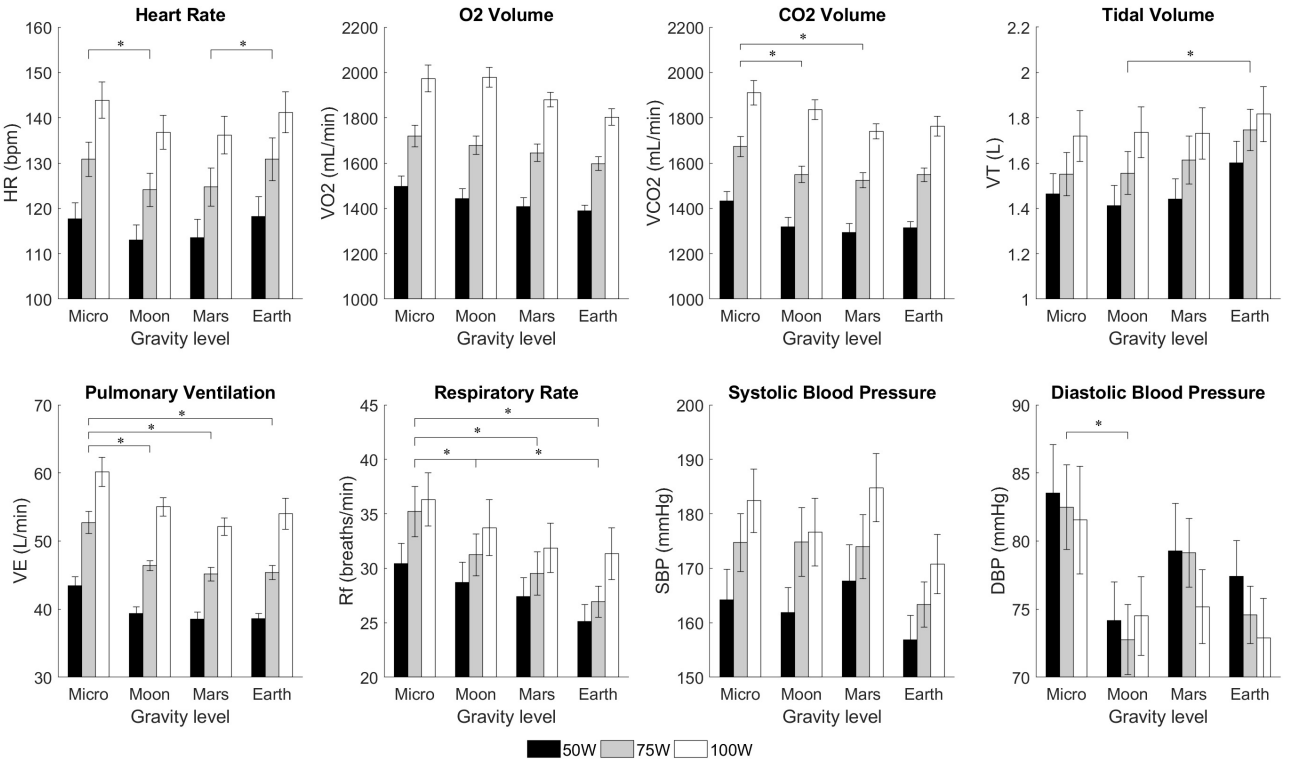

FIGURE 5 | Cardiopulmonary variables from 14 subjects (mean ± SE) at different workload intensities for each of the altered-gravity environments (Microgravity −6° HDT, Moon +9.5° HUT, Mars +22.3° HUT, Earth +90° upright). The figure highlights significant differences between altered-gravity levels (pairwise comparisons after a 2-factor repeated measures ANOVA with Bonferroni correction, *significantly different at $p < 0.05$). Statistical differences between workload intensities, including all possible pairwise comparisons, were also found in all variables except diastolic blood pressure. For clarity, these differences are not shown in the figure.

TABLE 2 | Regression coefficients for cardiopulmonary variables based on the following equation: $y_{ij} = \beta_0 + \beta_1^* AG^2 + \beta_2^* AG + \beta_3^* WR^2 + \beta_4^* WR + \beta_5^* AG^* WR + u_i + \varepsilon_{ij}$.

	β_0	β_1	β_2	β_3	β_4	β_5
HR (bpm)	70.29	15.46	NS	−0.003	1.025	−0.185
VO_2 (ml/min)	356.59	NS	NS	−0.109	26.93	−1.74
VCO_2 (ml/min)	370.78	347.71	−380.93	−0.099	25.07	−1.10
T_V (l)	0.702	0.165	NS	-8.42×10^{-5}	0.018	NS
V_E (l/min)	13.72	15.63	−16.27	−0.002	0.680	−0.059
R_f (min^{-1})	19.17	7.74	−13.07	−0.001	0.282	NS

*Only significant coefficients were included in the regression ($p < 0.05$). **Figure 6** shows the regression models fitted to the experimental data. Abbreviations: NS, non-significant; AG, artificial gravity (g); WR, work rate (W); HR, heart rate (beats per minute); VO_2, volume of oxygen uptake (mL/min); VCO_2, volume of carbon dioxide output (mL/min); V_E, pulmonary ventilation (L/min); V_T, tidal volume (mL); R_f, respiratory rate (breaths/min).*

effect two-way repeated measures ANOVA; for maximum foot forces: $F(1,22) = 0.008$, $p = 0.927$; for minimum foot forces: $F(1,22) = 0.269$, $p = 0.609$). Consequently, both feet were analyzed together.

Maximum foot forces were all positive and therefore compression forces, and they are indicated in **Figure 7**. Statistical analysis showed a significant increase with workload intensity [$F(1.288, 29.625) = 46.534$, $p < 0.0005$] and simulated altered-gravity [$F(1.583, 36.405) = 204.137$, $p < 0.0055$]. Pairwise comparisons revealed significant differences between all work rates ($p < 0.0005$) and all altered-gravity conditions ($p < 0.0005$). Additionally, when compared to Earth's values (paired, two-sided *t*-test), maximum foot forces were statistically different in Microgravity (all work rates, $p < 0.0005$), Moon (all work rates $p < 0.0005$), and Mars at 100W ($p < 0.014$).

Minimum foot forces were both negative (in the Microgravity configuration) and positive (in the rest of configurations). Thus, minimum foot forces in Microgravity were traction forces, while in the rest of configurations they were compression forces (see **Figure 7**). A two-way repeated-measures ANOVA showed a significant increase in minimum foot forces with altered-gravity [$F(1.407, 34.045) = 45.985$, $p < 0.0005$] and a significant decrease with workload intensity [$F(1.443, 33.19) = 16.055$, $p < 0.0005$]. Pairwise comparisons yielded statistically significant

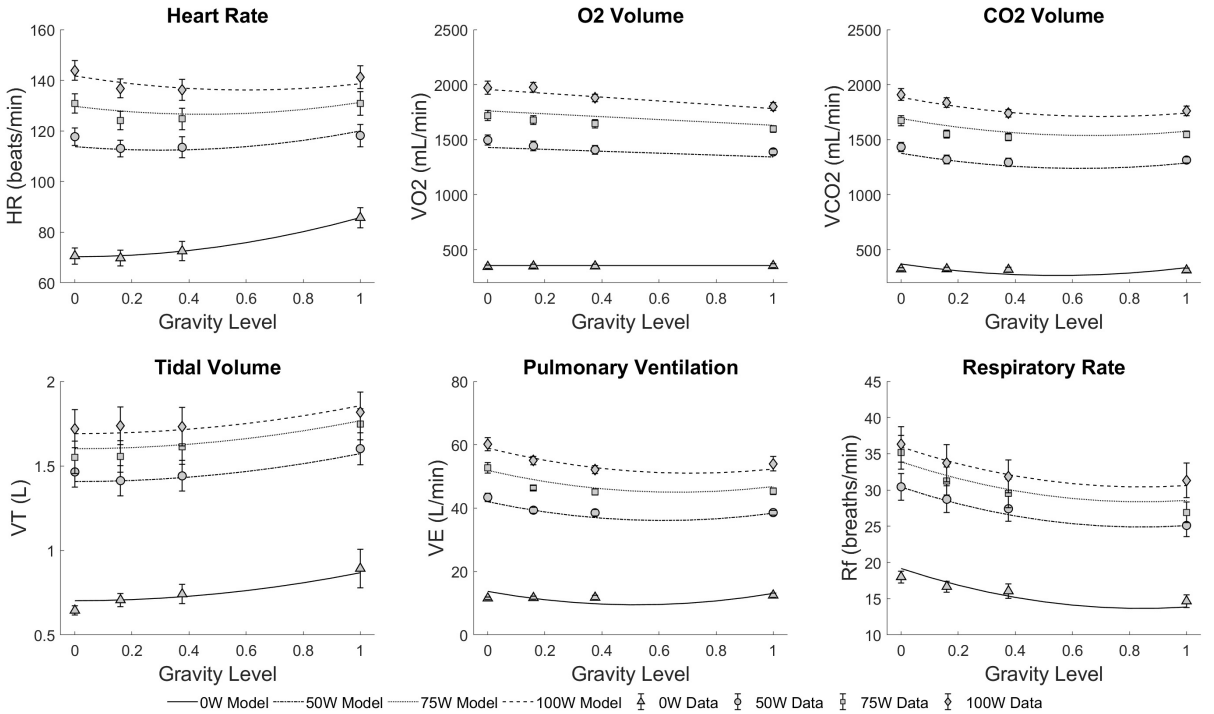

FIGURE 6 | Statistically significant regression models fitted to the cardiopulmonary experimental data across all conditions: four altered-gravity levels (Microgravity −6° HDT, Moon +9.5° HUT, Mars +22.3° HUT, Earth +90° upright) and four workload intensities (0, 50, 75, and 100W). Symbols and error bars correspond to experimental data from 14 subjects (mean ± SE) at each condition.

TABLE 3 | Calculated minimum and maximum foot force averages [mean (SE), including 12 subjects] during each work rate of the exercise protocol (50W, 75W, 100W) at the different simulated altered-gravity positions (Microgravity −6° HDT, Moon +9.5° HUT, Mars +22.3° HUT, Earth +90° upright).

		Right Foot (N)		Left Foot (N)	
		Maximum	**Minimum**	**Maximum**	**Minimum**
Microgravity −6° HDT	50W	89.63 (6.71)	−1.49 (7.23)	94.94 (7.64)	−0.11 (5.78)
	75W	94.66 (6.77)	−5.16 (8.32)	98.44 (7.72)	−7.30 (5.60)
	100W	105.42 (6.59)	−6.42 (10.26)	106.46 (6.90)	−6.91 (6.48)
Moon +9.5° HUT	50W	125.36 (5.71)	28.90 (4.72)	125.12 (6.42)	23.75 (4.70)
	75W	141.08 (6.14)	26.84 (5.58)	136.54 (7.07)	18.18 (4.65)
	100W	150.44 (7.54)	22.79 (6.72)	144.74 (8.19)	16.88 (4.54)
Mars +22.3° HUT	50W	153.07 (8.64)	41.77 (6.52)	149.60 (9.64)	36.89 (4.70)
	75W	162.27 (9.33)	34.88 (8.05)	160.61 (10.66)	29.31 (6.68)
	100W	170.19 (8.05)	31.54 (8.65)	167.21 (10.39)	27.67 (6.67)
Earth +90° upright	50W	147.61 (8.24)	53.09 (6.01)	152.44 (10.71)	49.50 (4.69)
	75W	167.33 (8.88)	51.63 (7.20)	169.96 (11.47)	46.67 (6.12)
	100W	185.42 (9.01)	55.22 (7.23)	186.96 (10.63)	53.20 (5.24)

differences between all altered-gravity conditions: Microgravity and Moon ($p < 0.0005$), Microgravity and Mars ($p < 0.0005$), and Moon and Mars ($p = 0.007$). Work rate pairwise comparisons showed statistically significant differences between 50W and 75W ($p < 0.005$), and 50W and 100W ($p < 0.0005$). Additionally, when compared to Earth's values (paired, two-sided t-test), minimum foot forces were statistically different in Microgravity (all work rates $p < 0.0005$), Moon (all work rates $p < 0.0005$), and Mars (50W: $p = 0.004$; 75W and 100W $p < 0.0005$).

Subjective Data

Subjective data related to "comfort" and "strenuousness" (or difficulty of exercise) are summarized in **Table 4**. Results show a significant increase in comfort level with increased AG [χ^2 (3) = 23.59, $p < 0.0005$]. Earth was reported as the most natural position with few discomfort issues, mainly related with the bike saddle. In reclined configurations, main causes of discomfort were pressure in the lower back and use of handlebars to avoid sliding. Some cases of numbness in the feet were also

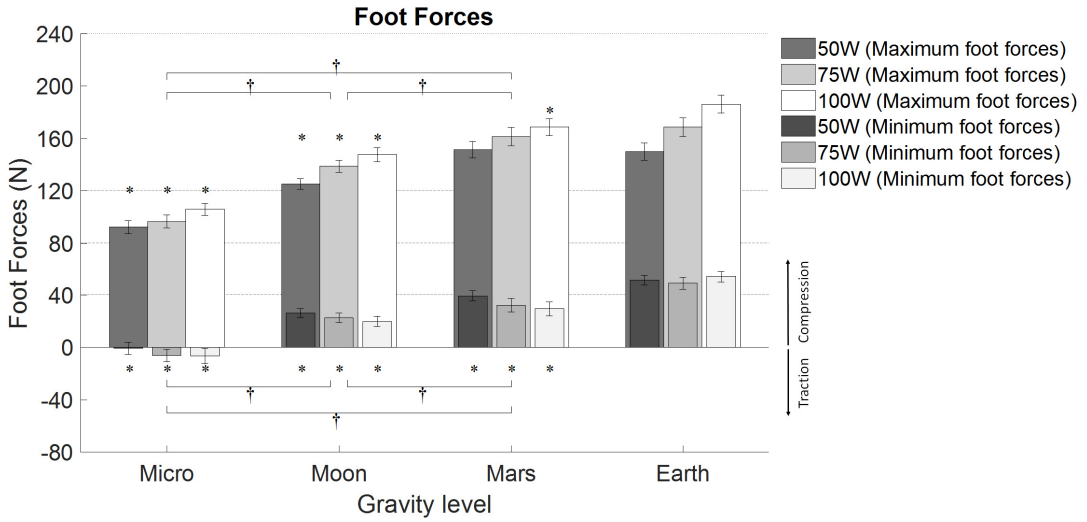

FIGURE 7 | Average minimum and maximum foot forces (12 subjects, mean ± SE at different workload intensities for each of the altered-gravity environments (Microgravity 6° HDT, Moon 9.5° HUT, Mars 22.3° HUT, Earth upright). The figure highlights significant differences between altered-gravity conditions Microgravity, Moon, and Mars (pairwise comparisons after a 2-factor repeated measures ANOVA with Bonferroni correction, † significantly different at $p < 0.05$). Additionally, significant differences compared to Earth are also included (*paired *t*-test, $p < 0.05$). For clarity, pairwise comparisons between workload levels are not shown.

TABLE 4 | Exit survey results concerning perceived comfort and strenuousness during the experimental sessions [mean (SE), including 14 subjects] for all altered-gravity conditions (Microgravity −6° HDT, Moon +9.5° HUT, Mars +22.3° HUT, Earth +90° upright).

Ag level	Comfort	Strenuousness
Microgravity −6° HDT	4.4 (2.0)	6.1 (2.1)
Moon +9.5° HUT	5.9 (1.5)	4.9 (2.0)
Mars +22.3° HUT	6.7 (2.2)	4.2 (1.6)
Earth +90° upright	7.4 (2.0)	3.4 (1.7)

Data was collected using a 10-point Likert scale (Comfort: 1 – very uncomfortable/unnatural, 10 – very comfortable/natural. Strenuousness: 1 – easy, 10 – very strenuous).

reported in the Microgravity configuration, probably due to the head-down tilt of the body and the upper position of the legs. The Friedman test also yielded a statistically significant effect of AG on strenuousness [$\chi^2(3) = 27.51$, $p < 0.0005$]. Thus, Microgravity was the most challenging position, and the perception of difficulty of exercise was progressively reduced with increasing AG. Subjects were also asked to choose between workload intensity and protocol duration as the main cause of strenuousness. Workload intensity was selected in the majority of the cases. Other factors such as cycling frequency and position discomfort were also mentioned.

DISCUSSION

This study measured cardiopulmonary responses to submaximal ergometer exercise under multiple postural conditions using a HDT/HUT paradigm. Although a few studies have reported cardiorespiratory responses to exercise in upright, supine, and −6° HDT, this is the first study to include additional tilt angles representing Moon and Mars gravitational conditions, which allowed the generation of additional data points to build cardiopulmonary dose-response curves in simulated hypogravity at multiple exercise intensities.

Head-down tilt posture at an angle of 6° has become the standard model for microgravity simulation (Pavy-Le Traon et al., 2007). In this position, fluids are redistributed toward the central cavity, causing an increase in ventricular preload, left-ventricular end-diastolic volume, and stroke volume compared to upright and also supine posture. It is important to note that in −6° HDT, the Gx hydrostatic gradient and a small Gz (foot-to-head) hydrostatic gradient exist, making this condition slightly different from supine posture (where Gz gradient does not exist), and different from true microgravity conditions (no hydrostatic gradients exist).

Cardiopulmonary responses at rest due to postural changes are consistent with previous studies. Prisk et al. (1995) measured resting pulmonary gas exchange in eight subjects in standing upright, supine, and microgravity conditions (Spacelab flights SLS-1 and SLS-2). Their results showed that V_T decreased in the supine position with respect to standing upright, and it decreased even more in real microgravity conditions. As a compensatory mechanism, they noted an increase in R_f when subjects were in microgravity (but not in supine). In our experiment, we found a significant decrease in V_T and a significant increase in R_f when transitioning from seated upright to −6° HDT condition, which is consistent with previous results given that our testing conditions differ slightly likely creating a larger perturbation to the pulmonary system. Our results also support the idea that changes in the gravitational conditions and thus hydrostatic pressures cause subjects to select a different combination of V_T and R_f to maintain the appropriate alveolar ventilation (Prisk et al., 1995). Given the adjustments in V_T and R_f, our subjects were able to also maintain a similar V_E, contrary to Prisk's study where subjects experienced a significant decrease in V_E both

in supine and microgravity. Our V_T and R_f results are also consistent with ventilatory responses gathered by Gisolf et al. (2004) on eight normal subjects in supine and standing position. With respect to gas exchange, we also found unaltered VO_2 and slightly elevated VCO_2 in −6° HDT compared with sitting upright. When comparing the upright seated baseline with the Earth condition baseline (i.e., subjects are seated on the bike saddle ready to start pedaling), we did see significant increases in VO_2, VCO_2. V_T, and V_E. This is consistent with subjects not being truly in a resting position similar to the other testing conditions (i.e., Microgravity, Mars, Moon) where subjects are laying on top of the tilt platform without exerting any effort to maintain themselves upright (Piotrowski et al., 2018).

Concerning cardiopulmonary responses during exercise, we found a slight tendency of VO_2 to decrease with increasing gravity levels (2-way repeated measures ANOVA). The average reduction across exercise conditions of VO_2 per unit of simulated AG-level was −97.88 mL/min/g. This slight reduction is also supported by a reduction in VCO_2 with increasing gravity levels (−95.10 mL/min/g averaged across exercise conditions). These changes in cardiopulmonary variables may be related to the suggestion that exercise performance decreases with reducing hydrostatic column (Egaña et al., 2006). The exact mechanisms may be attributed to a decrease in muscle perfusion at higher tilt angles with respect to upright (Fitzpatrick et al., 1996; Wright et al., 1999), potentially reducing blood flow to the exercising muscles (Nielsen, 1983), and an attenuated muscle pump effect in the presence of a reduced (or even absence in the case of HDT) venous hydrostatic column (Laughlin, 1987; Laughlin and Joyner, 2003). However, we did not find significant differences between conditions in VO_2 when tested for pairwise comparisons, indicating that if this effect exists, it does not seem to be very strong. This is consistent with previous results collected during submaximal cycling exercise at 100W in both upright and −6° HDT conditions reporting no significant differences in VO_2 or HR between the two postures, either before or after an 8-week training protocol (Ade et al., 2013). Also consistent with Ade et al. (2013), our HR data at 100W in upright (Earth condition), and −6° HDT (Microgravity condition) do not differ either. However, it is interesting to note that HR does decrease in intermediate postures (Moon and Mars conditions). This non-linear behavior could be related to differences between HUT and HDT and the reversal of the hydrostatic gradient along the Gz- body axis, as well as the discomfort and additional effort reported by our subjects associated to cycling during HDT when the legs are elevated above heart level (Ade et al., 2013).

Cardiopulmonary data on true microgravity during ergometer exercise are very scarce. One study was conducted onboard the Russian Space Station Mir (Girardis et al., 1999) to investigate metabolic consumption of two astronauts during cycle exercise at 50, 75, and 100W. Results showed that submaximal VO_2 at 0 g was significantly lower than all measurements taken at 1 g. These results are in disagreement with our ground-study as well as with results reported by others during HDT on Earth (Ade et al., 2013). This discrepancy between spaceflight and supine and/or HDT data raises again the question about the validity of −6° HDT as a good microgravity analog when studying submaximal exercise capacity. Other factors to take into account are that spaceflight data were collected in only two subjects, and the first data points were taken on flight day 12, and thus potential effects of muscle and aerobic capacity deconditioning might have occurred by then. Additionally, atmosphere composition at the time of the test (which was not reported) as well as pedaling frequency (which was not controlled by an operator) might have been additional factors affecting the results. All in all, further studies in true microgravity (and ideally true partial gravity) are warranted to better elucidate submaximal exercise pulmonary responses in these conditions.

Using these spaceflight data as well as additional hypergravity data, Bonjour et al. (2011) developed a model to predict cardio-pulmonary responses to submaximal cycling exercise in varying gravitational environments. Gravitational levels included 0 g (data from MIR reported above), as well as hypergravity data collected on centrifuges in Karolinska Institute in Sweden (1, 1.5, 2, and 2.5 g), and the Center for Research and Education in Special Environments in Buffalo (1, 2, and 3 g). Bonjour proposed a quadratic non-linear relationship between HR and AG, and he predicted HR responses at Mars and Moon gravity levels when cycling at 50, 75, and 100W. The comparison between his predictions and the results obtained in this study is shown in **Table 5**. When analyzing the responses at Earth condition (1 g), we can observe that our results showed higher HR responses than the ones obtained by Bonjour. Individual differences between the subjects could likely explain this effect, suggesting that the subjects participating in our study were less physically prepared than the ones participating in the studies he conducted. Another important factor is the difference in pedaling frequency. Bonjour considered studies performed at a pedaling frequency of 1 Hz whereas our study was conducted at 1.5 Hz. This difference leads to an increased cycling internal work (Bonjour et al., 2010), which makes our study more physically demanding.

During exercise, our results show a slight decrease in V_T, and an increase in Rf with lower tilt angles (i.e., lower simulated gravity levels). Averaged changes with simulated AG-level for V_T and Rf across exercise conditions were 0.165 L/g and −5.33 breaths/min/g, respectively. Changes in V_T are presumably related to the increase in thoracic pressure when being reclined (Gisolf et al., 2004). The decrease in the tilt angle reduces the gravity force in the longitudinal axis (Gz) but increases it in the direction perpendicular to the platform (i.e., Gx, the anterioposterior direction). As a consequence, there is a higher contribution of the weight forces of the thoracic cage,

TABLE 5 | Comparison between Bonjour's predictions of the heart rate responses to exercise on Moon and Mars with the results obtained in this study [mean (SE), including 14 subjects].

HR (beats/min)		50W	75W	100W
Moon	Prediction	87	96	105
	AEPS study	113.08 (3.31)	124.09 (3.66)	136.80 (3.75)
Mars	Prediction	88	97	106
	AEPS study	113.51 (4.14)	124.71 (4.16)	136.21 (4.14)
Earth	Prediction	93	102	112
	AEPS study	118.18 (4.44)	130.86 (4.74)	141.21 (4.55)

thus hampering lung expansion. To counteract for this effect, Rf increases at lower tilt-angles, causing also an increase in V_E. Finally, we did not find any significant changes in blood pressure, except of DBP in simulated microgravity conditions. Diastolic blood pressure significantly increased while exercising at −6° HDT, most likely driven by the introduction of the foot-to-head hydrostatic gradient, combined with the higher positioning of the exercising legs above the Gz line of the body. It is interesting to note that we did not find statistically significant differences between Mars and Earth in any of our cardiopulmonary variables, except for HR.

Previous studies performed onboard the ISS using the Cycle Ergometer with Vibration Isolation System (CEVIS) device measured foot forces between 7.0 and 19.0% of the body weight (BW) using work rates ranging from 75 to 210W (Genc et al., 2010). These results are in concordance with our results in −6° HDT where we obtained maximum peak forces between 12.7 and 14.6% BW. Other studies compared Earth with microgravity cycling loadings, obtaining a 20% and 10% BW, respectively (Cavanagh et al., 2010). Although these results are slightly lower compared to the ones obtained in our study, differences in pedaling rate or workload level can produce changes in foot forces, this being a possible reason for these differences. Foot forces during cycling activity at partial-gravity such as the Martian or the lunar gravitational environments have not been previously studied. However, ground reaction forces at reduced gravity levels during other exercise modalities have been investigated, including running (Cavanagh et al., 2017), hopping (Weber et al., 2019), and the use of stair-steppers (Edmonds et al., 2008). However, ergometer exercise does not provide foot forces as high as these other exercise modalities, and therefore, a straight comparison across different exercise disciplines is not directly applicable. Finally, it is interesting to note that, in our study on ergometer exercise, we did not find considerable differences in maximum foot forces between Mars and Earth conditions. Investigating this similarity could be key with regard to prescription exercise protocols during future long duration exploration missions.

Subjective data in simulated microgravity conditions showed the lowest comfort punctuation. Major complaints reported were lower back pain and discomfort in the arms due to the handlebars. Future suggestions that could improve these issues include a better platform lining, intermediate cycle ergometer positions, and different handlebar configurations to enable a more ergonomic positioning of the subject on the platform. However, no cycling difficulties or major discomfort problems were reported, validating the correct functioning of the platform. Strenuousness results showed an increased difficulty perception at lower artificial gravity levels, which was likely related to the more unnatural positioning of the body.

Limitations

We used a HDT/HUT paradigm to study the effect of postural changes during submaximal aerobic exercise. −6 °HDT has been adopted by the spaceflight community as a well-accepted analog to simulate microgravity, especially with regard to fluid shifts and cardiovascular adaptations. However, this is not a fully accurate ground-based simulation of spaceflight. The presence of a small longitudinal (Gz, foot-to-head) and transverse (Gx) gravitational effects, including the pressure of the ground's surface on the subject's back and their impact on intrathoracic volume and ventilation mechanics, is certainly a limitation when comparing pulmonary and cardiovascular function with true microgravity or true partial gravity (Regnard et al., 2001; Watenpaugh, 2016). A classic example of differences in cardiovascular responses between HDT and true microgravity is the "surprising" reduction of central venous pressure (CVP) in space relative to 1 g supine and upright values, while ground-based analogs such as HDT produce the "expected" increase in CVP related to the central fluid shift (Buckey et al., 1996a; Watenpaugh, 2016). Subjects also reported some discomfort during the exercise sessions in tilted positions, especially the HDT configuration, that should not occur in real microgravity and might have slightly affected the results. Despite these discrepancies, the tilt paradigm reproduced many of the physiological responses reasonably well (Watenpaugh, 2016), but it is important to acknowledge these differences when interpreting the results. In our study, we investigated the effects of gravity alterations through postural changes on Earth in an attempt to elucidate physiological responses in altered-gravity environments, but further studies in true hypogravity are warranted to fully capture those responses.

We included Earth configuration in our study since 1 g is one of the most interesting conditions when investigating gravitational physiology. However, we acknowledge some differences in configuration and body posture with respect to the reclined positions, such as the presence of a saddle and the need for subjects to keep themselves upright. Thus, a consequence of exercising while lying on the platform is the unloading of the back and trunk muscles, which might decrease the VO_2 requirements during exercise in these hypogravity configurations (Piotrowski et al., 2018). Given all these differences, subjects always experienced the upright configuration first (could be considered as the familiarization session) and was not included in the randomization scheme implemented with the rest of the sessions.

Other limitations of the study are related to the resources available to conduct the experiment. Subjects were selected from the college population and thus, their age (range between 20 and 32 years old) and most likely physical fitness (although capable of conducting aerobic exercise for an hour), were not truly representative of the astronaut population. Only two women participated in the study and therefore it is not possible to conduct a comprehensive analysis on gender effects. Additionally, the duration of the test sessions was limited to avoid excessive fatigue of subjects during the exercise protocol. Thus, some variables did not reach steady state and extrapolation of results outside the timeframes investigated should be done with caution.

CONCLUSION

For the first time, we characterized cardiopulmonary and musculoskeletal responses to submaximal ergometer exercise

during postural changes using a HDT/HUT paradigm. We investigated multiple simulated gravity levels (i.e., tilt angles), and exercise intensities, generating dose-response curves to inform future trade-offs and decisions regarding the effects of hydrostatic changes and altered-gravity on human performance. Our results showed that there are not significant differences in human cardiopulmonary and musculoskeletal responses between Mars and Earth experimental conditions. This indicates some degree of similarity in human performance during ergometer exercise under Martian and terrestrial gravitational environments, suggesting that this type of exercise conducted under a gravitational stress of ∼3/8 g could provide similar physiological stimuli than cycling under 1 g on Earth.

We also found some differences between −6° HDT and the (scarce) true microgravity data gathered during spaceflight, highlighting the limitations of using ground-based models to study the complex physiological processes that occur in true microgravity conditions, as well as the need of collecting additional flight data.

ETHICS STATEMENT

All subjects were informed about their right to withdraw from the experiment at any point and provided written informed consent to participate. The study was approved by Cornell University's Institutional Review Board for Human Participants.

AUTHOR CONTRIBUTIONS

AD-A served as an overall supervisor of the research project and provided advice regarding the experimental design, data analysis, and statistics, and she was the primary contributor to the manuscript. PNT assisted in the experimental design and conducted the human experiments, completed the statistical analysis, and contributed to the manuscript. FP contributed to the experimental design and execution of the experiment, and drafting of the manuscript. All authors approved the final manuscript.

FUNDING

This project was partially supported by the NASA/ New York Space Grant Consortium – Faculty Grants (2017–2018).

ACKNOWLEDGMENTS

We greatly appreciate our anonymous subjects for their participation in this experiment. We would also like to thank Evan Halloran, Eric Berg, Russell Silva, and Benjamin Roberge for designing and constructing the Altered-gravity Exercise Platform Simulator.

REFERENCES

Ade, C. J., Broxterman, R. M., and Barstow, T. J. (2013). Effects of body posture and exercise training on cardiorespiratory responses to exercise. *Respir. Physiol. Neurobiol.* 188, 39–48. doi: 10.1016/j.resp.2013.04.023

Akaike, H. (1974). A new look at the statistical model identification. *IEEE Trans. Automat. Contr.* 19, 716–723. doi: 10.1109/TAC.1974.1100705

Alessandro, C., Tafreshi, A. S., and Riener, R. (2016). "Increasing leg blood volume during head-down tilt by performing physical exercises, a preliminary study," in *Proceedings of the 6th IEEE International Conference on Biomedical Robotics and Biomechatronics (BioRob)*, (Singapore: IEEE), 888–893. doi: 10.1109/BIOROB.2016.7523740

Baranov, M. V., Katuntsev, V. P., Shpakov, A. V., and Baranov, V. M. (2016). A method of ground simulation of physiological effects of hypogravity on humans. *Bull. Exp. Biol. Med.* 160, 401–405. doi: 10.1007/s10517-016-3181-0

Bonjour, J., Bringard, A., Antonutto, G., Capelli, C., Linnarsson, D., Pendergast, D. R., et al. (2011). Effects of acceleration in the Gz axis on human cardiopulmonary responses to exercise. *Eur. J. Appl. Physiol.* 111, 2907–2917. doi: 10.1007/s00421-011-1917-0

Bonjour, J., Capelli, C., Antonutto, G., Calza, S., Tam, E., Linnarsson, D., et al. (2010). Determinants of oxygen consumption during exercise on cycle ergometer: the effects of gravity acceleration. *Respir. Physiol. Neurobiol.* 171, 128–134. doi: 10.1016/j.resp.2010.02.013

Buckey, J. C. (2006). *Space Physiology*. New York, NY: Oxford University Press.

Buckey, J. C., Gaffney, F. A., Lane, L. D., Levine, B. D., Watenpaugh, D. E., Wright, S. J., et al. (1996a). Central venous pressure in space. *J. Appl. Physiol.* 81, 19–25.

Buckey, J. C., Lane, L. D., Levine, B. D., Watenpaugh, D. E., Wright, S. J., Moore, W. E., et al. (1996b). Orthostatic intolerance after spaceflight. *J. Appl. Physiol.* 81, 7–18.

Cavanagh, P., Rice, A., Glauberman, M., Sudduth, A., Cherones, A., Davis, S., et al. (2017). Ground Reaction forces during reduced gravity running in parabolic flight. *Aerosp. Med. Hum. Perform.* 88, 730–736. doi: 10.3357/amhp.4779.2017

Cavanagh, P. R., Genc, K. O., Gopalakrishnan, R., Kuklis, M. M., Maender, C. C., and Rice, A. J. (2010). Foot forces during typical days on the international space station. *J. Biomech.* 43, 2182–2188. doi: 10.1016/j.jbiomech.2010.03.044

Charles, J. B., and Lathers, C. M. (1994). Summary of lower body negative pressure experiments during space flight. *J. Clin. Pharmacol.* 34, 571–583. doi: 10.1002/j.1552-4604.1994.tb02009.x

Clément, G. (2005). *Fundamentals of Space Medicine*. El Segundo, CA: Microcosm Press and Springer.

Clément, G. (2017). International roadmap for artificial gravity research. *npj Microgravity* 3, 29. doi: 10.1038/s41526-017-0034-8

Clément, G., and Bukley, A. P. (2007). *Artificial Gravity*. Hawthorne, CA: Springer.

Clement, G. R., Bukley, A. P., and Paloski, W. H. (2015). Artificial gravity as a countermeasure for mitigating physiological deconditioning during long-duration space missions. *Front. Syst. Neurosci.* 9:92. doi: 10.3389/fnsys.2015.00092

Clément, G. R., Charles, J. B., and Paloski, W. H. (2016). Revisiting the needs for artificial gravity during deep space missions. *Reach* 1, 1–10. doi: 10.1016/j.reach.2016.01.001

Cutuk, A. (2006). Ambulation in simulated fractional gravity using lower body positive pressure: cardiovascular safety and gait analyses. *J. Appl. Physiol.* 101, 771–777. doi: 10.2343/geochemj.2.0462

Diaz, A., Heldt, T., and Young, L. R. (2015a). "Cardiovascular responses to artificial gravity combined with exercise," in *Proceeding of the 2015 IEEE Aerospace Conference*, (Big Sky, MT).

Diaz, A., Trigg, C., and Young, L. R. (2015b). Combining ergometer exercise and artificial gravity in a compact-radius centrifuge. *Acta Astronaut* 113, 80–88. doi: 10.1016/j.actaastro.2015.03.034

Diaz Artiles, A. (2015). *Exercise Under Artificial Gravity – Experimental and Computational Approaches*. PhD Thesis. Cambridge, MA: Massachusetts Institute of Technology.

Diaz Artiles, A., Heldt, T., and Young, L. R. (2016). Effects of artificial gravity on the cardiovascular system: computational approach. *Acta Astronaut* 126, 395–410. doi: 10.1016/j.actaastro.2016.05.005

Diaz-Artiles, A., Heldt, T., and Young, L. R. (2018). Short-term cardiovascular response to short-radius centrifugation with and without ergometer exercise. *Front. Physiol.* 9:1492. doi: 10.3389/fphys.2018.01492

Edmonds, J. L., Jarchow, T., and Young, L. R. (2008). Physiological benefits of exercise in artificial gravity: a broadband countermeasure to space flight related deconditioning. *Acta Astronaut* 63, 2–7. doi: 10.1016/j.actaastro.2007.12.026

Egaña, M., Green, S., Garrigan, E. J., and Warmington, S. (2006). Effect of posture on high-intensity constant-load cycling performance in men and women. *Eur. J. Appl. Physiol.* 96, 1–9. doi: 10.1007/s00421-005-0057-9

Evans, J. M., Mohney, L., Wang, S., Moore, R. K., Elayi, S. C., Stenger, M. B., et al. (2013). Cardiovascular regulation during body unweighting by lower body positive pressure. *Aviat. Space Environ. Med.* 84, 1140–1146. doi: 10.3357/ASEM.3576.2013

Fitzpatrick, R., Taylor, J. L., and Mccloskey, D. I. (1996). Effects of arterial perfusion pressure on force production in working human hand muscles. *J. Physiol.* 495(Pt 3), 885–891. doi: 10.1113/jphysiol.1996.sp021640

Gaffney, F. A., Nixon, J. V., Karlsson, E. S., Campbell, W., Dowdey, A. B. C., and Blomqvist, C. G. (1985). Cardiovascular deconditioning produced by 20 hours of bedrest with head-down tilt (−5°) in middle-aged healthy men. *Am. J. Cardiol.* 56, 634–638. doi: 10.1016/0002-9149(85)91025-2

Genc, K. O., Gopalakrishnan, R., Kuklis, M. M., Maender, C. C., Rice, A. J., Bowersox, K. D., et al. (2010). Foot forces during exercise on the international space station. *J. Biomech.* 43, 3020–3027. doi: 10.1016/j.jbiomech.2010.06.028

Girardis, M., Linnarsson, D., Moia, C., Pendergast, D. R., and Ferretti, G. (1999). Oxygen cost of dynamic leg exercise on a cycle ergometer: effects of gravity acceleration. *Acta Physiol. Scand.* 166, 239–246. doi: 10.1046/j.1365-201x.1999.00564.x

Gisolf, J., Wilders, R., Immink, R. V., van Lieshout, J. J., and Karemaker, J. M. (2004). Tidal volume, cardiac output and functional residual capacity determine end-tidal CO2transient during standing up in humans. *J. Physiol.* 554, 579–590. doi: 10.1113/jphysiol.2003.056895

Hargens, A. R., Bhattacharya, R., and Schneider, S. M. (2013). Space physiology VI: exercise, artificial gravity, and countermeasure development for prolonged space flight. *Eur. J. Appl. Physiol.* 113, 2183–2192. doi: 10.1007/s00421-012-2523-5

Kostas, V. I., Stenger, M. B., Knapp, C. F., Shapiro, R., Wang, S., Diedrich, A., et al. (2014). Cardiovascular models of simulated moon and mars gravities: head-Up tilt vs. lower body unweighting. *Aviat. Space Environ. Med.* 85, 414–419. doi: 10.3357/ASEM.3687.2014

Lathers, C. M., Diamandis, P. H., Riddle, J. M., Mukai, C., Elton, K. F., Bungo, M. W., et al. (1990). Acute and intermediate cardiovascular responses to zero gravity and to fractional gravity levels induced by head-down or head-up tilt. *J. Clin. Pharmacol.* 30, 494–523. doi: 10.1002/j.1552-4604.1990.tb03614.x

Lathers, C. M., Riddle, J. M., Mulvagh, S. L., Mukai, C., Diamandis, P. H., Dussack, L. G., et al. (1993). Echocardiograms during six hours of bedrest at head-down and head-up tilt and during space flight. *J. Clin. Pharmacol.* 33, 535–543. doi: 10.1002/j.1552-4604.1993.tb04700.x

Laughlin, M. H. (1987). Skeletal muscle blood flow capacity: role of muscle pump in exercise hyperemia. *Am. J. Physiol. Circ. Physiol.* 253, H993–H1004. doi: 10.1152/ajpheart.1987.253.5.h993

Laughlin, M. H., and Joyner, M. (2003). Closer to the edge? Contractions, pressures, waterfalls and blood flow to contracting skeletal muscle. *J. Appl. Physiol.* 94, 3–5. doi: 10.2307/1320933

Lee, S. M. C., Feiveson, A. H., Stein, S., Stenger, M. B., and Platts, S. H. (2015). Orthostatic intolerance after ISS and space shuttle missions. *Aerospace Med. Hum. Perform.* 86, 54–67. doi: 10.3357/AMHP.EC08.2015

Levine, B. D., Lane, L. D., Watenpaugh, D. E., Gaffney, F. A., Buckey, J. C., Blomqvist, C. G., et al. (1996). Maximal exercise performance after adaptation to microgravity. *J. Appl. Physiol.* 81, 686–694. doi: 10.1152/jappl.1996.81.2.686

Louisy, F., Guezennec, C. Y., and Guell, A. (1994). Leg vein hemodynamics during bedrests simulating lunar trip. *J. Gravit. Physiol.* 1, 100–101.

Moore, A. D., Lynn, P. A., and Feiveson, A. H. (2015). The first 10 years of aerobic exercise responses to long-duration ISS flights. *Aerospace Med. Hum. Perform.* 86, 78–86. doi: 10.3357/amhp.ec10.2015

Nielsen, H. V. (1983). Arterial pressure–blood flow relations during limb elevation in man. *Acta Physiol. Scand.* 118, 405–413. doi: 10.1111/j.1748-1716.1983.tb07290.x

Nixon, J. V., Murray, R. G., Bryant, C., Johnson, R. L., Mitchell, J. H., Holland, O. B., et al. (1979). Early cardiovascular adaptation to simulated zero gravity. *J. Appl. Physiol.* 46, 541–548. doi: 10.1152/jappl.1979.46.3.541

Paloski, W. H., and Charles, J. B. (2014). *2014 International Workshop on Research and Operational Considerations for Artificial Gravity Countermeasures*. Mountain View, CA: Nasa Ames Research Center.

Pavei, G., Biancardi, C. M., and Minetti, A. E. (2015). Skipping vs. *running as the bipedal gait of choice in hypogravity*. *J. Appl. Physiol.* 119, 93–100. doi: 10.1152/japplphysiol.01021.2014

Pavei, G., and Minetti, A. E. (2016). Hopping locomotion at different gravity: metabolism and mechanics in humans. *J. Appl. Physiol.* 120, 1223–1229. doi: 10.1152/japplphysiol.00839.2015

Pavy-Le Traon, A., Allevard, A. M., Fortrat, J. O., Vasseur, P., Gauquelin, G., Guell, A., et al. (1997). Cardiovascular and hormonal changes induced by a simulation of a lunar mission. *Aviat. Space Environ. Med.* 68, 829–837.

Pavy-Le Traon, A., Heer, M., Narici, M. V., Rittweger, J., and Vernikos, J. (2007). From space to earth: advances in human physiology from 20 years of bed rest studies (1986-2006). *Eur. J. Appl. Physiol.* 101, 143–194. doi: 10.1007/s00421-007-0474-z

Pearson, R. K., Neuvo, Y., Astola, J., and Gabbouj, M. (2016). Generalized hampel filters. *EURASIP J. Adv. Signal. Process.* 2016:87. doi: 10.1186/s13634-016-0383-6

Petersen, N., Jaekel, P., Rosenberger, A., Weber, T., Scott, J., Castrucci, F., et al. (2016). Exercise in space: the European Space Agency approach to in-flight exercise countermeasures for long-duration missions on ISS. *Extrem. Physiol. Med.* 5, 1–13. doi: 10.1186/s13728-016-0050-4

Piotrowski, T., Rittweger, J., and Zange, J. (2018). A comparison of squatting exercise on a centrifuge and with earth gravity. *Front. Physiol.* 9:1759. doi: 10.3389/fphys.2018.01759

Pletser, V. (2004). Short duration microgravity experiments in physical and life sciences during parabolic flights: the first 30 ESA campaigns. *Acta Astronaut* 55, 829–854. doi: 10.1016/j.actaastro.2004.04.006

Pletser, V., Winter, J., Duclos, F., Bret-Dibat, T., Friedrich, U., Clervoy, J. F., et al. (2012). The first joint european partial-G parabolic flight campaign at moon and mars gravity levels for science and exploration. *Microgravity Sci. Technol.* 24, 383–395. doi: 10.1007/s12217-012-9304-y

Ploutz-Snyder, L. L., Downs, M., Goetchius, E., Crowell, B., English, K. L., Ploutz-Snyder, R., et al. (2018). Exercise training mitigates multi-system deconditioning during bed rest. *Med. Sci. Sports Exerc.* 50, 1920–1928. doi: 10.1249/mss.0000000000001618

Prisk, G. K., Elliott, A. R., Guy, H. J., Kosonen, J. M., and West, J. B. (1995). Pulmonary gas exchange and its determinants during sustained microgravity on Spacelabs SLS-1 and SLS-2. *J. Appl. Physiol.* 79, 1290–1298. doi: 10.1152/jappl.1995.79.4.1290

Regnard, J., Heer, M., Drummer, C., and Norsk, P. (2001). Validity of microgravity simulation models on earth. *Am. J. Kidney Dis.* 38, 668–674. doi: 10.1053/ajkd.2001.27753

Richter, C., Braunstein, B., Winnard, A., Nasser, M., and Weber, T. (2017). Human biomechanical and cardiopulmonary responses to partial gravity - A systematic review. *Front. Physiol.* 8:583. doi: 10.3389/fphys.2017.00583

Salkind, N. J., Dougherty, D. M., and Frey, B. (2010). "The greenhouse geisser correction," in *Encyclopedia of Research Design*, (Thousand Oaks, CA: Sage Publications), 544–548. doi: 10.1007/BF02289823

Schlabs, T., Rosales-Velderrain, A., Ruckstuhl, H., Stahn, A. C., and Hargens, A. R. (2013). Comparison of cardiovascular and biomechanical parameters of supine lower body negative pressure and upright lower body positive pressure to simulate activity in 1/6 G and 3/8 G. *J. Appl. Physiol.* 115, 275–284. doi: 10.1152/japplphysiol.00990.2012

Smith, S. M., Heer, M. A., Shackelford, L. C., Sibonga, J. D., Ploutz-Snyder, L., and Zwart, S. R. (2012). Benefits for bone from resistance exercise and nutrition in long-duration spaceflight: evidence from biochemistry and densitometry. *J. Bone Miner. Res.* 27, 1896–1906. doi: 10.1002/jbmr.1647

Trappe, T., Trappe, S., Lee, G., Widrick, J., Fitts, R., and Costill, D. (2006). Cardiorespiratory responses to physical work during and following 17 days of bed rest and spaceflight. *J. Appl. Physiol.* 100, 951–957. doi: 10.1152/japplphysiol.01083.2005

Watenpaugh, D. E. (2016). Analogs of microgravity: head-down tilt and waterimmersion. *J. Appl. Physiol.* 120, 904–914. doi: 10.1152/japplphysiol.00986.2015

Weber, T., Green, D. A., Attias, J., Sies, W., Frechette, A., Braunstein, B., et al. (2019). Hopping in hypogravity-A rationale for a plyometric exercise

countermeasure in planetary exploration missions. *PLoS One* 14:e0211263. doi: 10.1371/journal.pone.0211263

Widjaja, D., Vandeput, S., Van Huffel, S., and Aubert, A. E. (2015). Cardiovascular autonomic adaptation in lunar and martian gravity during parabolic flight. *Eur. J. Appl. Physiol.* 115, 1205–1218. doi: 10.1007/s00421-015-3118-8

Wright, J. R., McCloskey, D. I., and Fitzpatrick, R. C. (1999). Effects of muscle perfusion pressure on fatigue and systemic arterial pressure in human subjects. *J. Appl. Physiol.* 86, 845–851. doi: 10.1152/jappl.1999.86.3.845

Conflict of Interest Statement: The authors declare that the research was conducted in the absence of any commercial or financial relationships that could be construed as a potential conflict of interest.

frontiers in Physiology

ORIGINAL RESEARCH
published: 04 July 2019
doi: 10.3389/fphys.2019.00761

Alterations of Functional Brain Connectivity After Long-Duration Spaceflight as Revealed by fMRI

Ekaterina Pechenkova[1], Inna Nosikova[2], Alena Rumshiskaya[3], Liudmila Litvinova[3], Ilya Rukavishnikov[2], Elena Mershina[4], Valentin Sinitsyn[4], Angelique Van Ombergen[5], Ben Jeurissen[6], Steven Jillings[5,7], Steven Laureys[7], Jan Sijbers[6], Alexey Grishin[8], Ludmila Chernikova[2], Ivan Naumov[2], Ludmila Kornilova[2], Floris L. Wuyts[5], Elena Tomilovskaya[2] and Inessa Kozlovskaya[2]*

[1] Laboratory for Cognitive Research, Higher School of Economics, Moscow, Russia, [2] Institute of Biomedical Problems, Russian Academy of Sciences, Moscow, Russia, [3] Radiology Department, Federal Center of Treatment and Rehabilitation, Moscow, Russia, [4] Medical Research and Educational Center, Lomonosov Moscow State University, Moscow, Russia, [5] Lab for Equilibrium Investigations and Aerospace, Faculty of Science, University of Antwerp, Antwerp, Belgium, [6] iMec/Vision Lab, Faculty of Science, University of Antwerp, Antwerp, Belgium, [7] Coma Science Group, GIGA Consciousness Research Centre, Neurology Department, University Hospital of Liège, Liège, Belgium, [8] Gagarin Cosmonauts Training Center, Star City, Russia

OPEN ACCESS

Edited by:
Richard D. Boyle, National Aeronautics and Space Administration (NASA), United States

Reviewed by:
Donna R. Roberts, Medical University of South Carolina, United States
Rachael D. Seidler, University of Michigan, United States

***Correspondence:**
Ekaterina Pechenkova
evp@virtualcoglab.org

Specialty section:
This article was submitted to Environmental, Aviation and Space Physiology, a section of the journal Frontiers in Physiology

Received: *31 December 2018*
Accepted: *31 May 2019*
Published: *04 July 2019*

Citation:
Pechenkova E, Nosikova I, Rumshiskaya A, Litvinova L, Rukavishnikov I, Mershina E, Sinitsyn V, Van Ombergen A, Jeurissen B, Jillings S, Laureys S, Sijbers J, Grishin A, Chernikova L, Naumov I, Kornilova L, Wuyts FL, Tomilovskaya E and Kozlovskaya I (2019) Alterations of Functional Brain Connectivity After Long-Duration Spaceflight as Revealed by fMRI. Front. Physiol. 10:761. doi: 10.3389/fphys.2019.00761

The present study reports alterations of task-based functional brain connectivity in a group of 11 cosmonauts after a long-duration spaceflight, compared to a healthy control group not involved in the space program. To elicit the postural and locomotor sensorimotor mechanisms that are usually most significantly impaired when space travelers return to Earth, a plantar stimulation paradigm was used in a block design fMRI study. The motor control system activated by the plantar stimulation involved the pre-central and post-central gyri, SMA, SII/operculum, and, to a lesser degree, the insular cortex and cerebellum. While no post-flight alterations were observed in terms of activation, the network-based statistics approach revealed task-specific functional connectivity modifications within a broader set of regions involving the activation sites along with other parts of the sensorimotor neural network and the visual, proprioceptive, and vestibular systems. The most notable findings included a post-flight increase in the stimulation-specific connectivity of the right posterior supramarginal gyrus with the rest of the brain; a strengthening of connections between the left and right insulae; decreased connectivity of the vestibular nuclei, right inferior parietal cortex (BA40) and cerebellum with areas associated with motor, visual, vestibular, and proprioception functions; and decreased coupling of the cerebellum with the visual cortex and the right inferior parietal cortex. The severity of space motion sickness symptoms was found to correlate with a post- to pre-flight difference in connectivity between the right supramarginal gyrus and the left anterior insula. Due to the complex nature and rapid dynamics of adaptation to gravity alterations, the post-flight findings might be attributed to both the long-term microgravity exposure and to the readaptation to Earth's gravity that took place between the landing and post-flight MRI session. Nevertheless, the results have implications for the multisensory reweighting and gravitational motor system theories, generating hypotheses to be tested in future research.

Keywords: spaceflight, microgravity, cosmonauts, fMRI, functional connectivity, brain plasticity, vestibular function, support stimulation

INTRODUCTION

Recent advances in space vehicle engineering are expected to facilitate interplanetary space missions and space tourism. This will recruit what is known about the effects of space on the human body and mind, information which has been accumulating for more than a half century. Besides ionizing radiation, the most serious challenges for a human traveling to space are induced by microgravity. Body weightlessness and support unloading result in hypokinesia, vestibular sensory deprivation and an altered central interpretation of vestibular input (Young et al., 1984), as well as fluid redistribution (Smith et al., 1997), which in the aggregate cause detrimental effects on bones, muscles, cardiovascular function, neurovestibular function, and vision (Van Ombergen et al., 2017a). Such deterioration may progress into serious health issues and make long-term space flights impossible without proper microgravity countermeasures (Kozlovskaya et al., 2015; Shelhamer, 2015; Wang et al., 2018).

Besides issues that can be identified as health problems, microgravity induces many changes in behavior and performance, some of which may be considered as functional alterations and some as compensatory adaptations to the new environment (Newberg and Alavi, 1998; Bloomberg et al., 2015; Kornilova et al., 2017). The most pronounced among these changes are alterations in sensorimotor function, which, in its different aspects, recovers from days to weeks upon returning to the Earth (Lackner and DiZio, 1996). After a long-term space mission, many space travelers have difficulties standing upright and moving around just after landing (Clément et al., 2007). Later in post-flight period, the observed residual effects include disturbances in walking trajectories and postural stability, altered head position, tendency to raise arms to the sides, stamped gait or irregularly spaced steps (Mulavara et al., 2010), as well as increased reliance on visual feedback (Reschke et al., 1998) and increased time for motor task performance (Kubis et al., 1977; Kozlovskaya et al., 1982).

Alterations elicited by microgravity exposure are not limited to muscle "disuse" because of the weight unloading, but presumably affect all levels of the motor system and, according to the gravitational motor system theory, may be considered a dysfunction of the gravitational mechanisms in the motor system which provide reliability, accuracy, and stability of motor responses on the Earth's surface (Kozlovskaya et al., 1988). These mechanisms are studied in human participants and animal models in actual spaceflight settings and in ground-based analogs, such as parabolic flight (PF), dry immersion (DI), and head-down bed rest (HDBR) (Watenpaugh, 2016; Van Ombergen et al., 2017a; Tomilovskaya et al., 2019). Up to now, an extensive body of empirical evidence suggests that a cascade of motor system modifications in microgravity is triggered by the lack of support afference from deep skin mechanoreceptors (Kozlovskaya et al., 2007). The reorganization of the motor system elicited by the lack of support is complemented by changes in biomechanics such as altered relationships between the mass of a body part and the force required to move it, and by the degraded performance of vestibular and proprioceptive sensory feedback (Reschke et al., 1998) which results in a conflict in the input from different sensory modalities (vestibular, proprioceptive, and visual) (Kornilova and Kozlovskaya, 2003; Davis et al., 2008). Altogether, such changes lead not simply to the prioritization of visual feedback for motor control, but to a necessity to rebuild the motor act coordination in order to find new adaptive solutions to the degree-of-freedom problem (Bernstein, 1967). Results consistent with this view and suggesting a gradual reinterpretation of muscle proprioceptive signals during prolonged exposure to microgravity (Lackner and DiZio, 1996) have been obtained, for example, in research on functional synergies during spaceflight (Clément et al., 1984; Massion, 1992). Similar motor learning processes were documented not only in the posture and locomotion domain, but also in manual tasks (Sangals et al., 1999; Bock et al., 2003; see Seidler et al., 2015 for a review).

In light of the previous discussion, the idea that alterations of sensorimotor functioning after microgravity exposure are very likely to reflect not only peripheral, but also central nervous system modification (or brain plasticity) seems logical and even commonplace. It has also received extensive support from animal models (Krasnov and Dyachkova, 1990; Holstein et al., 1999; DeFelipe et al., 2002; Dyachkova, 2007). But although a number of studies were conducted to collect evidence for microgravity-induced plasticity of human brain functioning with electroencephalography (EEG), the results were interpreted with caution because effects attributed to central neuroplasticity were hard to disentangle from numerous low-level confounds introduced by the complex nature of both the space mission environment and the observed physiological effects (Marušč et al., 2014).

Structural and functional magnetic resonance imaging (MRI) is seen as a more perspective method to reveal the mechanisms of space-induced neuroplasticity, although the MRI data may also be contaminated by side effects such as fluid shifting to the upper body (Roberts et al., 2015). Early calls for neuroimaging studies to find signs of neuroplasticity evoked by the adaptation to the space station environment (Newberg and Alavi, 1998) had little effect for almost two decades.

The first evidence for structural changes in the human brain after the long-term spaceflight includes a narrowing of the central sulcus, a shrinking of the cortico-spinal fluid (CSF) spaces at the vertex, and an upward shift of the brain within the skull as revealed by a clinical assessment of MRI scans (Roberts et al., 2017). Quantitative approaches have also shown extensive but focal bilateral decreases in gray matter volume in the temporal and anterior frontal cortices, as well as in the occipital cortex (Koppelmans et al., 2016; Van Ombergen et al., 2018); a focal increase in gray matter volume in the medial paracentral lobule was also observed (Koppelmans et al., 2016). The results of the only three microgravity-analog (HDBR) studies performed to the date partially corroborated these findings (Li et al., 2015; Roberts et al., 2015; Koppelmans et al., 2017b). As for the white matter, volumetric studies have shown a reduction of white matter volume in the left temporal lobe (Van Ombergen et al., 2018), and diffusion MRI data have indicated structural connectivity disruption in the longitudinal fasciculus, the inferior fronto-occipital fasciculus and the corticospinal tract in the right

hemisphere, as well as in both inferior cerebellar peduncles (Lee et al., 2019).

The only published functional MRI (fMRI) study of a crew member after an actual spaceflight (compared to the preflight baseline) is a case study of a cosmonaut who spent 169 days on the ISS (Demertzi et al., 2016). The study used both task-based and resting-state fMRI techniques. While conventional task-based fMRI requires a participant to receive stimulation or to perform a motor or cognitive task while laying in the scanner, resting-state fMRI requires only relaxed wakefulness without any explicit stimulation or task being administered. The resting-state fMRI data are only used for analysis of intrinsic brain connectivity, especially within large-scale neural networks; the task-based fMRI data may be used for both activation and connectivity analyses. In the cosmonaut, the task-based analysis revealed higher activation in the supplementary motor area during the performance of an imaginary tennis task post-flight compared to preflight. The resting-state fMRI demonstrated reduced post-flight intrinsic connectivity in the right insula and between the left cerebellum and the right motor cortex (Demertzi et al., 2016).

Findings from over 10 microgravity analog studies published so far are very diverse, mainly due to the wide spectrum of study techniques or objectives (Roberts et al., 2010; Liao et al., 2012, 2013, 2015; Rao et al., 2014; Zhou et al., 2014; Cassady et al., 2016; Yuan et al., 2016, 2018a,b; Van Ombergen et al., 2017d). However, many of the brain regions that demonstrate microgravity-induced functional changes are associated with motor, vestibular and proprioceptive functions, or cognitive control (see Van Ombergen et al., 2017c for an extensive review).

Overall, the existing evidence advances the brain sensorimotor system and its connectivity with visual, vestibular, and proprioceptive brain regions as the primary target of neuroimaging research in microgravity-induced neuroplasticity. The ongoing prospective longitudinal studies that use different MRI methods (Koppelmans et al., 2013; Van Ombergen, 2017; Yuan et al., 2017) will be an important source of reliable evidence on this topic. The present paper reports preliminary results of an ongoing longitudinal task-based fMRI study devoted to the effects of long-duration spaceflight on cerebral motor function in humans. The research was conducted within the framework of the ESA/Roscosmos Brain DTI/Tractographia Project. To the best of our knowledge, it is the first published prospective controlled group fMRI study of large scale neural network plasticity in space travelers, and the first task-based functional connectivity MRI study of the effects of microgravity.

In this experiment, we compared brain activation and connectivity elicited by plantar stimulation in two groups: cosmonauts before and after long-term spaceflight, and healthy controls scanned twice with a comparable interval. Plantar stimulation produces support afference, which is believed to be a crucial factor for upright posture and normal terrestrial locomotion in humans (Layne et al., 1998; Kozlovskaya et al., 2007). During a long-term spacelight, prolonged support unloading takes place, which we expect to manifest in alterations of the functional connectivity between the brain areas contributing to motor control. Therefore, we hoped to elucidate those specific neural substrates that correspond to the postural and locomotor disturbances observed in cosmonauts upon re-entry to Earth. We also looked for correlations between the connectivity data and individual differences in the severity of the space motion sickness, which is believed to arise from the sensory conflict and to reflect the sensorimotor adaptation processes in microgravity (Heer and Paloski, 2006; Kornilova et al., 2013).

MATERIALS AND METHODS

Participants

Eleven Russian cosmonauts and healthy age- and gender-matched volunteers (11 men not involved in the space program) took part in the study. At the time of the first exam the mean age of the participants was 45 years old (SD = 5) for the cosmonauts and 44 (SD = 6) for the control group. The study was approved as a part of the Brain DTI project by Committee of Biomedicine Ethics of the Institute of Biomedical Problems of the Russian Academy of Sciences and the Human Research Multilateral Review Board (HRMRB) according to the 18th World Medical Assembly of Helsinki, Finland, June 1964, amended by the 41st Assembly, Hong Kong, September 1989. All participants gave written informed consent for the study at enrollment.

In cosmonauts, subjective space motion sickness symptoms during space flight were assessed by a questionnaire first introduced at the MIR orbital station during the 'ANKETA' experiment (Kornilova, 1997) and since then used at the Institute of Biomedical Problems at the Russian Academy of Sciences. The cosmonauts were interviewed after the spaceflight before their vestibular tests on the first or 2nd day post-landing. Space motion sickness symptoms comprised complaints about orientation illusions, dizziness, poor coordination, difficulties in gaze fixation and tracing visual objects, nausea and vomiting (see the full list of questions in **Supplementary Materials**). The combination, intensity, and duration of these reactions were qualified according to the classification accepted in Russia (Kornilova et al., 2002, 2013). For the purpose of the present study, points were ascribed to each cosmonaut's state after the flight: 0 corresponds to no complaints; 1 corresponds to moderately pronounced and rather short SMS syndrome; and 2 corresponds to complaints of pronounced and long lasting SMS syndrome with strong dizziness, vomiting, and discoordination. All control participants of the present study were ascribed zero points on this scale.

Study Design

A 2 × 2 experimental design was used, with group (cosmonauts vs. controls) as a between-subject factor and session (post-flight vs. pre-flight) as a within-subject factor (repeated measures). In the control group, the first scanning session was treated as 'preflight,' and the second as 'post-flight.' According to the study design, only significant Group × Session effects were attributed to spaceflight.

Each cosmonaut was scanned before and after completing a long-term mission to the International Space Station between 2014 and 2017. For one cosmonaut, the data were aggregated

TABLE 1 | General demographics, spaceflight-related information, and scan-to-scan intervals for the cosmonauts and control participants.

Parameter	Cosmonauts		Controls		Difference
	Mean	*SD*	*Mean*	*SD*	*p-value*
Age at the first scan (years)	45	5	44	6	0.680
Days to launch at the first scan	94	36			
Days after landing at the first scan	9.4	2.4			
Scan-to-scan interval (days)	282	63	249	57	0.212
Prior spaceflight experience (missions)	1.1	1.2			
Mission duration	183	55			
Space motion sickness score ('ANKETA')	0.72	0.64	0	0	

across two separate space missions (and counted as the data from one subject). The control participants were scanned twice with comparable time intervals between the scans. A detailed description of demographics and timing data is presented in **Table 1**.

The KORVIT System

The pneumatic KORVIT system (VIT, Saint Petersburg, Russia and Center of Aviaspace Medicine, Moscow, Russia) was used for mechanical stimulation of the soles support zones. The device was initially developed in the Institute of Biomedical Problems at the Russian Academy of Sciences (Grigor'ev et al., 2004; Kozlovskaya et al., 2007; Layne and Forth, 2008) as a mean of compensation of support afferentation deficit and therefore as a countermeasure to microgravity-induced motor impairment. The main component of the system is a pair of plastic boots with inflatable chambers mounted into the boot soles under the metatarsal and the heel zone. This layout of the chambers ensures stimulation of the zones with the highest density of mechanoreceptors and therefore elicits maximal response in the tonic muscle system. The chambers are connected to an air compressor by plastic cables. All parts of the system except for the air compressor are MR safe; during the scanning session the boots and cables were located in the scanner room, while the air compressor was located and operated upon in the scanner console room. The setup is illustrated in **Figure 1**. In the present study, the gait-like simulation mode was used with alternating pressure of 40 kPa cyclically administered to four zones on participants' feet (right heel, right toes, left heel, left toes) with the frequency equal to 75 steps per minute.

According to previous studies, this mode of support stimulation leads to an extensive activation of the sensorimotor cortex (SMC) that controls locomotion (Kremneva et al., 2013). It has also been shown that this paradigm does not reflect actual locomotion, because the person does not make any movements. However, it has been proven that the afferent impulses induced by rhythmic stimulation of the support zone of the sole at a frequency and load similar to those experienced during real walking play an important role in supraspinal control (Kozlovskaya et al., 2007). Moreover, these results are similar to the results of other research groups that used imaginary walking paradigms (Kremneva et al., 2013).

MRI Data Acquisition

All participants were scanned with a 3T GE Discovery MR750 scanner equipped with a 16-channel head, neck and spine (HNS) array coil. The scanner was located at the Federal Center of Medicine and Rehabilitation in Moscow, Russia.

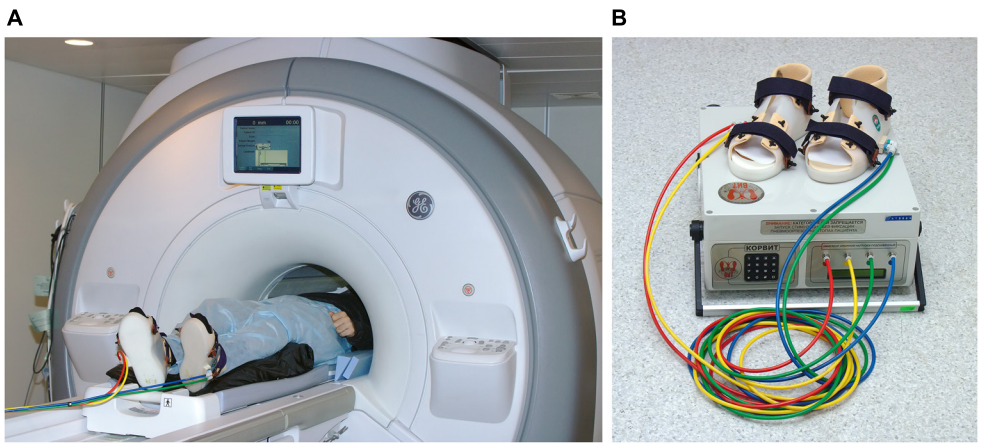

FIGURE 1 | Experimental setup. **(A)** A participant positioned in the scanner wearing the KORVIT system boots. **(B)** Components of the KORVIT system.

For each participant, 160 T2*-weighted functional images were acquired in a single session of the gait-like plantar stimulation paradigm. Four extra volumes were scanned and automatically discarded by the scanner software prior to the acquisition of the functional data in order to achieve magnetic equilibrium. The gradient-echo echo-planar imaging (GRE EPI) pulse sequence was used with the following parameters: TR/TE/FA = 2000 ms/30 ms/77°, FoV = 192 mm × 192 mm × 126 mm, matrix size = 64 × 64 × 42, isotropic voxel size 3 mm. Each volume covered the whole brain with slices oriented parallel to the AC/PC line. The session lasted for approximately 5 min and was administered within the final part of the over 1 h long assessment that included both structural and functional scans (BRAINDTI project protocol). T1-weighted structural images were acquired in the first part of this program using the 3D fast spoiled gradient-echo (FSPGR) pulse sequence with an isotropic voxel size of 1 mm (TR/TE/FA = 7.9 ms/3.06 ms/12°).

Procedure

During the plantar stimulation, a participant would lay in the scanner supine (head first) with KORVIT boots on his feet. He was instructed to keep his head still during the plantar stimulation. Extra foam padding was used to prevent excessive head motion elicited by the pulses of air pressure on the feet. The gait-like stimulation was administered in a block design with alternating 20-s blocks of two conditions: 'stimulation' and 'rest.' The stimulation cycle started with the rest period and was repeated eight times.

Task-Based Activation Data Analysis

Data processing was performed with SPM 12 (Wellcome Institute of Cognitive Neurology[1]) and GLMFlex2 software (Aaron Shultz[2]). Preprocessing included the following steps: slice timing correction; realignment; longitudinal spatial coregistration of structural images from the two scanning sessions; spatial coregistration of the mean structural image and functional images; segmentation of the average structural volume into six tissue volumes; normalization into Montreal Neurological Institute (MNI) space; and spatial smoothing of the functional images with a Gaussian kernel of 8 mm full width at half-maximum (FWHM). Six residual head motion parameters (three for translation and three for rotation) were extracted during the realignment step.

To reveal the task-based activation, data were modeled using the general linear model as implemented in SPM12 software. For each participant, the MR signal was modeled using the canonical hemodynamic response function (HRF) with temporal derivatives (Friston et al., 2007). Temporal derivatives of the HRF were included into the model to prevent possible artifactual differences between groups or conditions. This concern was raised because the influence of spaceflight on the neurovascular coupling and HRF parameters is not yet known, but some effect is highly plausible given the alterations in cardiovascular functioning in space (Zhu et al., 2015) and especially the alterations of brain hemodynamics (Kawai et al., 2003; Blaber et al., 2013; Taylor et al., 2013) due to fluid shifting to the upper body. The data were analyzed as a block design with one experimental (plantar stimulation) condition while the baseline condition was not explicitly modeled to avoid model redundancy. Six parameters describing the head motion throughout the experimental session were included into the model as nuisance regressors. *T*-test contrasts for the BOLD signal change evoked by the plantar stimulation were obtained from both HRF and HRF temporal derivative regressors and combined into a single image for further use in the second-level analysis with the 'derivative boost' method (Lindquist et al., 2009; Steffener et al., 2010) implemented in the *spmup_hrf_boost* script (Pernet, 2014). A 2 × 2 ANOVA with group (cosmonauts vs. healthy controls) as a between-subject factor and session (pre-flight vs. post-flight) as a within-subject factor was performed as a second-level analysis scheme with the GLMFlex2 software. The results were assessed with a FDR-corrected cluster-wise threshold of $q = 0.05$ based on an uncorrected voxel-wise threshold of $p = 0.001$. Lenient statistical thresholds ($p < 0.05$ uncorrected, $k = 5$) were additionally applied to the group activation map obtained from the data of all 22 participants (both experimental and control groups) in order to define ROIs and the sensorimotor system mask for subsequent connectivity analyses. Peak activation coordinates were labeled with either FSL Harvard-Oxford maximal likelihood cortical and subcortical atlases (Desikan et al., 2006) or the AAL atlas (Tzourio-Mazoyer et al., 2002) for the cerebellum.

Task-Based Connectivity Data Preprocessing

CONN Functional Connectivity Toolbox v. 17a (Whitfield-Gabrieli and Nieto-Castanon, 2012[3]) was used for the task-based connectivity preprocessing and further statistical analysis. Several standard procedures in the Conn toolbox were applied to the data already preprocessed for the task-based activation analysis in order to account for the residual motion-induced artifacts and physiological noise (denoising). First, head motion artifact detection was performed with the Artifact Detection Toolbox (ART[4]). Medium level thresholds that result in rejecting 3% of the normative sample data were applied; images demonstrating scan-to-scan head motion of more than 0.9 mm or global mean intensity change of more than 5 SDs were considered outliers. Outliers were subsequently included as nuisance regressors into the denoising linear model along with the residual head motion parameters. Another set of nuissance regressors was introduced by the anatomical component-based noise correction technique (aCompCor; Behzadi et al., 2007). With this method, noise ROIs are defined within the white matter and CSF masks individually segmented for each participant. The signal from the noise ROIs is decomposed with a principal component analysis (PCA) and time courses of the resulting components are regressed out from the data. The main BOLD-signal effects of the plantar

[1] www.fil.ion.ucl.ac.uk/spm

[2] http://mrtools.mgh.harvard.edu/

[3] http://www.nitrc.org/projects/conn

[4] http://www.nitrc.org/projects/artifact_detect

stimulation and rest blocks were also regressed out to restrict the analysis to within-condition connectivity alterations rather than global changes of the correlation evoked by the task onset or offset. The linear detrending term was also applied. Then a standard temporal high-pass filter with a cutoff of 0.008 Hz was applied on the time series in order to further restrict the analysis to signal fluctuations which characterize task-based fMRI BOLD frequency band.

Two approaches to the task-based functional connectivity analysis were taken: voxel-to-voxel (data-driven) and ROI-to-ROI (hypothesis-driven). Follow-up hypotheses-driven seed-to-voxel analyses were also used to aid interpretation of the results. The connectivity results were labeled with the Harvard-Oxford and AAL atlases as well as the activation data.

Task-Based Connectivity Voxel-to-Voxel Analysis

Firstly, voxel-to-voxel analysis was conducted to obtain the intrinsic connectivity contrast (ICC) values for each voxel in the whole brain. ICC was computed as a mean absolute value of the correlations of the time series for a given voxel with all other voxels included in the analysis (Martuzzi et al., 2011). The ICC values for each participant and condition (pre-flight and post-flight plantar stimulation and rest) were further used in the second-level ANCOVA with Group (cosmonauts vs. healthy controls) as a between-subject factor and session (post-flight vs. pre-flight) as a within-subject factor. Because of the imperfect cerebellum coverage in several scans, a concern was raised that the difference in the cerebellum ROIs between the preflight and post-flight sessions in the affected participants might also result in between-session differences in connectivity values. To account for this potential confound, the mean-centered difference in the total volume of the cerebellar network ROIs (defined with the Conn network atlas) for each participant was included in the analysis as a between-subject covariate. A Group × Session interaction was assessed with a FDR-corrected cluster-wise threshold of $p = 0.05$, $q = 0.05$ based on an uncorrected voxel-wise two-sided threshold of $p = 0.001$.

Task-Based Connectivity ROI-to-ROI Analysis

An exploratory ROI-to-ROI analysis was adopted to test for the possible effects of long-duration spaceflight. The set of ROI selected for the analysis covered the sensorimotor, visual, proprioceptive, and vestibular brain systems thus including all main sources of afference utilized by the motor control system.

First, we included eight clusters identified in the activation map obtained from the plantar stimulation versus rest contrasts in all participants (cosmonauts and controls) at the liberal statistical threshold, obtained as described above (**Table 3**). Then all clusters from the sensorimotor, cerebellar, and visual systems from the Conn Networks atlas were also included. Since the insula plays an important role in motor, vestibular and proprioceptive functions, we included the ROIs for the right and left anterior and posterior insula (outlines from Kelly et al., 2012 were used). The bilateral ROIs for the thalamus, which is believed to be a relay station for vestibular signals (Lopez and Blanke, 2011), and the putamen, which is believed to play a crucial role in proprioception (Goble et al., 2012), were taken from the Harvard-Oxford atlas. Other ROIs were constructed with the MarsBar toolbox (Brett et al., 2002) as spheres around coordinates taken from the literature. The selection of the vestibular ROI replicated that by Van Ombergen et al. (2017b), with a different outline of the thalamus ROI as the only exception. Besides the insula and thalamus, vestibular ROIs included the right parietal operculum area 2 (rOP2), which is currently believed to represent the human vestibular cortex; the precuneus; the inferior parietal lobule, which is believed to be a part of the multimodal vestibular cortex (Zu Eulenburg et al., 2012; Dieterich and Brandt, 2015); and the bilateral vestibular nuclei (Kirsch et al., 2016). Proprioception ROIs were selected on the basis of data presented by Goble et al. (2012) and, besides the putamen, included the inferior frontal gyrus (IFG) and the inferior parietal cortex (BA40) bilaterally. The initially selected set of ROIs was further cross-checked for intersections, and only one of the two ROIs were included if a significant overlap was found (for example, the spherical ROI for the rOP2 was almost entirely covered by the activation-based rOP ROI). Since only differential contrasts of connectivity across groups and conditions were further considered, the residual marginal ROI overlap was not taken into account. Characteristics of the 27 areas forming the resulting ROI set are presented in **Table 2**.

The signal from each ROI was extracted only from gray matter voxels of the unsmoothed functional volumes, in order to avoid any additional risk of contaminating the data with white matter or CSF signals or with signals from other ROIs. Then, the task modulation of the ROI-to-ROI functional connectivity was assessed for the 'preflight' and the 'post-flight' sessions with the individual general psychophysiological interaction model (gPPI; McLaren et al., 2012) for each participant. The resulting differential ROI-to-ROI connectivity values for the active plantar stimulation condition over the implicitly modeled baseline were further used in the second-level ANCOVA with group (cosmonauts vs. healthy controls) as a between-subject factor and session (pre-flight vs. post-flight) as a within-subject factor, and the mean-centered difference in the total volume of the cerebellar network ROIs as a covariate. The results were considered at the levels of (a) individual modified connection (two-sided t-test, analysis-level FDR-corrected, $p_{corr} < 0.05$); (b) ROI demonstrating a modified connectivity pattern; and (c) network (clusters of modified connections). At the latter two levels we used network-based statistics, taking into account the connection intensity (NBS; Zalesky et al., 2010) for the correction for multiple comparisons (FDR at the ROI level and FWE at the network level, $p_{corr} < 0.05$, cluster-defining threshold $p < 0.05$ uncorrected).

The NBS statistic utilizes the permutation test and may be understood as an analog of the topological correction for multiple comparisons in the connectivity domain (with individual connections in place of voxels and subnetworks as clusters of connections). Therefore the NBS statistics is more

TABLE 2 | Characteristics of the ROIs selected for the ROI-to-ROI analysis of the functional connectivity between the sensorimotor, visual, proprioceptive, and vestibular systems.

ROI	System	Source/reference	Shape	Center of mass MNI coordinates		
				x	*y*	*z*
SensoriMotor. Lateral (L)	Sensorimotor	Conn Networks	Cluster	−55	−12	29
SensoriMotor. Lateral (R)	Sensorimotor	Conn Networks	Cluster	56	−10	29
SensoriMotor. Superior	Sensorimotor	Conn Networks	Cluster	0	−31	67
Cerebellar.Anterior (Lobules VI–IX)	Cerebellar	Conn Networks	Cluster	0	−63	−30
Cerebellar.Posterior (Crus)	Cerebellar	Conn Networks	Cluster	0	−79	−32
Visual.Primary	Visual	Conn Networks	Cluster	2	−79	12
Visual.Ventral	Visual	Conn Networks	Cluster	0	−93	−4
Visual. Dorsal (L)	Visual	Conn Networks	Cluster	−37	−79	10
Visual. Dorsal (R)	Visual	Conn Networks	Cluster	38	−72	13
Anterior Insula (L)	Proprioception, vestibular	Kelly et al., 2012	Cluster	−35	12	−5
Posterior Insula (L)	Proprioception, vestibular	Kelly et al., 2012	Cluster	−38	−9	2
Anterior Insula (R)	Proprioception, vestibular	Kelly et al., 2012	Cluster	38	8	−5
Posterior Insula (R)	Proprioception, vestibular	Kelly et al., 2012	Cluster	39	−12	6
Putamen (LR)	Proprioception	Harvard-Oxford atlas, subcortical; Goble et al., 2012	Cluster	−25/26	0/2	0/0
Thalamus (LR)	Vestibular	Harvard-Oxford atlas, subcortical	Cluster	−10/11	−19/−18	6/7
IFG (L)	Proprioception	Goble et al., 2012	10-mm sphere	−49	13	5
IFG (R)	Proprioception	Goble et al., 2012	10-mm sphere	53	16	7
IPC.BA40 (L)	Proprioception, vestibular	Goble et al., 2012	10-mm sphere	−62	−48	40
IPC.BA40 (R)	Proprioception, vestibular	Goble et al., 2012	10-mm sphere	60	−44	48
Vestibular nuclei (LR)	Vestibular	Kirsch et al., 2016	Two 5-mm spheres (L and R)	−16/16	−36/36	−32/−32
Precuneus	Vestibular	Zu Eulenburg et al., 2012	10-mm sphere	0	−52	27
Operculum (L)	Sensorimotor, proprioception	Task-based activation	Cluster	−52	−31	22
Operculum (R)	Sensorimotor, proprioception, vestibular	Task-based activation	Cluster	53	−28	22
Parahippocampal Gyrus	Visual	Task-based activation	Cluster	17	−24	−15
Cerebellum-01	Cerebellar	Task-based activation	Cluster	2	−42	−8
Cerebellum-02	Cerebellar	Task-based activation	Cluster	−15	−37	−24
Cerebellum-03	Cerebellar	Task-based activation	Cluster	17	−37	−26

sensitive but less spatially specific than the more conventional analysis at the level of individual connection. Due to the nature of the NBS statistics, inference limitations apply: the subnetworks may only be discussed in their integrity; no individual connection change may be considered significant on the basis that it belongs to a significantly changing NBS network. As implemented in Conn, the ROI-level NBS analysis treats only connections originating from the ROI under consideration and involves an extra FDR correction for the number of ROIs.

Follow-Up Seed-to-Voxel Analysis

To aid interpretation of the results, we performed a follow-up whole-brain seed-to-voxel analysis using as seeds the ROIs that demonstrated significant effects of Group × Scanning session interaction in the NBS ROI-to-ROI analysis (ROI

TABLE 3 | Clusters of activation revealed by the plantar stimulation in all participants.

Cluster		Volume, voxels (mm^3)	*T*-statistics	MNI coordinates (center of mass/peak)			Region labels+
				x	*y*	*z*	
(1) SMC/SMA bilateral	FDR_C-corr.	181 (4887)		−1	−36	67	Precentral gyrus, post-central gyrus
	$p < 0.05$ uncorr.	430 (11610)		−1	−35	66	Post-central gyrus, precentral gyrus, precuneous cortex, superior parietal lobule
	Peaks		8.91*	0	−34	65	Post-central gyrus
			4.67*	−3	−19	68	Precentral gyrus
			4.23*	15	−40	71	Post-central gyrus
			3.31	6	−13	68	Juxtapositional lobule cortex (formerly supplementary motor cortex)
(2) Right operculum	FDR_C-corr.	93 (2511)		51	−29	22	Parietal operculum cortex, planum temporale
	$p < 0.05$ uncorr.	308 (8316)		53	−28	22	Parietal operculum cortex, planum temporale, supramarginal gyrus (anterior division)
	Peaks		5.59*	45	−33	22	Parietal operculum cortex
			5.09*	66	−31	17	Superior temporal gyrus, posterior division
			4.92*	48	−22	20	Parietal operculum cortex
			3.31	32	−24	16	Insular cortex
			2.60	66	−19	17	Post-central gyrus
(3) Left operculum	FDR_C-corr.	68 (1836)		−49	−30	21	Parietal operculum cortex, central opercular cortex
	$p < 0.05$ uncorr.	294 (7938)		−52	−31	22	Parietal operculum cortex, planum temporale, supramarginal gyrus (anterior division)
	Peaks		6.26*	−48	−31	23	Parietal operculum cortex
			3.83*	−54	−22	17	Central opercular cortex
			2.23	−33	−28	20	Central opercular cortex
(4) Cerebellum-01	$p < 0.05$ uncorr.	55 (1485)		2	−42	−8	Vermis III–IV, brain stem
	Peaks		3.68	0	−46	−10	Vermis IV–V
			3.11	0	−31	−4	Brain stem
(5) Right temporal pole/insula	$p < 0.05$ uncorr.	41 (1107)		42	6	−15	Temporal pole, planum polare, insular cortex
	Peaks		2.44	45	−4	−7	Planum polare
			2.21	39	11	−25	Temporal pole
			2.10	44	13	−12	Temporal pole
(6) Cerebellum-02	$p < 0.05$ uncorr.	36 (972)		−15	−37	−24	Left cerebellum III, IV–V lobules
	Peaks		2.83	−9	−40	−25	Left cerebellum III
			3.33	−18	−34	−25	Left cerebellum IV–V
(7) Parahippocampal gyrus	$p < 0.05$ uncorr.	11 (297)		17	−24	−15	Parahippocampal gyrus, posterior
	Peaks		2.55	15	−25	−16	Parahippocampal gyrus, posterior
(8) Cerebellum-03	$p < 0.05$ uncorr.	10 (270)		17	−37	−26	Right cerebellum IV–V lobules
	Peaks		2.50	21	−37	−28	Right cerebellum IV–V

+*Only labels covering at least 5% of the cluster volume are listed.* **Peaks within the clusters that survived* FDR_C *correction.*

level). While the NBS analysis does not allow for any inference regarding individual, pairwise connections between ROIs, the seed-to-voxel analysis aims at testing whether the observed connectivity alterations are diffuse in their nature or have any compact localizable addressees. We also performed a whole-brain seed-to-voxel analysis using as a seed the cluster revealed by the ICC analysis as sensitive to the cosmonaut vs. control, post- vs. pre-, task vs. baseline interaction.

In each seed-to-voxel analysis, we used the PPI connectivity data computed between the seed region and every brain voxel outside the seed region. These differential values were entered into the second-level ANCOVA, analogous to what was implemented for the ROI-to-ROI analysis: group (cosmonauts vs. healthy controls) as a between-subject factor, session (pre-flight vs. post-flight) as a within-subject factor, and the mean-centered difference in the total volume of the cerebellar network ROIs as a covariate. Seeds were tested one at a time.

Additionally, we conducted a set of second-level ANCOVAs, testing for possible correlations between the post-flight vs. pre-flight difference in connectivity of the seeds and the individual scores of space motion sickness severity (the mean-centered difference in the total volume of cerebellar network ROIs was also included as a covariate of no interest). Again, seeds were tested one at a time.

Besides the correction for multiple comparisons performed at the level of each resulting spatial map (cluster-wise topographic FDR correction; $p < 0.05$, $q < 0.05$; voxel-wise cluster-forming two-sided threshold $p < 0.001$ uncorrected), the statistical thresholds for the results were also corrected for the total number of seed-to-voxel analyses ($p < 0.05/12 = 0.004$).

RESULTS

Assessment of Potential Confounds

There were no significant differences in the mean age of the groups at the first scanning session (see **Table 1**). No statistically significant differences were found between groups or sessions in the standard deviations of displacement or rotation across any of the six registered head motion parameters. The percentage of the scans classified by the ART toolbox as invalid varied from 0 to 8% per participant; the total of 1.22% scans were discarded as invalid for the entire dataset. No participant was excluded from the analysis due to excessive head motion. The scan-to-scan head motion before scrubbing averaged 0.15 mm, *SD*: 0.05 mm per participant with a mean maximum motion of 1.14 mm, *SD*: 1.28 mm. No effects of the group, session or interaction of these factors on the general voxel-to-voxel correlation (GCOR; Saad et al., 2013) were revealed.

Brain Activation

A 2 × 2 ANOVA showed no effect of Group × Scanning session interaction on brain activation evoked by the plantar stimulation paradigm. The aggregated statistical map for both groups revealed an activation pattern that included the primary SMC, the supplementary motor cortex (SMA), extensive regions in operculum bilaterally, and, when applying low statistical thresholds, areas of the right insula and the temporal pole and of the anterior cerebellum (see **Figure 2** and **Table 3**).

Voxel-to-Voxel Connectivity

The whole-brain analysis revealed a cluster in the right posterior supramarginal gyrus (pSMG; 567 mm^3; center of mass: $x = 63$, $y = -37$, $z = 13$; see **Figure 3A**) demonstrating the effect of a Group × Scanning session interaction for the ICC change during the task blocks over the baseline.

ROI-to-ROI Connectivity

ROI-to-ROI analysis exploring the connectivity between the motor, somatosensory, visual, proprioceptive, cerebellar and vestibular brain systems, demonstrated significant post-flight alterations compared to the between-session differences observed in the control group.

Alterations were found at the levels of individual connection, ROI and subnetwork. The following individual connections showed modifications significant at the $p < 0.05$ threshold after analysis-level FDR-correction. Functional coupling between the right and left posterior insulae significantly increased in cosmonauts post-flight, while connections degraded between the posterior cerebellum and the primary visual cortex, and between the anterior cerebellum (activation cluster Cerebellum-03) and right parietal cortex (BA40).

In order to detect more subtle although less spatially specific changes, we computed ROI-level and network-level network-based statistics by intensity (NBS; Zalesky et al., 2010). The network-level NBS identified a subnetwork demonstrating effects of a Group × Scanning session interaction (at $p < 0.05$, FWE-corrected; see **Figure 4**). This subnetwork included five regions also showing significant connectivity modifications at the ROI level (at $p < 0.05$, FDR-corrected), namely: the vestibular nuclei (intensity = 22.88, size = 8), the right parietal cortex (intensity = 20.24, size = 6), the anterior part of the cerebellar network (Conn Networks atlas; intensity = 17.47, size = 7), the right posterior insula (intensity = 16.87, size = 5) and the left anterior insula (intensity = 16.47, size = 6). It is noteworthy that all suprathreshold connections of the vestibular nuclei, the right parietal cortex and the cerebellar network (anterior part) ROIs demonstrated a negative shift in PPI values (task vs. baseline differential connectivity) in cosmonauts post-flight vs. pre-flight. Connections comprising the altered networks of the affected ROIs are also presented in **Figure 5** and **Table 4**.

Seed-to-Voxel Connectivity

Regions identified in the NBS ROI-to-ROI and ICC results as sites involved into connectivity alterations due to the spaceflight were used as seeds for the follow-up seed-to-voxel analyses performed according to the same scheme as in the main analysis (cosmonauts vs. controls, post-flight vs. pre-flight). This approach aimed to check whether the observed connectivity changes are diffuse in their

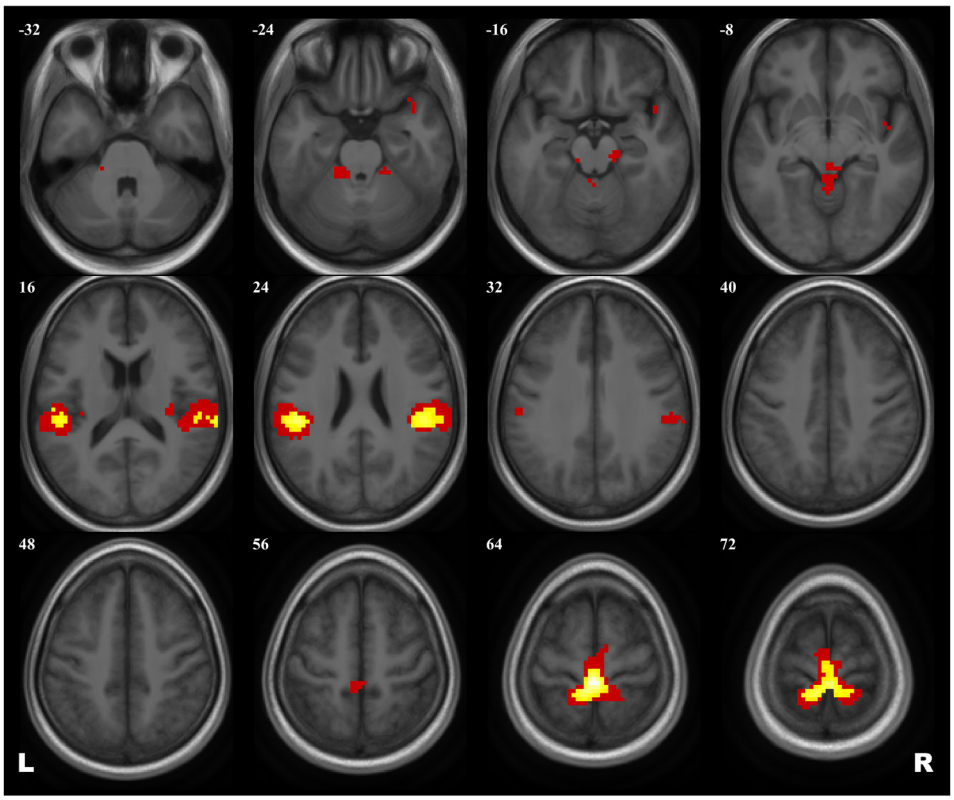

FIGURE 2 | Group map of the activation elicited by plantar stimulation in all participants (both cosmonauts and healthy controls). Yellow areas depict activation at a reliable statistical threshold (cluster-wise FDR correction, $q < 0.05$, $p < 0.05$; voxel-wise cluster-defining threshold, $p < 0.001$ uncorrected). Activation at a lenient statistical threshold ($p < 0.05$ uncorrected voxel-wise, $k = 5$) is shown in red. The statistical images are presented as overlays upon the average structural image of all participants converted to the MNI space.

nature or have any compact localizable addressees across the whole brain.

The second set of the seed-to-voxel analysis employed the same six seeds as described above (five ROIs from the NBS results, and the rpSMG cluster from the ICC results). Now the post-flight vs. pre-flight differences in PPI values characterizing the connectivity of these regions with the rest of the brain were tested for significant correlations with the individual SMS scores.

The results showed a positive correlation of the severity of space motion sickness with differential post-to-preflight, task-to-baseline connectivity between the rpSMG seed and the left insular, opercular, and frontal orbital cortices (**Figure 3B** and **Table 5**; cluster-defining threshold $p < 0.001$, cluster-level FDR correction with correction for the total number of seed-to-voxel follow-up analyses: $p < 0.05/12 = 0.004$).

DISCUSSION

The present study reports on alterations of task-based functional brain connectivity in a group of 11 cosmonauts after spaceflight as compared to a healthy control group. To recruit the postural and locomotor sensorimotor mechanisms that are usually most significantly impaired when space travelers return to the Earth, a plantar stimulation paradigm was used in a block design fMRI study.

Task-specific functional connectivity modifications were revealed within a set of regions involving the sensorimotor, visual, proprioceptive, and vestibular neural networks. The most notable post-flight findings include an increase in stimulation-specific connectivity of the right posterior supramarginal gyrus with the rest of the brain (as revealed by the ICC measure); strengthened connections between the left and right insulae and decreased coupling of the cerebellum with the visual cortex and with the right inferior parietal cortex (BA40) (revealed by the connection-wise ROI-to-ROI approach); and altered connectivity of the bilateral insulae, vestibular nuclei, right inferior parietal cortex (BA40) and cerebellum with other areas associated with motor, visual, vestibular, and proprioception functions (revealed by the NBS approach). A correlation was also observed between the severity of space motion sickness symptoms and connectivity between the right posterior supramarginal gyrus and the left insular region.

Since no previous studies have reported data on task-based functional brain connectivity after an actual space flight, we are unable to perform a direct comparison of our results with the previous findings. However, our data are

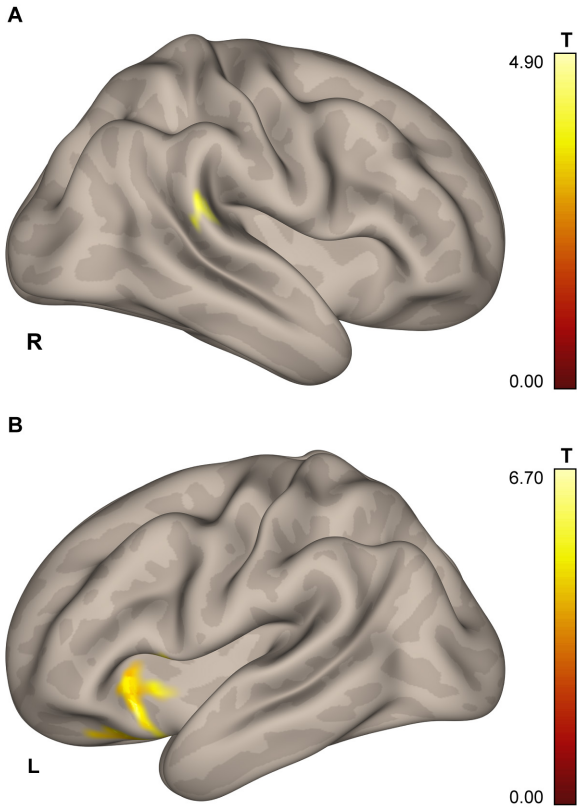

FIGURE 3 | Results of the ICC and follow-up seed-to-voxel analysis. **(A)** Area in the lower portion of the right posterior supramarginal gyrus demonstrating higher connectivity with the rest of the brain for cosmonauts vs. controls, post- vs. pre-flight, plantar stimulation vs. rest, as revealed by the ICC analysis (cluster-wise FDR correction, $q < 0.05$, $p < 0.05$; voxel-wise cluster-defining threshold, $p < 0.001$ uncorrected). **(B)** Cluster in the left orbitofrontal cortex, insula and operculum, demonstrating correlation between the severity of space motion sickness and post- vs. pre-flight, plantar stimulation over the resting baseline difference in functional connectivity, with the seed in the rpSMG area shown in the **(A)**. Results are shown after the cluster-wise FDR correction, $q < 0.05$, $p < 0.004 = 0.05/12$; voxel-wise cluster-defining threshold, $p < 0.001$ uncorrected.

consistent with many aspects of the broader literature, including structural neuroimaging and microgravity analog research. At the same time, as shown by the example of the EEG, which is so far the only neuroimaging technique accessible both in space and in terrestrial settings, neurophysiological data from actual and simulated microgravity may be substantially inconsistent due to multiple factors such as details of the environment, stressors and emotional states that might contaminate the observed effects (Marušč et al., 2014; Van Ombergen et al., 2017c).

Given the lack of data available for direct comparison in the field, later in the discussion we introduce some speculations that we believe to be helpful for hypothesis generating and future research. We hope that subsequent progress in neuroimaging studies of microgravity would rule out some of the theories discussed below in favor of the others.

Task-Based Activation

The task-based fMRI activation pattern evoked by the KORVIT plantar stimulation system in our study included the primary SMC, the SMA, the SII cortex (operculum) bilaterally, and, at a liberal statistical threshold, cerebellar and insular areas. Such a pattern is typical for passive gait-like plantar stimulation (Dobkin et al., 2004; Golaszewski et al., 2006; Kremneva et al., 2013; Jaeger et al., 2014; Labriffe et al., 2017) and is characterized by reduced insular and cerebellar activation compared to active foot stimulation paradigms (Sahyoun et al., 2004). KORVIT gait-like stimulation was applied to the sole zones with the maximal density of mechanoreceptors, and we believe that through proper modeling of the support afference our fMRI paradigm evoked the neural circuits essential for human upright posture and normal bipedal locomotion (Kozlovskaya et al., 2007) which might be modified in microgravity and, therefore, were the target of our research. At the same time, it should be noted that KORVIT gait-like stimulation does not activate the neural representation of the tonic muscle system exclusively. This is due to the involvement of other skin receptors, the low spatial resolution of the fMRI, and, last but not the least, the complex principles of individual muscle representation in the SMC (Kakei et al., 1999), resulting in a substantial overlap of different muscle projections (Melgari et al., 2008). Therefore, we refer to the pattern of activation obtained in our study as the neural correlates of plantar stimulation rather than the neural correlates of support afference, or tonic muscle system.

The present study failed to reveal any spaceflight-related significant differences in brain activation evoked by the plantar stimulation. In the presence of substantial individual variability among the cosmonauts (reported also by Roberts et al., 2010 in a pilot HDBR study), this null result may indicate insufficient statistical power. However, it may also mean that the 'core' neural system associated with the reaction to support loading remains intact after microgravity exposure, or that it completely recovers by the time of the examination (9th day after landing). The latter interpretation is supported by a recent study by Yuan et al. (2018a), who found altered activation in the cerebellum, hippocampus, and visual areas elicited by an active foot tapping fMRI paradigm in a group of volunteers during 70-day HDBR, an effect which was not found a week after HDBR. Also, microgravity-induced changes within the human sensorimotor system are likely to be paradigm-dependent, as was illustrated by our earlier case study (Demertzi et al., 2016) that reported enhanced activation in the SMA during an imaginary tennis task, but not a task involving imagery navigation through a house, after spaceflight.

Intrinsic Connectivity Contrast Data

Our data-driven approach revealed altered ICC for the plantar stimulation over baseline within the right posterior SMG in cosmonauts after spaceflight in comparison to the control group. This part of the SMG belongs to the temporoparietal junction (TPJ) region which also contains a part of the angular gyrus and the most caudal portion of the superior

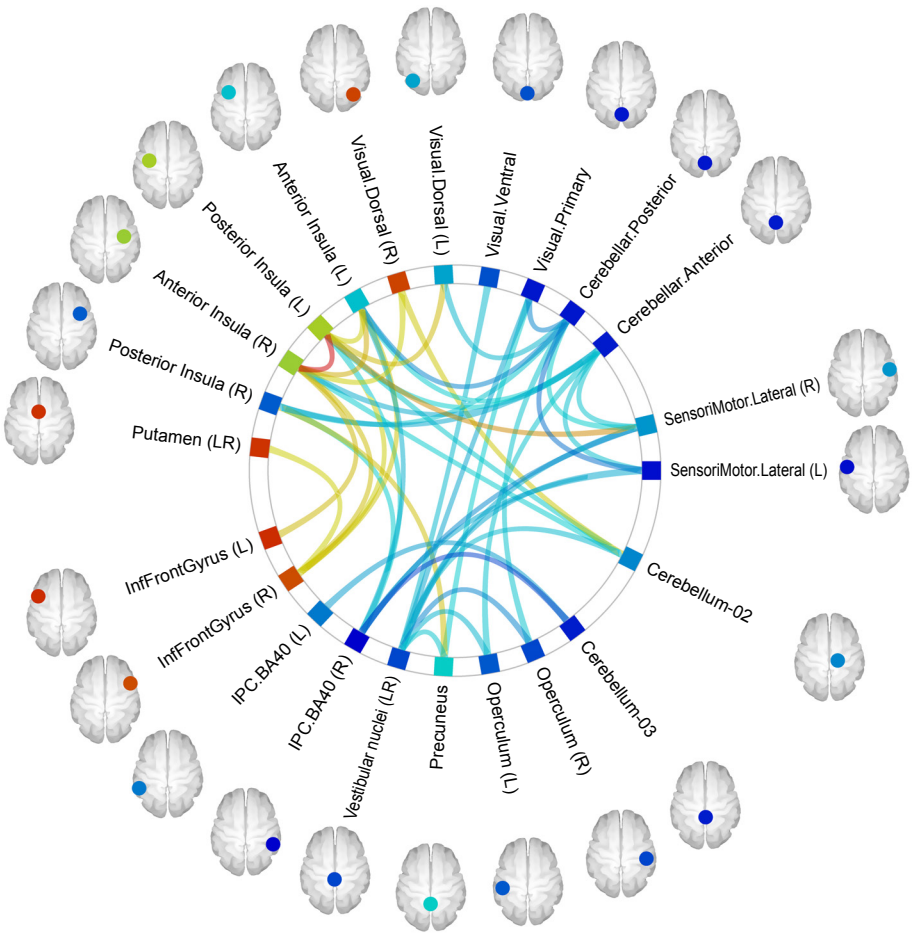

FIGURE 4 | A subnetwork identified by the NBS network-level ROI-to-ROI connectivity analysis and demonstrating changes in PPI connectivity values post-flight vs. pre-flight, cosmonauts vs. controls. Line color indicates the sign and magnitude of the effect for individual connections comprising the network. The network-defining threshold (connection-wise) was set to $p < 0.05$, and the network-level results were FWE-corrected for multiple comparisons (NBS by intensity, $p < 0.05$ at the network level).

temporal gyrus. The TPJ region in general is believed to play an important role in the processes of motor adaptation, multisensory integration (Grefkes and Fink, 2005) and bodily self-consciousness (Pfeiffer et al., 2014). Therefore our present finding resonates with the recent results by Van Ombergen et al. (2017d), who studied healthy participants exposed to acute alterations of gravity during a parabolic flight and found a decreased resting-state ICC in the right TPJ, specifically within the angular gyrus. Additionally, their results revealed increased connectivity of this region with the SMG bilaterally. The pSMG area is known to be involved in the processing of vestibular input (Bense et al., 2001), in the perception of being upright (Kheradmand et al., 2013), and in the visual perception of object motion according to the laws of gravity (Indovina et al., 2005); the angular gyrus is associated with coordination of sensory weighting and sensory realignment mechanisms during sensorimotor adaptation (Block et al., 2013). Interestingly, the two regions showing signs of structural connectivity disruption after the spaceflight that were found in a recent diffusion MRI study by Lee et al. (2019) also lie in the white matter below the right TPJ region next to the rpSMG. The involved white matter regions belong to the superior longitudinal fasciculus, the inferior longitudinal fasciculus, and the inferior fronto-occipital fasciculus, which are all important for connecting the parietal and frontal cortices and play a role in sensory integration (Lee et al., 2019).

While interpretations involving the functions listed above are appealing, they should be considered with caution because of the heterogeneity and polyfunctional nature of the TPJ (Lee and McCarthy, 2016; Schuwerk et al., 2017) and because of the lack of exact overlap between the coordinates reported in the discussed studies and the locus of our finding (except for the overlap with results by Indovina et al., 2005). The latter is especially important given the considerable spatial extension of both the

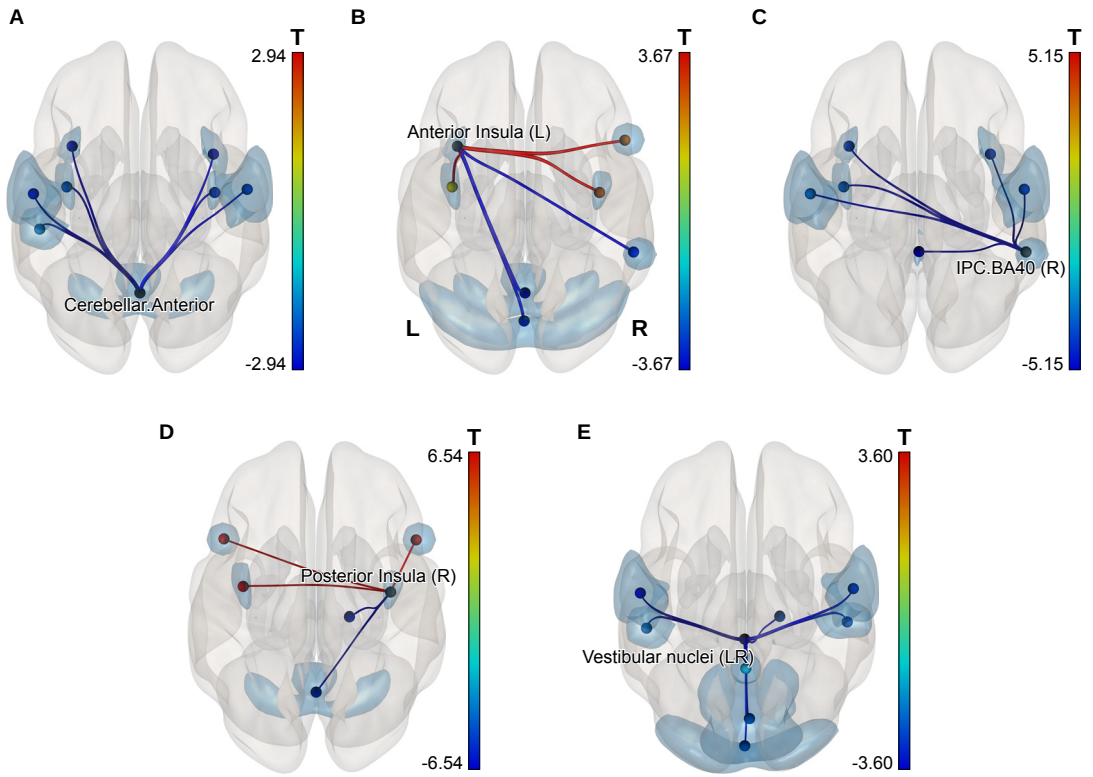

FIGURE 5 | ROI-level networks showing significant PPI connectivity modifications in the NBS analysis post-flight vs. pre-flight, cosmonauts vs. controls for the following regions: **(A)** the anterior part of the cerebellar network (Conn Networks atlas); **(B)** the left anterior insula; **(C)** the right inferior parietal cortex, BA40; **(D)** the right posterior insula; **(E)** the vestibular nuclei. The network-defining threshold (connection-wise) was set to $p < 0.05$, and the ROI-level results were FDR-corrected for multiple comparisons (NBS by intensity, $q < 0.05$, $p < 0.05$ at the ROI level). Line color indicates the sign and magnitude of the effect for individual connections comprising the networks. Note that due to the nature of the NBS analysis, no individual connection contributing to the significantly changed network may be considered as significantly altered on its own. Cyan blobs indicate the location of the ROIs for the illustrative purposes.

TPJ and the SMG. Remarkably, the region in the right inferior parietal cortex (BA40) that in the present study was identified as a region showing not increasing but decreasing connectivity after the spaceflight with the ROI-to-ROI approach, is also located within the rSMG, although at a distance from the cluster revealed by the ICC approach.

ROI-to-ROI Analysis

Decreased Connectivity of the Vestibular Nuclei

Altered connectivity of the vestibular nuclei was among the most predictable results of the current study because of the severe impact of microgravity on the vestibular system, starting with the deconditioned gravity sensing otolith system (Moore et al., 2003; Kornilova et al., 2012; Hallgren et al., 2016). Although the nature of the NBS results does not allow for discussion of any individual connection but only of the entire cluster of the assessed connections of the vestibular nuclei, our data make evident the decreased connectivity of the vestibular nuclei with multiple regions including other parts of the vestibular brain system (operculum, precuneus, inferior parietal cortex) as well as with motor, somatosensory, cerebellar, and visual regions in cosmonauts after spaceflight. Such disintegration cannot be accounted for by the decreased activity in the vestibular nuclei, because it was shown previously that monkeys traveling to space with chronically implanted electrodes exhibited not decreased but increased activity of the vestibular nuclei during gaze test performance both inflight and post-flight (Sirota et al., 1988; Badakva et al., 2000; Slenzka, 2003). Therefore, the more plausible explanation of the relative disconnection of the vestibular nuclei involves down-weighting of the vestibular input in order to reduce the conflict between the information from different sensory modalities (proprioception, visual, vestibular) (Block and Bastian, 2011). This idea is also supported by the co-activation pattern evoked by vestibular stimulation in a recent HDBR study by Yuan et al. (2018b) and by the results of the PF study (Van Ombergen et al., 2017d).

Increased Interinsular Connectivity

Interestingly, although the insula is considered to be an important part of the human vestibular cortex, and we found that spaceflight significantly alters connectivity of both insulae and the vestibular nuclei, no modifications of the functional connectivity between these two structures were found (even at a liberal, uncorrected threshold), suggesting that the down-weighting of the vestibular input occurs early within the stream of vestibular information processing. At the same time, the right posterior

TABLE 4 | Results of the ROI-level NBS analysis (NBS by intensity).

Analysis unit	Intensity	*t*(19)	*p*-unc.	*p*-FDR	*p*-FWE
Network_1/1 (Size = 71)	204.24		0.0084		0.0086
Seed Vestibular Nuclei (VNLR)	22.88		0.0015	0.0397	0.0332
VNLR—Visual.Primary		−3.60	0.0019	0.0261	
VNLR— Operculum (R)		−3.58	0.002	0.0261	
VNLR—SensoriMotor.Lateral (L)		−3.04	0.0067	0.0578	
VNLR—Operculum (L)		−2.72	0.0137	0.0715	
VNLR—SensoriMotor.Lateral (R)		−2.71	0.0138	0.0715	
VNLR—Cerebellum-02		−2.63	0.0166	0.072	
VNLR—Visual.Ventral		−2.37	0.0284	0.1054	
VNLR—Precuneus		−2.22	0.0384	0.1249	
Seed Proprio.IPC.BA40 (R)	20.24		0.0031	0.042	0.0637
IPC.BA40 (R)—Cerebellum-03		−5.15	0.0001	0.0015	
IPC.BA40 (R)—SensoriMotor.Lateral (R)		−4.06	0.0007	0.0087	
IPC.BA40 (R)—Anterior Insula (L)		−3.49	0.0025	0.0214	
IPC.BA40 (R)—SensoriMotor.Lateral (L)		−2.84	0.0105	0.0686	
IPC.BA40 (R)—Anterior Insula (R)		−2.45	0.024	0.1246	
IPC.BA40 (R)—Posterior Insula (L)		−2.26	0.0355	0.1536	
Seed Cerebellar.Anterior	17.47		0.0065	0.0457	0.124
Cerebellar.Anterior—Anterior Insula (R)		−2.94	0.0084	0.1186	
Cerebellar.Anterior—Posterior Insula (R)		−2.90	0.0091	0.1186	
Cerebellar.Anterior—SensoriMotor.Lateral (L)		−2.52	0.021	0.1456	
Cerebellar.Anterior—Operculum (L)		−2.40	0.0269	0.1456	
Cerebellar.Anterior—SensoriMotor.Lateral (R)		−2.38	0.028	0.1456	
Cerebellar.Anterior—Anterior Insula (L)		−2.19	0.041	0.1682	
Cerebellar.Anterior—Posterior Insula (L)		−2.14	0.0453	0.1682	
Seed Posterior Insula (R)	16.87		0.0076	0.0457	0.1417
Posterior Insula (R)—Posterior Insula (L)		6.54	0.000	0.0001	
Posterior Insula (R)—Cerebellar.Anterior		−2.77	0.0123	0.107	
Posterior Insula (R)—IFG (L)		2.76	0.0123	0.107	
Posterior Insula (R)—IFG (R)		2.62	0.0167	0.1086	
Posterior Insula (R)—Cerebellum-02		−2.17	0.0426	0.1713	
Seed Anterior Insula (L)	16.47		0.0085	0.0457	0.1554
Anterior Insula (L)—Cerebellar.Posterior		−3.67	0.0016	0.0422	
Anterior Insula (L)—Posterior Insula (R)		2.94	0.0084	0.103	
Anterior Insula (L)—IPC.BA40 (R)		−2.78	0.0119	0.103	
Anterior Insula (L)—Cerebellar.Anterior		−2.49	0.0222	0.14	
Anterior Insula (L)—IFG (R)		2.40	0.0269	0.14	
Anterior Insula (L)—Posterior Insula (L)		2.19	0.0409	0.1772	

The entire network revealed in the NBS analysis at the network level is comprised of 71 connections. The table is limited to connections of the seeds that demonstrated ROI-level effects significant at the $p < 0.05$ (FDR-corrected) level, NBS by intensity.

TABLE 5 | Correlation between the severity of space motion sickness and seed-to-voxel connectivity.

Seed	Resulting cluster center of mass, MNI			Cluster size, vx (mm^3)	Cluster *p* uncorr.	Cluster *p* FDR-corr.	FDR *p*-thresh*	Region labels+
	x	*y*	*z*					
rpSMG	−34	20	−9	165 (4455)	0.000	0.000	0.004	Frontal orbital cortex L Insular cortex L Frontal operculum cortex L

+*Only labels covering at least 5% of the cluster volume are listed.* **Threshold, corrected for the total number of the seed-to-voxel follow-up analyses.*

insula showed increasing connectivity with the left posterior insula and a broader area within the left insular and opercular cortex. Also the right posterior and the left anterior insulae significantly changed their connectivity within the set of regions including the proprioceptive cortex and cerebellum, as revealed by the ROI-level NBS analysis. Given that the insula is believed to play an important role not only in vestibular signal processing but also in proprioception, interoception, pain, sensory integration, motor control, and higher processes such as salience detection, emotion, and speech (Kelly et al., 2012), the increased interinsular connectivity may be hypothesized to be a compensatory aid for motor control in conditions of functional loss of vestibular modality and altered proprioception.

Changes in insular connectivity due to microgravity exposure or its ground-based analogs have been reported previously (Zhou et al., 2014; Demertzi et al., 2016). Both studies revealed a reduced resting-state functional connectivity in the insula: Demertzi et al. (2016) found this effect in the right insula of a single cosmonaut post-flight with the ICC measure, while Zhou et al. (2014) revealed it using the degree of centrality (DC) measure in the left anterior insula of a group of HDBR participants. Both findings seem to be inconsistent with our results exhibiting an intensification of insulae bilateral coupling. Since this difference might rise from the applied measure of connectivity, while the ROI-to-ROI approach is both more sensitive and more focused (and therefore it might neglect the insula's connectivity with areas not considered in the study), we extracted the ICC values for every participant and condition from the right insula ROI constructed as a 10-mm sphere around the coordinates reported by the 2016 study ($x = 48$, $y = -6$, $z = 4$). These data were further used with the same ANCOVA model as the main dataset, with the same contrast (cosmonauts > controls, post-flight > preflight, plantar stimulation > rest). While there was no significant interaction effect for the ICC connectivity measure, in the majority of the cosmonauts (8 out of 11) the individual ICC changes were positive, including the cosmonaut who was the subject of the earlier case study (Demertzi et al., 2016). Therefore, we may conclude that the discrepancy in the observed direction of insular connectivity alterations most likely reflects the specific features of the task-based vs. baseline resting-state connectivity.

Decreased Connectivity of the Cerebellum

Last but not least, the finding of degraded connectivity of the cerebellar regions with multiple areas that belong to the motor, somatosensory, parietal proprioceptive, and visual cortices after long-term spaceflight (revealed by the ROI NBS and individual connection ROI-to-ROI analysis) is highly consistent with the existing literature that identifies the cerebellum as a principal brain structure for human adaptation to gravity (Razumeev and Grigoryan, 1976; Sajdel-Sulkowska, 2013), sensorimotor adaptation in general (Martin et al., 1996a,b; Werner et al., 2010; Galea et al., 2011), motor learning and fine motor control (Della-Maggiore et al., 2009; Tomassini et al., 2011; Manto et al., 2012).

Presumably, the cerebellum should play an important role in the adaptation to microgravity alterations, and regional cerebellar volumes and cerebellar-cortical connectivity are considered as possible predictors of adaptation success in space travelers (Seidler et al., 2015). In line with this idea, a recent voxel-based morphometry (VBM) study in humans revealed massive volumetric gray matter reduction in the cerebellum after a HDBR analog of microgravity that does not imply active motor control adaptation, although not after an actual long-term spaceflight (Koppelmans et al., 2016). No massive gray matter volume changes after the long-term spaceflight were reported by Van Ombergen et al. (2018) as well. In rats, a microgravity-induced ultrastructural plasticity of the cerebellum was found even after a 24-h-long spaceflight (Holstein et al., 1999).

The spaceflight-associated decrement in structural connectivity found by Lee et al. (2019) in the inferior cerebellar peduncles is consistent with the evidence for the functional disconnection of both the cerebellum and the vestibular nuclei we observe in the present study, given that the inferior cerebellar peduncle embraces the link between the vestibular nuclei and the cerebellum (Splittgerber, 2019). However, considering the indirect correspondence between structural and functional connectivity, this analogy should be made with caution.

As for the alterations of functioning, a case study (Demertzi et al., 2016) revealed a reduced resting state connectivity between the left cerebellum and the right motor cortex. Similarly, our task-based data on the altered network of the lobules VI–IX (anterior part of the cerebellar network, ROI-level NBS analysis) included decreased connectivity with both right and left lateral motor cortex regions, although these changes did not survive the connection-wise correction for multiple comparisons. Meanwhile, our data do not corroborate the findings by Cassady et al. (2016), who found increased connectivity between the right OP2 and the cerebellum during HDBR and decreased intercerebellar connectivity after bed rest. Overall, the decreased cortico-cerebellum connectivity within the motor control circuit during the gait-like stimulation found in the present study may imply a higher impact of the controlled vs. automated processes in locomotion, as a result of the microgravity exposure or in the process of readaptation to Earth's gravity. As suggested by the degrading connection between the anterior cerebellum and the right parietal proprioceptive cortex (BA40 ROI), it also may imply the so-called cerebellum-dependent adaptation, or recalibration of the relationship between sensory input and motor output (Block and Bastian, 2012).

Connectivity of the Primary Motor and Somatosensory Cortex

Many researchers have found structural plasticity in the primary motor and somatosensory cortex after spaceflight and its analogs. One of the important findings in astronauts reported by Koppelmans et al. (2016) is a focal gray matter increase in the medial paracentral lobule, a region including the representation of the lower limbs within the primary SMC. Li et al. (2015) and Koppelmans et al. (2017b) have also found a volumetric increase of gray matter in the paracentral lobule after HDBR. Animal research has provided a detailed description of the ultrastractural plasticity in the primary motor and somatosensory cortices in rats during and after spaceflight

(Belichenko and Krasnov, 1991; DeFelipe et al., 2002; Dyachkova, 2007).

Surprisingly, our data did not reveal any significant alterations in the connectivity of primary motor and somatosensory cortex ROIs. One possible reason for this may be that the gray matter increase reported by Koppelmans et al. (2016) is driven mostly by fluid shift mechanisms, i.e., by the complementary decrease in CSF volume in this region (Van Ombergen et al., 2018) rather than neuroplasticity.

For further clarification, we conducted a seed-to-voxel analysis of the PPI connectivity measures with two seeds in the paracentral lobules (left and right), adopted from T1 MNI ICBM152 and Freesurfer in order to replicate the ROI used by Koppelmans et al. (2016) in their VBM analysis. The results revealed decreased connectivity of the left (but not the right) paracentral lobule with the contralateral frontal pole and middle and inferior temporal gyri in cosmonauts vs. controls at post- vs. pre-flight (see **Figure 6** and **Table 6**). This finding should be considered with caution due to the a posteriori character of the underlying analysis. It also does not rule out the idea that the post-flight alteration of gray matter volume is a mechanical effect. However, it shows that the major counterparts of the connectivity changes that engage the paracentral region lie beyond the set of areas chosen for the ROI-to-ROI analysis in the present study.

One possible explanation of this finding is that here we observed a correlate of the previously described phenomenon of an altered lower extremity functional asymmetry in cosmonauts. A change of the leading leg from right before launch to left during the flight was observed in about half of the cosmonauts, according to the data from support reaction registrations in a study of locomotion performance during long-duration spaceflight (Brykov et al., 2015). The plausibility of such an interpretation is increased given the evidence for inversion of other brain functional asymmetries due to support unloading. EEG recordings of presaccadic slow negative potentials (PSNPs) in a dry immersion model have shown that over the course of 7 days of simulated microgravity, the focus of presaccadic negativity shifted to the right hemisphere: the PSNP amplitude sharply decreased in the left and increased in the right hemisphere (Kirenskaya et al., 2006). The authors suggested that because of support unloading and a decrease in proprioceptive input, exposure to microgravity causes a corresponding decrease in the activity of the prefrontal and parietal cortices of the left hemisphere, initially involved in preparation and realization of motor responses. The activation of the right hemisphere in this case could be of compensatory character. The same logic seems to be applicable to our present results.

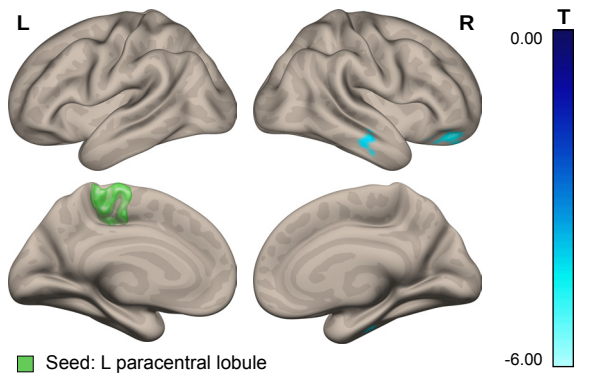

FIGURE 6 | Connectivity of the paracentral lobule. Areas demonstrating altered functional connectivity with the left paracentral lobule evoked by plantar stimulation over the resting baseline in cosmonauts compared to the control group, at post- vs. pre-flight. Blue indicates decreasing connectivity with the seed. Green indicates the location of the seed.

Neuroplasticity, Adaptation, and Readaptation

So far, the most unequivocal results advocating for microgravity-induced neuroplasticity in the sensorimotor system of the mammal brain have been obtained with animal models (Belichenko and Krasnov, 1991; DeFelipe et al., 2002; Dyachkova, 2007). As for the human data, even today microgravity-induced neuroplasticity is discussed in the literature only as a highly plausible theoretical speculation not sufficiently supported by empirical evidence (Koppelmans et al., 2017a; Van Ombergen et al., 2017a). The reason for this caution is not only a lack of data, but also the problems of inference. With non-invasive techniques, central neuroplasticity can hardly be disentangled from numerous low-level confounds arising from the upward displacement of the brain within the skull (Roberts et al., 2017), changes in CSF production and reabsorption (Nelson et al., 2014; Kramer et al., 2015), adaptations in cardiovascular functioning (Zhu et al., 2015) and brain hemodynamics (Kawai et al., 2003; Blaber et al., 2013; Taylor et al., 2013).

However, it is very unlikely that behavioral adaptation and motor learning in space travelers is acquired without any modifications in brain structure and function. Modern neuroscience has collected extensive evidence for experience-induced neuroplasticity in adults learning new skills, and such plasticity becomes visible with neuroimaging even in short periods of time (Dayan and Cohen, 2011; Sampaio-Baptista et al., 2018). This research may guide our understanding of spaceflight's consequences and their reversible nature (Seidler et al., 2015).

Upon returning to Earth, the space crewmembers pass through a readaptation period since the new motor control strategies acquired in microgravity become maladaptive in the terrestrial settings. Transition to another state of the sensorimotor system takes time, and may be traced for up to 2 weeks at least (Mulavara et al., 2010). The time-course of the readaptation demonstrates substantial individual differences and may be affected by a wide range of factors, from genetic to behavioral (Seidler et al., 2015). Therefore, the signs of the neuroplasticity observed in the readaptation period should be considered not only as residual consequences of the long-term microgravity exposure, but as a mixture of effects induced

TABLE 6 | Connectivity of the paracentral lobule.

Seed	Resulting cluster center of mass, MNI			Cluster size, vx (mm^3)	Cluster *p* uncorr.	Cluster *p* FDR-corr.	FDR *p*-thresh*	PPI value differential effect+	Region labels
	x	*y*	*z*						
Paracentral lobule, L	24	40	−19	75 (2025)	0.0005	0.006	0.025	−0.13	Frontal pole R Frontal orbital cortex R
Paracentral lobule, L	52	−18	−22	58 (1566)	0.0016	0.011	0.025	−0.12	Inferior temporal gyrus, posterior division R Middle temporal gyrus, posterior division R

*+To aid interpretation, the PPI values (connectivity between the seed and the target region for the task blocks differential from the implicit baseline) were averaged within each cluster. The cosmonaut vs. control, post-flight vs. pre-flight effect on PPI values is presented for illustrative purposes. *Threshold, corrected for the number of seeds.*

by spaceflight and the subsequent readaptation to Earth. This view is supported by evidence from animal research which shows continuing ultrastructural modifications in the rat somatosensory cortex, especially in terms of the functional activity or degeneration of axonal terminals in the first hours upon reentry to the Earth's gravity and even 14 days after landing (Dyachkova, 2007). With this consideration, the time period between landing and subsequent MRI examination, for example, the difference of 4 vs. 9 days discussed by Roberts et al. (2017) should be taken into account as an important variable in future research.

The results of the present study perfectly illustrate the inference problem arising from the mixture of adaptation and readaptation processes. Thus, the unchanged fMRI activation pattern elicited by the plantar stimulation may reflect either the preservation of the 'core' neural system associated with the reaction to support loading, or the fast and effective recovery of this system in the first days after spaceflight. Similarly, the observed modifications of the connectivity between different sensory inputs utilized by the motor system (vestibular, proprioceptive, visual) may reflect not only impairment in the default motor control connectivity due to the vestibular deprivation and biomechanic factors associated with microgravity, but also a dephasing of the motor control strategies adopted during spaceflight in favor of the neural implementation of ground-based locomotion.

Interestingly, the hypothesis that after a prolonged space flight the human brain features two co-existing neural networks supporting two modes of locomotion — one for 1 g-gravity and one for microgravity — could account for the fact that second-time flyers adapt more quickly and are less prone to microgravity-induced problems (Kozlovskaya et al., 2015). It also encourages a perspective on divergent signs between the task-based and resting-state connectivity alterations highlighted in the previous discussion (the right TPJ results in Van Ombergen et al., 2017d and in the present study; the insula connectivity results in Zhou et al., 2014; Demertzi et al., 2016 and in the present study). The task-based connectivity measures provide information about the current state of the functional brain organ accomplishing some motor activity such as locomotion. At the same time, it is widely believed that resting-state connectivity represents the background activity of large-scale neural networks that become active when triggered by certain stimulations or tasks (Heine et al., 2012). If so, the resting-state connectivity after a space flight provides amalgamated information about all co-existing motor networks, both the one presently used and the one adapted for microgravity conditions and unused in terrestrial settings. Therefore, a comparison of the connectivity data from these two sources may provide an important basis for future insights into the mechanisms of neuroplasticity within the motor system.

Implications for the Sensory Reweighting Theory

In microgravity, alterations in biomechanics such as modified relationships between the mass of a body part and the force required to move it call for a recalibration of the correspondence between sensory input and motor output (sensory realignment), which is believed to be the function of the cerebellum (Block and Bastian, 2012). At the same time, the otolith afferentation is substantially altered. Not only does it become unreliable, but the otherwise tight coupling of canal-otolith information gets lost, and a conflict in the input from different sensory modalities (vestibular, proprioceptive, and visual) is created (Kornilova and Kozlovskaya, 2003; Davis et al., 2008). The motion sickness syndrome is believed to be a consequence of such sensory mismatch (Reason and Brand, 1975; Schmäl, 2013) and is often experienced by space travelers and described as space motion sickness (Heer and Paloski, 2006; Kornilova et al., 2013).

This sensory conflict calls for a second type of sensorimotor adaptation that involves a recalibration of the relationship between several sensory modalities. Theoretically, this may be dealt with by reweighting the sensory inputs; that is, by downweighting the less reliable modality and prioritizing a more reliable one (Horak et al., 1990). The neural mechanisms of multisensory reweighting remain generally unclear. Reweighting has been studied predominantly in patients with postural pathologies and sensory loss, children and the elderly (e.g., Jeka et al., 2010; Polastri and Barela, 2013), but it has also been suggested as an important mechanism of motor adaptation

in astronauts who demonstrate increased reliance on visual and tactile information during and after spaceflight (Reschke et al., 1998; Speers et al., 1998; Clément et al., 2001). Evidence for multisensory reweighting in astronauts has been collected on the basis of kinematic and tactile sensitivity research and subsequent modeling (Speers et al., 1998; Clément et al., 2001; Lowrey et al., 2014).

Given the substantial individual differences between space travelers in their susceptibility to space motion sickness (and therefore in the supposed degree of the proposed sensory reweighting) and the small size of our sample, it may be the case that pronounced neural correlates of sensory reweighting may be found in some but not all cosmonauts. Therefore we examined the role of individual differences and looked for possible correlations between the severity of space motion sickness symptoms and connectivity of the areas changing their connectivity pattern during plantar stimulation in cosmonauts post-flight as shown by the ROI-to-ROI and ICC approaches. The observed correlations suggest the potential importance of connection between the left insula and the right TPJ regions for the neural mechanisms of space motion sickness and sensory reweighting in microgravity. The greater the post- vs. pre-flight difference in connectivity between the two regions, the more pronounced were the symptoms of space motion sickness, which is consistent with the idea of a possible compensatory role of the insula and its connectivity, as discussed above.

Implications for the Gravitational Motor System Theory

According to the gravitational motor system theory (Kozlovskaya et al., 1988), keeping an upright stance in humans is the function of specialized tonic muscle system mainly comprised of the tonic motor units of the extensors. The support afference from the deep skin mechanoreceptors is considered to be the most important sensory input driving motor control in this system. Empirical evidence comes from both actual spaceflights and ground-based models showing that withdrawal of support entails a reflectory decline of transverse stiffness and a voluntary force of tonic extensor (postural) muscles, limiting their participation in locomotion and increasing the involvement of phasic muscle units (Kozlovskaya et al., 1988, 2007; Shigueva et al., 2015). The prevalence of the flexor over the extensor activity leads to the adoption of a quasi-embryonic flexor posture (Margaria, 1966; Bogdanov and Gurfinkel, 1976) and to a changed pattern of coordinated muscle recruitment (Roy et al., 1996). Support unloading has also been found to result in increased sensitivity of the vestibular system in different types of dry immersion in humans (Kreidich, 2009; Kornilova et al., 2016). Similar increased vestibular excitability has also been revealed in the actual microgravity in primates (Sirota et al., 1988) and in cats and a monkey in parabolic flight (Grigorian et al., 1995). These findings were in line with the hypothesis that the vestibular system normally experiences an inhibitory influence from the support afferent system and activates when the influence is removed (Kreidich, 2009). Such inhibitory modulation may be implemented through inhibitory connections projecting from the cerebellum onto the vestibular nuclei (Ito, 1972).

Our present results are in agreement with this theory. In space travelers we did not find evidence for alterations in brain activation elicited by the support afferentation (gait-like plantar stimulation). This is likely to be a result of the fast recovery of the system processing support afference in cosmonauts within the very first days upon their return to the Earth's gravity. At the same time, evidence for the down-weighting of the vestibular input was still present on the 9th day upon return when most cosmonauts underwent their post-flight scan. Since in microgravity the support afferent system becomes effectively silent and therefore is not involved in sensory conflicts, we may suppose that it is also minimally involved in sensory re-weighting, unlike the vestibular system which produces massive but unreliable sensory signals during space flight. We may further suppose that the fast recovery of the support afferent system's activity upon return to Earth is accompanied by the restoration of its inhibitory modulation on the vestibular system, which in turn slows down the recovery of the vestibular function. Testing this hypothesis may become a prospective direction of future behavioral and neuroimaging research.

CONCLUSION

Our data show changes in functional brain connectivity specific for a plantar stimulation task in a group of the cosmonauts after long-term spaceflight as compared to a control group. The observed alterations included a disconnection of the vestibular nuclei, the superior part of the right supramarginal gyrus, and the cerebellum from a set of motor, somatosensory, visual, and vestibular areas. Increased connectivity was found between the left and right insulae as well as between the part of the right posterior supramarginal gyrus within the TPJ region and the rest of the brain. A post- to pre-flight difference in connectivity between the latter area in the right posterior temporal cortex and the left anterior insula demonstrated a correlation with the severity of space motion sickness symptoms. At the same time, no alterations were found in activation elicited by the gait-like plantar stimulation. The findings cannot be attributed solely to the lasting effects of long-term microgravity exposure since such effects are contaminated by the readaptation to Earth's gravity that took place between the landing and the post-flight MRI session. Nevertheless, the results suggest implications for the multisensory reweighting and gravitational motor system theories, generating hypotheses to be tested in future research.

ETHICS STATEMENT

This study was approved as a part of the Brain DTI project by Committee of Biomedicine Ethics of the

Institute of Biomedical Problems of the Russian Academy of Sciences and the Human Research Multilateral Review Board (HRMRB) according to the 18th World Medical Assembly of Helsinki, Finland, June 1964, amended by the 41st Assembly, Hong Kong, September 1989. All participants gave written informed consent for the study at enrollment.

AUTHOR CONTRIBUTIONS

EP helped with the design the study, made the fMRI data analysis, and wrote the draft of manuscript. InN, AG, IR, and SJ coordinated the study and participated in conducting research. AR and LL conducted fMRI procedure and contributed to analyzing the experiment results. FW, ET, and IK participated in conceiving and designing of the idea. LC contributed to methodology and participated in critically revising the manuscript. IvN and LK contributed in the part of observations and processing of vestibular function state. BJ and AVO helped with the design the study, took part in conducting research. SL and JS participated in discussions and critically revising the manuscript. EM and VS coordinated the study, participated in critically revising the manuscript. All the authors took part in writing, review and editing and read and approved the current manuscript.

FUNDING

The study was supported by the European Space Agency (ISLRA 2009-1062), the Belgian Science Policy (Belspo PRODEX), and the Russian Academy of Sciences (63.1). BJ was supported by the Research Foundation Flanders (FWO) under Grant No. 12M3119N.

ACKNOWLEDGMENTS

We appreciate contribution of our participants.

SUPPLEMENTARY MATERIAL

The Supplementary Material for this article can be found online at: https://www.frontiersin.org/articles/10.3389/fphys.2019.00761/full#supplementary-material

REFERENCES

Badakva, A. M., Zalkind, D. V., Miller, N. V., and Riazansky, S. N. (2000). Head pitch movement and vestibular neuronal activity in response to otolith stimulation of monkeys in space. *J. Gravit. Physiol.* 7, S99–S105.

Behzadi, Y., Restom, K., Liau, J., and Liu, T. T. (2007). A component based noise correction method (CompCor) for BOLD and perfusion based fMRI. *Neuroimage* 37, 90–101. doi: 10.1016/j.neuroimage.2007.04.042

Belichenko, P. V., and Krasnov, I. B. (1991). The dendritic spines of the pyramidal neurons in layer V of the rat sensorimotor cortex following a 14-day space flight. *Biull. Eksp. Biol. Med.* 112, 541–542.

Bense, S., Stephan, T., Yousry, T. A., Brandt, T., and Dieterich, M. (2001). Multisensory cortical signal increases and decreases during vestibular galvanic stimulation (fMRI). *J. Neurophysiol.* 85, 886–899. doi: 10.1152/jn.2001.85.2.886

Bernstein, N. A. (1967). *Coordination and Regulation of Movement*. London: Pergamon Press.

Blaber, A. P., Zuj, K. A., and Goswami, N. (2013). Cerebrovascular autoregulation: lessons learned from spaceflight research. *Eur. J. Appl. Physiol.* 113, 1909–1917. doi: 10.1007/s00421-012-2539-x

Block, H., Bastian, A., and Celnik, P. (2013). Virtual lesion of angular gyrus disrupts the relationship between visuoproprioceptive weighting and realignment. *J. Cognit. Neurosci.* 25, 636–648. doi: 10.1162/jocn_a_00340

Block, H. J., and Bastian, A. J. (2011). Sensory weighting and realignment: independent compensatory processes. *J. Neurophysiol.* 106, 59–70. doi: 10.1152/jn.00641.2010

Block, H. J., and Bastian, A. J. (2012). Cerebellar involvement in motor but not sensory adaptation. *Neuropsychologia* 50, 1766–1775. doi: 10.1016/j.neuropsychologia.2012.03.034

Bloomberg, J. J., Peters, B. T., Cohen, H. S., and Mulavara, A. P. (2015). Enhancing astronaut performance using sensorimotor adaptability training. *Front. Syst. Neurosci.* 9:129. doi: 10.3389/fnsys.2015.00129

Bock, O., Abeele, S., and Eversheim, U. (2003). Sensorimotor performance and computational demand during short-term exposure to microgravity. *Aviat. Space Environ. Med.* 74, 1256–1262.

Bogdanov, V. A., and Gurfinkel, A. S. (1976). *Biomechanics of Human Locomotion, in Fiziologiya Dvizhenii [Physiology of movements]*. Leningrad: Nauka, 276–315.

Brett, M., Anton, J.-L., Valabregue, R., and Poline, J.-B. (2002). Region of interest analysis using the MarsBar toolbox for SPM 99. *Neuroimage* 16:S497.

Brykov, V. I., Rukavishnikov, I. V., and Semenov Yu, S. (2015). "Kharakteristiki khodby i bega v usloviiakh nevesomosti: pervye rezultaty eksperimenta 'Motokard' [Walking and running locomotion under conditions of weightlessness: first results of 'Motokard' experiment]," in *Pilotiruemye Polety v Kosmos [Piloted Flights into Space]*, eds Yu. V. Lonchakov, V. A. Sivolap, and A. A. Kuritsin (Zvezdny Gorodok: Gagarin Cosmonauts Training Center), 357–358.

Cassady, K., Koppelmans, V., Reuter-Lorenz, P., De Dios, Y., Gadd, N., Wood, S., et al. (2016). Effects of a spaceflight analog environment on brain connectivity and behavior. *Neuroimage* 141, 18–30. doi: 10.1016/j.neuroimage.2016.07.029

Clément, G., Bukley, A., and Paloski, W. (2007). "The Gravity of the situation," in *Artificial Gravity*, eds G. Clemenat and A. Bukley (Hawthorne, CA: Microcosm Press and Springer), 1–32. doi: 10.1007/0-387-70714-x_1

Clément, G., Gurfinkel, V. S., Lestienne, F., Lipshits, M. I., and Popov, K. E. (1984). Adaptation of postural control to weightlessness. *Exp. Brain Res.* 57, 61–72. doi: 10.1007/BF00231132

Clément, G., Moore, S. T., Raphan, T., and Cohen, B. (2001). Perception of tilt (somatogravic illusion) in response to sustained linear acceleration during space flight. *Exp. Brain Res.* 138, 410–418. doi: 10.1007/s002210100706

Davis, J. R., Johnson, R., and Stepanek, J. (eds) (2008). *Fundamentals of Aerospace Medicine*. Philadelphia, PA: Lippincott Williams & Wilkins.

Dayan, E., and Cohen, L. G. (2011). Neuroplasticity subserving motor skill learning. *Neuron* 72, 443–454. doi: 10.1016/j.neuron.2011.10.008

DeFelipe, J., Arellano, J. I., Merchán-Péfirez, A., González-Albo, M. C., Walton, K., and Llinás, R. (2002). Spaceflight induces changes in the synaptic circuitry of the postnatal developing neocortex. *Cereb. Cortex* 12, 883–891. doi: 10.1093/cercor/12.8.883

Della-Maggiore, V., Scholz, J., Johansen-Berg, H., and Paus, T. (2009). The rate of visuomotor adaptation correlates with cerebellar white-matter microstructure. *Hum. Brain Mapp.* 30, 4048–4053. doi: 10.1002/hbm.20828

Demertzi, A., Van Ombergen, A., Tomilovskaya, E., Jeurissen, B., Pechenkova, E., Di Perri, C., et al. (2016). Cortical reorganization in an astronaut's brain after long-duration spaceflight. *Brain Struct. Funct.* 221, 2873–2876. doi: 10.1007/s00429-015-1054-3

Desikan, R. S., Ségonne, F., Fischl, B., Quinn, B. T., Dickerson, B. C., Blacker, D., et al. (2006). An automated labeling system for subdividing the human cerebral cortex on MRI scans into gyral based regions of interest. *Neuroimage* 31, 968–980. doi: 10.1016/j.neuroimage.2006.01.021

Dieterich, M., and Brandt, T. (2015). The bilateral central vestibular system: its pathways, functions, and disorders. *Ann. N. Y. Acad. Sci.* 1343, 10–26. doi: 10.1111/nyas.12585

Dobkin, B. H., Firestine, A., West, M., Saremi, K., and Woods, R. (2004). Ankle dorsiflexion as an fMRI paradigm to assay motor control for walking during rehabilitation. *Neuroimage* 23, 370–381. doi: 10.1016/j.neuroimage.2004.06.008

Dyachkova, L. N. (2007). Ultrastructural changes in somatosensory cortex of albino rats during space flight. *Biol. Bull.* 34, 307–309. doi: 10.1134/S1062359007030156

Friston, K. J., Ashburner, J., Kiebel, S., Nichols, T. E., and Penny, W. D. (eds) (2007). *Statistical Parametric Mapping: The Analysis of Functional BrainIimages*. London: Academic Press.

Galea, J. M., Vazquez, A., Pasricha, N., Orban de Xivry, J.-J., and Celnik, P. (2011). Dissociating the roles of the cerebellum and motor cortex during adaptive learning: the motor cortex retains what the cerebellum learns. *Cereb. Cortex* 21, 1761–1770. doi: 10.1093/cercor/bhq246

Goble, D. J., Coxon, J. P., Van Impe, A., Geurts, M., Van Hecke, W., Sunaert, S., et al. (2012). The neural basis of central proprioceptive processing in older versus younger adults: an important sensory role for right putamen. *Hum. Brain Mapp.* 33, 895–908. doi: 10.1002/hbm.21257

Golaszewski, S. M., Siedentopf, C. M., Koppelstaetter, F., Fend, M., Ischebeck, A., Gonzalez-Felipe, V., et al. (2006). Human brain structures related to plantar vibrotactile stimulation: a functional magnetic resonance imaging study. *Neuroimage* 29, 923–929. doi: 10.1016/j.neuroimage.2005.08.052

Grefkes, C., and Fink, G. R. (2005). The functional organization of the intraparietal sulcus in humans and monkeys. *J. Anat.* 207, 3–17. doi: 10.1111/j.1469-7580.2005.00426.x

Grigor'ev, A. I., Kozlovskaya, I. B., and Shenkman, B. S. (2004). Rol' opornoy afferentatsii v organizatsii tonicheskoy myshechnoy sistemy [The role of supporting afferentation in the organization of tonic muscular system]. *Rossiyskiy Fiziologicheskiy Zhurnal im. I.M. Sechenova Russ. J. Physiol.* 90, 508–521.

Grigorian, R. A., Aizikov, G. S., and Kreidich, J. V. (1995). Motor reactions and vestibular reflexes in cats and monkey in weightlessness. *J. Gravit. Physiol.* 2, P80–P81.

Hallgren, E., Kornilova, L., Fransen, E., Glukhikh, D., Moore, S. T., Clément, G., et al. (2016). Decreased otolith-mediated vestibular response in 25 astronauts induced by long-duration spaceflight. *J. Neurophysiol.* 115, 3045–3051. doi: 10.1152/jn.00065.2016

Heer, M., and Paloski, W. H. (2006). Space motion sickness: incidence, etiology, and countermeasures. *Auton. Neurosci.* 129, 77–79. doi: 10.1016/j.autneu.2006.07.014

Heine, L., Soddu, A., Gomez, F., Vanhaudenhuyse, A., Tshibanda, L., Thonnard, M., et al. (2012). Resting state networks and consciousness. *Front. Psychol.* 3:295. doi: 10.3389/fpsyg.2012.00295

Holstein, G. R., Kukielka, E., and Martinelli, G. P. (1999). Anatomical observations of the rat cerebellar nodulus after 24 hr of spaceflight. *J. Gravit. Physiol.* 6, 47–50.

Horak, F. B., Nashner, L. M., and Diener, H. C. (1990). Postural strategies associated with somatosensory and vestibular loss. *Exp. Brain Res.* 82, 167–177. doi: 10.1007/bf00230848

Indovina, I., Maffei, V., Bosco, G., Zago, M., Macaluso, E., and Lacquaniti, F. (2005). Representation of visual gravitational motion in the human vestibular cortex. *Science* 308, 416–419. doi: 10.1126/science.1107961

Ito, M. (1972). Cerebellar control of the vestibular neurones: physiology and pharmacology. *Prog. Brain Res.* 37, 377–390. doi: 10.1016/S0079-6123(08)63914-X

Jaeger, L., Marchal-Crespo, L., Wolf, P., Riener, R., Michels, L., and Kollias, S. (2014). Brain activation associated with active and passive lower limb stepping. *Front. Hum. Neurosci.* 8:828. doi: 10.3389/fnhum.2014.00828

Jeka, J. J., Allison, L. K., and Kiemel, T. (2010). The dynamics of visual reweighting in healthy and fall-prone older adults. *J. Mot. Behav.* 42, 197–208. doi: 10.1080/00222895.2010.481693

Kakei, S., Hoffman, D. S., and Strick, P. L. (1999). Muscle and movement representations in the primary motor cortex. *Science* 285, 2136–2139. doi: 10.1126/science.285.5436.2136

Kawai, Y., Doi, M., Setogawa, A., Shimoyama, R., Ueda, K., Asai, Y., et al. (2003). Effects of microgravity on cerebral hemodynamics. *Yonago Acta Med.* 46, 1–8.

Kelly, C., Toro, R., Di Martino, A., Cox, C. L., Bellec, P., Castellanos, F. X., et al. (2012). A convergent functional architecture of the insula emerges across imaging modalities. *Neuroimage* 61, 1129–1142. doi: 10.1016/j.neuroimage.2012.03.021

Kheradmand, A., Lasker, A., and Zee, D. S. (2013). Transcranial magnetic stimulation (TMS) of the supramarginal gyrus: a window to perception of upright. *Cereb. Cortex* 25, 765–771. doi: 10.1093/cercor/bht267

Kirenskaya, A. V., Tomilovskaya, E. S., Novototskii-Vlasov, Vlu., and Kozlovskaya, I. B. (2006). The effects of simulated microgravity on characteristics of slow presaccadic potentials. *Hum. Physiol.* 32, 131–139. doi: 10.1134/S0362119706020022

Kirsch, V., Keeser, D., Hergenroeder, T., Erat, O., Ertl-Wagner, B., Brandt, T., et al. (2016). Structural and functional connectivity mapping of the vestibular circuitry from human brainstem to cortex. *Brain Struct. Funct.* 221, 1291–1308. doi: 10.1007/s00429-014-0971-x

Koppelmans, V., Bloomberg, J. J., De Dios, Y. E., Wood, S. J., Reuter-Lorenz, P. A., Kofman, I. S., et al. (2017a). Brain plasticity and sensorimotor deterioration as a function of 70 days head down tilt bed rest. *PLoS One* 12:e0182236. doi: 10.1371/journal.pone.0182236

Koppelmans, V., Pasternak, O., Bloomberg, J. J., De Dios, Y. E., Wood, S. J., Riascos, R., et al. (2017b). Intracranial fluid redistribution but no white matter microstructural changes during a spaceflight analog. *Sci. Rep.* 7:3154. doi: 10.1038/s41598-017-03311-w

Koppelmans, V., Bloomberg, J. J., Mulavara, A. P., and Seidler, R. D. (2016). Brain structural plasticity with spaceflight. *NPJ Microgravity* 2:2. doi: 10.1038/s41526-016-0001-9

Koppelmans, V., Erdeniz, B., De Dios, Y. E., Wood, S. J., Reuter-Lorenz, P. A., Kofman, I., et al. (2013). Study protocol to examine the effects of spaceflight and a spaceflight analog on neurocognitive performance: extent, longevity, and neural bases. *BMC Neurol.* 13:205. doi: 10.1186/1471-2377-13-205

Kornilova, L., Grigorova, V., Myuller, C., Clarke, A., Cowings, P., and Glavachka, F. (2002). "The vestibular system. Intersensory interaction. Space perception and spatial orientation. Space adaptation syndrome and space motion sickness, in Orbital'naya stantsiya 'MIR'," in *Kosmicheskaya Biologiya i Meditsina [Orbital Station Mir: Space Biology and Medicine]*, Vol. 2, ed. A. I. Grigor'ev (Mozhaisk: RF SSC - Institute of Biomedical Problems of the Russian Academy of Sciences), 208–251.

Kornilova, L. N. (1997). Orientation illusions in spaceflight. *J. Vestib. Res.* 7, 429–440. doi: 10.1038/s41598-017-03311-w

Kornilova, L. N., Glukhikh, D. O., Naumov, I. A., Habarova, E. V., Ekimovskiy, G. A., Pavlova, A. S., et al. (2016). Effect of optokinetic stimulation on visual–manual tracking under the conditions of support-proprioceptive deprivation. *Hum. Physiol.* 42, 508–519. doi: 10.1134/S0362119716040071

Kornilova, L. N., and Kozlovskaya, I. B. (2003). Neurosensory mechanisms of space adaptation syndrome. *Hum. Physiol.* 29, 527–538. doi: 10.1023/A:1025899413655

Kornilova, L. N., Naumov, I. A., Azarov, K. A., and Sagalovitch, V. N. (2012). Gaze control and vestibular-cervical-ocular responses after prolonged exposure to microgravity. *Aviat. Space Environ. Med.* 83, 1123–1134. doi: 10.3357/asem.3106.2012

Kornilova, L. N., Naumov, I. A., Glukhikh, D. O., Ekimovskiy, G. A., Pavlova, A. S., Khabarova, V. V., et al. (2017). Vestibular function and space motion sickness. *Hum. Physiol.* 43, 557–568.

Kornilova, L. N., Naumov, I. A., and Kozlovskaya, I. B. (2013). "Neurosensory studies of the vestibular function in humans," in *Kosmicheskaya meditsina i Biologiya [Space Medicine and Biology]*, eds A. I. Grigor'ev and I. B. Ushakov (Voronezh: Nauchnaya Kniga), 278–298.

Kozlovskaya, I., Dmitrieva, I., Grigorieva, L., Kirenskaya, A., and Kreidich, Yu (1988). "Gravitational mechanisms in the motor system. studies in real and simulated weightlessness," in *Stance and Motion*, eds V. Gurfinkel, M. Ioffe, J. Massion, and J. Roll (Boston, MA: Springer), 37–48. doi: 10.1007/978-1-4899-0821-6_4

Kozlovskaya, I. B., Aslanova, I. F., Grigorieva, L. S., and Kreidich, YuV. (1982). Experimental analysis of motor effects of weightlessness. *Physiologist* 25, 49–52.

Kozlovskaya, I. B., Sayenko, I. V., Vinogradova, O. L., Miller, T. F., Khusnutdinova, D. R., Melnik, K. A., et al. (2007). Erratum to: new approaches to countermeasures of the negative effects of micro-gravity in long-term space flights [Acta Astronautica 59 (2006) 13–19]. *Acta Astronaut.* 60, 783–789. doi: 10.1016/j.actaastro.2006.09.038

Kozlovskaya, I. B., Yarmanova, E. N., Yegorov, A. D., Stepantsov, V. I., Fomina, E. V., and Tomilovaskaya, E. S. (2015). Russian countermeasure systems for adverse effects of microgravity on long-duration ISS flights. *Aerospace Med. Hum. Performan.* 86, A24–A31. doi: 10.3357/amhp.ec04.2015

Kramer, L. A., Hasan, K. M., Sargsyan, A. E., Wolinsky, J. S., Hamilton, D. R., Riascos, R. F., et al. (2015). MR-derived cerebral spinal fluid hydrodynamics as a marker and a risk factor for intracranial hypertension in astronauts exposed to microgravity. *J. Magn. Reson. Imaging* 42, 1560–1571. doi: 10.1002/jmri.24923

Krasnov, I. B., and Dyachkova, L. N. (1990). The effect of space flight on the ultrastructure of the rat cerebellar and hemisphere cortex. *Physiologist* 33 (1 Suppl.), S29–S30.

Kreidich, Y. V. (2009). *Osobennosti Vzaimodeystviya Opornoy i Vestibulyarnoy Afferentnykh System v Usloviyakh Mikrogravitatsii [Specifics of Interaction Between the Support and Vestibular Systems in Conditions of Microgravity]*. Ph.D. thesis, Institute of Biomedical Problems, Moscow.

Kremneva, E. I., Saenko, I. V., Chernikova, L. A., Cherviakov, A. V., Konovalov, R. N., and Kozlovskaia, I. B. (2013). Specifics of activation of cortex by stimulation of support receptors in healthy subjects and in patients with lesions of CNS. *Hum. Physiol.* 39, 524–529. doi: 10.1134/s0362119713050095

Kubis, J. F., McLaughlin, E. J., Jackson, J. M., Rusnak, R., McBride, G., and Saxon, S. V. (1977). "Task and work performance on Skylab missions 2, 3 and 4: Time and motion study experiment M-151," in *Biomedical Results from Skylab*, eds R. S. Johnson and L. F. Dietlein (Washington, DC: NASA), S–377.

Labriffe, M., Annweiler, C., Amirova, L. E., Gauquelin-Koch, G., Ter Minassian, A., Leiber, L.-M., et al. (2017). Brain activity during mental imagery of gait versus gait-like plantar stimulation: a novel combined functional MRI paradigm to better understand cerebral gait control. *Front. Hum. Neurosci.* 11:106. doi: 10.3389/fnhum.2017.00106

Lackner, J. R., and DiZio, P. (1996). Motor function in microgravity: movement in weightlessness. *Curr. Opin. Neurobiol.* 6, 744–750. doi: 10.1016/s0959-4388(96)80023-7

Layne, C. S., and Forth, K. E. (2008). Plantar stimulation as a possible countermeasure to microgravity-induced neuromotor degradation. *Aviat. Space Environ. Med.* 79, 787–794. doi: 10.3357/asem.2293.2008

Layne, C. S., Mulavara, A. P., Pruett, C. J., McDonald, P. V., Kozlovskaya, I. B., and Bloomberg, J. J. (1998). The use of in-flight foot pressure as a countermeasure to neuromuscular degradation. *Acta Astronaut.* 42, 231–246. doi: 10.1016/S0094-5765(98)00120-9

Lee, J. K., Koppelmans, V., Riascos, R. F., Hasan, K. M., Pasternak, O., Mulavara, A. P., et al. (2019). Spaceflight-associated brain white matter microstructural changes and intracranial fluid redistribution. *JAMA Neurol.* 76, 412–419. doi: 10.1001/jamaneurol.2018.4882

Lee, S. M., and McCarthy, G. (2016). Functional heterogeneity and convergence in the right temporoparietal junction. *Cereb. Cortex* 26, 1108–1116. doi: 10.1093/cercor/bhu292

Li, K., Guo, X., Jin, Z., Ouyang, X., Zeng, Y., Feng, J., et al. (2015). Effect of simulated microgravity on human brain gray matter and white matter – evidence from MRI. *PLoS One* 10:e0135835. doi: 10.1371/journal.pone.0135835

Liao, Y., Lei, M., Huang, H., Wang, C., Duan, J., Li, H., et al. (2015). The time course of altered brain activity during 7-day simulated microgravity. *Front. Behav. Neurosci.* 9:124. doi: 10.3389/fnbeh.2015.00124

Liao, Y., Miao, D., Huan, Y., Yin, H., Xi, Y., and Liu, X. (2013). Altered regional homogeneity with short-term simulated microgravity and its relationship with changed performance in mental transformation. *PLoS One* 8:e64931. doi: 10.1371/journal.pone.0064931

Liao, Y., Zhang, J., Huang, Z., Xi, Y., Zhang, Q., Zhu, T., et al. (2012). Altered baseline brain activity with 72 h of simulated microgravity – initial evidence from resting-state fMRI. *PLoS One* 7:e52558. doi: 10.1371/journal.pone.0052558

Lindquist, M. A., Loh, J. M., Atlas, L. Y., and Wager, T. D. (2009). Modeling the hemodynamic response function in fMRI: efficiency, bias and mis-modeling. *Neuroimage* 45, S187–S198. doi: 10.1016/j.neuroimage.2008.10.065

Lopez, C., and Blanke, O. (2011). The thalamocortical vestibular system in animals and humans. *Brain Res. Rev.* 67, 119–146. doi: 10.1016/j.brainresrev.2010.12.002

Lowrey, C. R., Perry, S. D., Strzalkowski, N. D. J., Williams, D. R., Wood, S. J., and Bent, L. R. (2014). Selective skin sensitivity changes and sensory reweighting following short-duration space flight. *J. Appl. Physiol.* 116, 683–692. doi: 10.1152/japplphysiol.01200.2013

Manto, M., Bower, J. M., Conforto, A. B., Delgado-Garcifmmode, J. M., da Guarda, S. N. F., Gerwig, M., et al. (2012). Consensus paper: roles of the cerebellum in motor control — the diversity of ideas on cerebellar involvement in movement. *Cerebellum* 11, 457–487. doi: 10.1007/s12311-011-0331-9

Margaria, R. (1966). Human locomotion on the Earth and in subgravity. *Schweiz. Z. Sportmed.* 14, 159–167.

Martin, T. A., Keating, J. G., Goodkin, H. P., Bastian, A. J., and Thach, W. T. (1996a). Throwing while looking through prisms I. Focal olivocerebellar lesions impair adaptation. *Brain* 119, 1183–1198. doi: 10.1093/brain/119.4.1183

Martin, T. A., Keating, J. G., Goodkin, H. P., Bastian, A. J., and Thach, W. T. (1996b). Throwing while looking through prisms II. Specificity and storage of multiple -gaze-throw calibrations. *Brain* 119, 1199–1211. doi: 10.1093/brain/119.4.1199

Martuzzi, R., Ramani, R., Qiu, M., Shen, X., Papademetris, X., and Constable, R. T. (2011). A whole-brain voxel based measure of intrinsic connectivity contrast reveals local changes in tissue connectivity with anesthetic without a priori assumptions on thresholds or regions of interest. *Neuroimage* 58, 1044–1050. doi: 10.1016/j.neuroimage.2011.06.075

Marušič, U., Meeusen, R., Pišot, R., and Kavcic, V. (2014). The brain in micro- and hypergravity: the effects of changing gravity on the brain electrocortical activity. *Eur. J. Sport Sci.* 14, 813–822. doi: 10.1080/17461391.2014.908959

Massion, J. (1992). Movement, posture and equilibrium: interaction and coordination. *Prog. Neurobiol.* 38, 35–56. doi: 10.1016/0301-0082(92)90034-C

McLaren, D. G., Ries, M. L., Xu, G., and Johnson, S. C. (2012). A generalized form of context-dependent psychophysiological interactions (gPPI): a comparison to standard approaches. *Neuroimage* 61, 1277–1286. doi: 10.1016/j.neuroimage.2012.03.068

Melgari, J.-M., Pasqualetti, P., Pauri, F., and Rossini, P. M. (2008). Muscles in "concert": study of primary motor cortex upper limb functional topography. *PLoS One* 3:e3069. doi: 10.1371/journal.pone.0003069

Moore, S. T., Clément, G., Dai, M., Raphan, T., Solomon, D., and Cohen, B. (2003). Ocular and perceptual responses to linear acceleration in microgravity: alterations in otolith function on the COSMOS and neurolab flights. *J. Vestib. Res.* 13, 377–393.

Mulavara, A. P., Feiveson, A. H., Fiedler, J., Cohen, H., Peters, B. T., Miller, C., et al. (2010). Locomotor function after long-duration space flight: effects and motor learning during recovery. *Exp. Brain Res.* 202, 649–659. doi: 10.1007/s00221-010-2171-0

Nelson, E. S., Mulugeta, L., and Myers, J. G. (2014). Microgravity-induced fluid shift and ophthalmic changes. *Life* 4, 621–665. doi: 10.3390/life4040621

Newberg, A. B., and Alavi, A. (1998). Changes in the central nervous system during long-duration space flight: implications for neuro-imaging. *Adv. Space Res.* 22, 185–196. doi: 10.1016/s0273-1177(98)80010-0

Pernet, C. R. (2014). Misconceptions in the use of the general linear model applied to functional MRI: a tutorial for junior neuro-imagers. *Front. Neurosci.* 8:1. doi: 10.3389/fnins.2014.00001

Pfeiffer, C., Serino, A., and Blanke, O. (2014). The vestibular system: a spatial reference for bodily self-consciousness. *Front. Integr. Neurosci.* 8:31. doi: 10.3389/fnint.2014.00031

Polastri, P. F., and Barela, J. A. (2013). Adaptive visual re-weighting in children's postural control. *PLoS One* 8:e82215. doi: 10.1371/journal.pone.0082215

Rao, L.-L., Zhou, Y., Liang, Z.-Y., Rao, H., Zheng, R., Sun, Y., et al. (2014). Decreasing ventromedial prefrontal cortex deactivation in risky decision making after simulated microgravity: effects of -6° head-down tilt bed rest. *Front. Behav. Neurosci.* 8:187. doi: 10.3389/fnbeh.2014.00187

Razumeev, A., and Grigoryan, R. (1976). *Cerebellum and Gravity*. Moscow: Nauka.

Reason, J. T., and Brand, J. J. (1975). *Motion Sickness*. Cambridge, MA: Academic Press.

Reschke, M. F., Bloomberg, J. J., Harm, D. L., Paloski, W. H., Layne, C., and McDonald, V. (1998). Posture, locomotion, spatial orientation, and motion sickness as a function of space flight. *Brain Res. Rev.* 28, 102–117. doi: 10.1016/S0165-0173(98)00031-9

Roberts, D. R., Albrecht, M. H., Collins, H. R., Asemani, D., Chatterjee, A. R., Spampinato, M. V., et al. (2017). Effects of spaceflight on astronaut brain structure as indicated on mri. *N. Engl. J. Med.* 377, 1746–1753. doi: 10.1056/nejmoa1705129

Roberts, D. R., Ramsey, D., Johnson, K., Kola, J., Ricci, R., Hicks, C., et al. (2010). Cerebral cortex plasticity after 90 days of bed rest: data from TMS and fMRI. *Aviat. Space Environ. Med.* 81, 30–40. doi: 10.3357/asem.2532.2009

Roberts, D. R., Zhu, X., Tabesh, A., Duffy, E. W., Ramsey, D. A., and Brown, T. R. (2015). Structural brain changes following long-term 6° head-down tilt bed rest as an analog for spaceflight. *Am. J. Neuroradiol.* 36, 2048–2054. doi: 10.3174/ajnr.A4406

Roy, R. R., Hodgson, J. A., Aragon, J., Day, M. K., Kozlovskaya, I., and Edgerton, V. R. (1996). Recruitment of the Rhesus soleus and medial gastrocnemius before, during and after spaceflight. *J. Gravit. Physiol.* 3, 11–15.

Saad, Z. S., Reynolds, R. C., Jo, H. J., Gotts, S. J., Chen, G., Martin, A., et al. (2013). Correcting brain-wide correlation differences in resting-state fMRI. *Brain Connect.* 3, 339–352. doi: 10.1089/brain.2013.0156

Sahyoun, C., Floyer-Lea, A., Johansen-Berg, H., and Matthews, P. M. (2004). Towards an understanding of gait control: brain activation during the anticipation, preparation and execution of foot movements. *Neuroimage* 21, 568–575. doi: 10.1016/j.neuroimage.2003.09.065

Sajdel-Sulkowska, E. M. (2013). *Cerebellum and Gravity: Altered Earth's Gravity Perception under Pathological Conditions and Response to Altered Gravity in Space*. Dordrecht: Springer.

Sampaio-Baptista, C., Sanders, Z.-B., and Johansen-Berg, H. (2018). Structural plasticity in adulthood with motor learning and stroke rehabilitation. *Annu. Rev. Neurosci.* 41, 25–40. doi: 10.1146/annurev-neuro-080317-062015

Sangals, J., Heuer, H., Manzey, D., and Lorenz, B. (1999). Changed visuomotor transformations during and after prolonged microgravity. *Exp. Brain Res.* 129, 378–390. doi: 10.1007/s002210050906

Schmäl, F. (2013). Neuronal mechanisms and the treatment of motion sickness. *Pharmacology* 91, 229–241. doi: 10.1159/000350185

Schuwerk, T., Schurz, M., Müller, F., Rupprecht, R., and Sommer, M. (2017). The rTPJ's overarching cognitive function in networks for attention and theory of mind. *Soc. Cogn. Affect. Neurosci.* 12, 157–168. doi: 10.1093/scan/nsw163

Seidler, R. D., Mulavara, A. P., Bloomberg, J. J., and Peters, B. T. (2015). Individual predictors of sensorimotor adaptability. *Front. Syst. Neurosci.* 9:100. doi: 10.3389/fnsys.2015.00100

Shelhamer, M. (2015). Trends in sensorimotor research and countermeasures for exploration-class space flights. *Front. Syst. Neurosci.* 9:115. doi: 10.3389/fnsys.2015.00115

Shigueva, T. A., Zakirova, A. Z., Tomilovskaya, E. S., and Kozlovskaya, I. B. (2015). Effect of support deprivation on the order of motor unit recruitment. *Hum. Physiol.* 41, 813–816. doi: 10.1134/S036211971507021X

Sirota, M. G., Babaev, B. M., Beloozerova, I. N., Nyrova, A. N., Yakushin, S. B., Kozlovskaya, I. B., et al. (1988). Neuronal activity of nucleus vestibularis during coordinated movement of eyes and head in microgravitation. *Physiologist* 31, 23–28.

Slenzka, K. (2003). Neuroplasticity changes during space flight. *Adv. Space Res.* 31, 1595–1604. doi: 10.1016/s0273-1177(03)00011-5

Smith, S. M., Krauhs, J. M., and Leach, C. S. (1997). Regulation of body fluid volume and electrolyte concentrations in spaceflight. *Adv. Space Biol. Med.* 6, 123–165. doi: 10.1016/s1569-2574(08)60081-7

Speers, R. A., Paloski, W. H., and Kuo, A. D. (1998). Multivariate changes in coordination of postural control following spaceflight. *J. Biomech.* 31, 883–889. doi: 10.1016/S0021-9290(98)00065-7

Splittgerber, R. (2019). *Snell's Clinical Neuroanatomy*, 8th Edn. Philadelphia, PA: Wolters Kluwer.

Steffener, J., Tabert, M., Reuben, A., and Stern, Y. (2010). Investigating hemodynamic response variability at the group level using basis functions. *Neuroimage* 49, 2113–2122. doi: 10.1016/j.neuroimage.2009.11.014

Taylor, C. R., Hanna, M., Behnke, B. J., Stabley, J. N., McCullough, D. J., Robert, T. D., et al. (2013). Spaceflight-induced alterations in cerebral artery vasoconstrictor, mechanical, and structural properties: implications for elevated cerebral perfusion and intracranial pressure. *FASEB J.* 27, 2282–2292. doi: 10.1096/fj.12-222687

Tomassini, V., Jbabdi, S., Kincses, Z. T., Bosnell, R., Douaud, G., Pozzilli, C., et al. (2011). Structural and functional bases for individual differences in motor learning. *Hum. Brain Mapp.* 32, 494–508. doi: 10.1002/hbm.21037

Tomilovskaya, E., Shigueva, T., Sayenko, D., Rukavishnikov, I., and Kozlovskaya, I. (2019). Dry Immersion as an onground model of microgravity physiological effects. *Front. Physiol.* 10:284. doi: 10.3389/fphys.2019.00284

Tzourio-Mazoyer, N., Landeau, B., Papathanassiou, D., Crivello, F., Etard, O., Delcroix, N., et al. (2002). Automated anatomical labeling of activations in SPM using a macroscopic anatomical parcellation of the MNI MRI single-subject brain. *Neuroimage* 15, 273–289. doi: 10.1006/nimg.2001.0978

Van Ombergen, A. (2017). *The Effect of Microgravity and Vestibular Disorders on Human Neuroplasticity*. Ph.D. thesis, University of Antwerpen, Belgium.

Van Ombergen, A., Demertzi, A., Tomilovskaya, E., Jeurissen, B., Sijbers, J., Kozlovskaya, I. B., et al. (2017a). The effect of spaceflight and microgravity on the human brain. *J. Neurol.* 264, 18–22. doi: 10.1007/s00415-017-8427-x

Van Ombergen, A., Heine, L., Jillings, S., Roberts, R. E., Jeurissen, B., Van Rompaey, V., et al. (2017b). Altered functional brain connectivity in patients with visually induced dizziness. *Neuroimage Clin.* 14, 538–545. doi: 10.1016/j.nicl.2017.02.020

Van Ombergen, A., Laureys, S., Sunaert, S., Tomilovskaya, E., Parizel, P. M., and Wuyts, F. L. (2017c). Spaceflight-induced neuroplasticity in humans as measured by MRI: what do we know so far? *NPJ Microgravity* 3:2. doi: 10.1038/s41526-016-0010-8

Van Ombergen, A., Wuyts, F. L., Jeurissen, B., Sijbers, J., Vanhevel, F., Jillings, S., et al. (2017d). Intrinsic functional connectivity reduces after first-time exposure to short-term gravitational alterations induced by parabolic flight. *Sci. Rep.* 7:3061. doi: 10.1038/s41598-017-03170-5

Van Ombergen, A., Jillings, S., Jeurissen, B., Tomilovskaya, E., Rühl, M. R., Rumshiskaya, A., et al. (2018). Brain tissue-volume changes in cosmonauts. *N. Engl. J. Med.* 379, 1678–1680. doi: 10.1056/nejmc1809011

Wang, L., Li, Z., Tan, C., Liu, S., Zhang, J., He, S., et al. (2018). Physiological effects of weightlessness: countermeasure system development for a long-term Chinese manned spaceflight. *Front. Med.* 2018, 1–11. doi: 10.1007/s11684-017-0587-7

Watenpaugh, D. E. (2016). Analogs of microgravity: head-down tilt and water immersion. *J. Appl. Physiol.* 120, 904–914. doi: 10.1152/japplphysiol.00986.2015

Werner, S., Bock, O., Gizewski, E. R., Schoch, B., and Timmann, D. (2010). Visuomotor adaptive improvement and aftereffects are impaired differentially following cerebellar lesions in SCA and PICA territory. *Exp. Brain Res.* 201, 429–439. doi: 10.1007/s00221-009-2052-6

Whitfield-Gabrieli, S., and Nieto-Castanon, A. (2012). Conn: a functional connectivity toolbox for correlated and anticorrelated brain networks. *Brain Connect.* 2, 125–141. doi: 10.1089/brain.2012.0073

Young, L. R., Oman, C. M., Watt, D. G., Money, K. E., and Lichtenberg, B. K. (1984). Spatial orientation in weightlessness and readaptation to earth's gravity. *Science* 225, 205–208. doi: 10.1126/science.6610215

Yuan, P., Koppelmans, V., Reuter-Lorenz, P., De Dios, Y., Gadd, N., Riascos, R., et al. (2018a). Change of cortical foot activation following 70 days of head down bed rest. *J. Neurophysiol.* 119, 2145–2152. doi: 10.1152/jn.00693.2017

Yuan, P., Koppelmans, V., Reuter-Lorenz, P., De Dios, Y., Gadd, N., Wood, S., et al. (2018b). Vestibular brain changes within 70 days of head down bed rest. *Hum. Brain Mapp.* 39, 2753–2763. doi: 10.1002/hbm.24037

Yuan, P., Koppelmans, V., Reuter-Lorenz, P., De Dios, Y., Gadd, N., Wood, S., et al. (2017). "Brain activations for vestibular stimulation and dual tasking change with spaceflight," in *Proceedings of the Neural Control of Movement Meeting*, Dublin.

Yuan, P., Koppelmans, V., Reuter-Lorenz, P. A., De Dios, Y. E., Gadd, N. E., Wood, S. J., et al. (2016). Increased brain activation for dual tasking with 70-days head-down bed rest. *Front. Syst. Neurosci.* 10:71. doi: 10.3389/fnsys.2016.00071

Zalesky, A., Fornito, A., and Bullmore, E. T. (2010). Network-based statistic: identifying differences in brain networks. *Neuroimage* 53, 1197–1207. doi: 10.1016/j.neuroimage.2010.06.041

Zhou,Y., Wang, Y., Rao, L.-L., Liang, Z.-Y., Chen, X.-P., Zheng, D., (2014). Disrupted resting-state functional architecture of the brain after 45-day simulated microgravity. *Front. Behav. Neurosci.* 8:200. doi: 10.3389/fnbeh.2014.00200

Zhu, H., Wang, H., and Liu, Z. (2015). Effects of real and simulated weightlessness on the cardiac and peripheral vascular functions of humans: a review. *Int. J. Occup. Med. Environ. Health* 28, 793-802. doi: 10.13075/ijomeh.1896.00301

Zu Eulenburg, P., Caspers, S., Roski, C., and Eickhoff, S. B. (2012). Meta-analytical definition and functional connectivity of the human vestibular cortex. *Neuroimage* 60, 162-169. doi: 10.1016/j.neuroimage.2011.12.032

Conflict of Interest Statement: The authors declare that the research was conducted in the absence of any commercial or financial relationships that could be construed as a potential conflict of interest.

frontiers in Physiology

BRIEF RESEARCH REPORT
published: 18 July 2019
doi: 10.3389/fphys.2019.00899

A Moderate Daily Dose of Resveratrol Mitigates Muscle Deconditioning in a Martian Gravity Analog

Marie Mortreux[1], Daniela Riveros[1], Mary L. Bouxsein[2] and Seward B. Rutkove[1]*

[1] Department of Neurology, Beth Israel Deaconess Medical Center, Harvard Medical School, Boston, MA, United States, [2] Center for Advanced Orthopaedic Studies, Beth Israel Deaconess Medical Center, Harvard Medical School, Boston, MA, United States

While there is a relatively good understanding of the effects of microgravity on human physiology based on five decades of experience, the physiological consequences of partial gravity remain far less well understood. Until recently, no model had been able to replicate partial gravity such as that experienced on Mars (0.38 g), which would be critical to help sustain long-term missions and ensure a safe return to Earth. Recent development of two partial weight bearing (PWB) models, one in mice and one in rats, now allows for quadrupedal partial unloading that mimics Martian gravity. Resveratrol (RSV), a polyphenol most commonly found in grapes and blueberries, has been extensively investigated for its health benefits, including its anti-inflammatory, anti-oxidative, and anti-diabetic effects. In the context of mechanical unloading, RSV has also been shown to preserve bone and muscle mass. However, there is a lack of research regarding its effect on the musculoskeletal system in partial gravity. We hypothesized that a moderate daily dose of RSV (150 mg/kg/day) would help mitigate muscle deconditioning in a Mars gravity analog. Indeed, our results demonstrate that RSV treatment during partial unloading significantly preserves muscle function (e.g., the average change in grip force after 14 days of PWB40 was of −6.18, and +10.92% when RSV was administered) and mitigates muscle atrophy (e.g., RSV supplementation led to an increase of 21.6% in soleus weight for the unloaded animals). This work suggests the potential of a nutraceutical approach to reduce musculoskeletal deconditioning on a long-term mission to Mars.

Keywords: partial gravity, resveratrol, rats, Mars, muscle function

OPEN ACCESS

Edited by:
Richard D. Boyle, National Aeronautics and Space Administration (NASA), United States

Reviewed by:
Boris Shenkman, Institute of Biomedical Problems (RAS), Russia
Nastassia Navasiolava, Centre Hospitalier Universitaire d'Angers, France
Susan Ann Bloomfield, Texas A&M University, United States

****Correspondence:***
Marie Mortreux
mmortreu@bidmc.harvard.edu

Specialty section:
This article was submitted to Environmental, Aviation and Space Physiology, a section of the journal Frontiers in Physiology

Received: *01 February 2019*
Accepted: *27 June 2019*
Published: *18 July 2019*

Citation:
Mortreux M, Riveros D, Bouxsein ML and Rutkove SB (2019) A Moderate Daily Dose of Resveratrol Mitigates Muscle Deconditioning in a Martian Gravity Analog. Front. Physiol. 10:899. doi: 10.3389/fphys.2019.00899

INTRODUCTION

After decades of manned low earth orbit missions, space agencies are now targeting other planets for human exploration. In the upcoming years, NASA plans to send astronauts to the Moon and to Mars (National Aeronautics and Space Administration [NASA], 2018), both of which display a significantly lower gravity than Earth (0.16 and 0.38 g, respectively). While there is an extensive literature reviewing the impact of microgravity (real or simulated) on the muscular system (Fitts et al., 2000; Morey-Holton et al., 2005; Baldwin et al., 2013; Chowdhury et al., 2013; Ohira et al., 2015;

Radugina et al., 2018), relatively little is known about the effects of partial gravity. Thus, mitigating strategies will be needed to prevent muscle deconditioning and allow astronauts to safely perform tasks upon arrival on Mars, especially after being reintroduced to gravity, even if at a reduced level.

Among potential medicinal interventions to prevent muscle deterioration, nutraceuticals are especially appealing since they are naturally occurring compounds that are present in the diet. Moreover, astronauts en route to Mars will not have the opportunity to exercise with the same devices currently deployed on the ISS (Petersen et al., 2016). Of potential candidates, resveratrol (RSV), a polyphenol, commonly found in grape skin, red wine, and blueberries and used as a dietary supplement, has been widely investigated (Tran et al., 2017; Yonamine et al., 2017; Zhang et al., 2017, 2018; Zhu et al., 2017; Franck et al., 2018), and declared safe for animals and humans (Williams et al., 2009). RSV has already been studied for its osteoprotective effects (Shen et al., 2012; Durbin et al., 2014; Ornstrup et al., 2014), and described as a physical exercise mimetic to prevent wasting disorders during hindlimb unloading (Momken et al., 2011). However, its mitigating effect has never been studied in a partial weight-bearing (PWB) model.

In this study, we hypothesized that daily supplementation with a moderate dose of RSV would mitigate muscle impairment in a ground-based partial gravity analog that mimics a Martian environment (0.4 g, PWB40). If correct, our results would offer proof of concept for such intervention with subsequent efforts devoted to unraveling potential underlying mechanisms of action.

MATERIALS AND METHODS

Animals and Supplementation

Twenty-four male Wistar rats (Charles River Laboratories Inc., Wilmington, MA, United States) weighing 425 ± 6.73 g (14 weeks of age) were obtained and housed in a temperature-controlled (22 ± 2°C) room with a 12:12-hour light-dark cycle. Water and rat chow were provided *ad libitum* and daily food intake was monitored. Animals were exposed to normal loading (PWB100) or Martian gravity (40% of normal loading: PWB40) for 14 days. Detailed description about the control group, the housing environment and the suspension apparatus can be found in our previous articles describing this model (Mortreux et al., 2018, 2019). Half of the animals in each group received resveratrol daily (RSV, 150 mg/kg/day, Transreveratrol HPLC Purified, megaresveratrol.net, Candlewood Stars, Inc, Danbury, CT, United States) starting at baseline (day 0). RSV was prepared daily by mixing the powder with 10% sucrose water into a 150 mg/ml solution that was administered orally using a 1 mL syringe. Animals were weighed weekly, free of their suspension apparatus. All experimental protocols were approved by the Beth Israel Deaconess Medical Center Institutional Animal Care and Use Committee.

Longitudinal Limb Muscle Assessment

Weekly, calf circumference was measured at the left tibia mid-shaft. Animals were anesthetized with isoflurane and placed in a prone position with their left hind limb taped at a 45-degree angle. Fur was removed using a hair clipper (Braintree Scientific, Braintree, MA, United States) and suture thread was used to obtain three circumference measurements and the average was recorded.

Using a 50 N grip force meter (Chatillon, Largo, FL, United States), both front and rear paw grip force were assessed weekly by performing three gentle pulls until the animals released their grip, allowing them to rest for 30 s between trials. The peak force of each trial was recorded and the three trials averaged.

Terminal Muscle Assessment

After 14 days, animals were sacrificed and the triceps surae (e.g., soleus and gastrocnemius muscles) was harvested and muscle wet mass was measured using a precision balance (Fisher Scientific, Pittsburgh, PA, United States). Muscles were fixed in 10% formalin for 48 h and embedded in paraffin. Immunohistochemical analysis was performed using anti-collagen VI (ab6588, Abcam, Cambridge, MA, United States) and anti-slow skeletal myosin heavy chain (ab11083, Abcam, Cambridge, MA, United States) antibodies. Images were obtained at 20× using an epifluorescence microscope (Zeiss Axio Imager M1) and a minimum of 100 myofibers were analyzed for each muscle with FIJI (ImageJ, NIH) using the muscle morphometry plug-in (Anthony Sinadinos using Eclipse IDE) to calculate the average myofiber cross sectional area (CSA) with the experimenter blinded for treatment and gravity level.

Statistical Analyses

Longitudinal measurements were analyzed using repeated measures 2-way ANOVA followed by Tukey's multiple comparisons test. Terminal measurements were analyzed using 1-way ANOVA followed by Tukey's *post hoc* test. All results were considered significant when $p < 0.05$ and performed using GraphPad Prism 7.

RESULTS

Resveratrol supplementation did not influence body weight (**Figure 1A**) in any group as compared to un-supplemented animals. Calf circumference was not impacted by the RSV supplementation and animals from both PWB40 and PWB40 + RSV groups displayed a significant reduction over time compared to either their baseline values or to the two control groups (**Figure 1B**). After 14 days, rats undergoing PWB40 were the only group performing below baseline values for front paw grip force, and significantly lower than all other groups (**Figure 1C**). In the hindlimbs (**Figure 1D**), a significant decline in grip force was evidenced as early as 7 days. RSV supplementation totally rescued grip

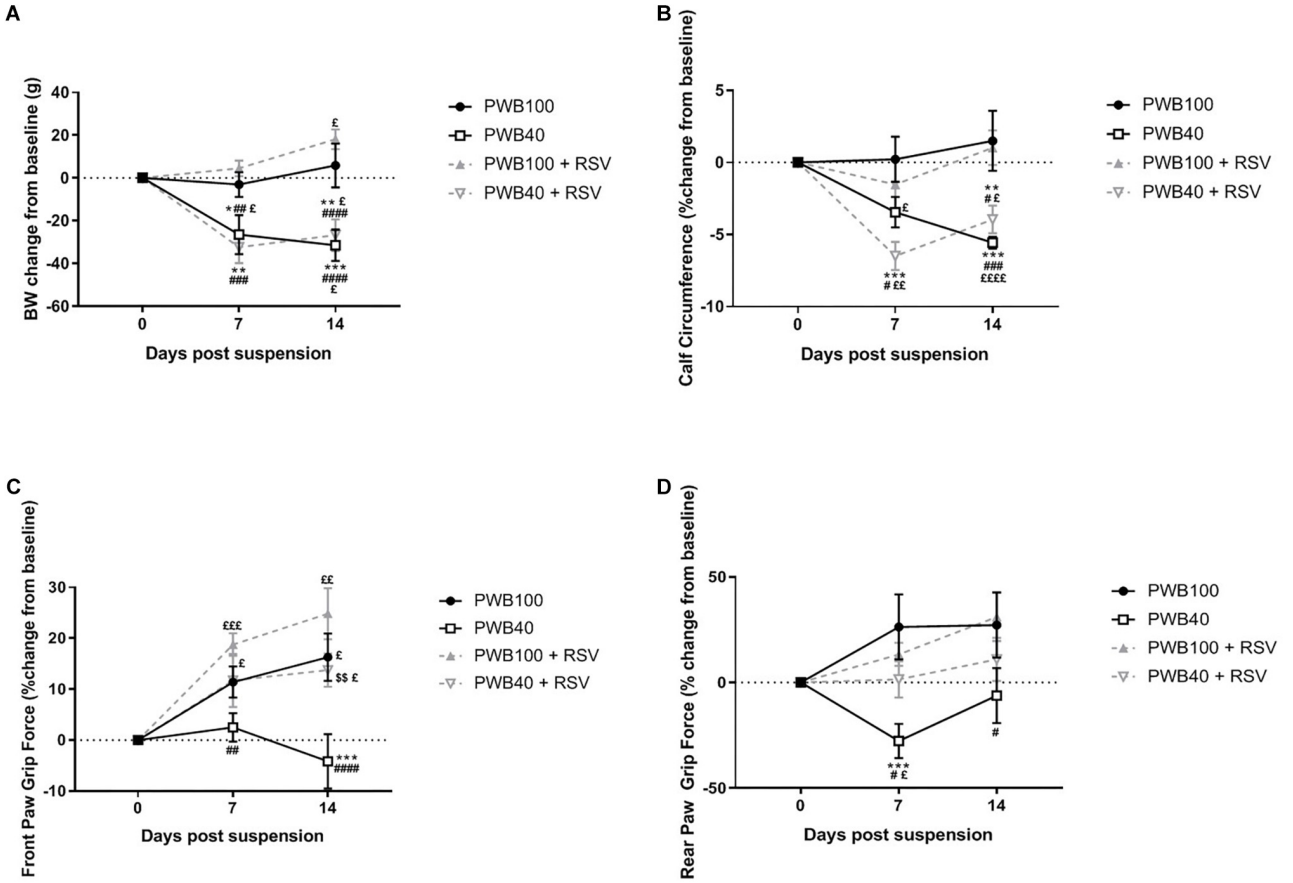

FIGURE 1 | Weekly changes in body weight **(A)**, calf circumference **(B)**, front paw **(C)** and rear paw **(D)** grip force compared to pre-suspension values (day 0). Data are presented as mean ± SEM; results of the *post hoc* tests following the ANOVA are indicated. $N = 6$ per group. $^{*}p < 0.05$, $^{**}p < 0.01$, $^{***}p < 0.001$, and $^{****}p < 0.0001$ vs. PWB100, respectively. $^{\#}p < 0.05$, $^{\#\#}p < 0.01$, $^{\#\#\#}p < 0.001$, and $^{\#\#\#\#}p < 0.0001$ vs. PWB100 + RSV, respectively. $^{\$\$}p < 0.01$ vs. PWB40. $^{£}p < 0.05$, $^{££}p < 0.01$, $^{£££}p < 0.001$, and $^{££££}p < 0.0001$ vs. baseline values (day 0), respectively.

force in both the front and hindlimbs of the rats exposed to partial unloading (**Figures 1C,D**).

Data on terminal muscle assessment are presented in **Figure 2** and **Supplementary Tables S1**, **S2**. Animals exposed to PWB40 alone displayed a significantly reduced soleus mass, average CSA, and slow-twitch-CSA compared to both non-unloaded groups. In contrast, RSV supplementation in animals exposed to PWB40 prevented muscle atrophy (**Figure 2A**) and partially rescued myofiber CSA (**Figure 2B** and **Supplementary Table S2**), but did not induce any significant change for the group at PWB100. As visualized in the images (**Figure 2C**), we observed a significant reduction of the myofiber type switch in the soleus of the rats undergoing PWB40 and supplemented with RSV ($p = 0.0269$ vs. PWB40, **Supplementary Table S1**). In the gastrocnemius, PWB40 induced a significant reduction of muscle mass (**Figure 2D**) and CSA (**Figures 2E,F**). RSV supplementation successfully increased muscle wet mass compared to non-treated animals (**Figure 2D**), but did not fully restore the average CSA (**Figure 2E**). However, the fiber-specific CSA did not significantly differ compared to the two non-unloaded groups (**Supplementary Table S2**). While a slight increase in slow-twitch myofibers was visible in the PWB40 + RSV group (**Figure 2F**), it was not significantly different compared to the other groups (**Supplementary Table S1**).

DISCUSSION

We previously demonstrated that our PWB system was well tolerated by the rats over a 14-day period (Mortreux et al., 2018, 2019) despite an initial body weight loss, similar to that observed in HLU models (Brooks et al., 2009) and analogous to what occurs in astronauts in flight (Matsumoto et al., 2011). As reported previously in healthy animals (Rauf et al., 2017), RSV did not affect food intake (**Supplementary Table S3**) or body weight (**Figure 1A**) in our study. In rodent models, grip force rapidly declines when animals are exposed to PWB (Wagner et al., 2010; Mortreux et al., 2018, 2019). Here we show that at all time-points, rats exposed to PWB40 + RSV did not score lower than their baseline values, or their non-unloaded counterparts. In both front and rear paw grip force experiments, the PWB40 cohort was the only group that displayed a significant decrease in

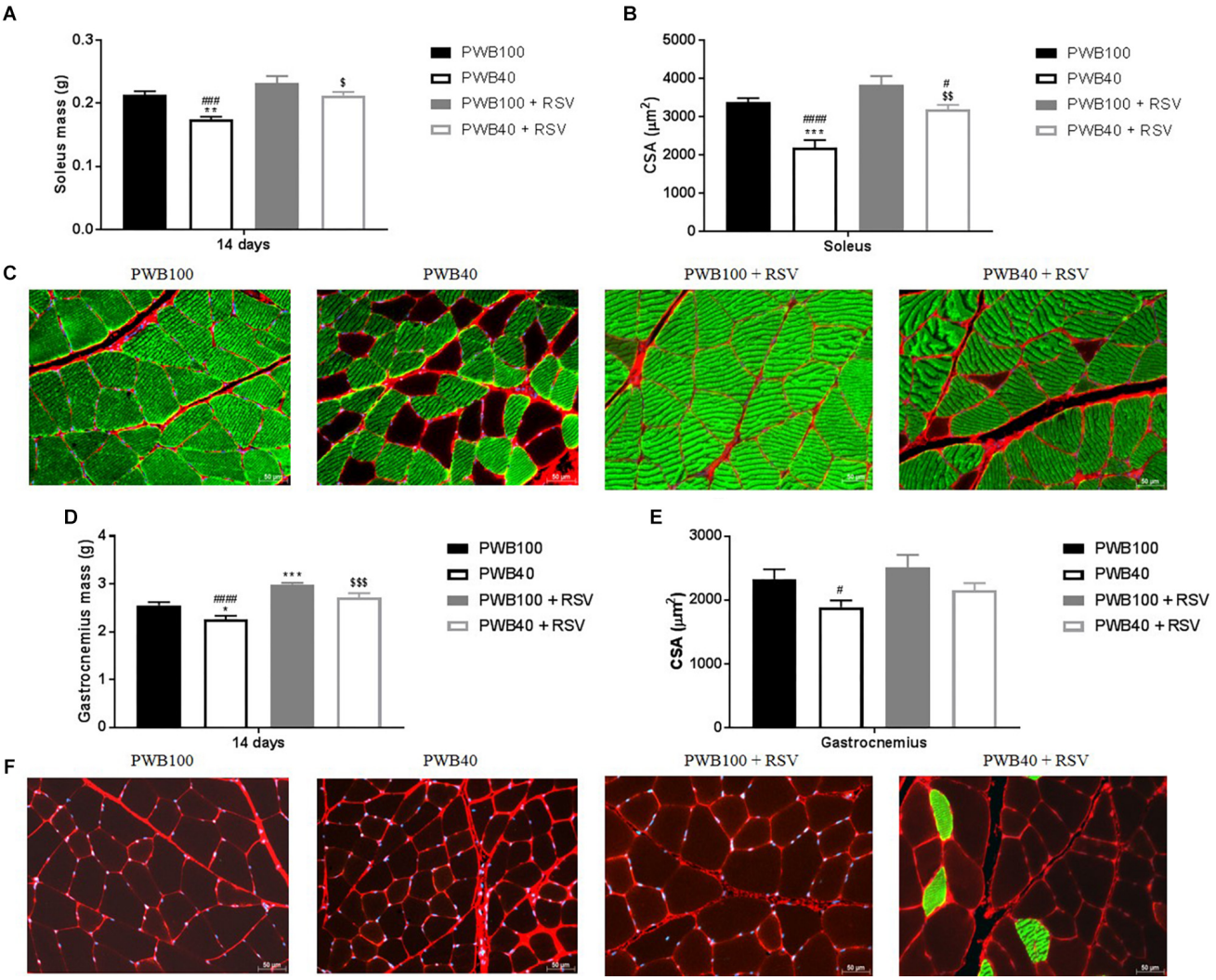

FIGURE 2 | Terminal assessment of the muscles of the triceps surae, including soleus **(A)** and gastrocnemius wet mass **(D)**, soleus **(B)** and gastrocnemius **(E)** average cross sectional area (CSA), and representative images of the soleus **(C)** and gastrocnemius **(F)** muscles stained with anti-collagen VI (red), anti-slow-skeletal myosin heavy chain (green), and DAPI (blue). $N = 6$ per group. The results are presented as mean ± SEM; the results of the *post hoc* tests following the ANOVA are indicated. $^{*}p < 0.05$, $^{**}p < 0.01$, and $^{***}p < 0.001$ vs. PWB100, respectively. $^{\#}p < 0.05$, $^{\#\#\#}p < 0.001$, and $^{\#\#\#\#}p < 0.0001$ vs. PWB100 + RSV, respectively. $^{\$}p < 0.05$, $^{\$\$}p < 0.01$, and $^{\$\$\$}p < 0.001$ vs. PWB40, respectively.

grip force compared to their baseline (rear paw, **Figure 1D**) and that of the other groups (front paw, **Figure 1C**). As previously reported (Mortreux et al., 2018), we observed a slight recovery in rear paw grip force after 14 days of PWB40. The reason for this improvement is uncertain, but may be due, in part, to an adaptation to partial unloading or adult growth.

Ex vivo analysis highlighted the muscle-protective effect of RSV (**Figure 2**). In both the gastrocnemius and soleus muscles, we observed a significant rescue of muscle wet mass comparable to the one observed by Momken et al. (2011) after 14 days of HLU. These findings are further confirmed by the histomorphometric analyses. In the soleus, the average CSA in the PWB40 + RSV group was significantly higher than in the PWB40 group, but remained significantly lower than the PWB100 + RSV group. No differences were seen between the PWB40 + RSV group and the PWB100 controls. In the gastrocnemius, only the PWB40 group displayed a significantly lower average CSA compared to the PWB100 + RSV group. This could be due to the limited number of slides analyzed.

During spaceflight and in rodent models of mechanical unloading, a myofiber type switch has been described (Desplanches, 1997; Lomonosova et al., 2016; Shenkman, 2016; McDonald et al., 2017) in static, weight-bearing muscles such as the soleus, which predominantly consists of slow-twitch fibers, thus providing endurance over dynamic strength. Muscle deconditioning increases the proportion of type two fast twitch fibers in weight-bearing muscles, therefore making them prone to muscle fatigue. While our PWB40 animals displayed a

significantly smaller percentage of type 1 fibers in the soleus compared to the normally loaded groups (**Supplementary Table S1**), rats undergoing PWB40 + RSV did not. This maintenance of muscle composition could explain the preservation of muscle function as demonstrated by our functional assessments. In contrast, gastrocnemius fiber type was not significantly altered by partial unloading or by RSV treatment, despite a 94.21% increase in type 1 myofiber compared to the PWB40 group.

Our initial functional study highlights the benefits of a moderate daily dose of RSV, however, several limitations are to be taken in consideration. First, our study involved only a modest number of male rats (n = 24), thus, we do not yet know if RSV supplementation would benefit females, similarly. Second, we assessed the effect of a single dosage of RSV (150 mg/kg/day). This choice was based on the literature and the known protective effects of RSV on bone (Durbin et al., 2014). Nevertheless, many dosages of RSV have been tested in animal models, up to 700 mg/kg/day (Williams et al., 2009), therefore, a more efficient dose to prevent muscle deconditioning during partial unloading could exist. Finally, our study assessed the functional outcomes of performance and composition of the main weight-bearing hindlimb muscles but did not focus on the deeper mechanisms and pathways that could be involved.

One possible explanation for our findings is that RSV could be responsible for maintaining skeletal muscle insulin sensitivity through its beneficial effect on glucose homeostasis and GLUT4 expression (Momken et al., 2011; Yonamine et al., 2017). Indeed, muscle is intrinsically linked to energy homeostasis since it is a major consumer of glucose during contraction. The transporter GLUT4 controls glucose uptake in the skeletal muscle, and when dysregulated, insulin resistance occurs (Dyar et al., 2014). This metabolic dysfunction has been observed in both astronauts and ground-based animal models of mechanical unloading (Tobin et al., 2002; Hughson et al., 2016; Gambara et al., 2017; Tascher et al., 2017). In diabetic animals, it has been shown that RSV treatment increases muscle weight and protein content by regulating GLUT4 expression in the skeletal muscle (Yonamine et al., 2017), while in healthy hypokinetic animals, RSV supplementation before, during, and after mechanical unloading, enhances insulin sensitivity and muscle recovery (Momken et al., 2011; Bennett et al., 2013), suggesting the presence of a significant link between glucose homeostasis and muscle health. Alternatively, this mitigating phenomenon could also be attributed to the anti-oxidative and anti-inflammatory effects of RSV, which could be crucial for the musculoskeletal system during a period of mechanical unloading, and are currently being investigated using other polyphenols such as dried plums (Simonavice et al., 2013; Schreurs et al., 2016). Further metabolic analyses will be required to unravel the cellular mechanisms involved in the muscle-protective effects of a moderate daily dose of RSV.

Taken together, our results highlight the therapeutic potential of RSV as a nutraceutical countermeasure to prevent muscle deconditioning in an animal model of Martian gravity. Further investigations should optimize the dose of RSV for the preservation of muscle function and explore the mechanisms involved. In addition, it will be important to confirm the lack of any potentially harmful interactions of RSV with other drugs administered to astronauts during space missions.

ETHICS STATEMENT

All studies were approved by the Institutional Animal Care and Use Committee of Beth Israel Deaconess Medical Center and conform to the National Research Council "Guide for the Care and Use of Laboratory Animals."

AUTHOR CONTRIBUTIONS

MM designed the methodology. MM and DR performed the experiments, and analyzed the data. MB and SR designed the study. All authors reviewed and approved the manuscript.

FUNDING

This work was funded by a grant from the National Aeronautics and Space Administration (NASA: NNX16AL36G).

ACKNOWLEDGMENTS

The authors would like to thank Dr. J. A. Nagy for her careful editing of the manuscript.

SUPPLEMENTARY MATERIAL

The Supplementary Material for this article can be found online at: https://www.frontiersin.org/articles/10.3389/fphys.2019.00899/full#supplementary-material

REFERENCES

Baldwin, K. M., Haddad, F., Pandorf, C. E., Roy, R. R., and Edgerton, V. R. (2013). Alterations in muscle mass and contractile phenotype in response to unloading models: role of transcriptional/pretranslational mechanisms. *Front. Physiol.* 4:284. doi: 10.3389/fphys.2013.00284

Bennett, B. T., Mohamed, J. S., and Alway, S. E. (2013). Effects of resveratrol on the recovery of muscle mass following disuse in the plantaris muscle of aged rats. *PLoS One* 8:e83518. doi: 10.1371/journal.pone.0083518

Brooks, N., Gj, C., Je, L., Am, F., Arbogast, S., Smith, J., et al. (2009). Countermeasures for spaceflight-induced muscle atrophy and loss of strength. *Aviat. Space. Environ. Med.* 80, 987–987. doi: 10.3357/asem.27009.2009

Chowdhury, P., Long, A., Harris, G., Soulsby, M. E., and Dobretsov, M. (2013). Animal model of simulated microgravity: a comparative study of hindlimb unloading via tail versus pelvic suspension. *Physiol. Rep.* 1:e00012. doi: 10.1002/phy2.12

Desplanches, D. (1997). Structural and functional adaptations of skeletal muscle to weightlessness. *Int. J. Sports Med.* 18, S259–S264. doi: 10.1055/s-2007-972722

Durbin, S. M., Jackson, J. R., Ryan, M. J., Gigliotti, J. C., Alway, S. E., and Tou, J. C. (2014). Resveratrol supplementation preserves long bone mass, microstructure, and strength in hindlimb-suspended old male rats. *J. Bone Miner. Metab.* 32, 38–47. doi: 10.1007/s00774-013-0469-2

Dyar, K. A., Ciciliot, S., Wright, L. E., Biensø, R. S., Tagliazucchi, G. M., Patel, V. R., et al. (2014). Muscle insulin sensitivity and glucose metabolism are controlled by the intrinsic muscle clock. *Mol. Metab.* 3, 29–41. doi: 10.1016/j.molmet.2013.10.005

Fitts, R. H., Riley, D. R., and Widrick, J. J. (2000). Physiology of a microgravity environment invited review: microgravity and skeletal muscle. *J. Appl. Physiol.* 89, 823–839. doi: 10.1152/jappl.2000.89.2.823

Franck, F. C., Benatti, B. B., Andia, D. C., Cirano, F. R., Casarin, R. C., Corrêa, M. G., et al. (2018). Impact of resveratrol on bone repair in rats exposed to cigarette smoke inhalation: histomorphometric and bone-related gene expression analysis. *Int. J. Oral Maxillofac. Surg.* 47, 541–548. doi: 10.1016/j.ijom.2017.08.004

Gambara, G., Salanova, M., Ciciliot, S., Furlan, S., Gutsmann, M., Schiffl, G., et al. (2017). Microgravity-induced transcriptome adaptation in mouse paraspinal longissimus dorsi muscle highlights insulin resistance-linked genes. *Front. Physiol.* 8:279. doi: 10.3389/fphys.2017.00279

Hughson, R. L., Robertson, A. D., Arbeille, P., Shoemaker, J. K., Rush, J. W. E., Fraser, K. S., et al. (2016). Increased postflight carotid artery stiffness and inflight insulin resistance resulting from 6-mo spaceflight in male and female astronauts. *Am. J. Physiol. Circ. Physiol.* 310, H628–H638. doi: 10.1152/ajpheart.00802.2015

Lomonosova, Y. N., Turtikova, O. V., and Shenkman, B. S. (2016). Reduced expression of MyHC slow isoform in rat soleus during unloading is accompanied by alterations of endogenous inhibitors of calcineurin/NFAT signaling pathway. *J. Muscle Res. Cell Motil.* 37, 7–16. doi: 10.1007/s10974-015-9428-y

Matsumoto, A., Storch, K. J., Stolfi, A., Mohler, S. R., Frey, M. A., and Stein, T. P. (2011). Weight loss in humans in space. *Aviat. Space Environ. Med.* 82, 615–621. doi: 10.3357/ASEM.2792.2011

McDonald, K. S., Blaser, C. A., and Fitts, R. H. (2017). Force-velocity and power characteristics of rat soleus muscle fibers after hindlimb suspension. *J. Appl. Physiol.* 77, 1609–1616. doi: 10.1152/jappl.1994.77.4.1609

Momken, I., Stevens, L., Bergouignan, A., Desplanches, D., Rudwill, F., Chery, I., et al. (2011). Resveratrol prevents the wasting disorders of mechanical unloading by acting as a physical exercise mimetic in the rat. *FASEB J.* 25, 3646–3660. doi: 10.1096/fj.10-177295

Morey-Holton, E., Globus, R. K., Kaplansky, A., and Durnova, G. (2005). The hindlimb unloading rat model: literature overview, technique update and comparison with space flight data. *Adv. Space Biol. Med.* 10, 7–40. doi: 10.1016/S1569-2574(05)10002-1

Mortreux, M., Nagy, J. A., Ko, F. C., Bouxsein, M. L., and Rutkove, S. B. (2018). A novel partial gravity ground-based analog for rats via quadrupedal unloading. *J. Appl. Physiol.* 125, 175–182. doi: 10.1152/japplphysiol.01083.2017

Mortreux, M., Riveros, D., Bouxsein, M. L., and Rutkove, S. B. (2019). Mimicking a space mission to mars using hindlimb unloading and partial weight bearing in rats. *J. Vis. Exp.* 146:e59327. doi: 10.3791/59327

National Aeronautics and Space Administration [NASA] (2018). *National Space Exploration Campaign Report*. Available at: https://www.nasa.gov/sites/default/files/atoms/files/nationalspaceexplorationcampaign.pdf (accessed October 24, 2018).

Ohira, T., Kawano, F., Ohira, T., Goto, K., and Ohira, Y. (2015). Responses of skeletal muscles to gravitational unloading and/or reloading. *J. Physiol. Sci.* 65, 293–310. doi: 10.1007/s12576-015-0375-6

Ornstrup, M. J., Harsløf, T., Kjær, T. N., Langdahl, B. L., and Pedersen, S. B. (2014). Resveratrol increases bone mineral density and bone alkaline phosphatase in obese men: a randomized placebo-controlled trial. *J. Clin. Endocrinol. Metab.* 99, 4720–4729. doi: 10.1210/jc.2014-2799

Petersen, N., Jaekel, P., Rosenberger, A., Weber, T., Scott, J., Castrucci, F., et al. (2016). Exercise in space: the european space agency approach to in-flight exercise countermeasures for long-duration missions on ISS. *Extrem Physiol. Med.* 5:9. doi: 10.1186/s13728-016-0050-4

Radugina, E. A., Almeida, E. A. C., Blaber, E., Poplinskaya, V. A., Markitantova, Y. V., and Grigoryan, E. N. (2018). Exposure to microgravity for 30 days onboard Bion M1 caused muscle atrophy and impaired regeneration in murine femoral Quadriceps. *Life Sci. Space Res.* 16, 18–25. doi: 10.1016/j.lssr.2017.08.005

Rauf, A., Imran, M., Sulera, H. A. R., Ahmad, B., Peters, D. G., and Mubarak, M. S. (2017). A comprehensive review of the health perspectives of resveratrol. *Food Funct.* 8, 4284–4305. doi: 10.1039/c7fo01300k

Schreurs, A. S., Shirazi-Fard, Y., Shahnazari, M., Alwood, J. S., Truong, T. A., Tahimic, C. G. T., et al. (2016). Dried plum diet protects from bone loss caused by ionizing radiation. *Sci. Rep.* 6:21343. doi: 10.1038/srep21343

Shen, C. L., von Bergen, V., Chyu, M. C., Jenkins, M. R., Mo, H., Chen, C. H., et al. (2012). Fruits and dietary phytochemicals in bone protection. *Nutr. Res.* 32, 897–910. doi: 10.1016/j.nutres.2012.09.018

Shenkman, B. S. (2016). From slow to fast: hypogravity-induced remodeling of muscle fiber myosin phenotype. *Acta Naturae* 8, 47–59. doi: 10.32607/20758251-2016-8-4-47-59

Simonavice, E., Liu, P.-Y., Ilich, J. Z., Kim, J.-S., Arjmandi, B., and Panton, L. B. (2013). The effects of a 6-month resistance training and dried plum consumption intervention on strength, body composition, blood markers of bone turnover, and inflammation in breast cancer survivors. *Appl. Physiol. Nutr. Metab.* 39, 730–739. doi: 10.1139/apnm-2013-0281

Tascher, G., Brioche, T., Maes, P., Chopard, A., O'Gorman, D., Gauquelin-Koch, G., et al. (2017). Proteome-wide adaptations of mouse skeletal muscles during a full month in space. *J. Proteome Res.* 16, 2623–2638. doi: 10.1021/acs.jproteome.7b00201

Tobin, B. W., Uchakin, P. N., and Leeper-Woodford, S. K. (2002). Insulin secretion and sensitivity in space flight. *Nutrition* 18, 842–848. doi: 10.1016/s0899-9007(02)00940-1

Tran, H. T., Liong, S., Lim, R., Barker, G., and Lappas, M. (2017). Resveratrol ameliorates the chemical and microbial induction of inflammation and insulin resistance in human placenta, adipose tissue and skeletal muscle. *PLoS One* 12:e0173373. doi: 10.1371/journal.pone.0173373

Wagner, E. B., Granzella, N. P., Saito, H., Newman, D. J., Young, L. R., and Bouxsein, M. L. (2010). Partial weight suspension: a novel murine model for investigating adaptation to reduced musculoskeletal loading. *J. Appl. Physiol.* 109, 350–357. doi: 10.1152/japplphysiol.00014.2009

Williams, L. D., Burdock, G. A., Edwards, J. A., Beck, M., and Bausch, J. (2009). Safety studies conducted on high-purity trans-resveratrol in experimental animals. *Food Chem. Toxicol.* 47, 2170–2182. doi: 10.1016/j.fct.2009.06.002

Yonamine, C. Y., Pinheiro-Machado, E., Michalani, M. L., Alves-Wagner, A. B., Esteves, J. V., Freitas, H. S., et al. (2017). Resveratrol improves glycemic control in Type 2 diabetic obese mice by regulating glucose transporter expression in skeletal muscle and liver. *Molecules* 22:E1180. doi: 10.3390/molecules22071180

Zhang, B., Xu, L., Zhuo, N., and Shen, J. (2017). Resveratrol protects against mitochondrial dysfunction through autophagy activation in human nucleus pulposus cells. *Biochem. Biophys. Res. Commun.* 493, 373–381. doi: 10.1016/j.bbrc.2017.09.015

Zhang, C., Yang, L., Zhao, X., Chen, X., Wang, L., and Geng, Z. (2018). Effect of dietary resveratrol supplementation on meat quality, muscle antioxidative capacity and mitochondrial biogenesis of broilers. *J. Sci. Food Agric.* 98, 1216–1221. doi: 10.1002/jsfa.8576

Zhu, X., Wu, C., Qiu, S., Yuan, X., and Li, L. (2017). Effects of resveratrol on glucose control and insulin sensitivity in subjects with type 2 diabetes: systematic review and meta-analysis. *Nutr. Metab.* 14:60. doi: 10.1186/s12986-017-0217-z

Conflict of Interest Statement: The authors declare that the research was conducted in the absence of any commercial or financial relationships that could be construed as a potential conflict of interest.

frontiers in Physiology

ORIGINAL RESEARCH
published: 20 September 2019
doi: 10.3389/fphys.2019.01221

Effect of L-Arginine on Titin Expression in Rat Soleus Muscle After Hindlimb Unloading

Anna Ulanova[1,2], Yuliya Gritsyna[1], Nikolai Salmov[1], Yuliya Lomonosova[3], Svetlana Belova[3], Tatyana Nemirovskaya[3], Boris Shenkman[3] and Ivan Vikhlyantsev[1]*

[1] Institute of Theoretical and Experimental Biophysics, Russian Academy of Sciences, Pushchino, Russia, [2] Pushchino State Institute of Natural Sciences, Pushchino, Russia, [3] State Scientific Center RF, Institute of Biomedical Problems, Russian Academy of Sciences, Moscow, Russia

Nitric oxide (NO), produced by NO-synthases via L-arginine oxidation, is an essential trigger for signaling processes involved in structural and metabolic changes in muscle fibers. Recently, it was shown that L-arginine administration prevented the decrease in levels of the muscle cytoskeletal proteins, desmin and dystrophin, in rat soleus muscle after 14 days of hindlimb unloading. Therefore, in this study, we investigated the effect of L-arginine administration on the degree of atrophy changes in the rat soleus muscles under unloading conditions, and on the content, gene expression, and phosphorylation level of titin, the giant protein of striated muscles, able to form a third type of myofilaments—elastic filaments. A 7-day gravitational unloading [hindlimb suspension (HS) group] resulted in a decrease in the soleus weight:body weight ratio (by 31.8%, $p < 0.05$), indicating muscle atrophy development. The content of intact titin (T1) decreased (by 22.4%, $p < 0.05$) and the content of proteolytic fragments of titin (T2) increased (by 66.7%, $p < 0.05$) in the soleus muscle of HS rats, compared to control rats. The titin gene expression and phosphorylation level of titin between these two groups were not significantly different. L-Arginine administration under 7-day gravitational unloading decreased the degree of atrophy changes and also prevented the decrease in levels of T1 in the soleus muscle as compared to HS group. Furthermore, L-arginine administration under unloading resulted in increased titin mRNA level (by 76%, $p < 0.05$) and decreased phosphorylation level of T2 (by 28%, $p < 0.05$), compared to those in the HS group. These results suggest that administration of L-arginine, the NO precursor, under unloading decreased the degree of atrophy changes, increased gene expression of titin and prevented the decrease in levels of T1 in the rat soleus muscle. The results can be used to search for approaches to reduce the development of negative changes caused by gravitational unloading in the muscle.

Keywords: L-arginine, titin, muscle atrophy, nitric oxide, skeletal muscle

OPEN ACCESS

Edited by:
Tatiana Borisova, Palladin Institute of Biochemistry (NAS Ukraine), Ukraine

Reviewed by:
Joan Ramon Torrella, University of Barcelona, Spain
Martina Krüger, Heinrich Heine University of Düsseldorf, Germany

****Correspondence:***
Anna Ulanova
ulanova.anna88@gmail.com; ivanvikhlyantsev@gmail.com

Specialty section:
This article was submitted to Environmental, Aviation and Space Physiology, a section of the journal Frontiers in Physiology

Received: *16 January 2019*
Accepted: *06 September 2019*
Published: *20 September 2019*

Citation:
Ulanova A, Gritsyna Y, Salmov N, Lomonosova Y, Belova S, Nemirovskaya T, Shenkman B and Vikhlyantsev I (2019) Effect of L-Arginine on Titin Expression in Rat Soleus Muscle After Hindlimb Unloading. Front. Physiol. 10:1221. doi: 10.3389/fphys.2019.01221

Abbreviations: C, cage control; HS, 7-day hindlimb suspension; HSL, 7-day hindlimb suspension + L-arginine; NO, nitric oxide; T1, Intact titin 1; T2, proteolytic fragments of T1.

INTRODUCTION

Nitric oxide (NO) is an essential trigger for signaling processes that lead to structural and metabolic changes in muscle fibers (Shenkman et al., 2015b). It is produced by NO-synthases during oxidation of the amino acid L-arginine. NO-synthase actively participates in the regulation of protein and energy metabolism in skeletal muscles, including the regulation of protein synthesis and degradation (Shenkman et al., 2015b).

Neuronal isoform (nNOSμ), associated with dystrophin in the subsarcolemmal region, is mostly expressed in skeletal muscles (Nakane et al., 1993; Brenman et al., 1995). Neuronal NO-synthase is regulated by intracellular Ca^{2+} via Ca^{2+}-dependent binding of the enzyme to the calcium-calmodulin complex (Forstermann et al., 1991). Neuronal NO-synthase is also activated by its substrate L-arginine, which is metabolized to NO (Shenkman et al., 2015b).

Muscle NO concentration has been shown to increase with an increase in muscle contractile activity (Perez et al., 2002; Vassilakopoulos et al., 2003; Pye et al., 2007) and decrease after muscle unloading (Lomonosova et al., 2011). Unloading leads to skeletal muscle atrophy accompanied with excessive degradation of the giant sarcomeric proteins, titin and nebulin (Shenkman et al., 2002; Udaka et al., 2008; Ulanova et al., 2015). The calcium-dependent cysteine proteases, μ-calpain (calpain-1) and m-calpain (calpain-2), have been reported to be involved in the initiation of proteolysis of titin and nebulin (Goll et al., 2003; Shenkman and Nemirovskaya, 2008; Mohrhauser et al., 2011).

It was found that NO inhibited m-calpain activity *in vitro* via S-nitrosylation of the active site cysteine (Koh and Tidball, 2000). It was also shown that NO produced endogenously by the skeletal muscles and other cell types has the potential to inhibit m-calpain activity and cytoskeletal proteolysis (Koh and Tidball, 2000; Samengo et al., 2012). Moreover, age-related loss of NO-synthase in the skeletal muscles was reported to decrease calpain S-nitrosylation, thereby leading to increased myofibril degradation and sarcopenia (Samengo et al., 2012). In addition, the proteolytic susceptibility of titin, the giant elastic protein present in vertebrate striated muscles (Tskhovrebova and Trinick, 2017; Herzog, 2018; Kellermayer et al., 2018; Linke, 2018), has been reported to be affected by titin phosphorylation (Gritsyna et al., 2017).

Nitric oxide is also known to be involved in the regulation of gene expression; brain-derived neurotrophic factor was reported to trigger NO synthesis and S-nitrosylation of histone deacetylase 2 in neurons, resulting in changes to histone modifications and gene activation (Nott et al., 2008).

Changes in titin gene expression were observed in mice skeletal muscles that were atrophied after a 30-day-long space flight (Ulanova et al., 2015). Increased titin degradation and reduced titin content were also observed. Studies of changes in the expression of the titin-coding gene (TTN) in conditions of simulated gravitational unloading have not been conducted. Recently, it was shown that L-arginine administration decreased the degree of atrophy changes and prevented the decrease in levels of the muscle cytoskeletal proteins, desmin and dystrophin, in rat soleus muscle during unloading (Lomonosova et al., 2011). However, the precise mechanism underlying the prevention of muscle atrophy by L-arginine is not yet known, and the effect of L-arginine on titin gene expression and degradation is not clear. Therefore, in this study, we investigated the effect of L-arginine administration on the (i) degree of atrophy changes in rat soleus muscles after hindlimb unloading, (ii) level and gene expression of titin, and (iii) changes in levels of titin phosphorylation in rat soleus during unloading. New data were obtained showing that administration of L-arginine, the NO precursor, under gravitational unloading decreased the degree of atrophy changes, increased gene expression of titin and prevented the decrease in levels of T1 in the rat soleus muscle.

MATERIALS AND METHODS

Animals and Ethical Approval

Fifteen 3-month-old male Wistar rats (190 ± 5 g) were obtained from the certified Nursery for laboratory animals, Institute of Bioorganic Chemistry of the Russian Academy of Sciences (Pushchino, Moscow region). The animals were housed in a temperature-controlled room under a 12:12 h light–dark cycle; food pellets and water were provided *ad libitum*. This study was carried out in accordance with the recommendations of Grundy (2015) and the European Convention for the protection of Vertebrate Animals used for Experimental and Scientific purposes (Council of Europe number 123, Strasbourg, 1986). The protocol was approved by the Biomedicine Ethics Committee of the Institute of Biomedical Problems of the Russian Academy of Sciences/Physiology section of the Russian Bioethics Committee (protocol no. 421 of April 14, 2016). All efforts were made to minimize the animal pain and suffering. Prior to all surgical procedures, the animals were anesthetized with an intraperitoneal injection of tribromoethanol (240 mg kg^{-1}). The depth of anesthesia was evaluated by testing the pedal withdrawal reflex (toe and foot pad pinch).

Hindlimb Unloading and L-Arginine Administration

The hindlimbs were unloaded using a standard rodent hindlimb suspension (HS)/unloading model (Morey-Holton and Globus, 2002). Briefly, a strip of adhesive tape was applied to the animal's tail, which was suspended by passing the tape through a swivel attached to a metal bar on the top of the cage. This setup allowed the forelimbs to be in contact with the grid floor and allowed the animals to move around the cage for free access to food and water. The suspension height was adjusted to prevent the hindlimbs from touching any supporting surface while maintaining a suspension angle of approximately 30°. The animals were randomly divided into three groups (n = 5/group): (1) C, cage control; (2) HS, 7-day hindlimb suspension; and (3) HSL, 7-day hindlimb suspension + L-arginine. 7 days were chosen because preliminary studies demonstrated the development of atrophy in human

soleus fibers and significant decrease in the titin content after 7 days gravitational unloading (Shenkman et al., 2004). Animals from the HSL group were daily administered 500 mg kg^{-1} L-arginine ("NOW Foods", United States) via intramuscular injections. The dose of L-arginine was previously tested and found to be optimal (Lomonosova et al., 2011). The rats from the C and HS groups were administered an equivalent dose of saline. Under anesthesia, the soleus muscles from the control and unloaded rats were surgically excised from both the hindlimbs, frozen in liquid nitrogen, and stored at –80°C until further analysis.

RNA Isolation

Total RNA was isolated from the samples using the Aurum™ Total RNA Fatty and Fibrous Tissue kit, according to the manufacturer's protocol (Bio-Rad Laboratories, Inc., Hercules, CA, United States). The total RNA quality was assessed by visualizing the integrity of the 18S and 28S rRNA after electrophoresis in 1% agarose gels. Total RNA concentration was determined via spectrophotometry (NanoDrop ND-1000 spectrophotometer; Nano-Drop Technologies, Waltham, MA, United States). RNA solutions were stored at −75°C.

Reverse Transcription-Quantitative Polymerase Chain Reaction

Isolated mRNA was reverse-transcribed to cDNA using the M-MLV reverse transcriptase (Evrogen, Moscow, Russia) and oligo-dT_{15} primers (catalog number SB001, Evrogen). Primers specific for gene fragments of titin and GAPDH were selected using Vector NTI software. The following primer pairs were used: titin (N2A isoform) 5′-CAGCAGCCAAGAAAGCCGCT-3′ (forward), 5′-CACCACTCTGATACTCTGAGGCTCTG-3′ (reverse) and GAPDH gene 5′-GCAAGAGAGAGGCCCTCAG-3′ (forward), 5′-TGTGAGGGAGATGCTCAGTG-3′ (reverse). Nucleotide gene sequences were obtained from the NCBI GenBank database. Real-time PCR was performed using a DT-322 amplifier (DNA-Technology, Moscow, Russia), Taq-DNA polymerase (Evrogen), and SYBR Green I fluorescent dye (Invitrogen, Carlsbad, CA, United States). PCR was performed as follows: (i) hot start at 95°C for 5 min, (ii) denaturation at 95°C for 15 s, (iii) primer annealing at 64°C for 20 s, and (iv) extension at 72°C for 20 s. Stages 2 to 4 were repeated 35 times. The amplification products were analyzed by electrophoresis in a 7% polyacrylamide gel. The PCR products were isolated from the gel according to the Cleanup Standard protocol (Evrogen, Russia). DNA fragments were sequenced in Evrogen. BLAST program software was used for identification of the PCR product (see **Supplementary Materials**). The changes in titin gene expression were determined according to the $2^{-\Delta\Delta ct}$ method (Livak and Schmittgen, 2001), and the housekeeping gene GAPDH was used for normalization.

SDS-PAGE Analysis of Titin

Changes in titin-1 (T1, intact titin) and T2 (proteolytic fragments) content were determined using polyacrylamide slab gels (2.2%, 10 × 10 × 0.1 cm). The gels were strengthened with agarose according to the Tatsumi–Hattori technique (Tatsumi and Hattori, 1995) with some modifications reported previously (Vikhlyantsev and Podlubnaya, 2017). Muscle tissues were homogenized in lysis buffer (12 mM Tris HCl, 1.2% SDS, 10% glycerol, 2% β-mercaptoethanol or 75 mM DTT, 5 μg/ml leupeptin, and E64, pH 6.8 to 7.0). To prevent titin degradation at high temperatures (Granzier and Wang, 1993), the samples were incubated for 30 to 40 min at 40°C instead of boiling them (Vikhlyantsev and Podlubnaya, 2017). Protein concentrations were measured using the NanoDrop ND-1000 Spectrophotometer. To ensure that equal protein amounts were loaded into the gels, samples from the control and experimental groups were all run on the same gel. SDS-PAGE analysis was performed using the Helicon VE–10 system (Moscow, Russia) at 8 mA. The gels were stained with Coomassie brilliant blue G-250 and R-250 mixed in a 1:1 ratio.

Determination of Titin Phosphorylation Levels

The level of titin phosphorylation was determined using a previously described method (Borbély et al., 2009) with minor modifications. The native level of protein phosphorylation was estimated in the gels using the fluorescent dye Pro-Q Diamond (Invitrogen). The gels were incubated in an aqueous solution of 50% ethanol and 10% acetic acid for 12–18 h, washed with distilled water for 30 min, and stained for 1.5 h. The gels were then rinsed in Pro-Q Diamond phosphoprotein gel destaining solution (Invitrogen), and the protein bands containing phosphate groups were visualized using the ChemiDoc™ Touch Imaging System (Bio-Rad). The data were processed using the Image Lab Software (Bio-Rad). Finally, the gels were stained with Coomassie brilliant blue G-250 and R-250, mixed in a 1:1 ratio, to determine the total protein content.

Densitometry and Statistical Analysis

Gels were digitized, and the data were processed using the TotalLab v1.11 software (Newcastle Upon Tyne, England). To determine the titin content relative to that of the myosin heavy chain, the total optical density of the myosin heavy chain peak and the total optical density of the T1 and T2 peak were determined on the same gel, as described previously (Cazorla et al., 2000). It is known that a specific titin-to-myosin ratio exists in the A-disk of the sarcomere (6 titin molecules per half of a myosin filament in a sarcomere) (Liversage et al., 2001). This approach for titin content measurement is more accurate than the estimation based on the total protein content in the sample. The values are presented as M ± SD, where M is the mean value and SD is the standard deviation. The statistical analysis of the results obtained was carried out with SigmaPlot 11.0 software (Systat Software, Inc., 2008). Since the distribution of some data samples was not normal (Shapiro–Wilk test), we estimated the significance of differences using non-parametric single-factor dispersion analysis for repeated

measurements (Kruskal–Wallis One Way Analysis of Variance on Ranks) with the following pairwise comparison by the Tukey test (see **Supplementary Materials**). The differences were considered statistically significant at $p < 0.05$.

RESULTS

Analysis of Atrophic Changes in Rat Soleus Muscle After Hindlimb Suspension

Decreased soleus muscle weight (by 40.5%, $p < 0.05$) and lower soleus weight:body weight ratio (by 31.8%, $p < 0.05$) was observed in the HS rats, compared to the C rats (**Table 1**). Compared to the C group, the HSL group showed both not significant decline in the soleus muscle weight (by 35.5%, $p = 0.073$), and tendency to reduction in the soleus muscle weight:body weight ratio (by 29.4%, $p = 0.086$) (**Table 1**).

Titin Content in Rat Soleus Muscle

Compared to the C group, the HS group showed a 22.4% decrease in T1 content ($p < 0.05$), and a 66.7% increase in T2 content ($p < 0.05$) in the soleus muscle (**Figure 1**). The difference in the T1 and T2 contents between the C and HSL groups was not statistically significant (**Figure 1**). Compared to the HS group rats, the HSL group rats showed a tendency to higher T1 content (by 23%, $p = 0.086$) in the soleus muscles.

Level of Titin Phosphorylation in Rat Soleus Muscle

Compared to the C group, the HS group showed a tendency to higher T2 phosphorylation levels (by 18.9%, $p = 0.333$) in the soleus muscles (**Figure 2**). The level of T2 phosphorylation in the soleus muscle in the HSL group was 14.4% ($p = 0.234$) and 28% ($p < 0.05$) lower than that in the C and HS groups, respectively, **Figure 2**. The levels of T1 phosphorylation in the soleus muscle in the C, HS, and HSL groups were not significantly different (**Figure 2**).

Titin Gene Expression in Rat Soleus Muscle

The differences between the titin mRNA levels on the C and HS groups were not statistically significant (**Figure 3**), but gene expression analysis revealed a tendency to higher the titin mRNA level (by 53%, $p = 0.073$; **Figure 3**) in the soleus muscle of rats with L-arginine administration (HSL group), compared to that in rats from the C group. Compared to the HS group, L-arginine administration under 7-day gravitational unloading showed a 76% increase in the titin mRNA level ($p < 0.05$; **Figure 3**).

TABLE 1 | Animal weight, weight of m. soleus and soleus muscle weight to body weight ratio.

Groups	Animal body weight, g	Weight of m. soleus, g	m. soleus weight/ animal weight, mg/g
"Control", $n = 5$	248.1 ± 14.3	0.121 ± 0.007	0.487 ± 0.006
"HS", $n = 5$	216.7 ± 5.8*	0.072 ± 0.007*	0.332 ± 0.025*
"HSL", $n = 5$	225.8 ± 13.1	0.078 ± 0.007	0.344 ± 0.010

*$P < 0.05$ as compared to control group.

DISCUSSION

The Effect of L-Arginine Administration on the Degree of Atrophy Changes and Level of Titin in Rat Soleus Muscles After Hindlimb Unloading

It is well known that disuse of muscles under conditions of simulated or real microgravity causes muscle atrophy (Fitts et al., 2001; Baldwin et al., 2013; Hargens and Vico, 2016; Mirzoev and Shenkman, 2018). Our results show a decrease in the weight of soleus muscle relative to the body weight after rat HS, suggesting the development of muscle atrophy. We found that L-arginine decreased the degree of atrophy changes and also prevented the decrease in levels of T1 in rat soleus muscle after 7 days of hindlimb unloading.

Titin is known to be a substrate for calcium-dependent proteases (calpains) (Goll et al., 2003; Huang and Zhu, 2016), and calpain activity is reported to increase in skeletal muscles from the first day of gravitational unloading (Enns et al., 2007). Recent studies have reported that unloading causes rapid skeletal muscle atrophy not only because of increased protein degradation via calpain activation but also because of decreased protein synthesis (Shenkman et al., 2015a; Mirzoev and Shenkman, 2018). Furthermore, it was found that treatment with PD150606 calpain inhibitor prevented the hindlimb suspension-induced atrophy in rat soleus muscle by inhibiting protein degradation pathways and preserving anabolic signaling (Shenkman et al., 2015a). Therefore, it is obvious that calpains play an essential role in the enhanced proteolysis of different proteins, including titin, under gravitational unloading (Enns et al., 2007; Shenkman et al., 2015a). In fact, the development of unloading-induced skeletal muscle atrophy has been shown to be accompanied with a decrease in the content of titin and an increase in the content of its proteolytic fragments T2 (Shenkman et al., 2002, 2004; Toursel et al., 2002; Udaka et al., 2008; Ulanova et al., 2015). Our results are consistent with these reports; compared to the control rats, those subjected to HS showed decreased T1 content and increased T2 content. However, the soleus muscle T1 content remained unaltered after unloading with L-arginine administration, compared to that in the control rats, suggesting a protective effect of L-arginine administration on the protein during unloading. The role of NO as a signaling molecule involved in the regulation of protein metabolism during unloading has recently been discussed (Shenkman et al., 2015b). Moreover, L-arginine administration was shown to prevent the increased proteolysis of desmin and dystrophin in the rat soleus after 14-day gravitational unloading (Lomonosova et al., 2011). In our study the HSL group showed a tendency to decline in the content of T2 proteolytic fragments compared

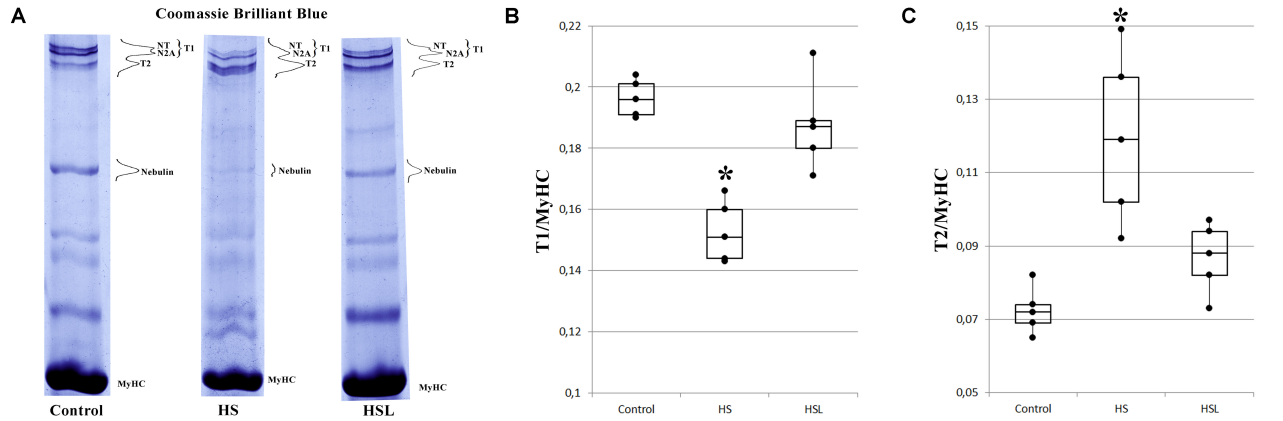

FIGURE 1 | Levels of intact titin-1 (T1) and proteolytic fragments (T2) in the soleus muscle of rats. **(A)** SDS-PAGE analysis of titin expression in the soleus muscle of rats. MyHC – myosin heavy chains. T2 (m.w. ~2000–2100 kDa) are proteolytic fragments of titin. NT and N2A are isoforms of intact titin-1 (T1, m.w. ~3400–3700 kDa in skeletal muscles). High molecular weight titin isoforms (denoted as NT-titin) were found in striated muscles of mammals (Vikhlyantsev and Podlubnaya, 2017). Plots of densitometric quantification of the T1 content **(B)** and T2 content **(C)** relative to MyHC content (n = 5). *P < 0.05 as compared to control group. Values are means ± SD.

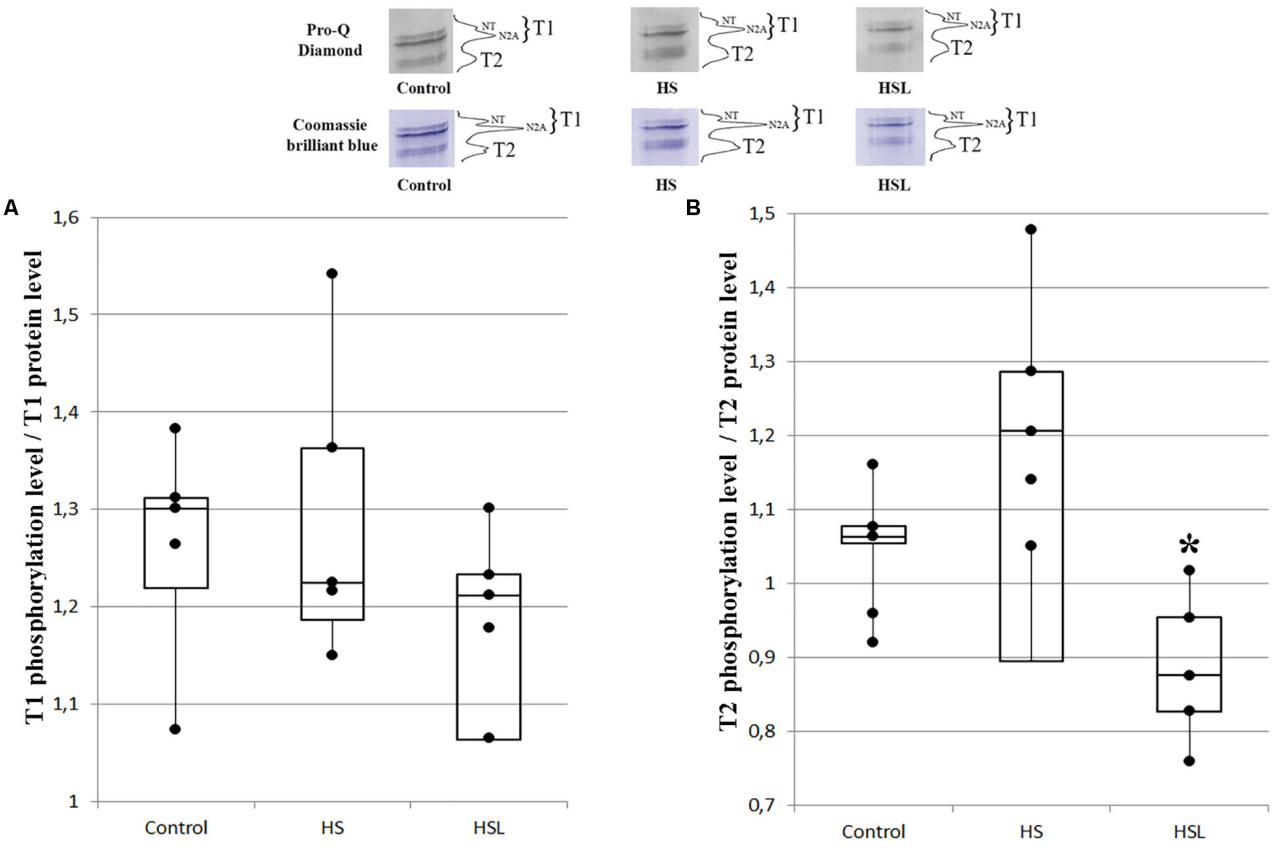

FIGURE 2 | Plots of titin phosphorylation levels in the soleus muscle of rats. **(A)** T1. **(B)** T2. *P < 0.05 when the 7-day hindlimb suspension + L-arginine (HSL) and the 7-day hindlimb suspension (HS) groups were compared, (n = 5). Values are means ± SD.

to the HS group. Collectively, our results indicated that NO production is essential for decreasing titin proteolysis under gravitational unloading. These results are consistent with the fact that NO increases calpain S-nitrosylation leading to a decrease in the activity of these proteases (Koh and Tidball, 2000; Samengo et al., 2012).

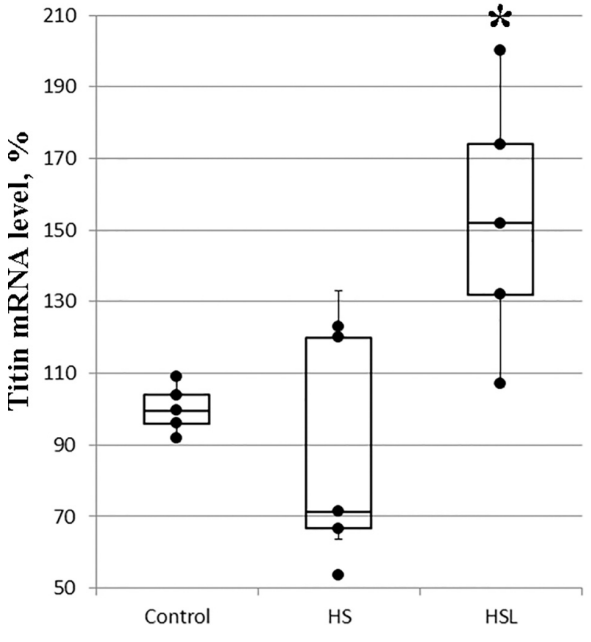

FIGURE 3 | Plots of titin mRNA levels in the soleus muscle of rats ($n = 5$). $^*P < 0.05$ as compared to hindlimb suspension (HS) group. Values are means ± SD.

The Effect of L-Arginine Administration on the Gene Expression of Titin in Rat Soleus Muscles After Hindlimb Unloading

Changes in titin gene expression and their possible role in alterations of the content of this protein under unloading remains unclear. Titin gene expression was shown to be increased (by 70%) in the atrophied gastrocnemius muscle of mice after a 30-day-long space flight (Ulanova et al., 2015). However, it should be noted that the animals were sacrificed 12 h after they landed; therefore, it was difficult to conclude whether an increase in titin gene expression was a consequence of the effects of microgravity on mice or a result of adaptation to the Earth's normal environment. We showed that there were no significant changes in titin gene expression in the rat soleus muscle after 7-day simulated gravitational unloading. Therefore, we concluded that alterations in titin gene expression do not play a significant role in unloading-induced changes in the content of this protein.

However, increased titin gene expression in the rat soleus muscle was observed after unloading with L-arginine administration in our work, suggesting the enhanced synthesis of this protein. This increase titin gene expression may be regulated via NO signaling. In 2008, it was shown that brain-derived neurotrophic factor triggers NO synthesis and S-nitrosylation of histone deacetylase 2, subsequently leading to gene activation in neurons (Nott et al., 2008). A later study concluded that cytoskeleton rearrangement and regulation of protein stability and turnover could potentially be modulated through NO-dependent changes in histone deacetylase activity (Watson and Riccio, 2009). NO-dependent machineries are known to be involved in the control of the key protein expression by means of inhibition of sumoylation of most SUMO targets (Qu et al., 2007) or GSK3β inhibition (Drenning et al., 2008; Sharlo et al., 2018). Our data show that NO is involved in the regulation of titin gene expression.

The Effect of L-Arginine Administration on the Changes in Titin Phosphorylation Levels in Rat Soleus Muscles After Hindlimb Unloading

In vivo titin phosphorylation is well known (Somerville and Wang, 1988) and the phosphorylation sites of this protein, located over the length of its molecule in the A-band (T2-titin part), I-band, and Z-disk in the sarcomere, have been determined (Linke and Hamdani, 2014). Many potential phosphorylation sites of titin molecule have also been discovered (Huttlin et al., 2010; Lundby et al., 2012)[1,2]. Phosphorylation is known to modify the stiffness of titin molecules (Linke and Hamdani, 2014). In recent years, the role of titin phosphorylation in the development of unloading-induced changes in muscles has been discussed. In particular, it was shown that titin hypophosphorylation, reducing the stiffness of titin molecules, may be involved with the development of diaphragm weakness caused by mechanical unloading (Ottenheijm et al., 2011; van Hees et al., 2012; van der Pijl et al., 2019). The role of phosphorylation of titin in change of its susceptibility to proteolysis has also been discussed. Phosphorylation is known to modify the sensitivity of proteins to their degradation by calpain-1 (Di Lisa et al., 1995). For instance, protein kinase A (PKA)-mediated phosphorylation of troponin-I reduced its sensitivity to degradation by calpain-1, whereas phosphorylation of protein kinase C (PKC), contrariwise, increased the sensitivity of troponin-I to proteolysis (Di Lisa et al., 1995). We found no direct experimental evidence to confirm a change in the sensitivity of titin to proteolysis mediated by a change in its phosphorylation level. However, there are indirect data testifying that titin hyperphosphorylation is accompanied by an increase in its proteolytic degradation. Using a fluorescent dye for protein phosphate group staining Pro-Q Diamond, it has been shown that atrophic changes in the gastrocnemius muscle of mice under real microgravity conditions are attended not only by a decrease in the T1 content, but also by a 1.3- and 3.3-fold increase in the degree of phosphorylation of T1 and T2, respectively, Ulanova et al. (2015). Similar changes have been registered in the gastrocnemius and soleus muscles of rats upon the development of alcohol-induced muscle atrophy (Gritsyna et al., 2017). According to certain results, obtained using monoclonal antibodies to phosphoserine pS26, a three-fold increase in the degree of phosphorylation of the PEVK region (located in zone I of the molecule) of titin in the quadriceps muscle of patients

[1]https://gygi.med.harvard.edu/phosphomouse/index.php
[2]http://cpr1.sund.ku.dk/cgi-bin/PTM.pl

with Ehlers-Danlos syndrome was accompanied by a decrease (by ∼20%) in the content of this protein (Ottenheijm et al., 2012). It has been suggested that titin hyperphosphorylation favors an increase in the sensitivity of this protein to proteolysis (Gritsyna et al., 2017).

In the present study, we showed a tendency to higher T2 phosphorylation level after HS. This tendency was accompanied by the enhanced proteolytic degradation of T1. These findings are in agreement with the assumption mentioned above. Administration of L-arginine during unloading caused hypophosphorylation of titin in the rat soleus muscle, that accompanied by a smaller decrease in the level of T1. Collectively, these results suggest that hypophosphorylation of titin, especially T2-part, decreases the susceptibility of this protein to proteolysis. This may be indirectly supported by finding that GSK3β inhibition in mice prevented the phosphorylation and depolymerization of desmin and blocked atrophy upon fasting or denervation. Mass spectrometry analysis identified GSK3-β and calpain-1 bound to desmin and catalyzing its disassembly (Aweida et al., 2018). This study proved that phosphorylation of desmin filaments by GSK3β is a key molecular event required for calpain-1–mediated depolymerization, and the subsequent myofibril destruction.

CONCLUSION

In conclusion, we showed that administration of L-arginine, the NO precursor, under gravitational unloading decreased the degree of atrophy changes, increased gene expression of titin and prevented the decrease in levels of T1 in rat soleus muscle. The results can be used to search for approaches to reduce the development of negative changes caused by gravitational unloading in the muscle. Because of limited n-number and high data variability, further research is required to provide evidence of changes in the phosphorylation level of titin and gain insight into how the post-translational modification affect the susceptibility of titin to proteolysis. To find answers to these research questions is the aim of our future studies.

ETHICS STATEMENT

This study was carried out in accordance with the recommendations of Grundy (2015) and the European Convention for the protection of Vertebrate Animals used for Experimental and Scientific purposes (Council of Europe number 123, Strasbourg, 1986). The protocol was approved by the Biomedicine Ethics Committee of the Institute of Biomedical Problems of the Russian Academy of Sciences/Physiology Section of the Russian Bioethics Committee (protocol no. 421 of April 14, 2016). All efforts were made to minimize the animal pain and suffering.

DATA AVALIABILITY STATEMENT

All datasets generated/analyzed for this study are included in the manuscript/**Supplementary Files**.

AUTHOR CONTRIBUTIONS

TN, BS, and IV conceived and designed the work. AU, YG, NS, YL, and SB performed the experiments. AU, BS, and IV analyzed the data and wrote the manuscript. AU and YG prepared the figures. AU, BS, and IV reviewed the manuscript.

FUNDING

This work was supported by the Russian Foundation for Basic Research (Grant Nos. 16-04-00529 and 17-04-01838) using the equipment of the Center for Collective Employment of ITEB (RAS) and Institute of Biomedical Problems (RAS).

ACKNOWLEDGMENTS

We would like to thank Editage (www.editage.com) for English language editing. We are grateful to Dr. A. V. Tankanag for help in statistical processing.

SUPPLEMENTARY MATERIAL

The Supplementary Material for this article can be found online at: https://www.frontiersin.org/articles/10.3389/fphys.2019.01221/full#supplementary-material

REFERENCES

Aweida, D., Rudesky, I., Volodin, A., Shimko, E., and Cohen, S. (2018). GSK3-β promotes calpain-1-mediated desmin filament depolymerization and myofibril loss in atrophy. *J. Cell. Biol.* 217, 3698–3714. doi: 10.1083/jcb.201802018

Baldwin, K. M., Haddad, F., Pandorf, C. E., Roy, R. R., and Edgerton, V. R. (2013). Alterations in muscle mass and contractile phenotype in response to unloading models: role of transcriptional/pretranslational mechanisms. *Front. Physiol.* 4:284. doi: 10.3389/fphys.2013.00284

Borbély, A., Falcao-Pires, I., van Heerebeek, L., Hamdani, N., Edes, I., Gavina, C., et al. (2009). Hypophosphorylation of the stiff N2B titin isoform raises cardiomyocyte resting tension in failing human myocardium. *Circ. Res.* 104, 780–786. doi: 10.1161/circresaha.108.193326

Brenman, J. E., Chao, D. S., Xia, H., Aldape, K., and Bredt, D. S. (1995). Nitric oxide synthase complexed with dystrophin and absent from skeletal muscle sarcolemma in duchenne muscular dystrophy. *Cell* 82, 743–752. doi: 10.1016/0092-8674(95)90471-9

Cazorla, O., Freiburg, A., Helmes, M., Centner, T., McNabb, M., Wu, Y., et al. (2000). Differential expression of cardiac titin isoforms and modulation of cellular stiffness. *Circ. Res.* 86, 59–67. doi: 10.1161/01.RES.86.1.59

Di Lisa, F., De Tullio, R., Salamino, F., Barbato, R., Melloni, E., Siliprandi, N., et al. (1995). Specific degradation of troponin T and I by mu-calpain and its modulation by substrate phosphorylation. *Biochem. J.* 308(Pt 1), 57–61. doi: 10.1042/bj3080057

Drenning, J. A., Lira, V. A., Simmons, C. G., Soltow, Q. A., Sellman, J. E., and Criswell, D. S. (2008). Nitric oxide facilitates NFAT-dependent transcription in

mouse myotubes. *Am. J. Physiol. Cell Physiol.* 294, C1088–C1095. doi: 10.1152/ajpcell.00523.2007

Enns, D. L., Raastad, T., Ugelstad, I., and Belcastro, A. N. (2007). Calpain/calpastatin activities and substrate depletion patterns during hindlimb unweighting and reweighting in skeletal muscle. *Eur. J. Appl. Physiol.* 100, 445–455. doi: 10.1007/s00421-007-0445-4

Fitts, R. H., Riley, D. R., and Widrick, J. J. (2001). Functional and structural adaptations of skeletal muscle to microgravity. *J. Exp. Biol.* 204, 3201–3208.

Forstermann, U., Pollock, J. S., Schmidt, H. H., Heller, M., and Murad, F. (1991). Calmodulin-dependent endothelium-derived relaxing factor/nitric oxide synthase activity is present in the particulate and cytosolic fractions of bovine aortic endothelial cells. *Proc. Natl. Acad. Sci. U.S.A.* 88, 1788–1792. doi: 10.1073/pnas.88.5.1788

Goll, D. E., Thompson, V. F., Li, H., Wei, W., and Cong, J. (2003). The calpain system. *Physiol. Rev.* 83, 731–801. doi: 10.1152/physrev.00029.2002

Granzier, H. L., and Wang, K. (1993). Gel electrophoresis of giant proteins: solubilization and silver-staining of titin and nebulin from single muscle fiber segments. *Electrophoresis* 14, 56–64. doi: 10.1002/elps.1150140110

Gritsyna, Y. V., Salmov, N. N., Bobylev, A. G., Ulanova, A. D., Kukushkin, N. I., Podlubnaya, Z. A., et al. (2017). Increased autolysis of μ-calpain in skeletal muscles of chronic alcohol-fed rats. *Alcohol. Clin. Exp. Res.* 41, 1686–1694. doi: 10.1111/acer.13476

Grundy, D. (2015). Principles and standards for reporting animal experiments in the journal of physiology and experimental physiology. *Exp. Physiol.* 100, 755–758. doi: 10.1113/EP085299

Hargens, A. R., and Vico, L. (2016). Long-duration bed rest as an analog to microgravity. *J. Appl. Physiol.* 120, 891–903. doi: 10.1152/japplphysiol.00935.2015

Herzog, W. (2018). The multiple roles of titin in muscle contraction and force production. *Biophys. Rev.* 10, 1187–1199. doi: 10.1007/s12551-017-0395-y

Huang, J., and Zhu, X. (2016). The molecular mechanisms of calpains action on skeletal muscle atrophy. *Physiol. Res.* 65, 547–560.

Huttlin, E. L., Jedrychowski, M. P., Elias, J. E., Goswami, T., Rad, R., Beausoleil, S. A., et al. (2010). A tissue-specific atlas of mouse protein phosphorylation and expression. *Cell* 143, 1174–1189. doi: 10.1016/j.cell.2010.12.001

Kellermayer, M., Sziklai, D., Papp, Z., Decker, B., Lakatos, E., and Mártonfalvi, Z. (2018). Topology of interaction between titin and myosin thick filaments. *J. Struct. Biol.* 203, 46–53. doi: 10.1016/j.jsb.2018.05.001

Koh, T. J., and Tidball, J. G. (2000). Nitric oxide inhibits calpain-mediated proteolysis of talin in skeletal muscle cells. *Am. J. Physiol. Cell Physiol.* 279, 806–812. doi: 10.1152/ajpcell.2000.279.3.C806

Linke, W. A. (2018). Titin gene and protein functions in passive and active muscle. *Ann. Rev. Physiol.* 80, 389–411. doi: 10.1146/annurev-physiol-021317-121234

Linke, W. A., and Hamdani, N. (2014). Gigantic business: titin properties and function through thick and thin. *Circ. Res.* 114, 1052–1068. doi: 10.1161/CIRCRESAHA.114.301286

Livak, K. J., and Schmittgen, T. D. (2001). Analysis of relative gene expression data using real-time quantitative PCR and the 2(-Delta Delta C(T)) Method. *Methods* 25, 402–408. doi: 10.1006/meth.2001.1262

Liversage, A. D., Holmes, D., Knight, P. J., Tskhovrebova, L., and Trinick, J. (2001). Titin and the sarcomere symmetry paradox. *J. Mol. Biol.* 305, 401–409. doi: 10.1006/jmbi.2000.4279

Lomonosova, Y. N., Kalamkarov, G. R., Bugrova, A. E., Shevchenko, T. F., Kartashkina, N. L., Lysenko, E. A., et al. (2011). Protective effect of L-arginine administration on proteins of unloaded m. *soleus*. *Biochemistry* 76, 571–580. doi: 10.1134/S0006297911050075

Lundby, A., Secher, A., Lage, K., Nordsborg, N. B., Dmytriyev, A., Lundby, C., et al. (2012). Quantitative maps of protein phosphorylation sites across 14 different rat organs and tissues. *Nat. Commun.* 3:876. doi: 10.1038/ncomms1871

Mirzoev, T. M., and Shenkman, B. S. (2018). Regulation of protein synthesis in inactivated skeletal muscle: signal inputs, protein kinase cascades, and ribosome biogenesis. *Biochemistry* 83, 1299–1317. doi: 10.1134/S0006297918110020

Mohrhauser, D. A., Underwood, K. R., and Weaver, A. D. (2011). In vitro degradation of bovine myofibrils is caused by μ-calpain, not caspase-3. *J. Anim. Sci.* 89, 798–808. doi: 10.2527/jas.2010-3149

Morey-Holton, E. R., and Globus, R. K. (2002). Hindlimb unloading rodent model: technical aspects. *J. Appl. Physiol.* 92, 1367–1377. doi: 10.1152/japplphysiol.00969

Nakane, M., Schmidt, H. H., Pollock, J. S., Fiirstermann, U., and Murad, F. (1993). Cloned human brain nitric oxide synthase is highly expressed in skeletal muscle. *FEBS Lett.* 316, 175–180. doi: 10.1016/0014-5793(93)81210-Q

Nott, A., Watson, P. M., Robinson, J. D., Crepaldi, L., and Riccio, A. (2008). S-nitrosylation of histone deacetylase 2 induces chromatin remodelling in neurons. *Nature* 455, 411–415. doi: 10.1038/nature07238

Ottenheijm, C. A., van Hees, H. W., Heunks, L. M., and Granzier, H. (2011). Titin-based mechanosensing and signaling: role in diaphragm atrophy during unloading? *Am. J. Physiol. Lung Cell Mol. Physiol.* 300, L161–L166. doi: 10.1152/ajplung.00288.2010

Ottenheijm, C. A., Voermans, N. C., Hudson, B. D., Irving, T., Stienen, G. J., van Engelen, B. G., et al. (2012). Titin-based stiffening of muscle fibers in ehlers-danlos syndrome. *J. Appl. Physiol.* 112, 1157–1165. doi: 10.1152/japplphysiol.01166.2011

Perez, A. C., de Oliveira, C. C., Prieto, J. G., Ferrando, A., Vila, L., and Alvarez, A. I. (2002). Quantitative assessment of nitric oxide in rat skeletal muscle and plasma after exercise. *Eur. J. Appl. Physiol.* 88, 189–191. doi: 10.1007/s00421-002-0693-2

Pye, D., Palomero, J., and Kabayo, T. (2007). Real-time measurement of nitric oxide in single mature mouse skeletal muscle fibres during contractions. *J. Physiol.* 581, 309–318. doi: 10.1113/jphysiol.2006.125930

Qu, J., Liu, G. H., Wu, K., Han, P., Wang, P., Li, J., et al. (2007). Nitric oxide destabilizes Pias3 and regulates sumoylation. *PLoS One* 2:e1085. doi: 10.1371/journal.pone.0001085

Samengo, G., Avik, A., Fedor, B., Whittaker, D., Myung, K. H., Wehling-Henricks, M., et al. (2012). Age-related loss of nitric oxide synthase in skeletal muscle causes reductions in calpain S-nitrosylation that increase myofibril degradation and sarcopenia. *Aging Cell* 11, 1036–1045. doi: 10.1111/acel.12003

Sharlo, C. A., Lomonosova, Y. N., Turtikova, O. V., Mitrofanova, O. V., Kalamkarov, G. R., Bugrova, A. E., et al. (2018). The Role of GSK-3β phosphorylation in the regulation of slow myosin expression in soleus muscle during functional unloading. *Biochemistry Suppl.Ser. A* 12, 85–91. doi: 10.1134/S199074781801009

Shenkman, B. S., Belova, S. P., Lomonosova, Y. N., Kostrominova, T. Y., and Nemirovskaya, T. L. (2015a). Calpain-dependent regulation of the skeletal muscle atrophy following unloading. *Arch. Biochem. Biophys.* 584, 36–41. doi: 10.1016/j.abb.2015.07.011

Shenkman, B. S., Nemirovskaya, T. L., and Lomonosova, Y. N. (2015b). NO-dependent signaling pathways in unloaded skeletal muscle. *Front. Physiol.* 6:298. doi: 10.3389/fphys.2015.00298

Shenkman, B. S., and Nemirovskaya, T. L. (2008). Calcium-depedent signaling mechanisms and soleus fiber remodeling under gravitational unloading. *J. Muscle Res. Cell Motil.* 29, 221–230. doi: 10.1007/s10974-008-9164-7

Shenkman, B. S., Nemirovskaya, T. L., Belozerova, I. N., Vikhlyantsev, I. M., Matveeva, O. A., Matveeva, O. A., et al. (2002). Effects of Ca2+-binding agent on unloaded rat soleus: muscle morphology and sarcomeric titin content. *J. Gravit. Physiol.* 9, 139–140.

Shenkman, B. S., Podlubnaya, Z. A., Vikhlyantsev, I. M., Litvinova, K. S., Nemirovskaya, T. L., et al. (2004). Contractile characteristics and sarcomeric cytoskeletal proteins of human soleus fibers in muscle unloading: role of mechanical stimulation from the support surface. *Biophysics* 49, 807–815.

Somerville, L. L., and Wang, K. (1988). Sarcomere matrix of striated muscle: in vivo phosphorylation of titin and nebulin in mouse diaphragm muscle. *Arch. Biochem. Biophys.* 262, 118–129. doi: 10.1016/0003-9861(88)90174-9

Strasbourg (1986). *European Convention for the Protection of Vertebrate Animals Used for Experimental and Other Scientific Purposes, European Treaty Series - No. 123*. Strasbourg: Council of Europe.

Tatsumi, R., and Hattori, A. (1995). Detection of giant myofibrillar proteins connectin and nebulin by electrophoresis in 2% polyacrylamide slab gels strengthened with agarose. *Anal. Biochem.* 224, 28–31. doi: 10.1006/abio.1995.1004

Toursel, T., Stevens, L., Granzier, H., and Mounier, Y. (2002). Passive tension of rat skeletal soleus muscle fibers: effects of unloading conditions. *J. App. Physiol.* 92, 1465–1472. doi: 10.1152/japplphysiol.00621.2001

Tskhovrebova, L., and Trinick, J. (2017). Titin and nebulin in thick and thin filament length regulation. *Subcell. Biochem.* 82, 285–318. doi: 10.1007/978-3-319-49674-0_10

Udaka, J., Ohmori, S., Terui, T., Ohtsuki, I., Ishiwata, S., Kurihara, S., et al. (2008). Disuse-induced preferential loss of the giant protein titin depresses muscle

performance via abnormal sarcomeric organization. *J. Gen. Physiol.* 131, 33–41. doi: 10.1085/jgp.200709888

Ulanova, A., Gritsyna, Y., Vikhlyantsev, I., Salmov, N., Bobylev, A., Abdusalamova, Z., et al. (2015). Isoform composition and gene expression of thick and thin filament proteins in striated muscles of mice after 30-day space flight. *BioMed Res. Int.* 2015:104735. doi: 10.1155/2015/104735

van der Pijl, R. J., Granzier, H. L., and Ottenheijm, C. A. (2019). Diaphragm contractile weakness due to reduced mechanical loading: role of titin. *Am. J. Physiol. Cell Physiol.* 317, C167–C176. doi: 10.1152/ajpcell.00509.2018

van Hees, H. W., Schellekens, W. J., Andrade Acuña, G. L., Linkels, M., Hafmans, T., Ottenheijm, C. A., et al. (2012). Titin and diaphragm dysfunction in mechanically ventilated rats. *Intensive Care Med.* 38, 702–709. doi: 10.1007/s00134-012-2504-5

Vassilakopoulos, T., Deckman, G., Kebbewar, M., Rallis, G., Harfouche, R., and Hussain, S. N. (2003). Regulation of nitric oxide production in limb and ventilator muscles during chronic exercise training. *Am. J. Physiol. Lung Cell. Mol. Physiol.* 284, 452–457. doi: 10.1152/ajplung.00270.2002

Vikhlyantsev, I. M., and Podlubnaya, Z. A. (2017). Nuances of electrophoresis study of titin/connectin. *Biophys. Rev.* 9, 189–199. doi: 10.1007/s12551-017-0266-6

Watson, P. M., and Riccio, A. (2009). Nitric oxide and histone deacetylases: a new relationship between old molecules. *Commun. Integr. Biol.* 2, 11–13. doi: 10.4161/cib.2.1.7301

Conflict of Interest: The authors declare that the research was conducted in the absence of any commercial or financial relationships that could be construed as a potential conflict of interest.

Advantages of publishing in Frontiers

OPEN ACCESS
Articles are free to read for greatest visibility and readership

FAST PUBLICATION
Around 90 days from submission to decision

HIGH QUALITY PEER-REVIEW
Rigorous, collaborative, and constructive peer-review

TRANSPARENT PEER-REVIEW
Editors and reviewers acknowledged by name on published articles

Frontiers
Avenue du Tribunal-Fédéral 34
1005 Lausanne | Switzerland

Visit us: www.frontiersin.org
Contact us: info@frontiersin.org | +41 21 510 17 00

REPRODUCIBILITY OF RESEARCH
Support open data and methods to enhance research reproducibility

DIGITAL PUBLISHING
Articles designed for optimal readership across devices

FOLLOW US
@frontiersin

IMPACT METRICS
Advanced article metrics track visibility across digital media

EXTENSIVE PROMOTION
Marketing and promotion of impactful research

LOOP RESEARCH NETWORK
Our network increases your article's readership